CONFIDENTIAL DECLASSIFIED

THE PERFORMANCE OF ADSORBENTS IN GAS MASK CANISTERS

BY

Frank G. Pearce

B.S., Rose Polytechnic Institute
1940

SUBMITTED IN PARTIAL FULFILMENT OF THE REQUIREMENTS
FOR THE DEGREE OF
DOCTOR OF SCIENCE

From the

MASSACHUSETTS INSTITUTE OF TECHNOLOGY
1945, i.e. 1946

Signature of Author _____
Department of Chemical Engineering, June 21, 1946
Signature of Professor in Charge of Research _____
Signature of Chairman of Departmental Committee on Graduate Students _____
Signature of Head of Department _____

MASS. INST. TECH.
FEB 20 1969
LIBRARIES

CONFIDENTIAL DECLASSIFIED

[redacted]

DECLASSIFIED

This document contains information affecting the national defense of the United States within the meaning of the Espionage Act, 50, U.S.C; 31 and 32, as amended. Its transmission or the revelation of its contents in any manner to an unauthorized person is prohibited by law.

GROUP - 4
Downgraded at 3 year intervals; declassified after 12 years.
per D. L. ADDERLEY

Classification Changed
TO: UNCLASSIFIED
By Authority of: ISM APPEN II F3C
DAVID L.
ADDERLEY 1 NOV 68
Name Date
EDGEWOOD ARSENAL
MARYLAND
MB.

[redacted]

DECLASSIFIED

CONFIDENTIAL

DECLASSIFIED

June 21, 1946

Professor George W. Swett
Secretary of the Faculty
Massachusetts Institute of Technology
Cambridge, Massachusetts

Dear Sir:

In accordance with the regulationsof the Faculty, I submit herewith a thesis entitled "The Performance of Adsorbents in Gas Mask Canisters" in partial fulfilment of the requirements for the degree of Doctor of Science.

Very truly yours,

Frank G. Pearce

CONFIDENTIAL

DECLASSIFIED

[redacted] DECLASSIFIED

ACKNOWLEDGEMENT

This research was carried out under the general supervision of Professor Harold C. Weber whose encouragement and suggestions are greatly appreciated.

The investigation was closely related to the development of gas mask and collective protector canisters at the Chemical Warfare Service Development Laboratory, M.I.T. Since several other persons at that installation were also engaged in these developments, they showed considerable interest in the results of this research and offered valuable suggestions. Many thanks are extended to Dr. F.F. Diwoky, Dr. O.A. Short, and Mr. J.T. Kaufman.

Other organizations within the Chemical Warfare Service were also interested in these investigations, and personnel at those installations had valuable suggestions to offer at conferences which were attended by the author. Thanks are due to Dr. I. Klotz of the N.D.R.C., Northwestern University, and to Dr. D. McRae and Mr. S. Hormatz of the Technical Command, Edgewood Arsenal, Maryland.

Much of the experimental work was conducted by the Canister Testing Section of the Test Division which was under the direction of Mr. W. Cunningham. Thanks are due to him and to his assistants.

[redacted] DECLASSIFIED

[redacted] DECLASSIFIED

TABLE OF CONTENTS

		Page
I.	Summary	1
II.	Introduction	8
III.	Previous Work	24
	A. Adsorption Isotherm	24
	B. Rate of Establishment of Equilibrium with Pure Fluids	26
	C. Mass Transfer Coefficients-Gas Film-From Gas Absorption Studies	27
	D. Mass Transfer Coefficients-Small Diameter Packing	31
	E. Integrated Equations for Unsteady State Mass Transfer in Packed Adsorbent Beds	32
	F. Experimental Data for Mass Transfer from Flowing Air Streams to Adsorbent Beds	41
IV.	Purpose of this Research	57
V.	Experimental Procedure	61
VI.	Results	69
VII.	Discussion of Results	107
	A. Experimental Results	107
	1. Axial Flow Adsorbent Beds	107
	a. Mechanixm of Removal of the Five Standard Agents by Type ASC Impregnated Whetlerite	107
	b. Chloropicrin Performance	111
	c. Phosgene, Cyanogen Chloride, Hydrocyanic Acid, and Arsine	122
	d. Cumulative Penetration	146

[redacted] DECLASSIFIED

[redacted]

DECLASSIFIED

TABLE OF CONTENTS (CONTINUED)

Page

e. Effect of Adsorbed Moisture on Bed Depth-Break Time Relationships 148

f. Air Resistance 150

g. Summarized Results-Axial Flow Beds 158

2. Radial Flow Adsorbent Beds 169

B. Practical Canister Design 174

VIII. Conclusions 178

IX. Recommendations 182

X. Appendix 184

Appendix A. Derivation of Equation for Cases of Reversible, Physical Adsorption 185

Appendix B. Derivation of Equation for Cumulative Break 224

Appendix C. Adaptation of Equations for Breather Flow 227

Appendix D. Adaptation of Equations to Radial Flow 235

Appendix E. Removal of Agents by Chemical Reaction with Impregnants 241

Appendix F. Theoretical Adaptation of Equations for Blends of Several Sieve Fractions 268

Appendix G. Summarized Data 271

Appendix H. Accuracy of Data 292

Appendix I. Sample Calculations 298

Appendix J. Location of Original Data 308

Appendix K. Nomenclature 309

[redacted]

DECLASSIFIED

[redacted]

DECLASSIFIED

TABLE OF CONTENTS (CONTINUED)

		Page
Appendix L.	Literature Citations	313
Appendix M.	Biographical Sketch	316

DECLASSIFIED

[redacted]

[redacted] DECLASSIFIED

I. SUMMARY

The object of the work described in this thesis was to obtain an exact or approximating relationship among the variables controlling the removal of gaseous impurities from air streams drawn through beds of granular adsorbents. This was necessary for the efficient design of the adsorbent sections of gas mask canisters for use by the United States Army during the recent conflict.

The Chemical Warfare Service has developed a very active adsorbent from wood, coal, fruit pits, and other carbonaceous materials, but it has been found that certain of the war gases are not adsorbed to any appreciable extent by reasonable volumes of this adsorbent. Therefore, impregnants such as copper oxide, metallic silver, and chromic oxide have been added to the base charcoal to produce Type ASC impregnated whetlerite. This material has a high capacity for all of the standard war gases.

It is important that this adsorbent be used as efficiently as possible, for the canisters must be as small and light as practical for the convenience and comfort of the soldier in the field. Also, such factors as air resistance and interference with normal combat duties must be considered, but all of these must be consistent with a high degree of protection.

For the most part, previous canister design has been performed by the "cut and try" method. While this proce-

[redacted] DECLASSIFIED

dure can accurately establish the performance of a particular design, it is time-consuming, expensive, and it is not easily utilized to obtain the optimum design. In the design of large collective protector canisters this procedure is impractical, for large volumes of air are handled (up to 300 cubic feet per minute) and large amounts of charcoal are wasted; also, the danger of casualties resulting from leaks during a test is high when such large quantities of noxious agents are being handled.

The removal of gases by passage through adsorbent beds can be accomplished by physical adsorption or by chemical reaction with the impregnants or with adsorbed water. Theoretical equations have been derived in Appendix A which predict the performance of adsorbent beds for physically adsorbed gases. Similar equations have been derived in Appendix E to predict the performance of adsorbent beds for gases which are removed by chemical reaction.

The theoretical equation relating break time of an axial flow adsorbent bed with the test variables for those agents which are removed by physical adsorption (Type I kinetics) is as follows: (See Nomenclature, p. 309).

$$t = \frac{N_o A}{C_1 Q} \left[\lambda - H_t \left(\ln \frac{C_1}{C_2} - \beta \right) \right] \qquad (1)$$

No general theoretical equation could be derived for those gases which are removed by a combination of physical adsorption and chemical reaction. However, for the particular case in which the rate of reaction is independent of the previous utilization of the impregnant, it is shown in

Appendix E that the following equation applies for axial flow adsorbent beds:

$$t = \frac{(N_o + N_r)\,A}{C_1 Q}\left[\lambda - (H_t + H_r)\left(\ln\frac{C_1}{C_2} - 1\right)\right] \qquad (2)$$

Both of these equations predict a straight line relationship between bed depth and time to a specific effluent concentration. They also predict that this straight line shall intersect the bed depth axis at a positive value; i.e., there is a certain positive bed depth which results in an immediate break. This intercept is called the apparent critical bed depth.

These theoretical equations suggested the use of bed depth-break time measurements to analyze the factors governing the adsorbent performance. Such tests were conducted varying the cross-sectional area, flow rate, particle diameter (sieve size), and effluent concentration. The effect of each of these variables on the slope of the bed depth-break time curve and on the apparent critical bed depth was determined for each of the agents.

These tests showed that chloropicrin is removed by reversible, physical adsorption and that the relationship among the variables is as predicted by Equation 1.

The remaining four standard Chemical Warfare agents (phosgene, cyanogen chloride, hydrocyanic acid, and arsine) were shown to be removed by a combination of chemical reaction and physical adsorption. The rate of chemical reaction was shown to be dependent on the previous utilization of the impregnant; therefore, Equation 2 does not

apply. Although no theoretical equation was derived for kinetics of this type (Type III-B kinetics, see Appdx. E), the experimental results could be correlated very well by the following semi-empirical equation:

$$t = \frac{N A}{C_1 Q}\left[\lambda - H\left(\ln\frac{C_1}{C_2} + 3\right)\right] \qquad (3)$$

This equation is strikingly similar to that for Type I kinetics (Equation 1). N_o and H_t have been replaced by two experimental constants, N and H, respectively, and β has been set equal to (-3). It is apparent that this equation also represents a straight line relationship between bed depth and break time with a positive intercept on the bed depth axis. Over the range of variables investigated, it was found that N is independent of flow rate and particle diameter but varies with different adsorbents. H behaves in a manner analagous to H_t in that it varies as a power of the linear air velocity and the particle diameter and is independent of the whetlerite.

The above equations (1, 2, and 3) are applicable for the evaluation of axial flow beds when tested at steady flow rates. In the last three years, the "Sine Wave Breather Tester" has been developed and used extensively for the evaluation of adsorbent beds. This machine simulates the breathing cycle of the average person under conditions of heavy exercise. Gas-laden air is drawn into the canister at a variable flow rate approximating the positive half of a sine wave (simulating inspiration), and

no air is drawn through the canister for the other half of the sine wave cycle (simulating expiration). The minute volume (integrated volume of contaminated air drawn through the canister per minute) is held at 50 liters per minute.

Theoretical equations are derived in Appendix C for these conditions of canister testing, and it has been shown that, for reversible, physical adsorption, Equation 1 is applicable if H_t is determined at an equivalent flow rate instead of at the average flow rate. The experimental data show that this theoretical argument is correct, and they also show that Equation 3, for Type III-B kinetics, can be modified in a similar manner. The equivalent flow rate is a function of the ratio of the influent concentration to the break concentration and of the power that H_t (or H) varies with velocity. This function is shown in Fig. 92.

Certain of the standard United States gas mask canisters are of the radial flow type; i.e., the adsorbent is retained between two concentric cylinders, the contaminated air stream entering the bed perpendicular to and at the surface of the outer cylinder. For this type construction, it has been shown in Appendix D that there is a critical diameter which is analagous to the apparent critical bed depth of an axial flow canister. The equations relating the break time to the test variables for reversible physical adsorption are as follows:

$$D_c = \left[D_i^{x+1} + 2(x+1)k_1 \left(\frac{1000\ Q}{\pi\ L} \right)^x \ln \frac{C_1}{C_2} \right]^{\frac{1}{x+1}} \qquad (4)$$

$$t = \frac{\pi L N_o}{4 Q C_1}\left[D_2^2 - D_c^2 + 4D_c k_1 \beta\left(\frac{1000\ Q}{\pi D_c L}\right)^{\bar{x}}\right] \qquad (5)$$

These equations have been proved to be equally applicable for Types I and III-B kinetics, and it has been shown that they may also be modified for breather testing in a manner analagous to the modification of Equation 1 for axial flow canisters.

Most of the Chemical Warfare agents are not cumulative poisons, and tests with these are conducted to a fixed effluent concentration usually approximating the minimum physiologically detectable concentration. Arsine, however, is a cumulative poison, and tests with this agent are continued to a fixed cumulative penetration. Theoretical equations for these test conditions are derived in Appendix B, and for axial flow beds and Type I kinetics the following general equation was obtained:

$$t = \frac{N_o A}{C_1 Q}\left[\lambda - H_t\left(\ln \frac{N_o H_t A}{F} - \beta\right)\right] \qquad (6)$$

This equation has been found to be equally applicable for Types I and III-B kinetics, and it has also been shown that the equations for radial flow canisters may be modified in a similar manner to predict cumulative penetration break times.

These equations, and the modifications thereof, have been used at the Chemical Warfare Service Development Lab., M. I. T., for the design of the adsorbent sections of gas mask canisters and have proved quite valuable. They have

also been used in the design of collective protector canisters (15-300 cubic feet per minute capacity), and actual spot measurements of the break times of these large canisters have proved the validity of the foregoing equations for other than small gas mask canisters.

II. INTRODUCTION

A. Field of Research

The general problem investigated concerned the rate of removal of war gases from air streams by the standard Chemical Warfare impregnated whetlerites. The knowledge of these rates is important in the design of the gas removal section of gas mask canisters so as to be able to select the particular design which affords the desired degree of protection with a minimum expenditure of canister weight, canister volume (shape being considered), and air resistance. All of these factors are of great importance, for any slight additional impediment to the soldier in the field is conducive to his discarding the mask, an act which has frequently occurred with soldiers carrying the bulky, old-type service masks.

The removal of gases by porous adsorbents has been investigated extensively in the past by a great number of research workers. However, the vast bulk of this work has been devoted to measurement of the equilibrium relationships and the rate of attainment of equilibrium when the adsorbents are brought into contact with a pure vapor of the adsorbate. Very little work has been done to determine the rate of removal of adsorbates from carrier air streams flowing through the adsorbent bed.

The same type of problem is encountered in the case of absorption of a gas from an air stream by liquid flowing downward through a packed tower. The major differences be-

tween removal by this method and by a granular porous adsorbent are (1) the equilibrium relationships for liquid-vapor absorption processes are a unique function of the liquid and the gas, independent of the nature of the packing; whereas, for removal of a gas by a porous adsorbent, they are different with each adsorbent and (2) the liquid-gas absorption process is a continuous, steady-state process (i.e., conditions at a point do not change with time); whereas, the removal of a gas by passage through an adsorbent bed is an unsteady state process in which conditions at any point in the bed are changing continually.

The most obvious variables whose interdependency is desired are (1) time, (2) adsorbent bed depth, (3) agent concentration in the carrier air stream, (4) air velocity, (5) air resistance, and (6) particle size of the adsorbent. The agent content of the adsorbent is a variable of secondary importance for prediction of performance, but it is quite important in explaining the relationships which are obtained.

The problems of gas adsorption by passage through fixed adsorbent beds is not limited to the removal of war gases by gas mask canisters. It is equally applicable to such commercial operations as removal of noxious agents from waste gases, purification of gaseous products, stripping of gasoline from low-boiling hydrocarbon vapors, and solvent recovery. Another application which is not so obvious is the use of the rate constants to determine one rate controlling factor in the catalysis of reactions involving

flow through solid catalyst beds.

It is believed that the results of this research will be of assistance in offering a basis for the engineering design of equipment to perform the above operations.

B. Nature of Adsorbents

At the outbreak of the present war, all U.S. gas mask canisters were filled with "Type A Impregnated Whetlerite". This adsorbent was a very porous material with a high surface area per unit volume. There are many reports available in the Chemical Warfare Service files describing the preparation of this material. Basically, it was a highly activated cocoanut shell charcoal, activated by high pressure steam distillation of the hydrocarbon constituents. After activation it was impregnated with an ammoniacal solution of copper hydroxide. After drying a cupric oxide impregnated whetlerite was obtained. The purpose of the impregnation was to improve the phosgene (CG) and the hydrocyanic acid (AC) capacity of the adsorbent.

Shortly after the outbreak of World War II a new impregnant, metallic silver, was added to enhance the arsine (SA) capacity of the material after it had become saturated with water. Since the supply of cocoanut shell was stopped by the Japanese expansion into the Phillipine-Burma-Australia area, wood and coal base whetlerites were developed which eventually surpassed the adsorptive capacity of the earlier cocoanut shell materials. Simultaneously various fruit pit whetlerites were developed. All of these

base whetlerites were capable of impregnation with cupric oxide and metallic silver to yield an adsorbent designated as "Type AS Impregnated Whetlerite".

This material was never used to any appreciable extent, for it became necessary to add a new impregnant before Type AS Impregnated Whetlerite was out of the pilot plant stage of development. This third impregnant was chromic oxide, added to enhance the cyanogen chloride (CK) capacity of the whetlerite after it had become saturated with water. These three materials--cupric oxide, metallic silver, and chromic oxide--were added simultaneously by a simgle impregnating solution. This resulted in the standard adsorbent now used in all currently produced U.S. Army and Navy gas mask canisters, "Type ASC Impregnated Whetlerite". These impregnants were used to produce Grade I adsorbents from whetlerite bases prepared from wood, coal, fruit pits, and nut shells. The development and improvement of this impregnated whetlerite is described im many Chemical Warfare Service reports.

Thus, it is evident that the use of an adsorbent for its adsorptive capacity is now balanced by its use as an impregnant carrier, each impregnant having been added to enhance the protection against certain of the Chemical Warfare agents intended for use by the United States Army in event of the initiation of Chemical Warfare by our enemies.

C. The Diffusion and Physical Adsorption Concept

The theory of diffusion of a gas through a stagnant

inert gas film is well known and is thoroughly described in Sherwood's book "Absorption and Extraction" (1). Most of the previous work, however, has dealt with the transfer of a diffusing material from the gas stream to a liquid interface under steady state conditions. The following is a brief summary of the diffusion theory and proposes its application to the case of diffusion of an agent from the carrier stream to the surface of a solid adsorbent under unsteady state conditions.

As in all diffusion processes, the rate at which a gas is transferred across an interface is considered to be proportional to the difference between its partial pressure in the carrier air stream and the partial pressure at the surface of the adsorbent and inversely proportional to the resistance to transfer by diffusion. For all cases pertaining to Chemical Warfare canister testing, the concentrations of the diffusing component is less than two per cent by volume so that negligible error is introduced if concentration units are employed in lieu of partial pressure units.

If it can be assumed that the rate of adsorption is infinite (the rate at which equilibrium is established within the adsorbent granule after material has been transferred to the surface is infinite), the rate of diffusion is the only factor which controls the rate of transfer to the adsorbent. The may be expressed mathematically by the following equation:

$$dN_a/dt = k_g(C - C^*) \qquad (7)$$

The term, k_g, commonly called the gas film mass transfer coefficient, represents the reciprocal of the diffusional resistance in the gas film.

Since the transfer area cannot be measured conveniently, it is customary to multiply both sides of Equation 7 by a factor, a, which represents the transfer area per unit volume of adsorbent and to group $k_g a$ into a single coefficient which is on a volume basis. This results in the following equation:

$$a \frac{dN_a}{dt} = dm/dt = k_g a \ (C - C^*) \qquad (8)$$

It must be remembered in using this equation that, since $k_g a$ is on a gross volume basis, it is a function of the density of packing. Practically, however, in the range of sieve sizes employed in the Chemical Warfare Service (12 to 40 mesh), little variation in packing density is obtained. In addition, the standard method of assembling adsorbent beds insures a constant packing density for a particular charcoal at a particular sieve size (see Appendix H).

If the rate of transfer through the stagnant film surrounding the granules controls, the only other factor which determines the performance of an adsorbent bed is the equilibrium relationship. There are a number of theoretical and empirical equations which have been developed to express these relationships. The most widely used relationships are the adsorption isotherms of Freundlich (2) and Langmuir (3).

Freundlich's isotherm is expressed by the following equation:

$$C^* = k\, m^n \qquad (9)$$

Langmuir's isotherm may be expressed as follows:

$$C^* = \frac{m}{k_1 - k_2 m} \qquad (10)$$

These two equations, over a limited range of the variables, fit most data for organic adsorbates on charcoal equally well and either may be used to correlate the data. In this particulat thesis, the correlation of Freundlich has been used because it results in more easily handled mathematical relationships.

Another factor which affects the performance of a granular bed is the heat generated by adsorption. This has two effects: (1) it changes the equilibrium relationship and (2) it has a very slight effect on the diffusion resistance. This complication is handled quite easily in a continuous process: e.g., liquid-gas absorption column systems. A heat balance can be employed to determine the temperature at any point in the column and corrections can be made. For the adsorption of gases by a porous adsorbent, however, conditions are continually changing, and the solution becomes greatly involved. Even more complicating is the fact that the point rate of adsorption and the heat generation are mutually dependent and both are unsteady state processes.

Since the prediction of the performance of an adsorbent bed is so involved, even when isothermal conditions are assumed, no attempt has been made, in the derivation of the equations, to account for the effect of heat liberation. The derivations are based on the assumption of isothermal operation and are interpreted bearing in mind the qualitative effects of non-isothermal conditions.

If Equation 8 is combined with a material balance, the following partial differential equation is obtained for the removal of agents from inert air streams by passage through adsorbent beds of constant cross sectional area:

$$\frac{\alpha}{1000k_g a}\frac{\partial^2 m}{\partial t^2} + \frac{V}{1000k_g a}\frac{\partial^2 m}{\partial \lambda \partial t} + \frac{\partial m}{\partial t} + \frac{\alpha}{1000}\frac{\partial C^*}{\partial t} + \frac{V}{1000}\frac{\partial C^*}{\partial \lambda} = 0 \quad (11)$$

The solubility of this equation depends on the relationship between C^* and m. The only conditions for which analytical solutions are known are those wherein n in Freundlich's adsorption isotherm is equal to zero or unity. However, the relationship between C^* and m for organic adsorbates on charcoal always results in a value of n of unity or greater; therefore, no general analytical solution exists.

Particular solutions for chosen values of the variables can be obtained by a tedious step-wise integration. These calculations were carried through for a number of the values of the independent variables, and analysis of the results showed that the following equation correlates the variables extremely well over the range of any practical importance:

$$t = \frac{N_o A}{C_1 Q}\left[\lambda - H_t\left(\ln \frac{C_1}{C_2} - \beta\right)\right] \qquad (1)$$

The derivation of Equation 11, its solution for particular values of the variables, and the interpretation of the particular solutions resulting in the establishment of Equation 1 are given in Appendix A. The effects of the heat of adsorption on the results predicted by Equation 1 are also discussed in Appendix A.

D. The Diffusion and Chemical Reaction Concept

It was stated previously that various metallic impregnants have been added to the base whetlerite during the development of the present Type ASC Impregnated Whetlerite. Obviously, the addition of these impregnants could not increase the adsorptive capacity of the charcoal to any appreciable extent. Actually, the tendency of added metallic impregnants is to decrease the adsorptive capacity. However, the increased capacity is obtained, and it is always associated with a non-reversible adsorption. The conclusion is that the impregnant either acts as a catalyst or reacts chemically with the impregnant. The facts that the adsorbents have fixed, maximum capacities for the agents and that the impregnants are always changed chemically after use indicate that the action is not catalytic.

If reaction occurs on the surface, a second rate function, the rate of chemical reaction, must be considered. This is somewhat analogous to the case of mass transfer in

a liquid-gas absorption tower wherein the diffusion resistance in the liquid film is important.

The general equation for the rate of chemical reaction may be expressed mathematically by the following equation:

$$dM/dt = k_r a' f(m) \qquad (12)$$

In this equation, $k_r a'$ may be a function of the amount of impregnant which has previously been consumed, and the term, $f(m)$, indicates that the rate is some unknown function of the amount of physically adsorbed (unreacted) adsorbate.

For the particular case where $k_r a'$ is very large as compared to $k_g a$, it is shown in Appendix E that Equation 1 is applicable if the adsorptive capacity, N_o, is replaced by the sum of the adsorptive and reactive capacities, $N_o + N_r$.

For another particular case wherein $k_r a'$ is assumed to be independent of the previous utilization of the impregnant and wherein $f(m)$ is assumed to be directly proportional to the equilibrium concentration (based on the equilibrium relationship and the amount of physically adsorbed agent on the adsorbent), it is shown in Appendix E that Equation 1 is applicable with the following modification:

$$t = \frac{(N_o + N_r)\, A}{C_1 Q} \left[\lambda - (H_t + H_r)\left(\ln \frac{C_1}{C_2} - 1\right) \right] \qquad (2)$$

It is to be noticed that, for all these cases, a linear relationship is obtained between the time elapsed to a fixed effluent concentration and bed depth and that the straight line graph relating these variables would intersect the bed depth axis at a point dependent on the rate functions and the ratio of the test to the break concentration.

The most difficult and most general case is encountered when the reaction rate constant is a function of the amount of impregnant which has been previously utilized and when f(m) is an involved function of m. One example of this type of kinetics has been calculated in Appendix E, and, although a practically linear relationship was obtained between break time and bed depth (at lives in excess of five minutes), no correlation could be obtained which would adapt the results of this type kinetics to Equation 1. However, the striking similarity between the bed depth-break time relationships obtained and those represented by Equations 1 and 2 suggested that a semi-empirical relationship of the same type might be obtained which would be sufficiently accurate for design calculations.

E. General Technique of Research

Fellinger (4) stated that:

"The ultimate goal of a broad program of research upon gas absorption in packed towers would be to obtain the following information for the various packing available: A collection of the individual film coefficients, pressure

drop data, and loading and flooding characteristics, and a correlation of these data with the main variables assumed to control absorption tower operation such as gas and liquor rates, diffusivity, viscosity, density, and possibly surface tension."

This type of data is equally desirable for the removal of vapors by granular adsorbents with the elimination of the variables which are peculiar to absorption tower operation and the inclusion of additional variables which are peculiar to adsorption by fixed beds, the most obvious example of which is the time variable.

It has been pointed out previously that the rate of transfer from an air stream may be controlled by the rate of diffusion or by the rate of chemical reaction with the impregnants on the adsorbent. The initial problem is to determine which resistance is controlling (if either) and to determine the rate functions and the equilibrium relationships.

Theoretical, analytical relationships have been derived, based on the assumptions that certain of the resistances or combinations of the resistances control the rate of transfer, and these serve as an excellent guide for the investigations. For example, Equation 1, which was derived on the assumption that diffusion through the stagnant air film surrounding the granules controls, immediately suggests experiments to determine the relationship between bed depth (constant cross section ad-

sorbent bed) and time to a fixed effluent concentration. The slope of the plot relating these functions can then be compared to the theoretical slope predicted by Equation 1, all the controlling variables of which can be measured.

The intercept of this plot on the bed depth axis can also be measured and experiments can be conducted to test its dependency on the logarithm of the concentration ratio as predicted by the equation. If correlation is obtained, tests may then be conducted to determine the dependency of the mass transfer coefficients, reflected by H_t, on such variables as particle diameter, velocity, and agent diffusivity which would be expected to affect the mass transfer coefficient.

Other experiments which can be conducted to establish the rate controlling functions include (1) agent pick-up by thin beds of adsorbent as a function of time and (2) measurement of the effluent concentration as a function of time.

Since the breathing resistance (resistance to air flow) is also important in the design of gas mask canisters, measurements were made of this quantity to determine the effects of bed depth, flow rate, and particle diameter.

F. Further Development of Equations

In order that the equations might be handled as easily as possible, a simplification was made in the development of Equation 1 by the introduction of the function, H_t,

commonly called the "height of a transfer unit" and originally presented by Chilton and Colburn (5) for use in absorption tower design. This function, which is directly proportional to the diffusional resistance, has the dimensions of length. For the particular case involving low gas concentrations, the following equations apply:

$$(HTU)_g = H_t = \frac{V}{1000\ k_g a} \qquad (13)$$

$$(HTR)_s = H_r = \frac{V}{1000\ k_r a'} \qquad (14)$$

These functions shall be used throughout instead of the mass transfer coefficient, $k_g a$, and the reaction rate constant, $k_r a'$. In order to simplify the calculations, H_t was assumed to vary as some power of air velocity. This assumption was verified later during the investigation.

In order to simulate actual use conditions as closely as possible, the "Sine Wave Breather Canister Tester" was developed by the Chemical Warfare Service in 1943. This apparatus was designed to approximate the breathing characteristics of the average man under conditions of heavy exercise that might be anticipated in the field. It differs from the constant flow rate machine only in that the average flow was regulated to 50 liters per minute and was made to approximate a sine wave. Gas-laden air is drawn into the canister being tested for 180 degrees of the sine wave; the air flow is stopped for a time interval corresponding to the other 180 degrees of the complete sine wave cycle;

and this process is repeated 33 cycles per minute. The resulting maximum or peak flow rate is 157 liters per minute.

Equation 1 was derived for conditions of constant flow rate. However, it is shown in Appendix C that it is theoretically equally applicable to "breather" testing if H_t is evaluated at an equivalent flow rate differing from the average flow rate. This equivalent flow rate depends upon the ratio of the test to the break concentration and upon the relationship between H_t and the linear air velocity. For the proof of this similarity and the details of the application of the resulting relationships, see Appendix C.

Equation 1 was derived for a canister of constant cross section. This type of canister is commonly termed an "axial flow canister" in the Chemical Warfare Service.

The other major design used by the United States Army is the "radial flow canister". In this type canister, the adsorbent bed is retained between two concentric cylinders made of perforated metal. The air stream enters the adsorbent bed at the surface of and perpendicular to the outer cylinder and leaves through the inner cylinder, commonly termed the inner tube.

The relationships between the variables for this type of canister are derived in Appendix D. They are as follows:

$$D_c = \left[D_1^{x+1} + 2(x+1) \left(\frac{1000\ Q}{\pi\ L} \right)^x \ln \frac{C_1}{C_2} \right]^{\frac{1}{x+1}} \qquad (4)$$

$$t = \frac{\pi}{4} \frac{L}{Q} \frac{N_o}{C_1} \left[D_2^2 - D_c^2 + 4 D_c k_1 \beta \left(\frac{1000Q}{\pi D_c L} \right)^x \right] \qquad (5)$$

III. PREVIOUS WORK

A. Adsorption Isotherm

The amount of a gas adsorbed by an adsorbent when equilibrium is established is a function both of the adsorbent and the adsorbate. Such factors as surface area, pore size, and pore shape of the adsorbent and the chemical composition of the adsorbate play important roles. The earliest attempt at correlation of adsorption data was made by de Saussere (6) in 1814. He found that the most easily condensed gases were adsorbed to the greatest extent by a given adsorbent. Since that time, innumerable investigations have been made to determine the factors which control the quantity of gas which will be adsorbed under any set of conditions.

The most common method of correlation of this type of data has been by the adsorption isotherm which is the relationship between the quantity of gas adsorbed and pressure at constant temperature. A large number of empirical and theoretical expressions have been derived relating these variables. The most common of these are the Freundlich equation (2) and the Langmuir equation (3). These equations, although not universally valid, fit a large proportion of the experimental data very well. The Freundlich isotherm is represented by the following expression:

$$C^* = k\, m^n \qquad (9)$$

In this equation, n is always greater than unity and approaches unity with increasing temperature for any particular adsorbate. The value of k decreases with increasing temperature.

In general, for a given adsorbent, the values of k and n increase as the boiling point of the adsorbate increases. This general relationship is exemplified by the data of Homfray (7) as analyzed by Freundlich (8) for the adsorption of nitrogen, carbon monoxide, argon, methane, ethane, and carbon dioxide on cocoanut charcoal.

Very little experimental data is available in the literature concerning the equilibrium relationships of the common war gases adsorbed on charcoals. No significance could be attached to the experimental values of k, for these are a very sensitive function of the extent of the surface of the adsorbent which can vary over extremely wide limits. However, data which would be indicative of the order of magnitude of n would be desirable.

Bunbury (9) showed that, for the adsorption of phosgene on activated charcoal at 18°C., n was equal to 4.33. Arii and Huzita (10), studying the adsorption of phosgene on sugar charcoal, obtained a value for n of 5.12.

An analysis of the data of Kubelka (11), who determined the equilibrium relationships of chloropicrin and activated charcoals, shows that, for the four charcoals investigated, n varied from 3 to 4 for pressures below one-tenth of the saturation value. At pressures above

CONFIDENTIAL

DECLASSIFIED

one-tenth of the saturation value, deviation was obtained from the Freundlich isotherm with the deviation toward a higher value of n.

B. Rate of Establishment of Equilibrium with Pure Fluids

It has long been realized that physical adsorption cannot be instantaneous, for activation energies are known to exist. In addition, some time is required for diffusion of the adsorbate into the pores of the adsorbent. However, the rates are extremely rapid, oftentimes so rapid that they cannot be measured.

Freundlich (12) found that charcoal adsorbed the equilibrium quantity of carbon dioxide in 20 seconds. Other investigators (13, 14, 15, 16, 17, 18, 19, 20, 21) have verified these extremely rapid rates, and, in practically all cases where chemical reaction does not occur, equilibrium is established within two minutes with over 90 per cent of the equilibrium quantity being adsorbed within 30 seconds. Hougen and Dodge (22) found that water is an exception to this generalization, the rate of adsorption being quite slow.

Marc (23) conducted measurements of the rates of adsorption of colloidal substances from aqueous dispersions by activated charcoals. In his investigations, the dispersions were agitated by a mechanical paddle, and it was found that, by extreme agitation, equilibrium could be established within six seconds as compared to hours

CONFIDENTIAL

DECLASSIFIED

when little or no agitation was used.

Chemosorption can also be rapid as was shown by Emmet and Brunauer (24), but generally it is much slower than physical adsorption because of the higher activation energies. An example of extremely slow chemical adsorption was found by Taylor and Williamson (25) in the adsorption of hydrogen on a manganese oxide catalyst.

C. Mass Transfer Coefficients-Gas Film-From Gas Absorption Studies

The determination of mass transfer coefficients in packed absorption towers (liquid-gas) has been an important topic of research in chemical engineering in the past twenty years. In general, there are two resistances which can control the rate of transfer. These are the resistances of the liquid and of the gas film. Experiments have been conducted wherein the liquid film resistance was virtually eliminated. These include studies of the rates of adiabatic vaporization of a pure liquid into an air stream and of the rates of transfer to or from a liquid in which they are very soluble.

Since the gas film resistance for these conditions is controlled by the same factors as for the adsorption of a gas by granular solids, the effect of such factors as particle diameter and velocity of gas flow should be correlative.

Sherwood and Holloway (26) made an excellent review

of the reliable gas film data up to 1940. They reviewed the work of the following investigators:

a. Kowalke, Hougen, and Watson (27) and Chilton, Duffy, and Vernon (28) who obtained extensive data on the ammonia-water system.

b. Borden and Squires (29) who obtained limited data on the ammonia-water system.

c. Johnstone and Singh (30) who studied the vaporization of water into air.

d. Doherty and Johnson (31) who obtained data on the ammonia-water system and the ammonia-acqueous sulfuric acid system.

e. Holloway (32) who obtained data on the vaporization of water into air.

As a result of this survey, Sherwood and Holloway presented a correlation of the data in which the mass transfer coefficient (gas film) varied as the 0.7 power of the mass rate of flow. At a constant temperature and pressure this is equivalent to a similar variation with linear air velocity.

The data of Kowalke, Hougen, and Watson also showed that the effect of temperature on the transfer coefficients was very slight.

All the work referred to above was done in large absorption towers, using various commercial packings such as Raschig rings, spiral tile, etc. with nominal sizes of one

inch or greater. These packings bear no resemblance to charcoal granules and are especially designed for high transfer area per unit volume consistent with low resistance to air flow. For this reason and because of the great differences in size (normal Chemical Warfare Whetlerites vary from 0.4 to 2 millimeters in diameter), no useful data can be obtained from the above experiments as to the effect of particle diameter on the mass transfer coefficient.

Although little data are available on the effect of packing diameter on the mass transfer coefficient, data are available which show the effect of column diameter (wetted wall) on the gas film coefficient. The following is an extract and recombination of the relationships given in Chapter II of Sherwood's "Absorption and Extraction" (1).

It has been established that the following correlation exists for wetted wall columns:

$$d/l = k_1 \left(\frac{d\ V \rho}{\mu}\right)^{.83} \left(\frac{\mu}{\rho D_v}\right)^{.44} \qquad (15)$$

The amount of material transferred across an interface per unit time may be expressed by the following equation:

$$N_a = \frac{D_v P}{RTl} \left(\frac{P_g - P^*}{P_{bm}}\right) \qquad (16)$$

The gas film mass transfer coefficient, k_g, is the

rate of transfer per unit time per unit area per unit concentration (or pressure) gradient. This is represented by the following equation:

$$k_g = \frac{N_a}{P_g - P^*} = \frac{D_v P}{R T l} \qquad (17)$$

Substituting the value of l obtained from Equation 16 into Equation 17, the following equation is obtained:

$$k_g = \frac{D_v P k_2}{R T d}\left(\frac{d V \rho}{\mu}\right)^{.83}\left(\frac{\mu}{\rho D_v}\right)^{.44} \qquad (18)$$

This equation predicts the effect of all the pertinent variables on the mass transfer coefficient in wetted wall towers. As a working assumption, it is proposed that the equation might be equally valid for packed towers if particle diameter is substituted for column diameter and the constant changed. This substitution results in the following equation:

$$k_g = \frac{D_v P k_3}{R T D_p}\left(\frac{D_p V \rho}{\mu}\right)^{.83}\left(\frac{\mu}{\rho D_v}\right)^{.44} \qquad (19)$$

Since k_g can not be measured, it is convenient to transform the equation to a volume basis by incorporating the transfer area factor, a. This factor, which represents the mass transfer area per unit volume of adsorbent, varies inversely as the particle diameter if all the area is equally active for mass transfer. Substituting this relationship into Equation 19, the following equation is obtained:

$$k_g a = \frac{D_v P k_3}{R T D_p} \left(\frac{D_p V \rho}{\mu}\right)^{.83} \left(\frac{\mu}{\rho D_v}\right)^{.44} \frac{1}{D_p} \qquad (20)$$

Regrouping this equation to show the effect of each of the variables, the following equation is obtained:

$$k_g a = \frac{P k_3}{R T} \frac{(D_v)^{.56}(V)^{.83}(\rho)^{.39}}{(D_p)^{1.17}(\mu)^{.56}} \qquad (21)$$

In normal chemical warfare adsorbent testing, P, R, T, ρ, and μ are held constant so that the equation can be simplified to the following:

$$k_g a = \frac{k_4 (D_v)^{.56}(V)^{.83}}{(D_p)^{1.17}} \qquad (22)$$

That this equation is not completely applicable is shown by the difference between the exponent of the velocity term (equivalent to the mass flow rate) and the value of 0.7 obtained by Sherwood and Holloway. However, the agreement is sufficiently accurate to warrant further testing of the equation. Experiments of this nature have been conducted by Gamson, Thodos, and Hougen (33) and by Hurt (34).

D. Mass Transfer Coefficients-Small Diameter Packing

A limited amount of work has been done quite recently to determine the mass transfer coefficients in beds of small, granular solids. Gamson, Thodos, and Hougen made measurements of the mass transfer coefficients for the vaporization of water from wetted granules into a flowing

air stream. The data were correlated by the method of transfer units which were related to the Reynolds and the Prandtl numbers. The results of their investigations are shown in Fig. 1. These data show that H_t varies directly as the 0.67 power of the Prandtl number and inversely as the surface area, a. For modified Reynolds numbers in excess of 300, H_t varies as the 0.42 power of the Reynolds number. For values of the Reynolds number below 60, H_t varies as the 1.0 power of the Reynolds number.

Hurt made similar measurements and, in addition, determined the transfer coefficients from data on the rate of vaporization of naphthalene into a flowing air stream. The results of his investigations are shown in Fig. 2. These data also show that H_t varies directly as the 0.67 power of the Schmidt number, but the variation with "a", the surface area, is inconclusive. Over the range of Reynolds numbers investigated, H_t varies as the 0.25-0.45 power of the Reynolds number. This is in variance with the data of Gamson, Thodos, and Hougen.

E. Integrated Equations for Unsteady State Mass Transfer in Packed Adsorbent Beds

1. Introduction

Several investigators have considered the mathematics involved in the calculation of the performance of an adsorbent or catalyst bed. The ultimate aim of these investigations was to obtain analytical relation-

DECLASSIFIED

FIGURE 1

a (HTU) NUMBERS FOR MASS TRANSFER IN GASES FLOWING THROUGH GRANULAR SOLIDS

VALUES OF a IN FT^{-1} WHEN HTU IS IN FT.

D_p		MESH SIZE OPENING	VALUES OF a, SQ FT PER CU FT PER CENT VOID SPACE			
INCHES	FEET	(TYLER)	26%	30%	40%	50%
.50	.0417	—	107	101	86.4	72
.40	.0333	2	133	126	108	90
.30	.0250	2.5	178	168	144	120
.20	.0167	3.5	266	252	216	180
.10	.00833	7-8	533	504	432	360
.05	.00417	12-14	1066	1008	864	720
.01	.000833	60	5330	5040	4320	3600

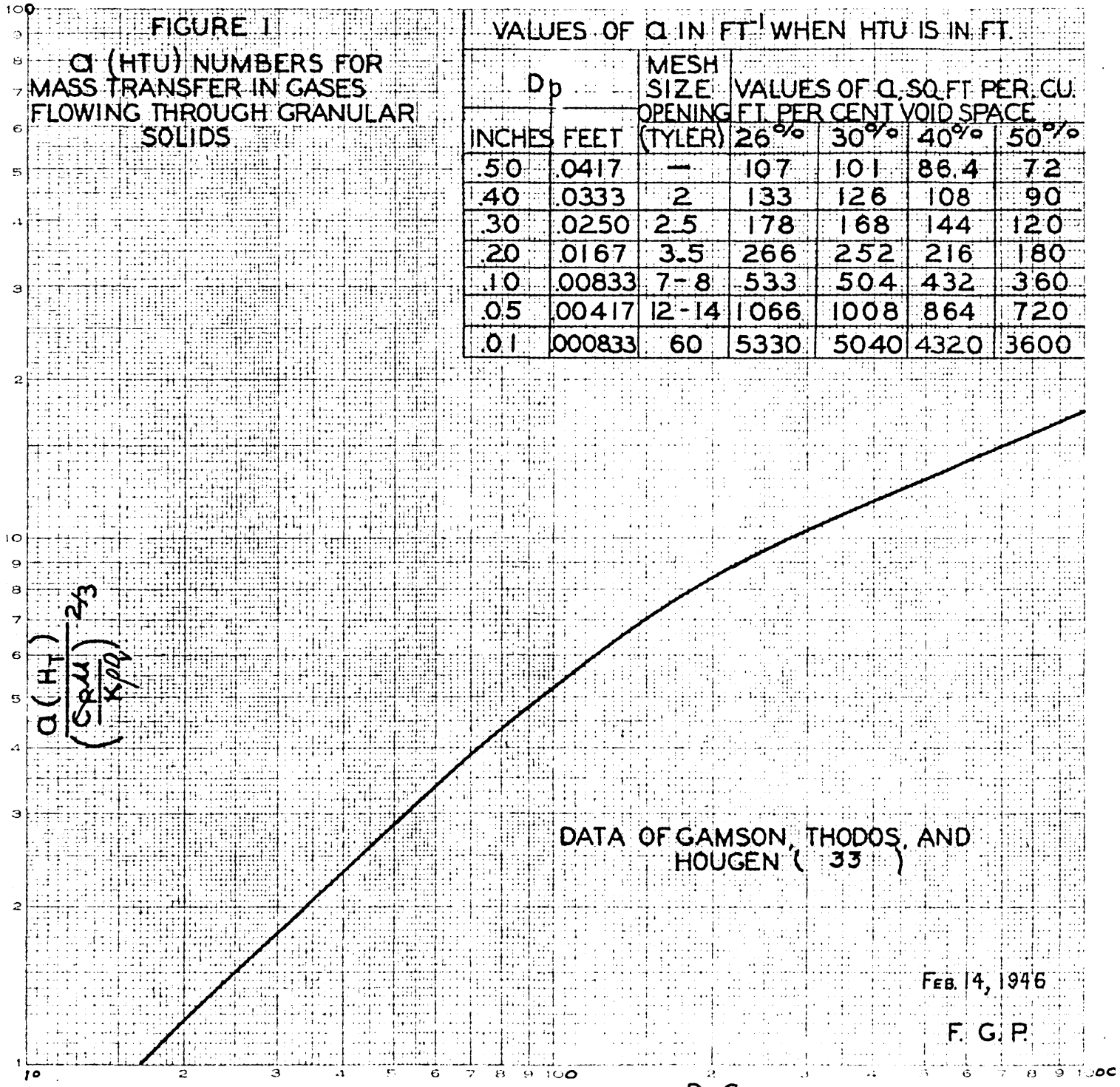

DECLASSIFIED

[redacted] DECLASSIFIED

FIGURE 2

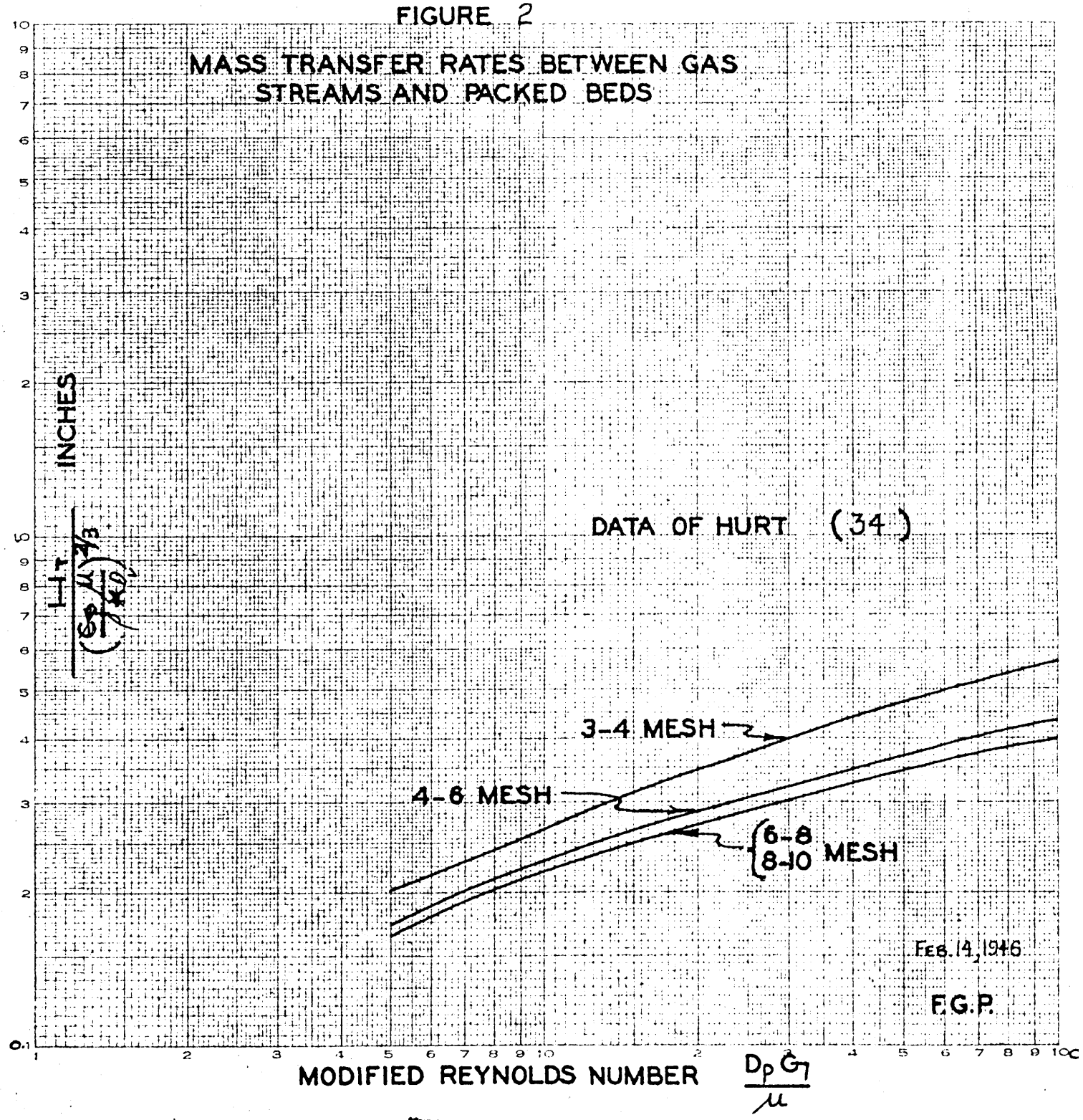

EUGENE DIETZGEN CO.
NO. 340-L22 DIETZGEN GRAPH PAPER
LOGARITHMIC 2 CYCLES X 2 CYCLES

[redacted] DECLASSIFIED

ships between concentration, time, and bed depth. The analyses of this problem differ in the assumptions made as to the rate-controlling factors and the form of the rate function. The following is a summary of the contributions of the known investigators--their assumptions and the resulting relationships.

2. Particular Equations

a. Bohart and Adams (35)

The earliest investigators in the field were Bohart and Adams who became interested in the problem during their investigations of the behavior of charcoal in the removal of chlorine from humid air streams. They assumed that the rate of chemical reaction between adsorbed chlorine and water controlled the rate of removal from the air stream and expressed the rate function by the following equation:

$$\partial m/\partial t = k (N_o - m) C \qquad (23)$$

This equation states that the rate of chemical reaction is directly proportional to the unused capacity, $N_o - m$, and to the concentration in the air stream. The solution of this equation, in combination with a material balance, results in the following expression:

$$C_2/C_1 = e^{-kC_1 t} \left(e^{\frac{k N_o \lambda (1000)}{V}} - 1 \right) \qquad (24)$$

Except for very small bed depths, it was shown that the exponential term inside the parentheses

is very large as compared to unity and that the unity term could be neglected. This results in the following simplified relationships:

$$t = \frac{1000\, N_o \lambda}{C_1 V} - \frac{1}{k\, C_1} \ln\left(\frac{C_1}{C_2} - 1\right) \qquad (25)$$

$$t = \frac{N_o\, A}{C_1\, Q}\left[\lambda - \frac{Q}{A\, K\, N_o} \ln\left(\frac{C_1}{C_2} - 1\right)\right] \qquad (26)$$

This equation was derived later by Hinshelwood (36) who assumed that the rate of adsorption after transfer to the surface controlled the overall rate. Therefore, in Hinshelwood's analysis, k is an adsorption rate constant and not a chemical reaction rate constant. The integrated relationships (Equations 25 and 26) are commonly known as the Hinshelwood Equations.

b. Mecklenberg (37, 38)

Mecklenberg assumed that the rate of diffusion from the carrier air stream to the surface of the adsorbent controlled the rate of removal from the air stream and expressed the rate by the following equation:

$$\partial C/\partial \lambda = -\frac{D_v\, a}{1}\,(C - C^*) \qquad (27)$$

This equation was combined with a material balance, and, in order to allow integration, C^* was assumed to be constant regardless of the adsorbate content of the adsorbent. The integration resulted in the following

equation:

$$t = \frac{1000\ N_o}{C_1 V}\left[\lambda - \frac{V\ 1}{1000\ D_v a \alpha}\left(\ln\frac{C_1 - C^*}{C_2 - C^*} - \frac{C_1}{C_1 - C^*}\right)\right] \quad (28)$$

Mecklenberg defined a new term which he called the "dead layer" by the following equation:

$$h = \frac{V\ 1}{1000\ D_v a \alpha}\ln\frac{C_1 - C^*}{C_2 - C^*} - \frac{C_1}{C_1 - C^*} \quad (29)$$

Substitution of this expression into Equation 28 results in the following equation:

$$t = \frac{1000\ N_o}{C_1 V}(\lambda - h) = \frac{N_o\ A}{C_1\ Q}(\lambda - h) \quad (30)$$

Mecklenberg's data showed that, for the removal of chloropicrin, the slope of the bed depth-break time plot was as predicted by Equation 30. He also showed that the following relationships were valid: (1) the dead layer varied as the square root of the velocity, (2) the dead layer varied directly as the particle diameter, and (3) at a constant effluent concentration, the dead layer varied as the logarithm of the influent concentration.

c. Beaton and Furnas (39)

Beaton and Furnas also assumed that the rate of diffusion from the fluid stream to the surface of the granules controlled the rate of transfer. They expressed this assumption by the following equation:

$$\partial m/\partial t = k_g a\ (C - C^*) \quad (8)$$

They further assumed that C^* was directly proportional to the adsorbate content of the adsorbent (in their particular case, the cation content of a base-exchange zeolite). This assumption is equivalent to the assumption that the adsorption isotherm follows Freundlich's adsorption equation with n equal to unity. The integrated relationships obtained by combination of these assumptions with a material balance is discussed in detail in Appendix A.

d. Engel and Coull (40)

Engel and Coull made measurements of the effluent concentration as a function of time for the removal of ether vapor from an air stream flowing through an activated charcoal bed. They did not attempt to derive a theoretical equation, but they obtained the following empirical relationships:

$$\frac{C_1 - C}{C_1} = 0.50 \left[1 + \frac{2}{\sqrt{\pi}} \int_0^{\frac{t-a}{b}} e^{-x^2} dx \right] \qquad (31)$$

$$a = 1260 \, (C_1 V)^{-1.12} + 3 \qquad (32)$$

$$b = 380 \, (C_1 V)^{-1.13} + 2 \qquad (33)$$

3. Discussion of Particular Equations

a. Bohart and Adams (Hinshelwood) Equation

The differential equation (Equation 23) which was proposed by Bohart and Adams is the result of several assumptions. The first of these is that the rate of chemical reaction is controlling and that it is pro-

portional to the agent concentration in the air stream. Since chemical reaction must occur on the adsorbent, it is not immediately obvious why the rate should depend on the concentration in the air stream. However, if the chemical reaction rate does control, it can be shown that the equilibrium concentration from the adsorbent rapidly approaches the concentration in the air stream. Since the equilibrium concentration from the adsorbent is a measure of the mobility of the molecules on the surface of the adsorbent, it is logical that, for a first order reaction, the reaction rate should be proportional to it.

The second assumption is that the rate of chemical reaction is proportional to the unused capacity of the adsorbent. This is equivalent to assuming that all surfaces on the adsorbent are equally active.

The equation neglects the time required for the adsorbent to become saturated with physically adsorbed gas and the chemical reaction which occurs during the "physical saturation" period.

The validity of the foregoing assumptions, and the effect of neglecting the time required for physical saturation must be demonstrated before the integrated relationship (Equation 24) can be used to correlate adsorption data or to predict performance.

b. Mecklenberg Equation

The differential equation proposed by Mecklenberg (Equation 27) is in agreement with the present knowledge of mass transfer through a stagnant air film.

The assumption that C^*, the equilibrium concentration, is constant for all values of the adsorbate content is believed to be very weak, for if such were the case the effluent concentration would be constant. It is interesting to note that, if C^* is assumed to be negligible, Mecklenberg's integrated relationship (Equation 28) reduces to the following:

$$t = \frac{1000\ N_o}{C_1 V}\left[\lambda - \frac{V\ l}{1000\ D_v a \alpha}\left(\ln \frac{C_1}{C_2} - 1\right)\right] \qquad (34)$$

This equation is identical to that derived in Appendix A for the particular case wherein the rate of diffusion through the stagnant air film controls and n in Freundlich's isotherm is equal to infinity.

c. Equation of Beaton and Furnas

The differential equation proposed by Beaton and Furnas (Equation 8) is identical to that of Mecklenberg except that certain terms have been consolidated into a single function. In the use of this equation it must be borne in mind that the integrated relationships were obtained on the assumption that the adsorption isotherm is linear and that it is not applicable for any other type of isotherm. This limitation has not always been realized in the application of the integrated relationships to experimental results.

d. Equation of Engel and Coull

The empirical equation of Engel and Coull

must be used with caution, for dimensionally, it is unsound. The term, t-a/b, is a mixed function, dimensionally.

F. Experimental Data for Mass Transfer from Flowing Air Streams to Adsorbent Beds

1. Reversible Physical Adsorption

a. Experimental Data

Several Chemical Warfare Service reports have been concerned with the so-called "adsorption wave". These investigations were devoted to measurements of effluent concentrations as a function of time. The majority of these reports, however, do not include data for effluent concentrations below ten per cent of the influent concentration and are, therefore, dealing with the region wherein the back pressure is significant and the plot of the logarithm of the effluent concentration vs. time is not a straight line and can not be analyzed. Furthermore, very few of these reports specify all the pertinent variables.

A very excellent investigation of this type was conducted by Dole and Klotz (41) who measured effluent concentrations near the normal break values (approximately one per cent of the influent concentration) to the influent concentration with high accuracy. Instantaneous concentrations were obtained by the use of an ultraviolet photometer, a great improvement in technique over the standard chemical indicators which have an appreciable time lag.

Measurements were made for the adsorption

of phosgene and chloropicrin from moisture-free air by dry charcoal. This precaution eliminated the hydrolysis of phosgene thereby limiting the mechanism of removal to physical adsorption. Selected data from the above report are shown in Figures 3, 4, 5, 6, and 7.

b. Correlation of Data by Equation 1

(1) Correlation of N_o with Slope of Bed Depth-Break Time Relationship

Equation 1 states that the slope of the bed depth-break time plot should be represented by the following equation:

$$S = \frac{1000\ N_o}{C_1 V} \tag{35}$$

$$N_o = \frac{C_1\ V\ S}{1000} \tag{36}$$

Bed depth-break time plots were made from the data of Figs. 3, 4, and 5 for a break concentration of 20 parts per million (20 p.p.m.) Break times were adjusted to a nominal influent concentration (7 mg./L. for the phosgene tests and 51 mg./L. for the chloropicrin tests) by a linear scaling. This method of adjustment has been found to be valid if the actual influent concentration does not differ by more than ten per cent from the nominal concentration; it is a standard Chemical Warfare Service canister testing procedure. The resulting plots are shown in Figs. 8 and 9. Table I shows the values of the variables and the values of N_o calculated by Equation 36.

FIGURE 3

PHOSGENE ADSORPTION

EFFECT OF BED DEPTH ON EFFLUENT CONCENTRATION-TIME RELATIONSHIPS

NOMINAL INFLUENT CONCENTRATION - 7.0 MG./L ≃ 1780 P.P.M.
DRY AIR, DRY CHARCOAL, 8 - 10 MESH (U.S. STD.)
VELOCITY - 325 CM/MIN.
DATA OF DOLE AND KLOTZ (41)

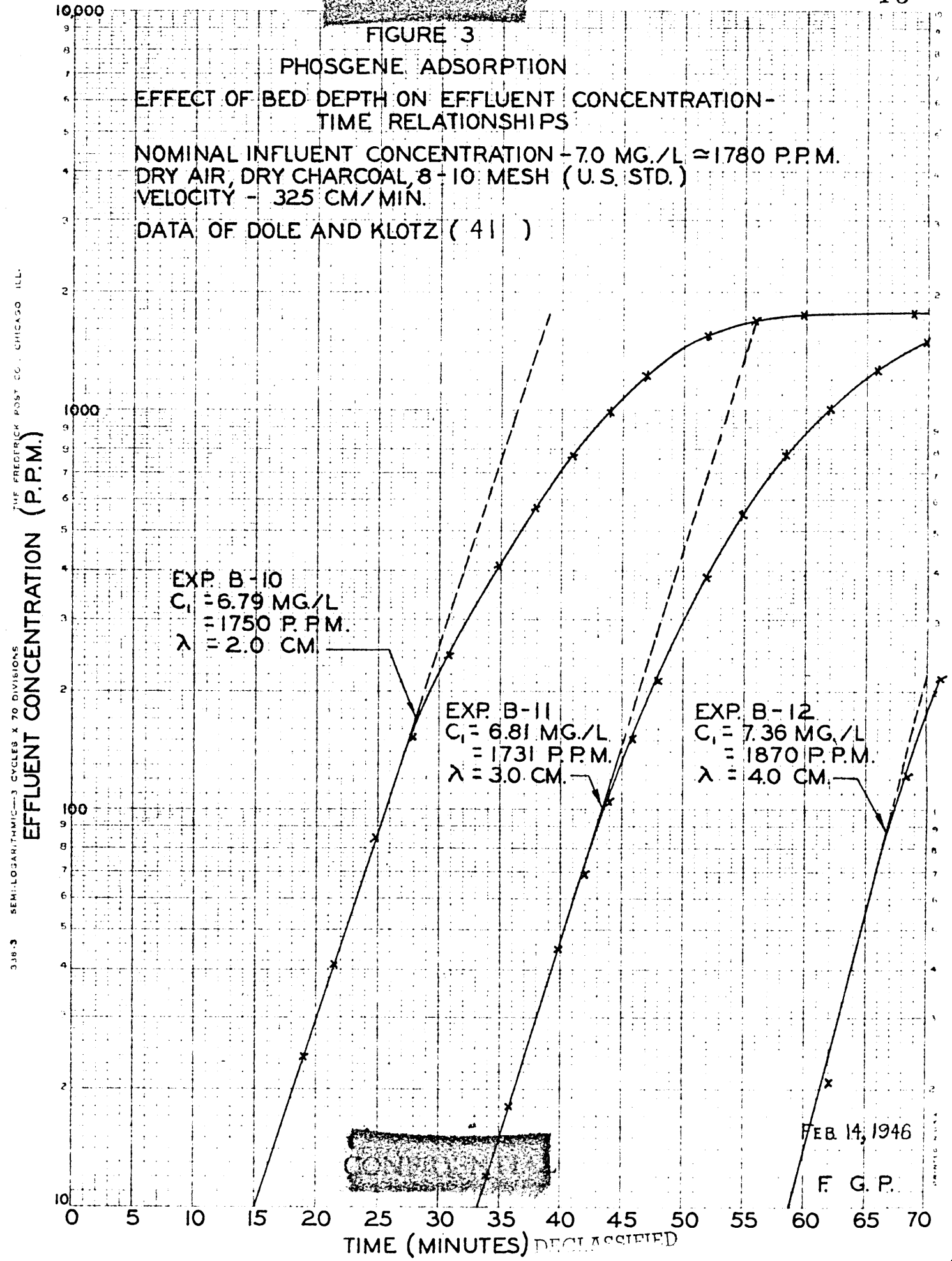

DECLASSIFIED

DECLASSIFIED

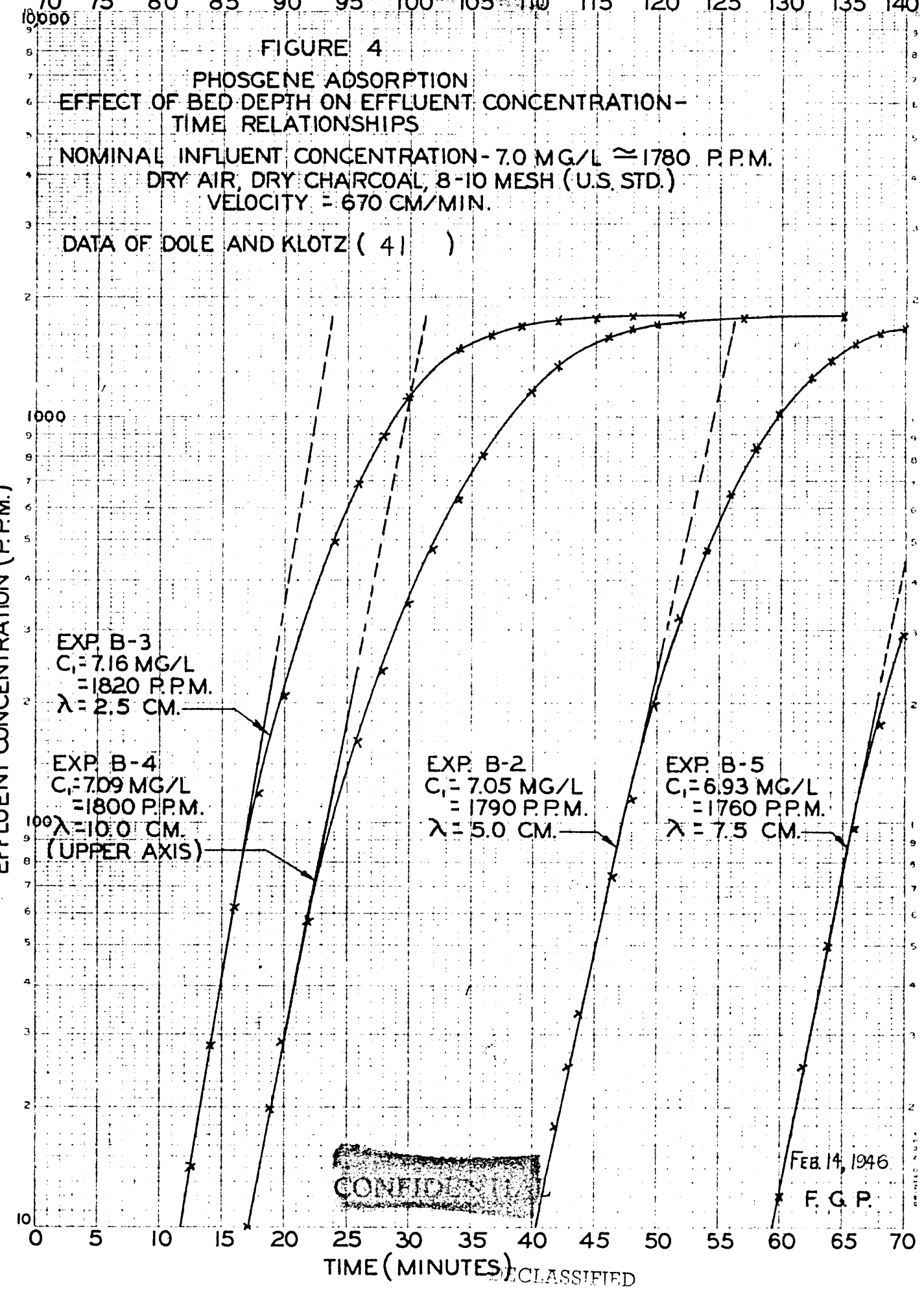

DECLASSIFIED

DECLASSIFIED

FIGURE 5

CHLOROPICRIN ADSORPTION
EFFECT OF BED DEPTH ON EFFLUENT CONCENTRATION
TIME RELATIONSHIPS

NOMINAL INFLUENT CONC.-50mg/L = 7650ppm.
DRY AIR DRY CHARCOAL, MESH ?
UNKNOWN

DATA OF DOLE AND KLOTZ (1)

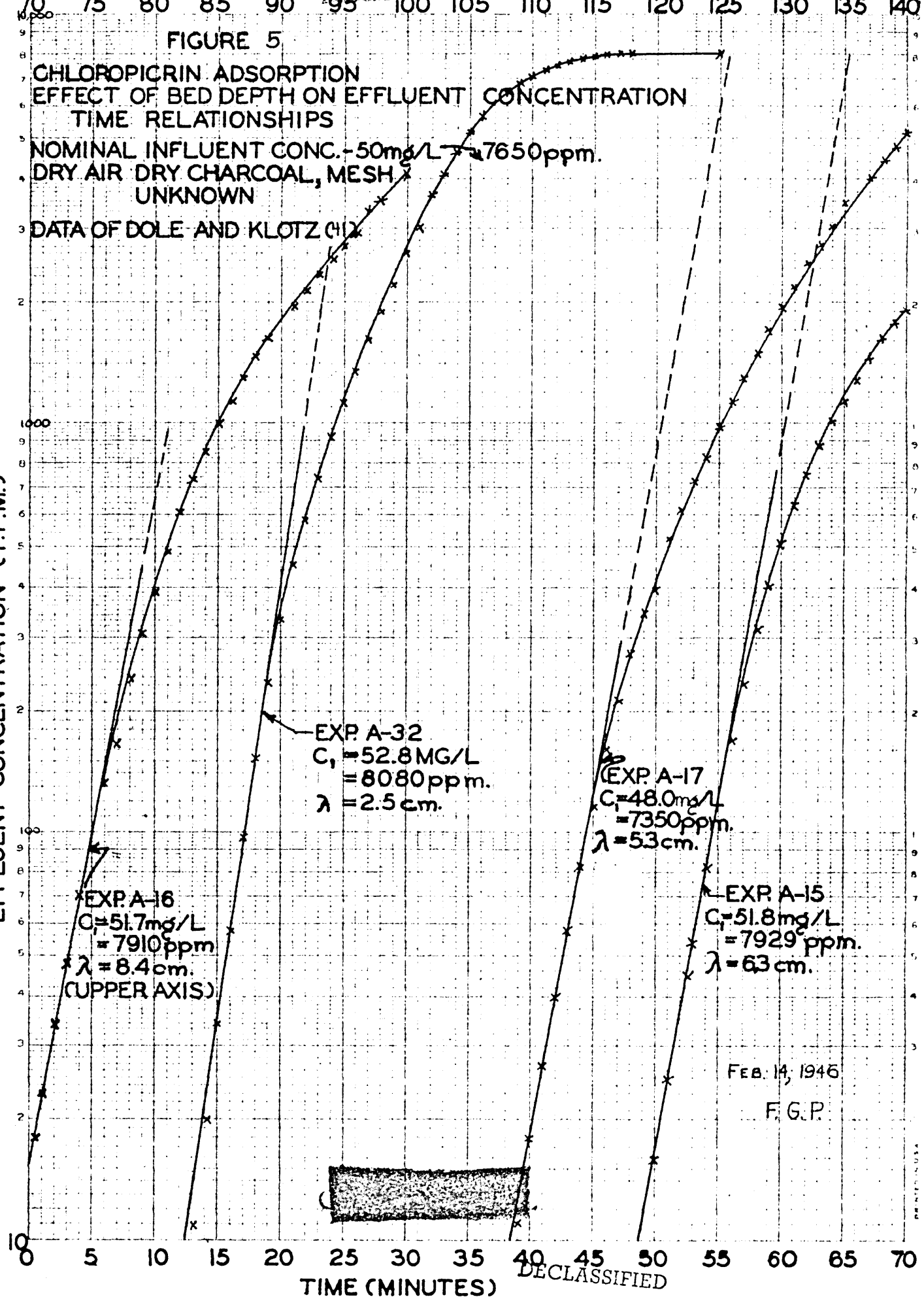

DECLASSIFIED

DECLASSIFIED

FIGURE 6

PHOSGENE ADSORPTION
EFFECT OF VELOCITY ON EFFLUENT CONCENTRATION
—TIME RELATIONSHIPS (LINEAR REGION ONLY)

NORMAL INFLUENT COCENTRATION - 7 mg/L ≙ 1780 ppm
DRY AIR, DRY CHARCOAL

DATA OF DOLE AND KLOTZ (41)

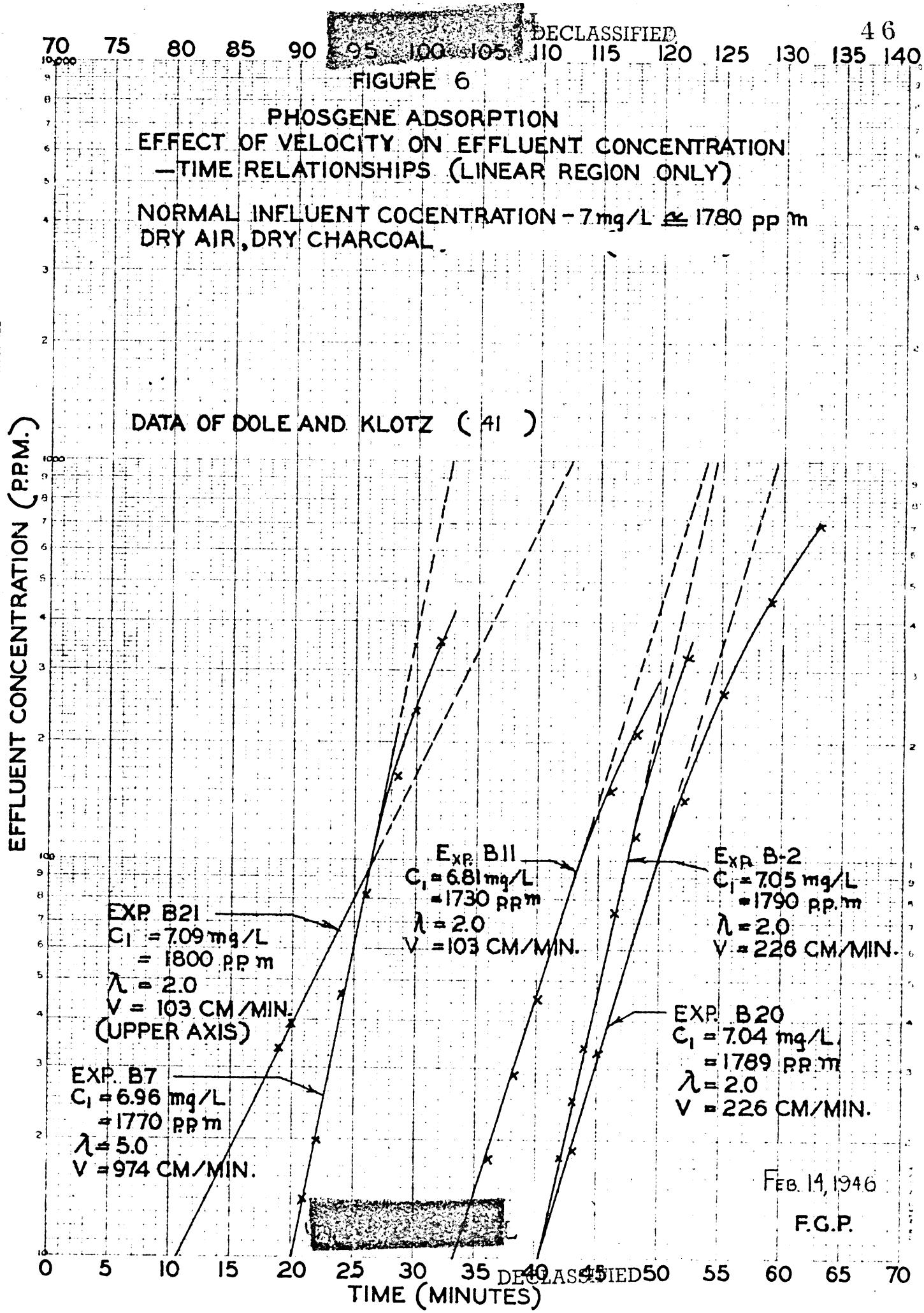

DECLASSIFIED

DECLASSIFIED

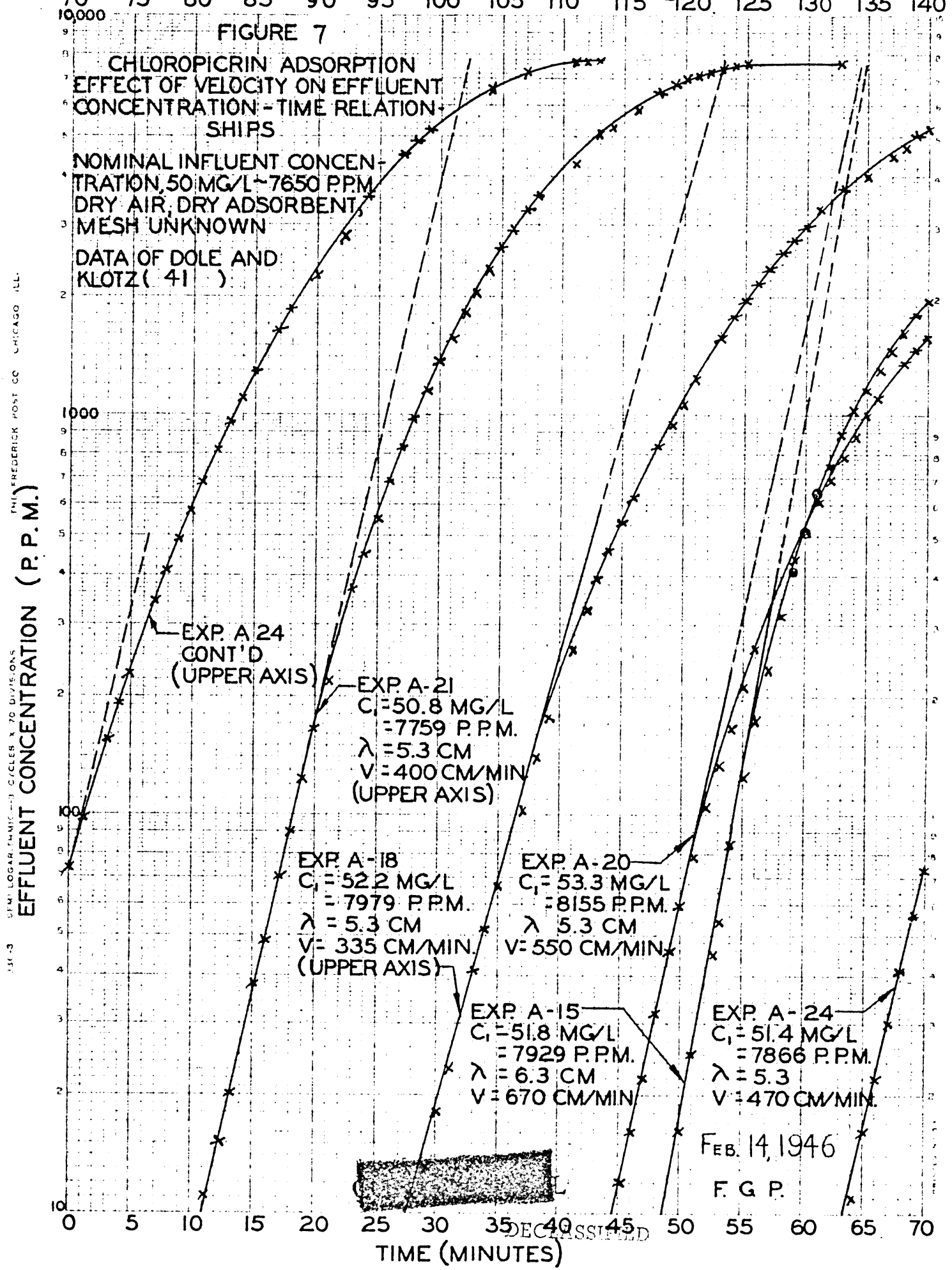

DECLASSIFIED

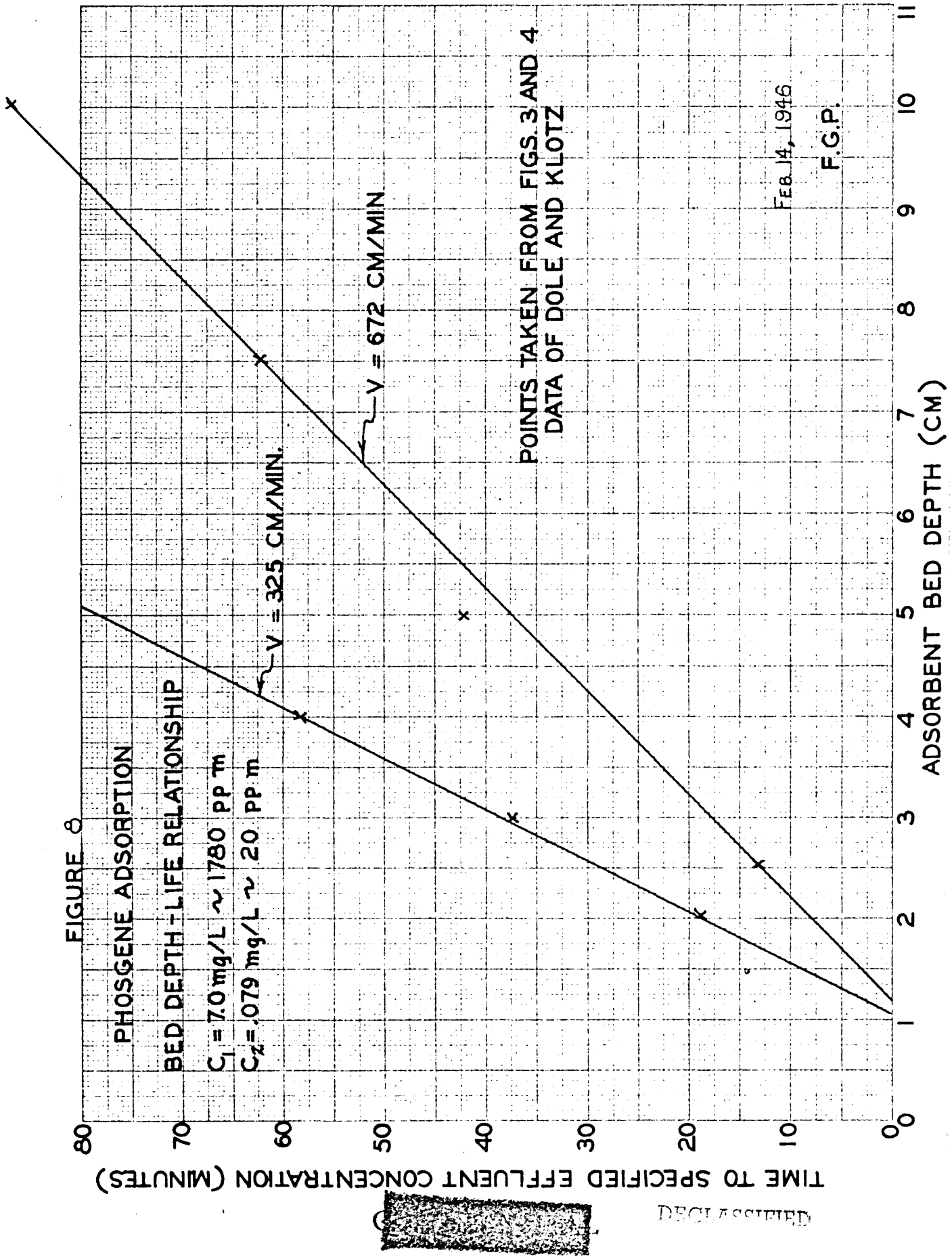
FIGURE 8
PHOSGENE ADSORPTION
BED DEPTH - LIFE RELATIONSHIP
C_1 = 7.0 mg/L ~ 1780 PP m
C_2 = .079 mg/L ~ 20 PP m
V = 325 CM/MIN.
V = 672 CM/MIN
POINTS TAKEN FROM FIGS. 3 AND 4
DATA OF DOLE AND KLOTZ
FEB. 14, 1946
F.G.P.
TIME TO SPECIFIED EFFLUENT CONCENTRATION (MINUTES)
ADSORBENT BED DEPTH (CM)
0
10
20
30
40
50
60
70
80
1
2
3
4
5
6
7
8
9
10
11

DECLASSIFIED

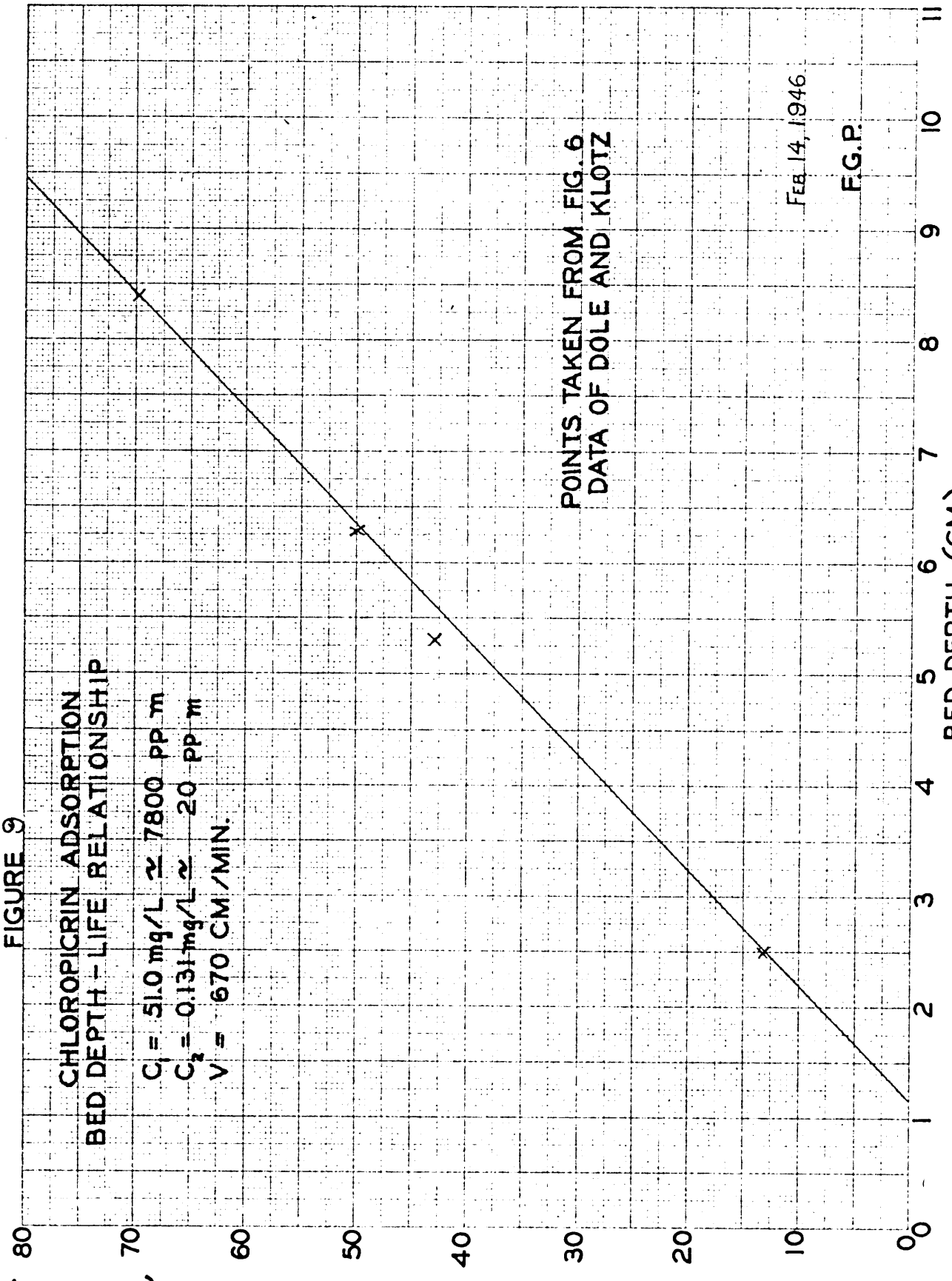

DECLASSIFIED

Table I

Determination of N_o for Phosgene and Chloropicrin from Bed Depth-Break Time Plots

Agent	V (cm./min.)	C_1 (mg./L)	S (min./cm.)	N_o (mg./ml.)
Phosgene	325	7.0	19.7	45
Phosgene	672	7.0	9.60	45
Chloropicrin	670	51.0	9.65	330

The data of Table I show that, for phosgene, N_o is a true constant at a fixed influent concentration as predicted by Equation 1. Insufficient data were available to test its constancy for chloropicrin.

(2) Determination of Mass Transfer Coefficients

Rearrangement of Equation 1 results in the following equation:

$$\ln C_2 = \frac{C_1 \ V \ t}{1000 \ N_o H_t} - \frac{\lambda}{H_t} + \ln C_1 - \beta \qquad (37)$$

This equation states that the slope of the straight line portion of the plot of the logarithm of the effluent concentration as a function of time may be represented by the following equation:

$$S' = \frac{C_1 \ V}{1000 \ N_o H_t} \qquad (38)$$

$$H_t = \frac{C_1 V}{1000 \ N_o S'} \qquad (39)$$

Figs. 6 and 7 show the plots (data of Dole and Klotz) of effluent concentration as a function of time for phosgene and chloropicrin at several air velocities. Only the linear, lower portion of several of the plots is shown. Tables II and III list the values of the variables and the values of H_t calculated by Equation 39.

Table II

Determination of H_t for Phosgene from Effluent Concentration-Time Relationships

V (cm./min.)	C_1 (mg./L.)	N_o (mg./ml.)	S' $(min)^{-1}$	H_t (cm.)
103	7.09	45	.145	.112
226	7.04	45	.243	.146
325	6.81	45	.227	.217
672	7.15	45	.325	.324
974	6.96	45	.382	.405

Table III

Determination of H_t for Chloropicrin from Effluent Concentration-Time Relationships

V (cm./min.)	C_1 (mg./L.)	N_o (mg./ml.)	S' $(min)^{-1}$	H_t (cm.)
335	52.2	330	.262	.197
400	50.8	330	.312	.197
470	51.4	330	.308	.237
550	53.3	330	.328	.272
670	51.8	330	.408	.258

The calculated values of H_t are plotted

in Figs. 10 and 11 as a function of velocity. Fig. 10 shows that, for phosgene, H_t varies approximately as the 0.5 power of the superficial linear velocity. The data which were employed for Fig. 11 do not cover a sufficiently large velocity range to warrant relating by a straight line. A dotted line with a slope of 0.5 was drawn through the points to approximate the relationship.

(3) Determination of β

Equation 1 predicts that the intercept of the straight line portion of the break time-bed depth plot (apparent critical bed depth) may be expressed by the following equation:

$$\lambda_c = H_t\left(\ln \frac{C_1}{C_2} - \beta\right) \qquad (40)$$

$$\beta = \ln \frac{C_1}{C_2} - \frac{\lambda_c}{H_t} \qquad (41)$$

The values of λ_c obtained from Figs. 8 and 9 are the result of a long extrapolation and are not sufficiently accurate for the determination of β, for the value of β is extremely sensitive to the value of λ_c.

2. Effect of Moisture Vapor in Air Stream on Phosgene Removal

Dole and Klotz conducted several tests to determine the effect of moisture in the air stream on the phosgene effluent concentration-time relationships. Selected data from these measurements are shown in Fig. 12.

DECLASSIFIED

[redacted]

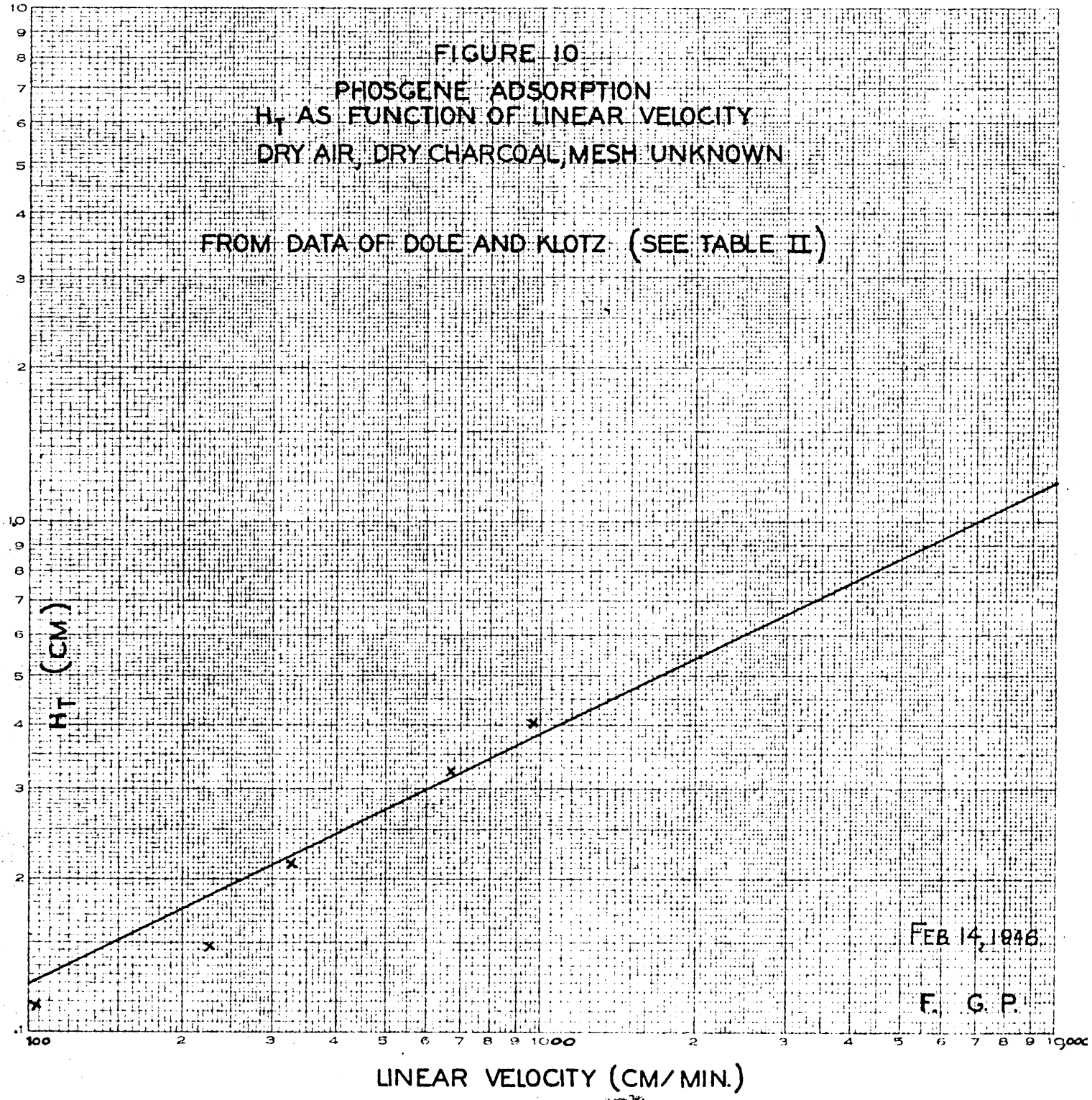

[redacted]

DECLASSIFIED

[redacted]

DECLASSIFIED

FIGURE II

CHLOROPICRIN ADSORPTION
H_T AS A FUNCTION OF VELOCITY
DRY AIR, DRY CHARCOAL, MESH UNKNOWN

FROM DATA OF DOLE AND KLOTZ
SEE TABLE III

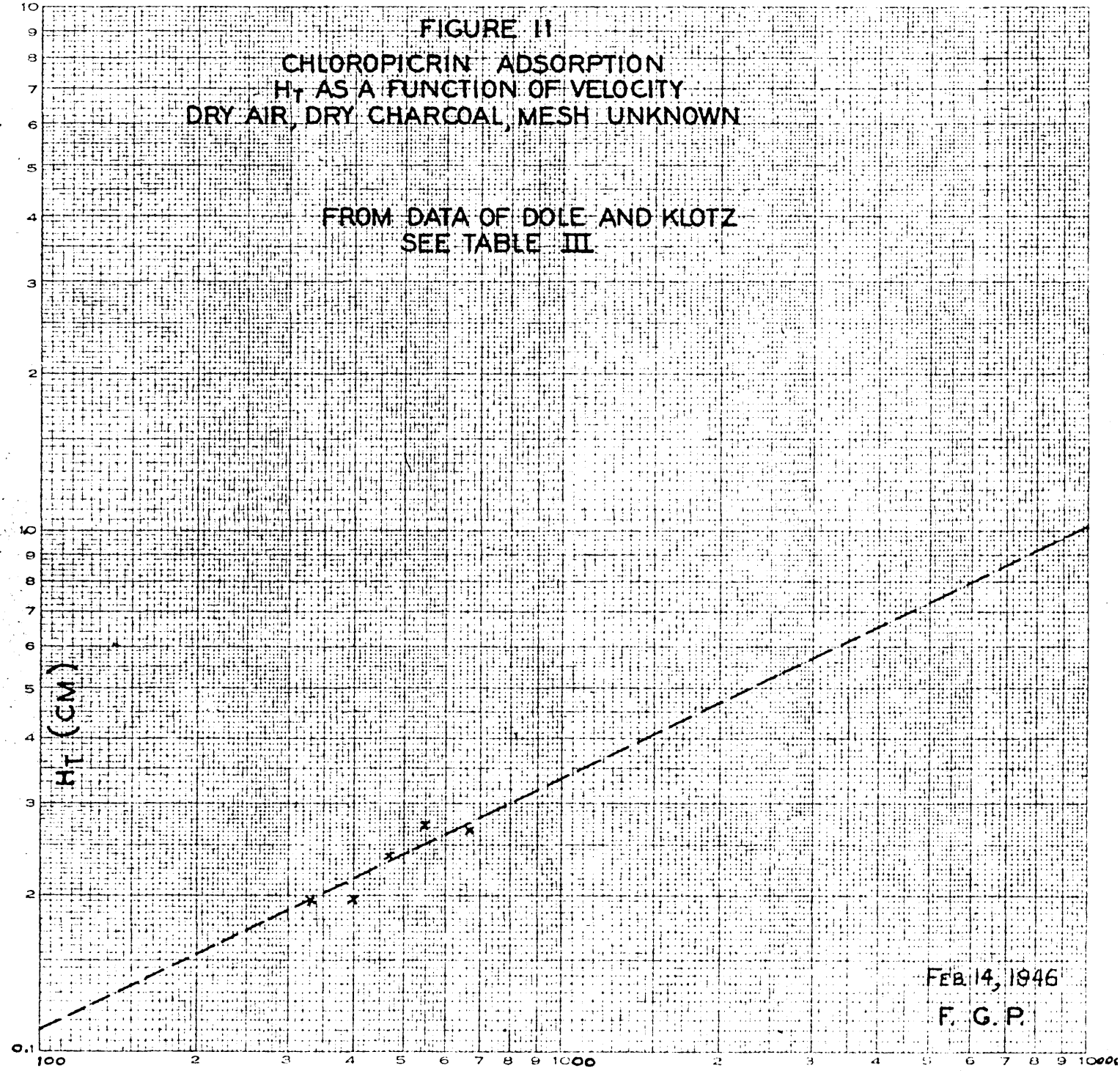

[redacted]

DECLASSIFIED

DECLASSIFIED

FIGURE 12

PHOSGENE ADSORPTION

EFFECT OF MOISTURE IN AIR STREAM ON EFFLUENT CONCENTRATION

FROM DATA AT DOLE AND KLOTZ (41)

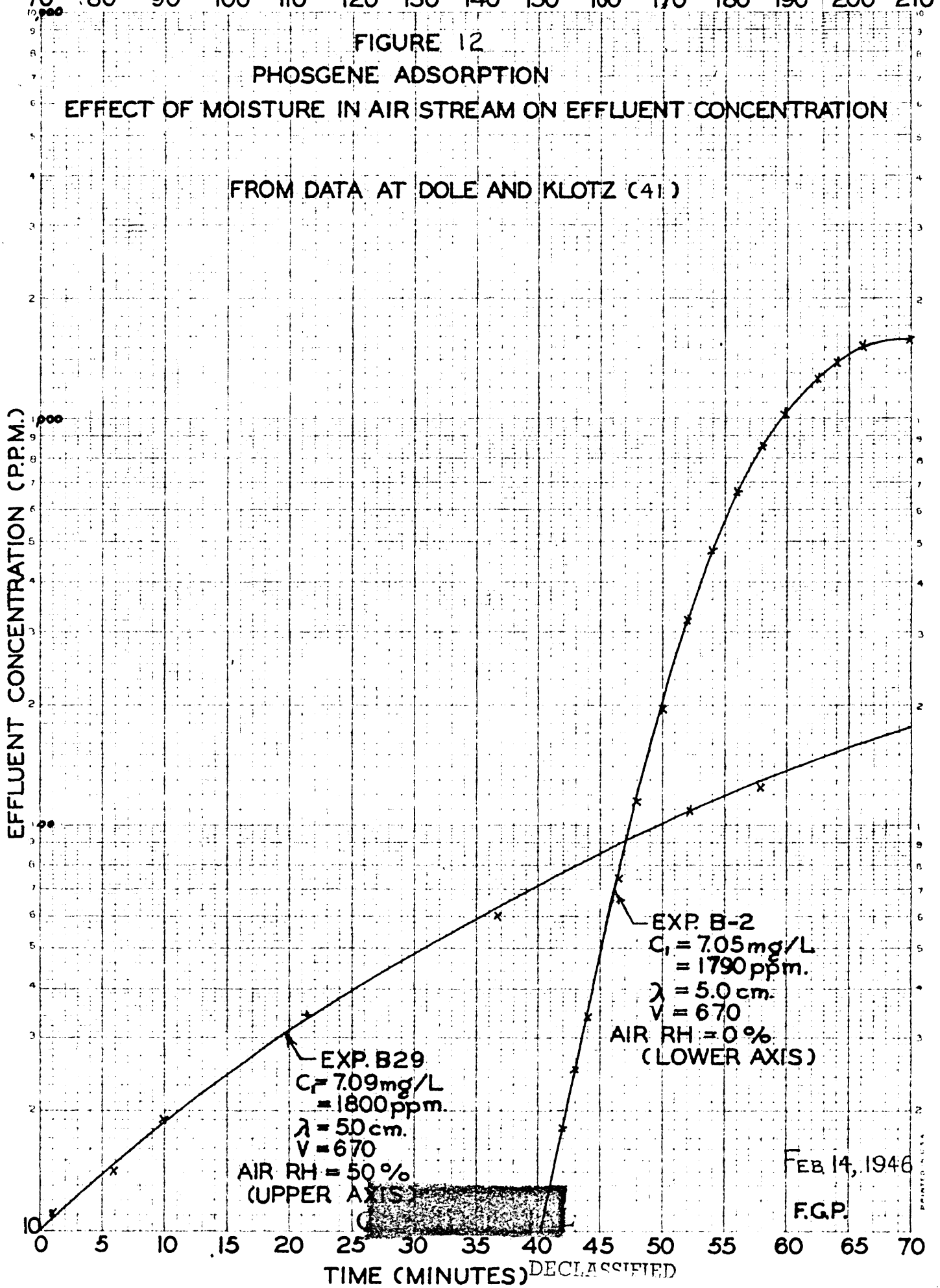

DECLASSIFIED

The data show the difference between the effluent concentration-time relationships for two tests made under identical conditions except that in one instance the relative humidity of the air stream was zero and in the other instance it was 50 per cent. The data show that the time to a specified effluent concentration is increased by the presence of moisture in the air stream and that the rate at which the effluent concentration approaches the influent concentration is greatly retarded.

These facts indicate that moisture in the air stream is transferred to the surface of the adsorbent, resulting in a slow chemical reaction between the adsorbed phosgene and water which increases the life and retards the attainment of equilibrium.

IV. Purpose of This Research

The purpose of this research was to obtain data which would serve as a basis for the design of the adsorbent sections of gas mask canisters. In the past canisters were designed by the trial and error method. This necessitated a myriad of tests for each particular proposed construction. Interpolation and extrapolation from any chosen, proved design to a slightly or radically different design was impossible.

In the design of collective protector canisters, such a procedure is impractical, for large volumes of air must be purified and trial and error methods would result in exorbitant wastage of whetlerite which is a relatively expensive material. In addition, the handling of such large volumes (up to 300 cubic feet per minute) of contaminated air at the high test concentrations is dangerous, for even small leaks can result in lethal concentrations.

The author was engaged in the design of collective protector canisters for the Chemical Warfare Service at the time this research was initiated. The above arguments were the basis for the instigation of a program to determine the factors which control the performance of an adsorbent bed so that the design could be calculated and the calculations checked with a minimum of experiment.

Another advantage of the development of mathematical relationships is the ease with which optimum designs can

be established. The method of trial and error design, although it can accurately establish the performance of a particular design, can not easily be used to establish the optimum design, for there are many independent variables which affect the performance.

The knowledge of mass transfer rates in packed adsorbent beds composed of small particles was practically non-existant at the time this research was initiated, and the results obtained during this investigation should add to such data as that obtained by Gamson, Thodos, and Hougen (33) and Hurt (34). This data should aid in the design of such commercial equipment as solvent recovery systems, noxious gas removal systems, water softening (base exchange) equipment, catalyst beds, etc.

Choice of the operating variables to be investigated and the ranges of these variables to be covered was dictated by the Chemical Warfare Service standard test procedures and the known practical limits of adsorbent bed size as governed by size and volume of the resulting complete canister. The following variables were considered:

1. Linear Air Velocity

The air flow rates of the standard Chemical Warfare Service test methods were employed. These are 32 liters per minute, constant flow, and 50 liters per minute, breather flow. In addition, tests were run at 64 liters per minute, constant flow. Canisters with two different cross sectional areas (axial flow canisters)

were employed in the tests so that a maximum of six velocities was studied.

2. Particle Diameter

It was mentioned in Appendix F that the standard Chemical Warfare Service whetlerite is a 12-30 mesh material (U. S. Standard Sieves). These standard whetlerites were separated by screening into 12-16, 16-20, 20-30, and 30-40 sieve sizes. Tests were made with blends of these sieve sizes as well as with the pure fractions.

3. Adsorbents

Several standard Chemical Warfare Service whetlerites were tested. These consisted of two unimpregnated whetlerites, one Type A impregnated whetlerite, one Grade II (inferior quality) Type ASC impregnated whetlerite, and several Grade I (superior quality) Type ASC impregnated whetlerites.

4. Adsorbent Bed Depth

The adsorbent bed depths investigated were governed by the test conditions so that excessively long break times would not be obtained. Generally, the bed depths were maintained so that the break time fell between five and 120 minutes. The range of bed depths was from 0.5 to 5.5 centimeters.

5. Test Gases

All tests were conducted with the five standard Chemical Warfare Service non-persistent agents: chloropicrin (PS), phosgene (CG), cyanogen chloride (CK),

DECLASSIFIED

hydrocyanic acid (AC), and arsine (SA).

6. Concentrations

For the great majority of the tests, the influent and effluent concentrations were held constant for each particular agent at their standard test values. However, in order to establish the validity of the equations, several tests were made to determine the effect of these variables on the apparent critical bed depth.

7. Temperature

The standard Chemical Warfare Service test methods prescribe only that the temperature of test shall not be less than 70° F. In these investigations, the additional stipulation was made that the temperature should not exceed 95° F. No attempt was made to deter- the effect of temperature within this range.

It was, therefore, the object of this thesis to investigate the removal of the standard Chemical Warfare Service non-persistent agents by the standard Chemical Warfare Service whetlerites and to determine the effects of linear air velocity, particle diameter, adsorbent bed depth, type whetlerite, and influent and effluent concentrations on the performance of beds of these adsorbents.

V. Experimental Procedure

A. Test Apparatus

The equipment which was used for the measurement of adsorbent bed performance was the standard Chemical Warfare Service canister testing apparatus described in Chemical Warfare Pamphlet No. 2, Part I, Sections A, B, I, J, and L. For a complete description of the apparatus, which differ slightly for each agent, the reader is referred to the above pamphlet. A brief description, however, is shown in Fig. 13 for the chloropicrin, constant flow test apparatus.

For chloropicrin testing, a controlled quantity of air is forced under pressure through a bottle of liquid chloropicrin the temperature of which is held constant by a thermo-regulator. This air stream passes through the chloropicrin at such a rate that practical saturation is obtained. The saturated air stream is then mixed with the main air stream, and the ratio of the two streams is regulated to give the desired concentration. This concentration is checked periodically by sampling a designated volume of the air-gas mixture and analyzing chemically for chloropicrin.

This mixed stream is drawn through the canister and the pressures are so regulated that the air stream entering the canister is essentially at atmospheric pressure. A sample of the effluent air stream is continually drawn at a steady rate through a bubbler. This bubbler contains

FIG. 13

REPRESENTATION OF PS APPARATUS

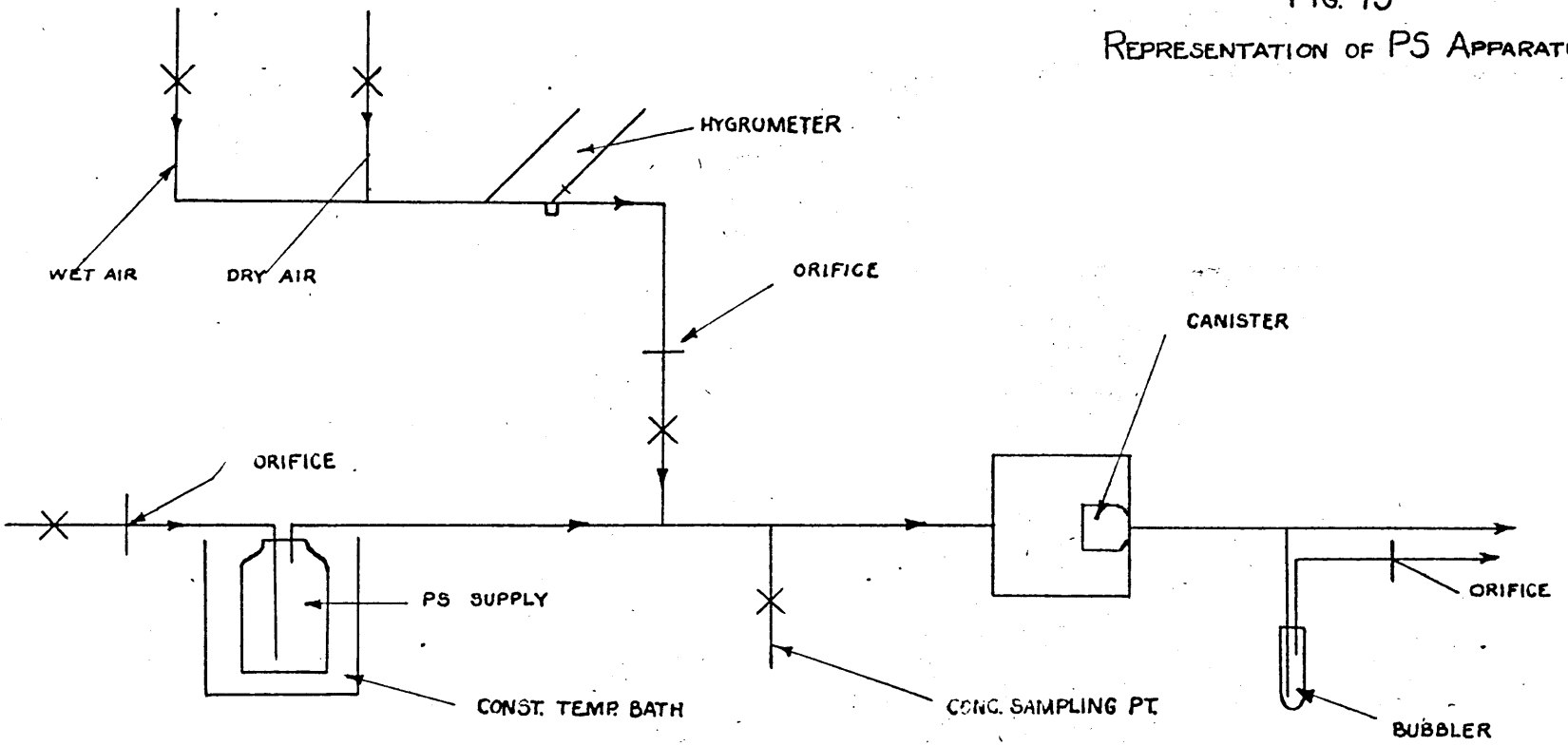

FEB. 16, 1946

F.G.P.

DECLASSIFIED

a chemical and an indicator, and the volume and concentration are such that a color change occurs when a designated quantity of agent has been drawn into the bubbler. Thus, this indicator measures a cumulative penetration by means of a time titration.

The differences among the test apparatus for the various agents are in the method of obtaining the desired concentration in the influent air stream. Cyanogen chloride and hydrogen cyanide concentrations are obtained in the same manner as chloropicrin concentrations. Phosgene concentrations are obtained by bleeding the required amount of pure phosgene into the main air stream from a tank of liquid phosgene, the rate being controlled by an orifice in the phosgene line. Arsine concentrations are obtained in a similar manner except that a reservoir of compressed arsine gas (made by chemical reaction during the test) is used as the supply source.

B. Procedure for Test Measurements

1. Separation of Particle Sizes

All whetlerites available for test contained particle sizes varying over a considerable range. Therefore, prior to any test, all whetlerites were separated into 12-16, 16-20, 20-30, and 30-40 sieve size fractions. This separation was performed by the procedure prescribed in Chemical Warfare Service Pamphlet No. 2, Part III, Section L. One hundred grams of the whetlerite was placed on the top screen (8 mesh) of a series of 8, 12, 16, 20,

30, and 40 U. S. Standard sieves. These were placed in a standard "Ro-Tap" machine and screened for three minutes. After this period, the whetlerite from each screen was removed, dried for eight hours at 250° F., and sealed in separate air-tight containers for future use.

2. Measurement of Adsorbent Volume and Apparent Density

The volume of adsorbent used in each test was measured with the standard Charcoal Volume Meter, E1, which is described in Chemical Warfare Service Pamphlet No. 2, Part III, Section L. Essentially, this meter measures the "free fall" volume of the adsorbent. The adsorbent is allowed to fall freely for approximately two feet and is distributed over the entire area of the meter by a series of wires arranged in checker board fashion at three levels of the fall. The charcoal falls into a graduated cylinder which affords a means of measuring the volume. A slide valve is located at the bottom of the cylinder to facilitate removal of the measured volume of whetlerite.

The apparent density of the adsorbent was determined by weighing a measured volume of the adsorbent and dividing the weight by the volume, the result being expressed in grams per milliliter.

3. Packing of Adsorbent into Canister for Evaluation

A measured volume of the adsorbent was filled by free-fall into the canisters in a manner identical to the measurement of the adsorbent volume except that the

canister replaced the graduated cylinder. The diameter of the free-fall column was maintained equal to the diameter of the canister being filled.

In order to avoid any possible differences in bed depth which might result from an unequal distribution in the filling tower, the canisters were rotated at approximately 5 R.P.M. This would not eliminate large differences in distribution, but it would minimize small differences.

The adsorbent was restrained from movement in the canister by means of spacers located at each end of the adsorbent bed. The top spacer (effluent side) was permanently beaded into the canister and supported the charcoal during the filling operation. After filling, the bottom spacer was forced onto the surface of the adsorbent bed with a light load and was held in that position by friction with the canister wall. No measureable compression of the charcoal occurred during the insertion of this spacer.

The spacers were so designed that they did not interfere with air flow to any appreciable extent except at the periphery where a 0.25-inch baffle was located. This baffle, which was designed during the development of the M11 Combat Canister, served to prevent channeling along the canister wall (especially after rough usage) and to strengthen the spacers which are normally subjected to appreciable loads.

Fig. 14 shows the general construction of the canisters and spacers used for these tests.

4. Measurement of Air Resistance

Air was drawn through the adsorbent beds at a rate measured by a calibrated orifice. The difference in the pressure at the influent and effluent sides of the adsorbent bed was measured by an Ellison Draft Gage accurate to 0.1 millimeters of water differential pressure.

5. Measurement of Break Time

The agent-contaminated air stream was drawn through the adsorbent bed, and a record was kept of the time the air stream passed through the bed. When the first bubbler "broke" (changed color) it was replaced immediately be a new bubbler. This process was repeated until the time interval between bubbler breaks was equal to or less than the time required to break the bubbler with the specified break concentration. The time interval from the start of the test to the start of the time interval during which the break occurred within the specified time interval was taken as the break time.

A variation of plus or minus ten per cent from the nominal test concentration was allowed, and the results were adjusted to the nominal test concentration by a linear scaling.

These test procedures are in accordance with Chemical Warfare Service Pamphlet No. 2, Part I; further details of the experimental procedure can be obtained from this pamphlet.

FIG. 14

CONSTRUCTION OF M11 CANISTER

CENTER SPACER

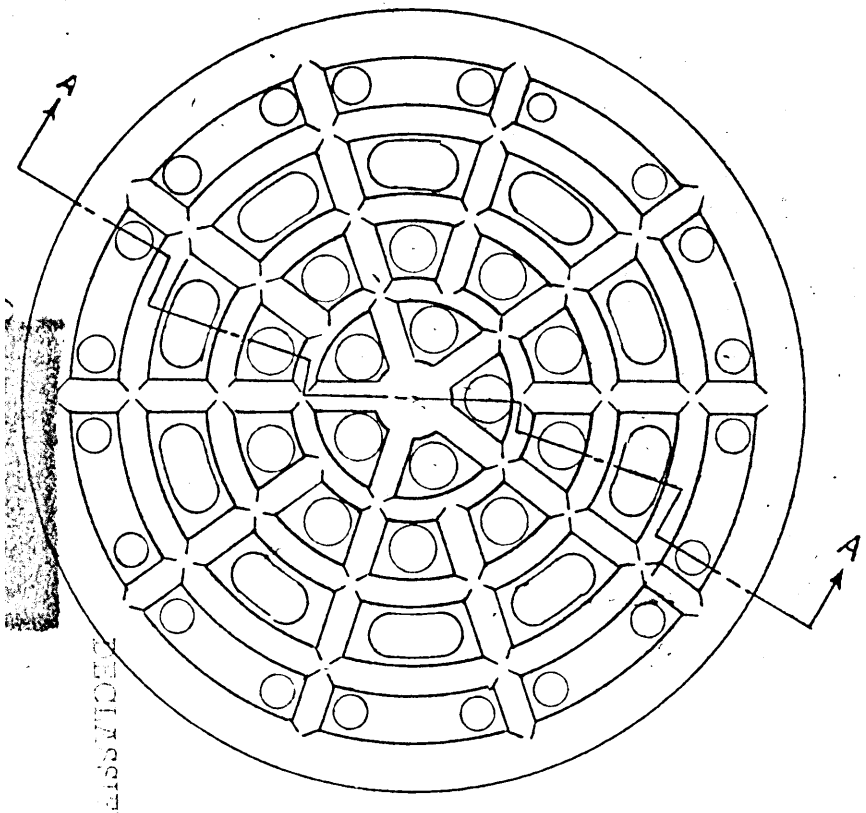

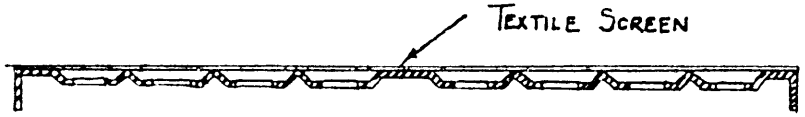

SECTION A-A

CANISTER BODY

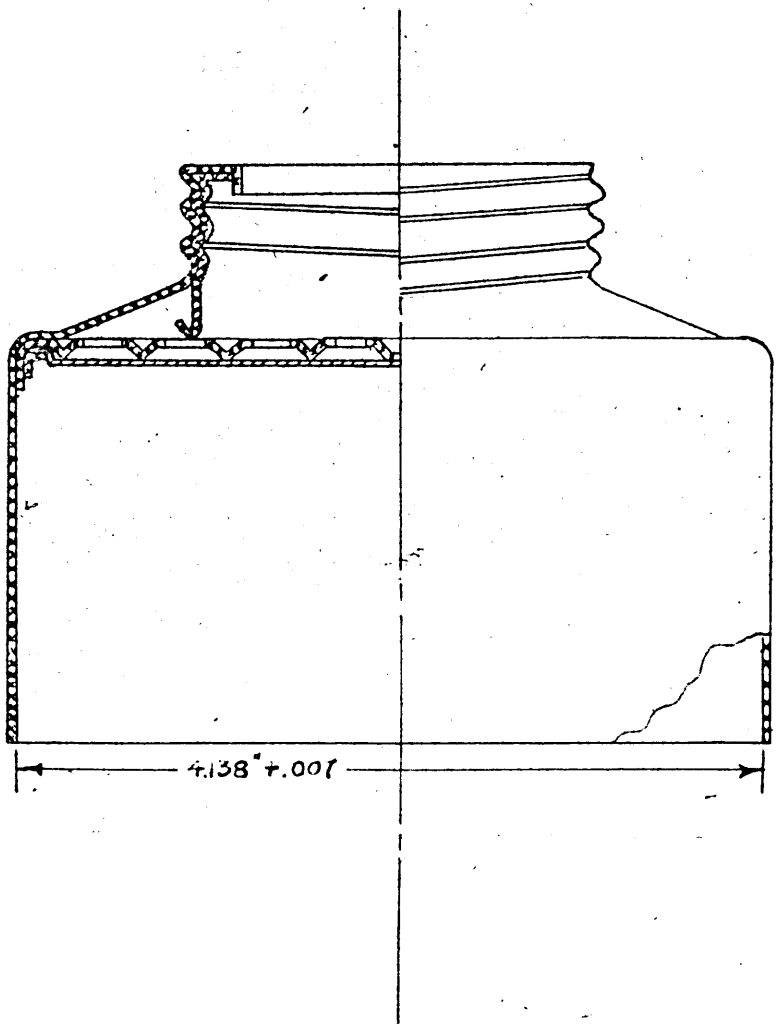

FEB. 17, 1940
F.G.P.

DECLASSIFIED

6. Measurement of Saturation Capacity

The saturation capacity of the adsorbent for chloropicrin was measured by drawing chloropicrin-laden air through a measured volume of adsorbent and measuring the gain in weight at constant weight. In these tests, bone-dry air was employed to avoid moisture gain by the adsorbent.

DECLASSIFIED

VI. RESULTS

Table IV

Variation of Air Resistance with Whetlerite Type
Blended Misture of Thirty Production Lots*
250 ml., M11 Canister, 85 L./min.

Type Whetlerite	Sieve Analysis 12-16	16-20	20-30	30-40	Air Resistance (mm. Water)
		(per cent)			
HH	100	-	-	-	18.6
AD	100	-	-	-	21.0
CC	100	-	-	-	24.4
HH	-	100	-	-	26.4
AD	-	100	-	-	27.8
CC	-	100	-	-	31.0
HH	-	-	100	-	44.1
AD	-	-	100	-	45.3
CC	-	-	100	-	48.9
HH	23.2	44.6	29.2	3.0	35.5
AD	23.2	50.9	23.0	2.9	34.8
CC	16.9	50.6	29.2	3.3	40.5

*HH Lots: HH3-455 to HH3-485
AD Lots: AD3-1079 to AD3-1107
CC Lots: CC3-1737 to CC3-1833

Table V

Variation of Air Resistance with Whetlerite Type
Single Production Lots
250 ml., M11 Canister, 85 L./min.

Type Whetlerite	Sieve Analysis 12-16	16-20	20-30	30-40	Air Resistance (mm. Water)
		(Per Cent)			
AD3-1760	100	-	-	-	19.1
BD3-1750	100	-	-	-	20.3
HH3-465	100	-	-	-	18.8
CC3-1088	100	-	-	-	20.3
CC3-900	100	-	-	-	19.4
AD3-1760	-	100	-	-	27.5
BD3-1750	-	100	-	-	27.2
HH3-465	-	100	-	-	26.8
CC3-1088	-	100	-	-	29.8
CC3-900	-	100	-	-	27.2
AD3-1760	-	-	100	-	42.0
BD3-1750	-	-	100	-	43.4
HH3-465	-	-	100	-	41.2
CC3-1088	-	-	100	-	46.6
CC3-900	-	-	100	-	46.2
AD3-1760	20.0	50.0	30.0	-	32.0
BD3-1750	20.0	50.0	30.0	-	34.2
HH3-465	20.0	50.0	30.0	-	31.8
CC3-1088	20.0	50.0	30.0	-	36.8
AD3-1760	19.8	47.9	28.6	4.7	35.5
BD3-1750	19.8	47.9	28.6	4.7	38.0
HH3-465	19.8	47.9	28.6	4.7	35.4
CC3-1088	19.8	47.9	28.6	4.7	40.2
CC3-900	30.0	60.0	10.0	-	28.1
CC3-900	30.0	40.0	30.0	-	33.3
CC3-900	30.0	-	70.0	-	40.9

Table VI

Sieve Analyses for Blends Used in Break Time Studies
(12-30 Mesh Whetlerite)

Whetlerite Designation	Whetlerite Type	Sieve Analysis (Per Cent) 12-16	16-20	20-30	30-40
AD3-255	ASC	37.4	40.7	20.7	1.2
MIT3-4713	A	30.3	43.3	23.8	2.6
HC3-361	ASC	31.1	40.2	25.7	3.0
CC3-900	ASC	20.5	47.5	28.4	3.6

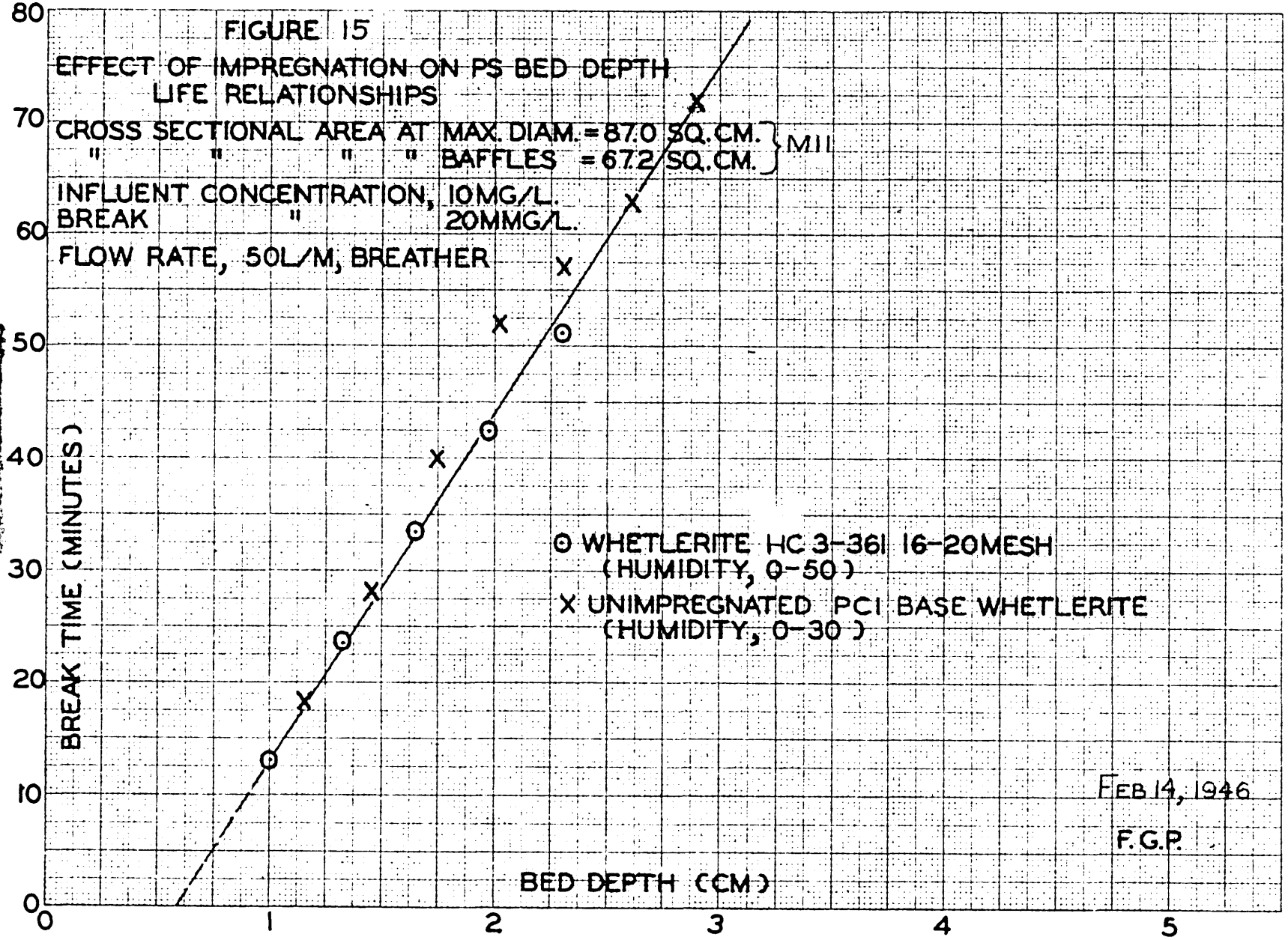

DECLASSIFIED

DECLASSIFIED.

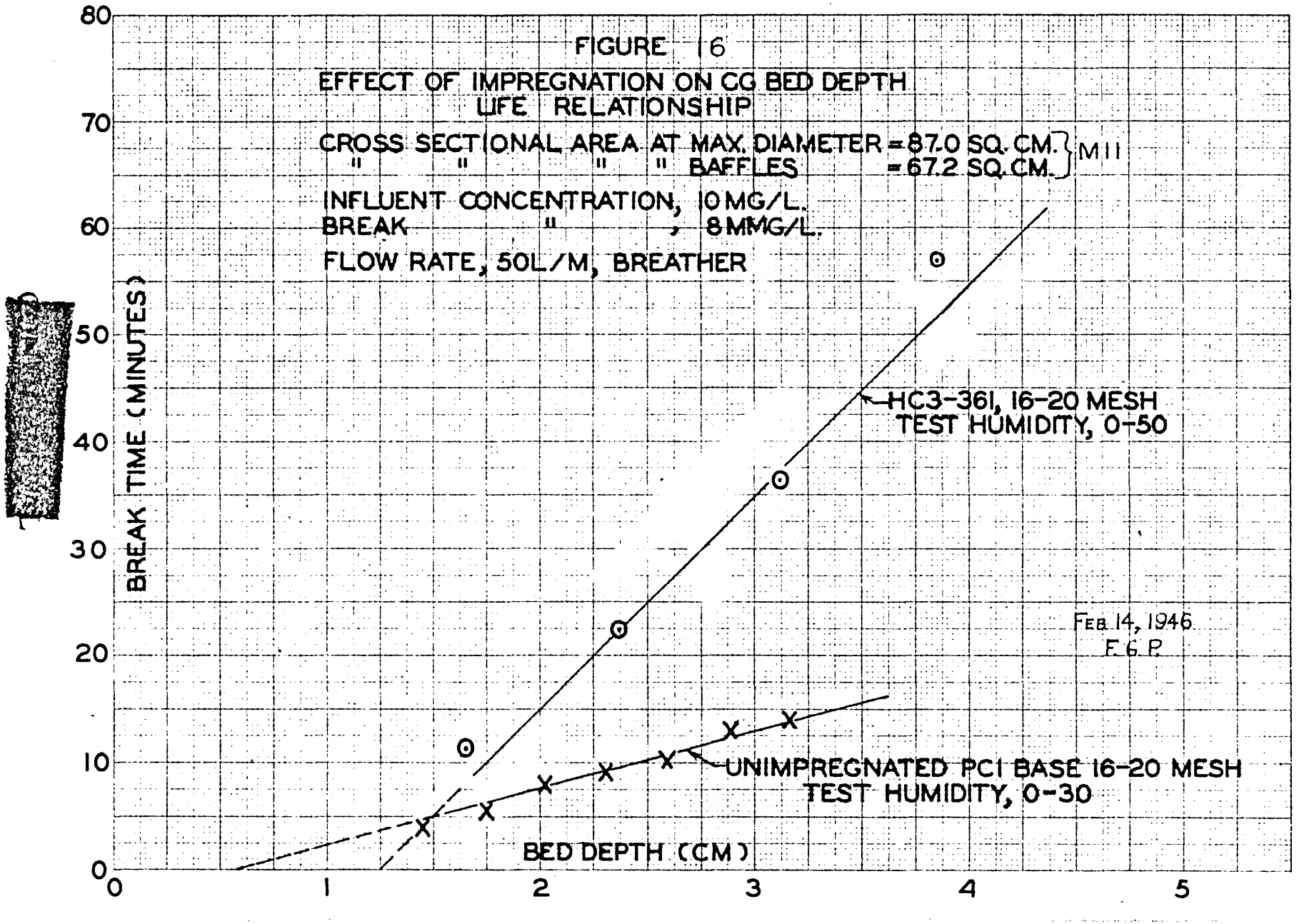
FIGURE 16
EFFECT OF IMPREGNATION ON CG BED DEPTH
LIFE RELATIONSHIP
CROSS SECTIONAL AREA AT MAX. DIAMETER = 87.0 SQ. CM.
" " " " BAFFLES = 67.2 SQ. CM.
M11
INFLUENT CONCENTRATION, 10 MG/L.
BREAK " , 8 MMG/L.
FLOW RATE, 50L/M, BREATHER
HC3-361, 16-20 MESH
TEST HUMIDITY, 0-50
UNIMPREGNATED PCI BASE 16-20 MESH
TEST HUMIDITY, 0-30
FEB. 14, 1946
F.G.P.
BREAK TIME (MINUTES)
BED DEPTH (CM)
0
10
20
30
40
50
60
70
80
1
2
3
4
5

FIGURE 17

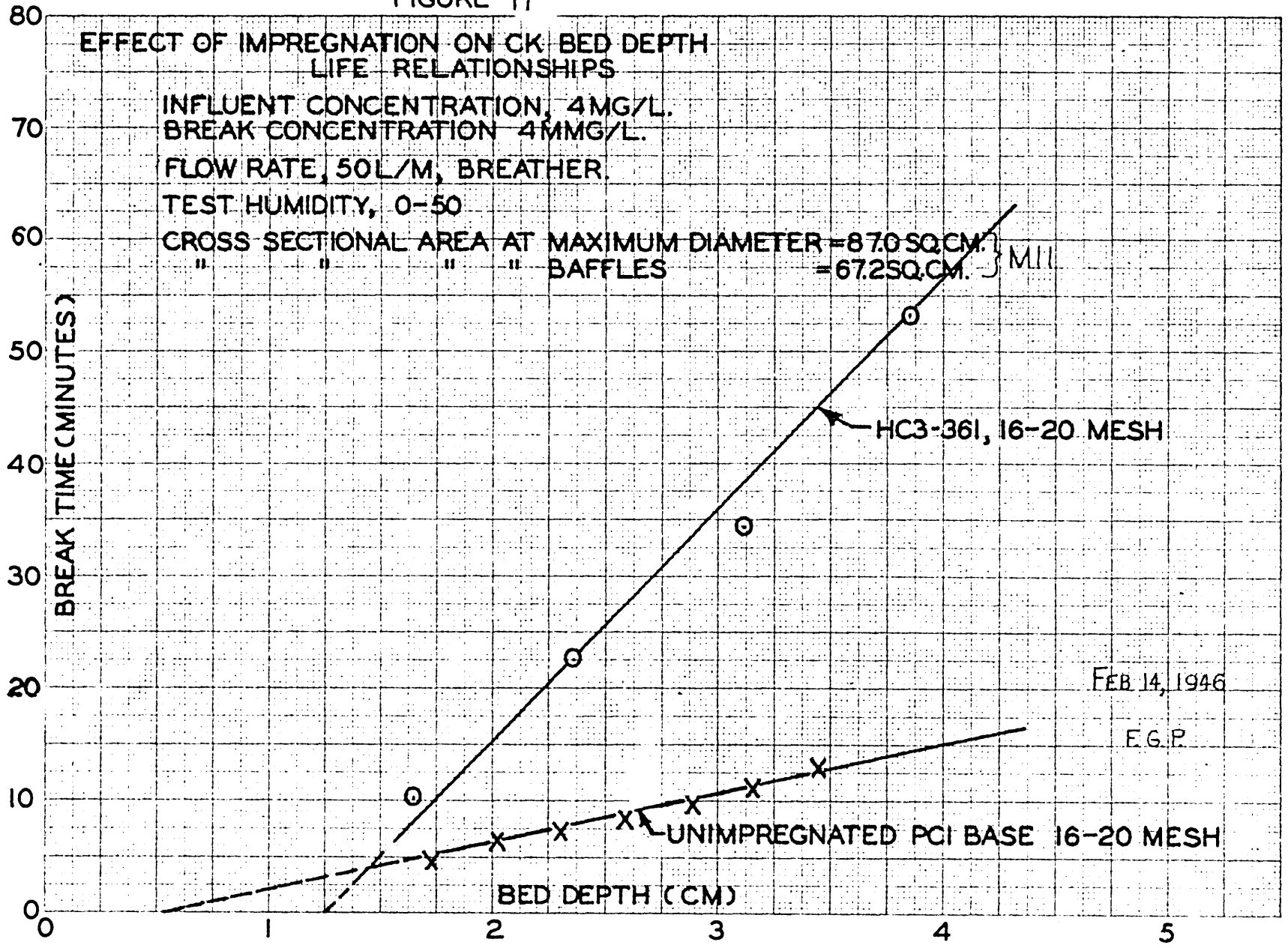

DECLASSIFIED

DECLASSIFIED

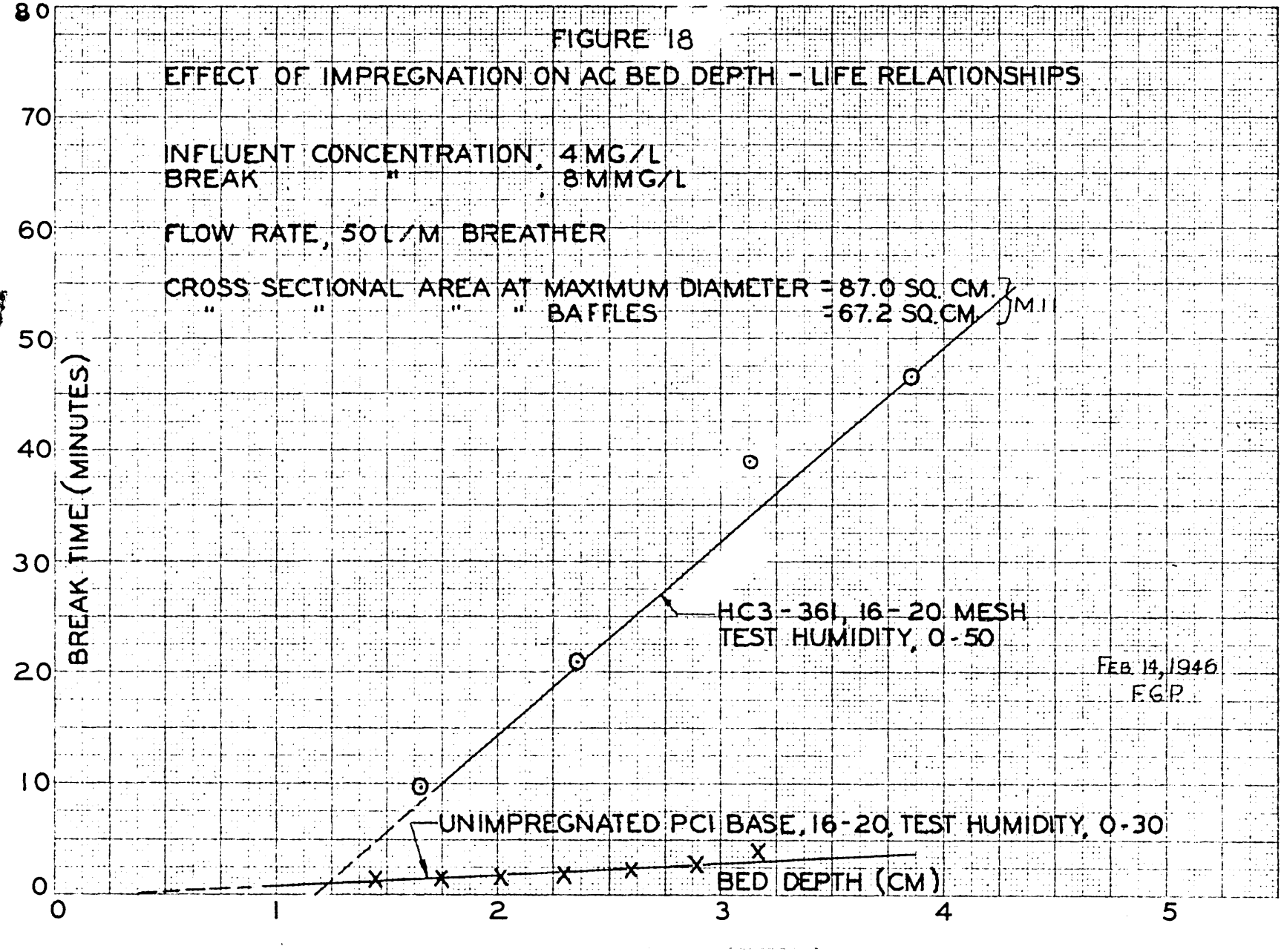
FIGURE 18
EFFECT OF IMPREGNATION ON AC BED DEPTH - LIFE RELATIONSHIPS
INFLUENT CONCENTRATION, 4 MG/L
BREAK " , 8 MMG/L
FLOW RATE, 50 L/M BREATHER
CROSS SECTIONAL AREA AT MAXIMUM DIAMETER = 87.0 SQ. CM.
" " " " BAFFLES = 67.2 SQ. CM.
M.I.T.
HC3-361, 16-20 MESH
TEST HUMIDITY, 0-50
FEB. 14, 1946
F.G.P.
UNIMPREGNATED PCI BASE, 16-20, TEST HUMIDITY, 0-30
BREAK TIME (MINUTES)
BED DEPTH (CM)
0
10
20
30
40
50
60
70
80
0
1
2
3
4
5

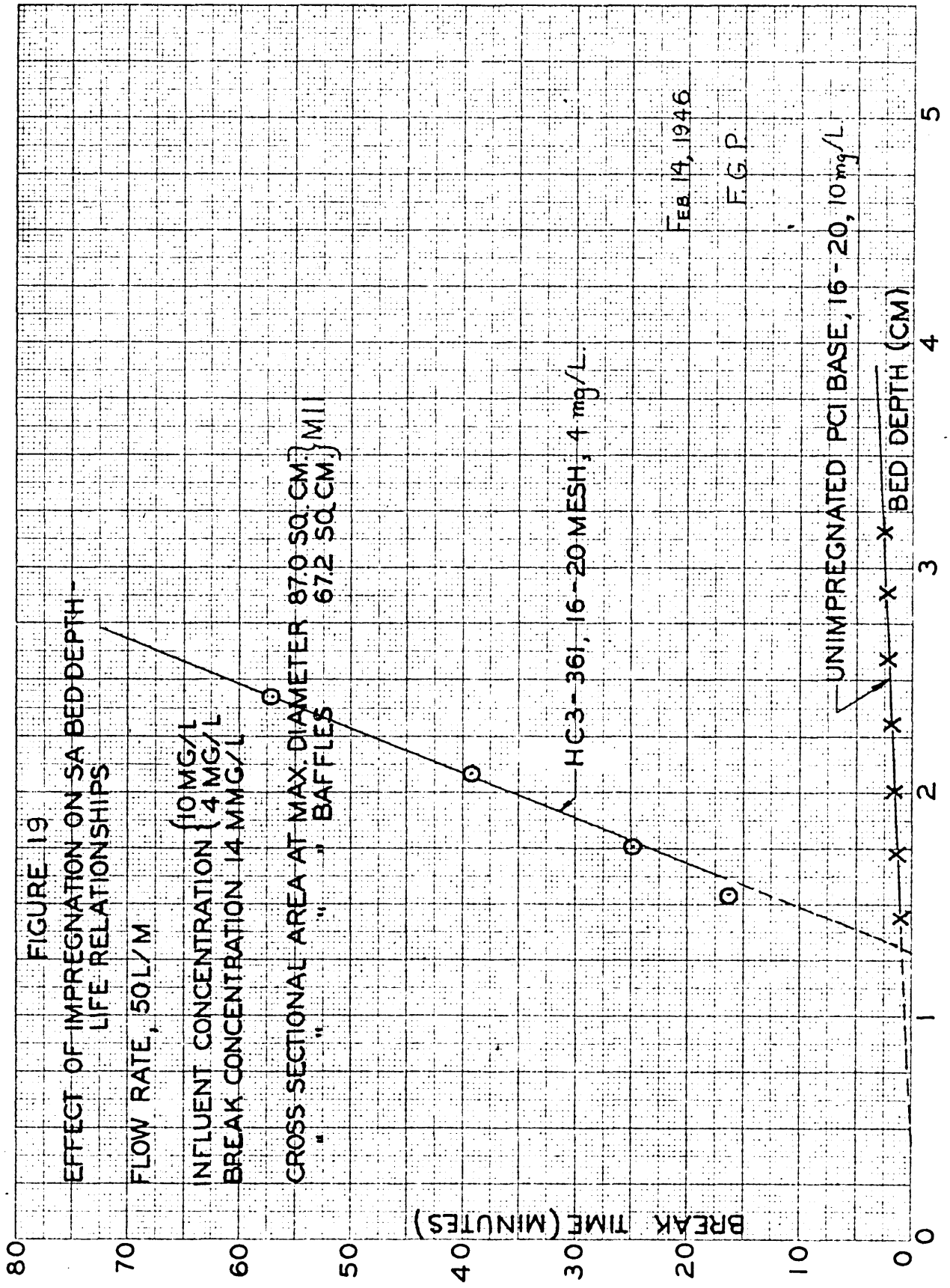
FIGURE 19
EFFECT OF IMPREGNATION ON SA BED DEPTH-
LIFE RELATIONSHIPS
FLOW RATE, 50 L/M
INFLUENT CONCENTRATION { 10 MG/L
4 MG/L
BREAK CONCENTRATION 14 MMG/L
CROSS SECTIONAL AREA AT MAX. DIAMETER 87.0 SQ. CM.
" " " BAFFLES 67.2 SQ. CM.
HC3-361, 16-20 MESH, 4 mg/L
UNIMPREGNATED PCI BASE, 16-20, 10 mg/L
FEB 14, 1946
F.G.P.
BREAK TIME (MINUTES)
BED DEPTH (CM)
0
10
20
30
40
50
60
70
80
1
2
3
4
5

Logarithmic 3 × 5 Cycles.
K. C. C. Sheet.
MADE IN U. S. A.

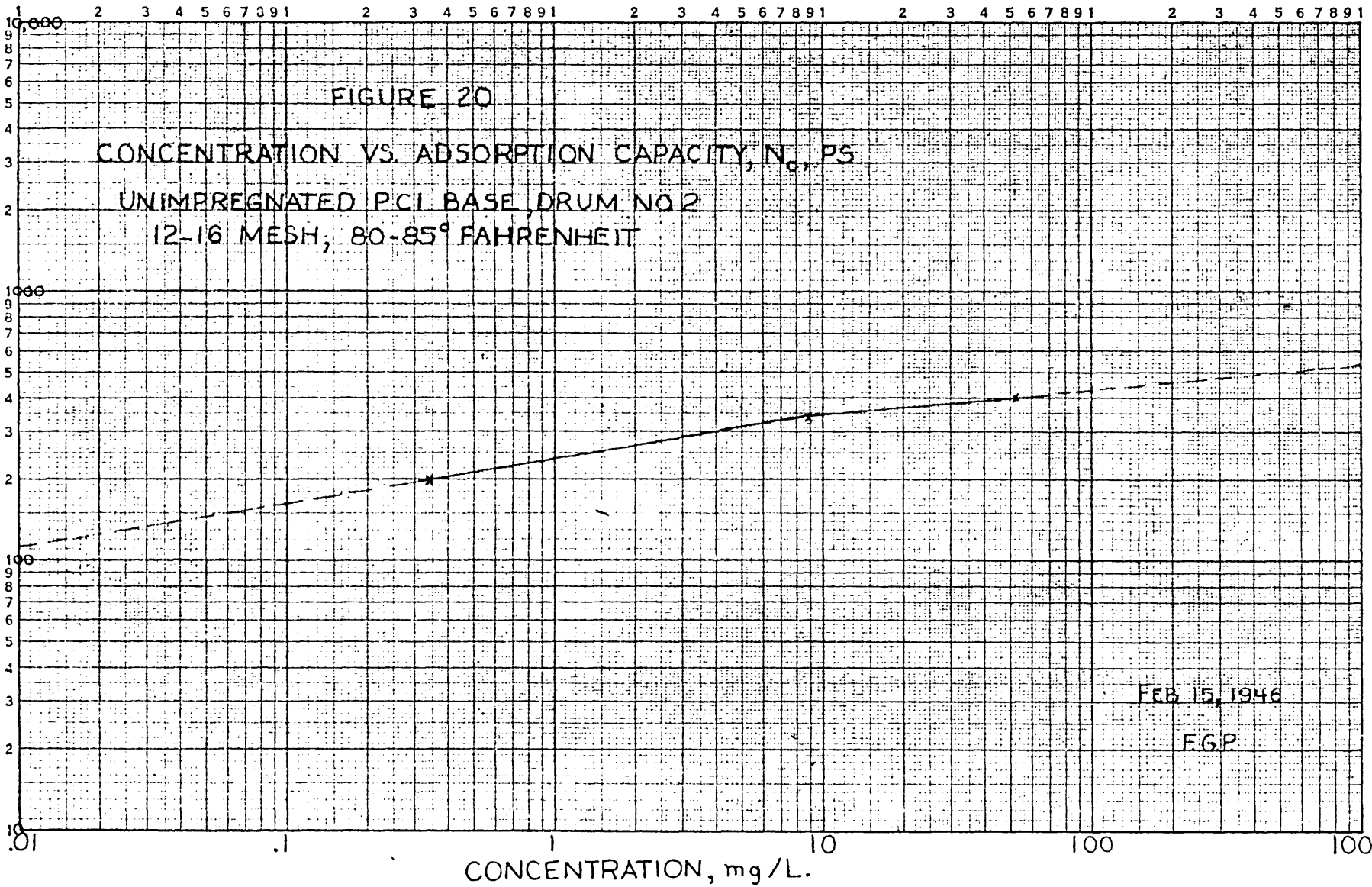

DECLASSIFIED

DECLASSIFIED

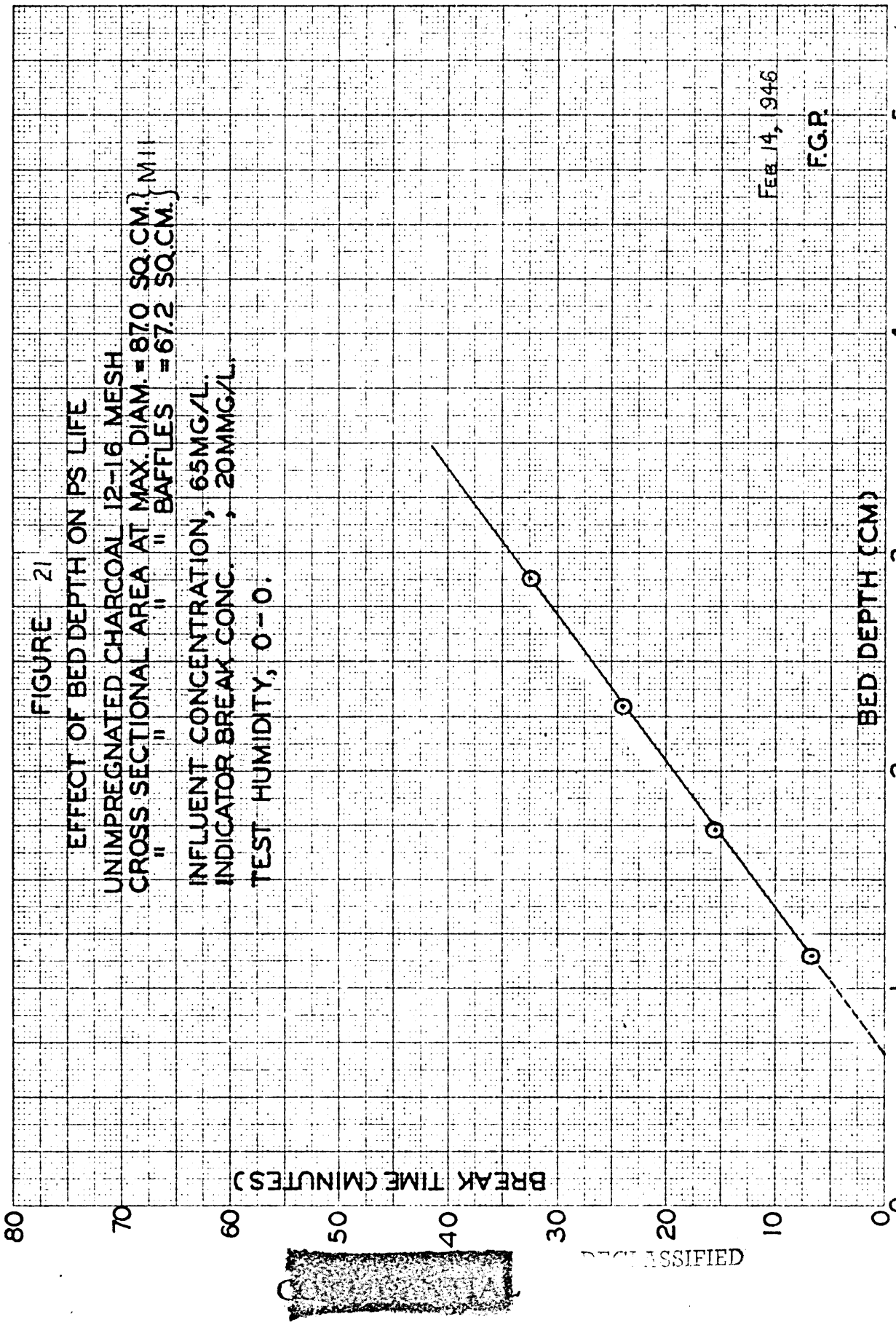

DECLASSIFIED

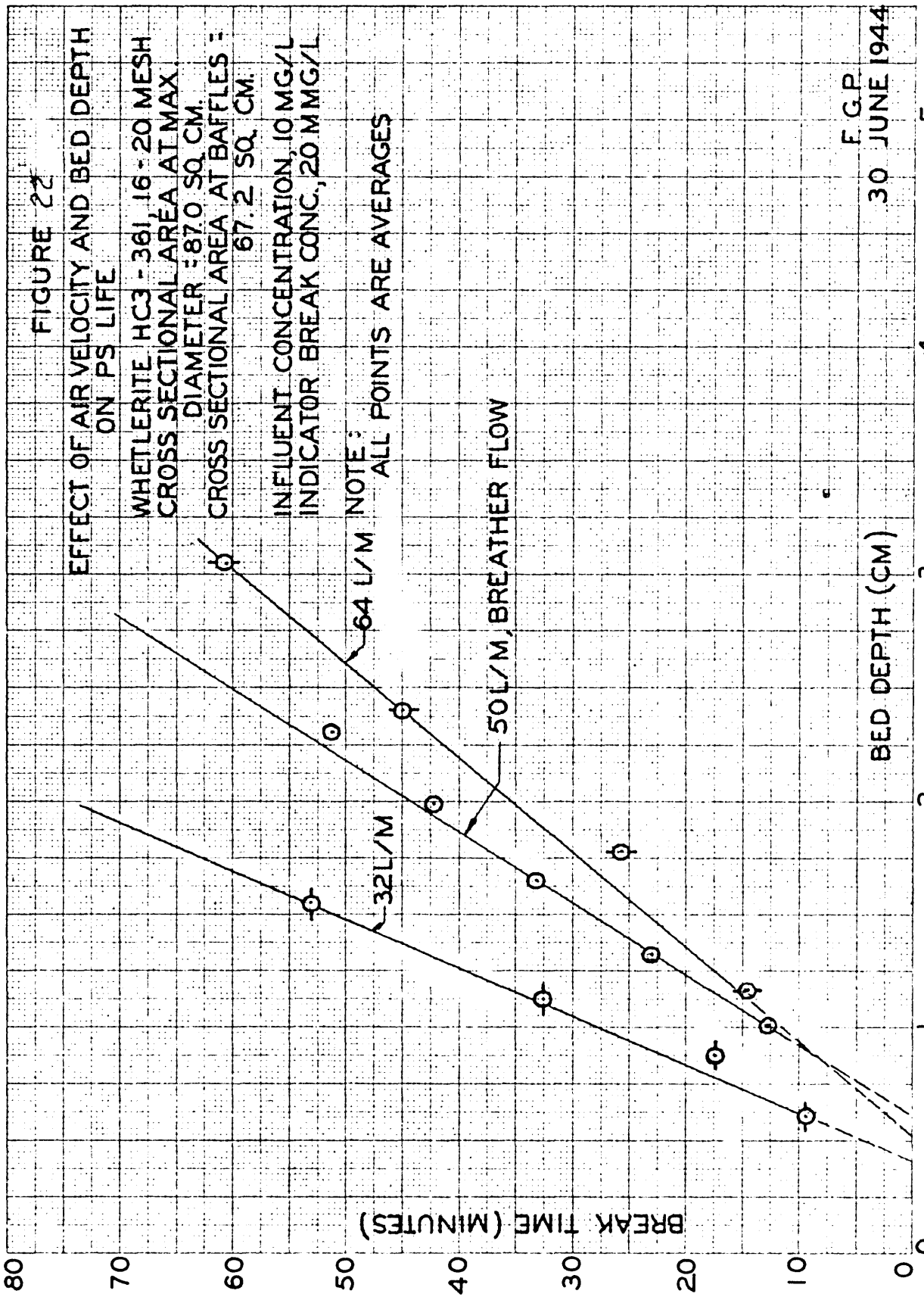
FIGURE 22
EFFECT OF AIR VELOCITY AND BED DEPTH ON PS LIFE
WHETLERITE HC3 - 361, 16 - 20 MESH
CROSS SECTIONAL AREA AT MAX. DIAMETER = 87.0 SQ. CM.
CROSS SECTIONAL AREA AT BAFFLES = 67.2 SQ. CM.
INFLUENT CONCENTRATION, 10 MG/L
INDICATOR BREAK CONC., 20 M MG/L
NOTE: ALL POINTS ARE AVERAGES
64 L/M
50 L/M, BREATHER FLOW
32 L/M
BREAK TIME (MINUTES)
BED DEPTH (CM)
0
10
20
30
40
50
60
70
80
1
2
3
4
5
F.G.P.
30 JUNE 1944

DECLASSIFIED

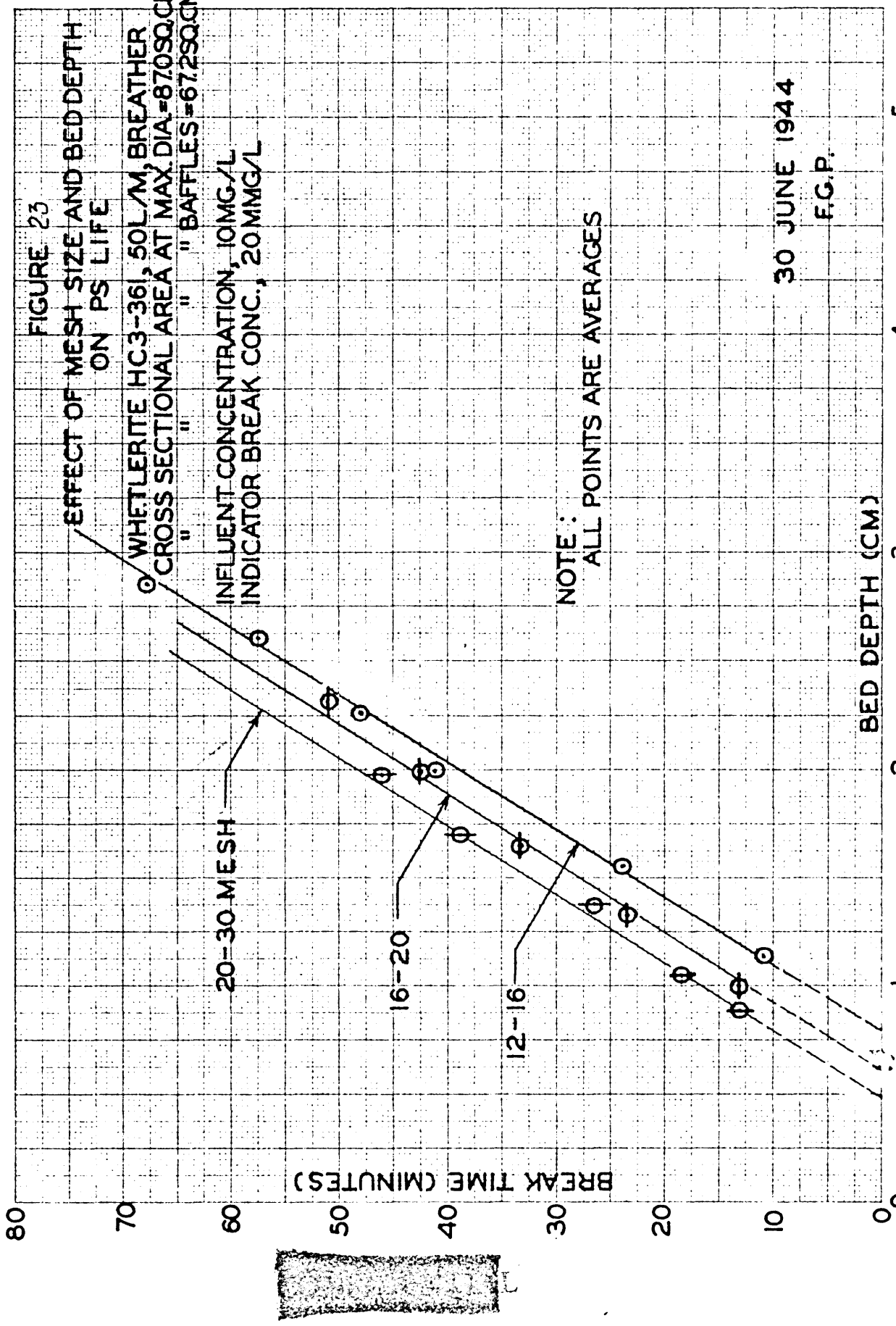

FIGURE 24

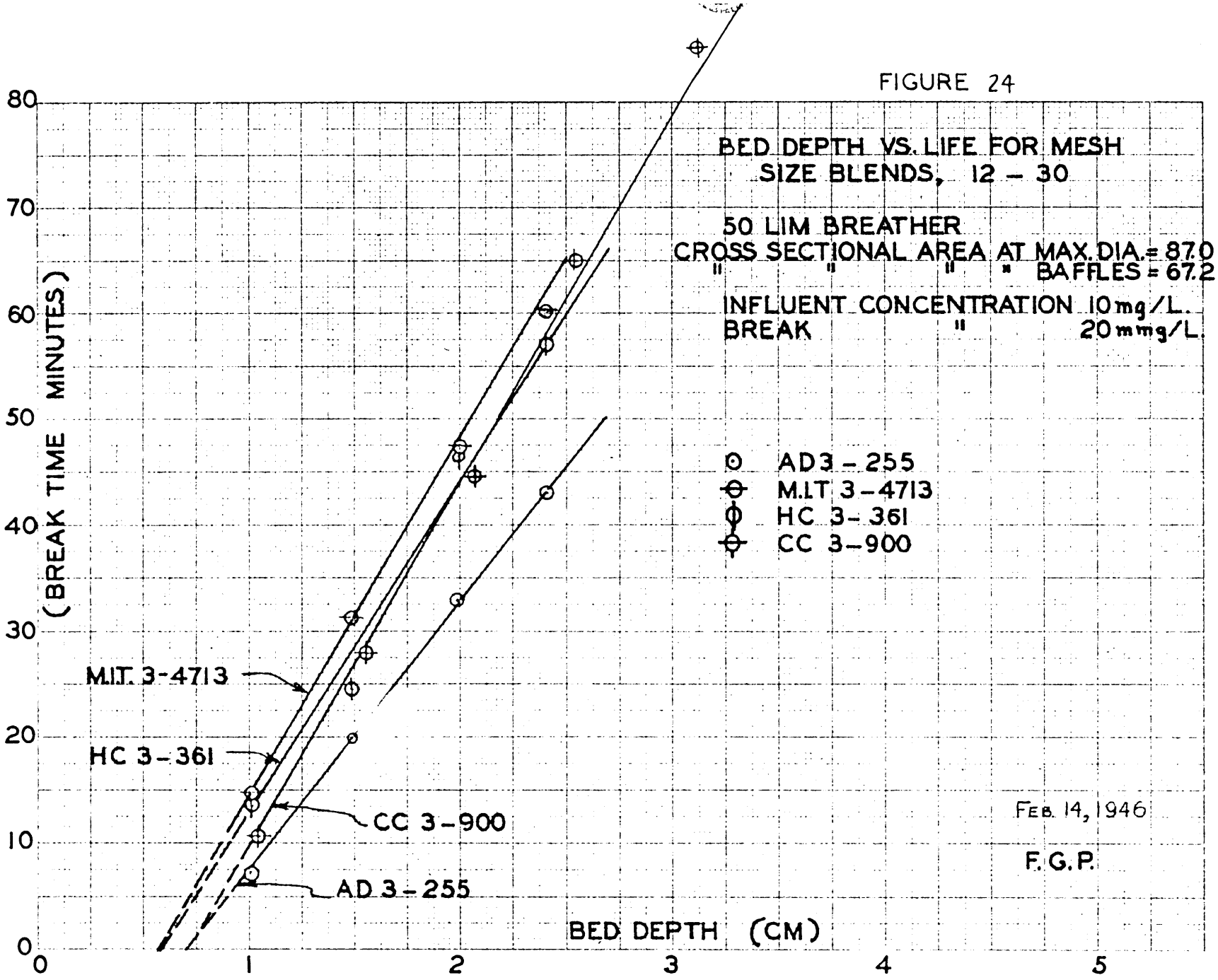

DECLASSIFIED

DECLASSIFIED

FIGURE 25

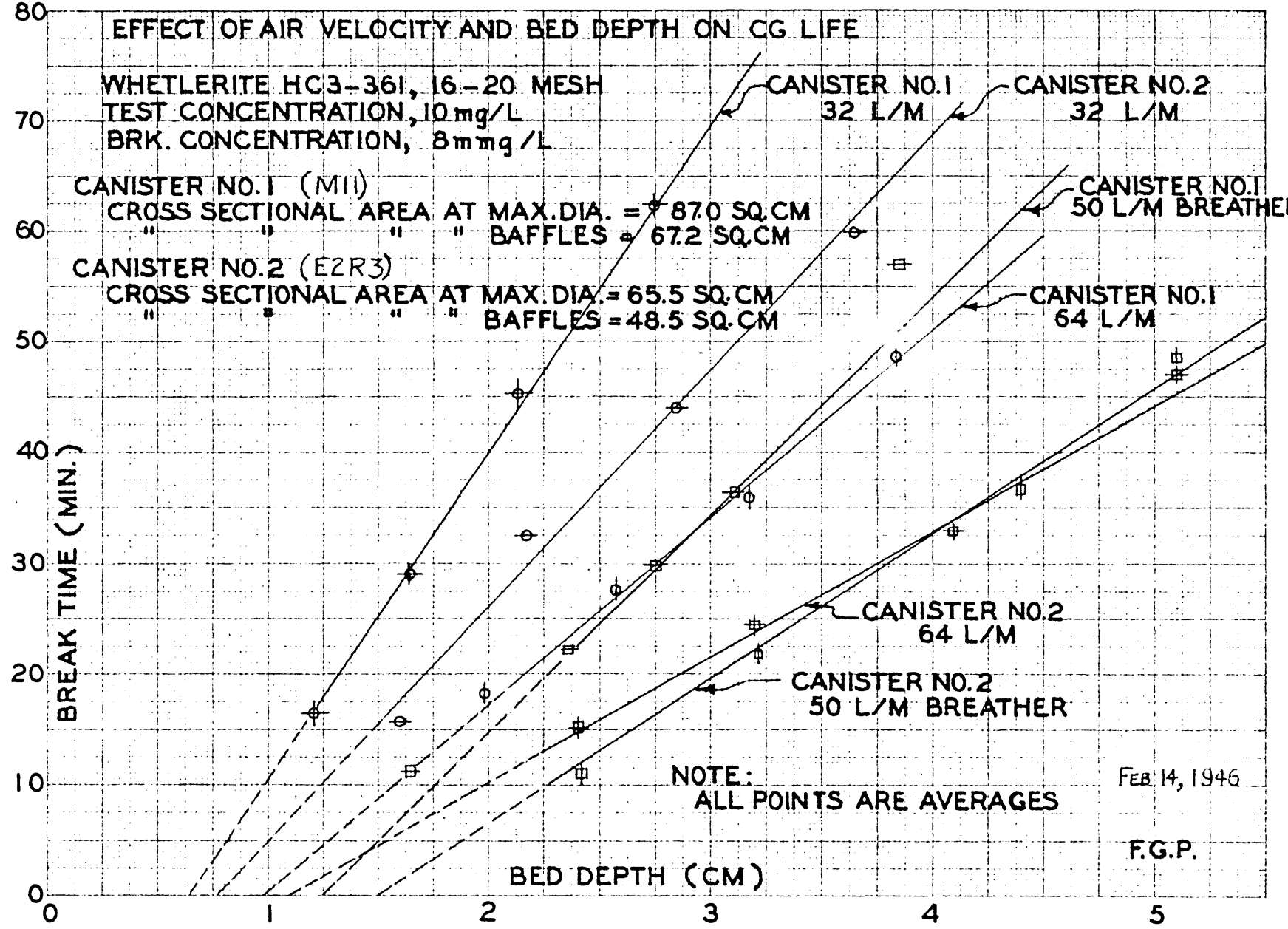

DECLASSIFIED
DECLASSIFIED
DECLASSIFIED
83

FIGURE 26

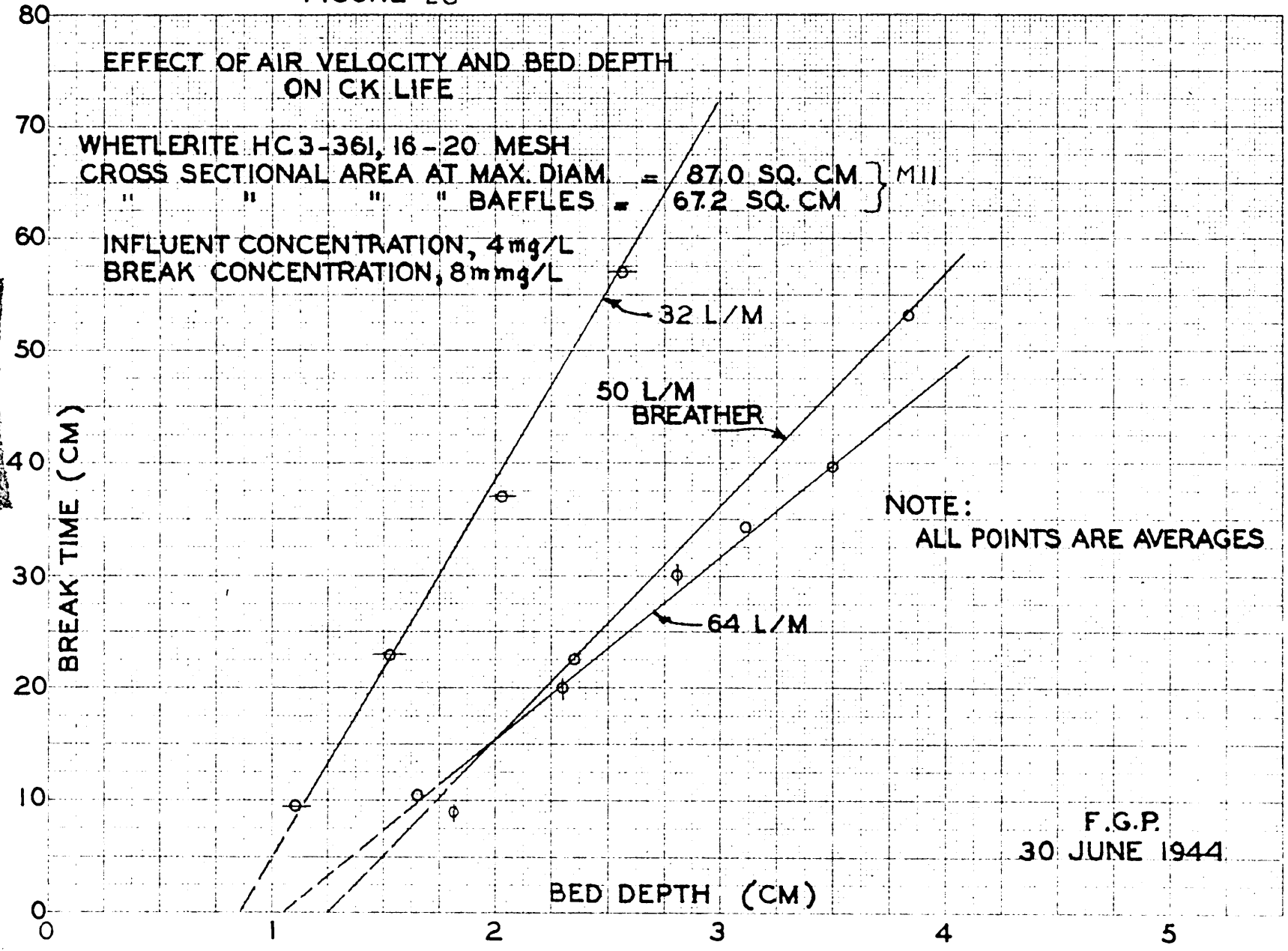

DECLASSIFIED

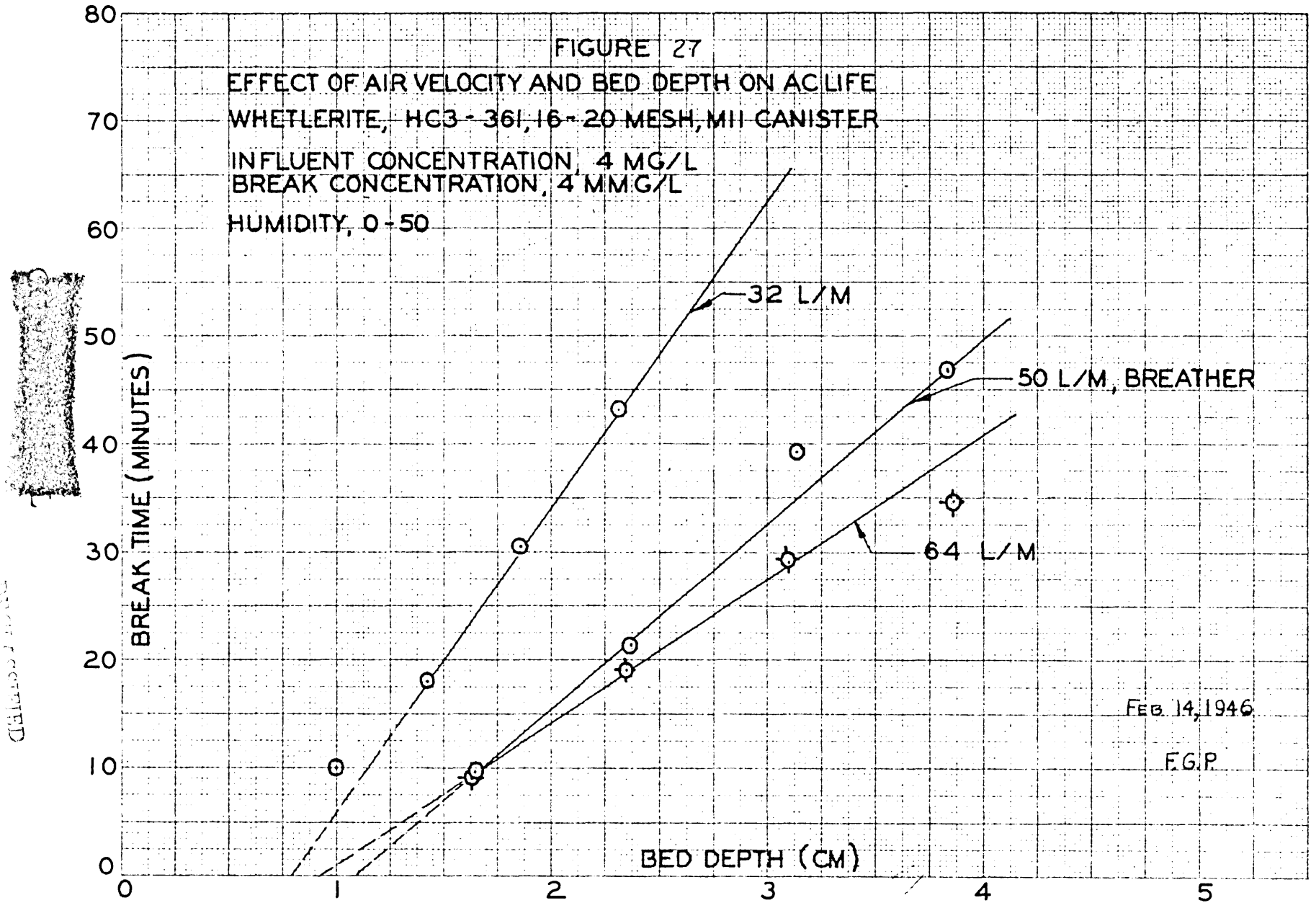

DECLASSIFIED

FIGURE 28

CK EFFLUENT CONCENTRATION AS FUNCTION OF TIME AND BED DEPTH

WHETLERITE, H H3 - 20-30 MESH
FLOW RATE, 50 L/M, BREATHER
CROSS SECTIONAL AREA AT MAX. DIA. = 87.0 SQ. CM. } M11
" " " " BAFFLES = 67.2 " "
TEST HUMIDITY, 0-30

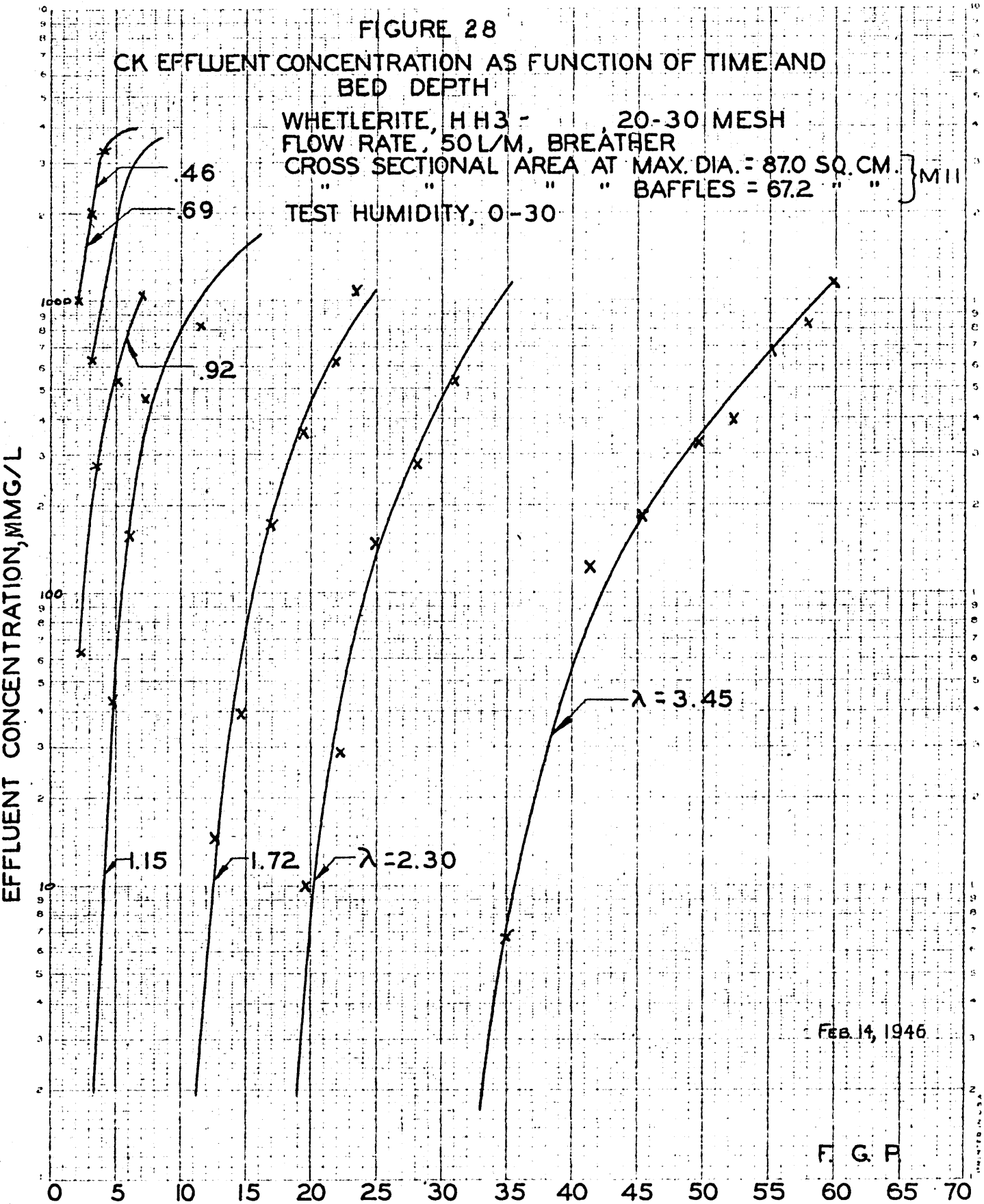

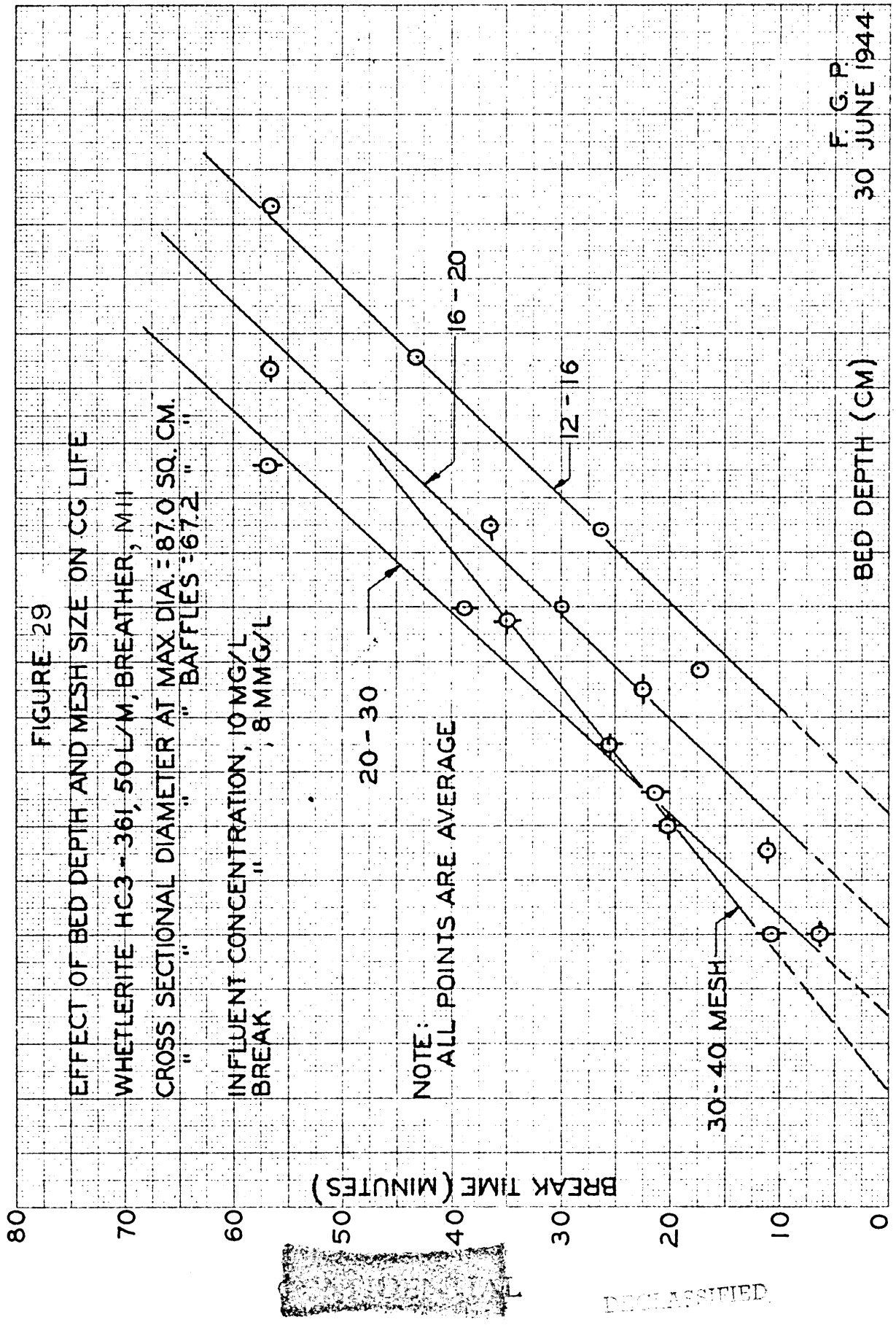
FIGURE 29
EFFECT OF BED DEPTH AND MESH SIZE ON CG LIFE
WHETLERITE HC3 - 361, 50 L/M, BREATHER, MH
CROSS SECTIONAL DIAMETER AT MAX. DIA. = 87.0 SQ. CM.
" " " BAFFLES = 67.2 " "
INFLUENT CONCENTRATION, 10 MG/L
BREAK , 8 MMG/L
NOTE:
ALL POINTS ARE AVERAGE
20 - 30
16 - 20
12 - 16
30 - 40 MESH
BREAK TIME (MINUTES)
BED DEPTH (CM)
F. G. P.
30 JUNE 1944
0
10
20
30
40
50
60
70
80
0
1
2
3
4
5

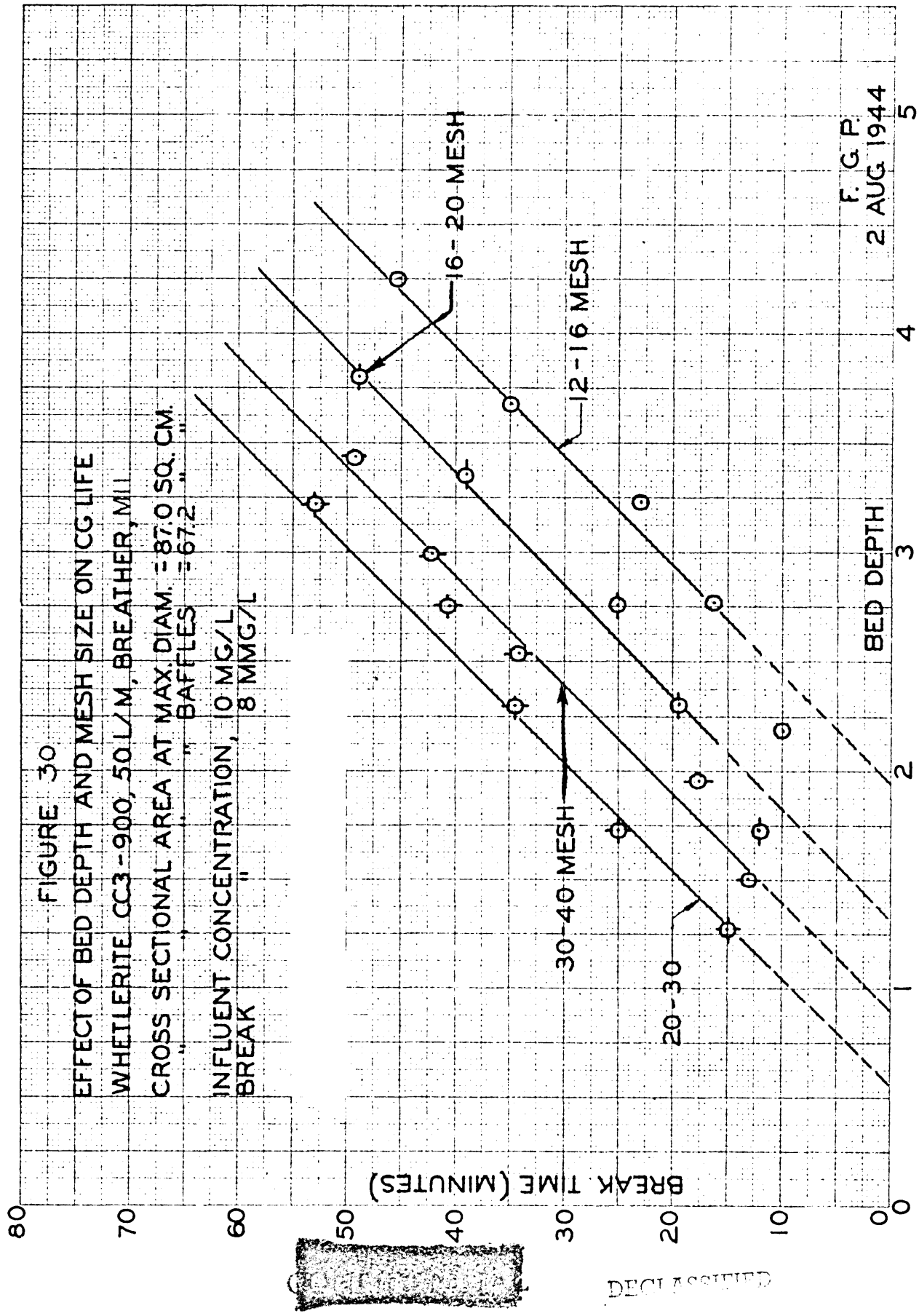

DECLASSIFIED

DECLASSIFIED

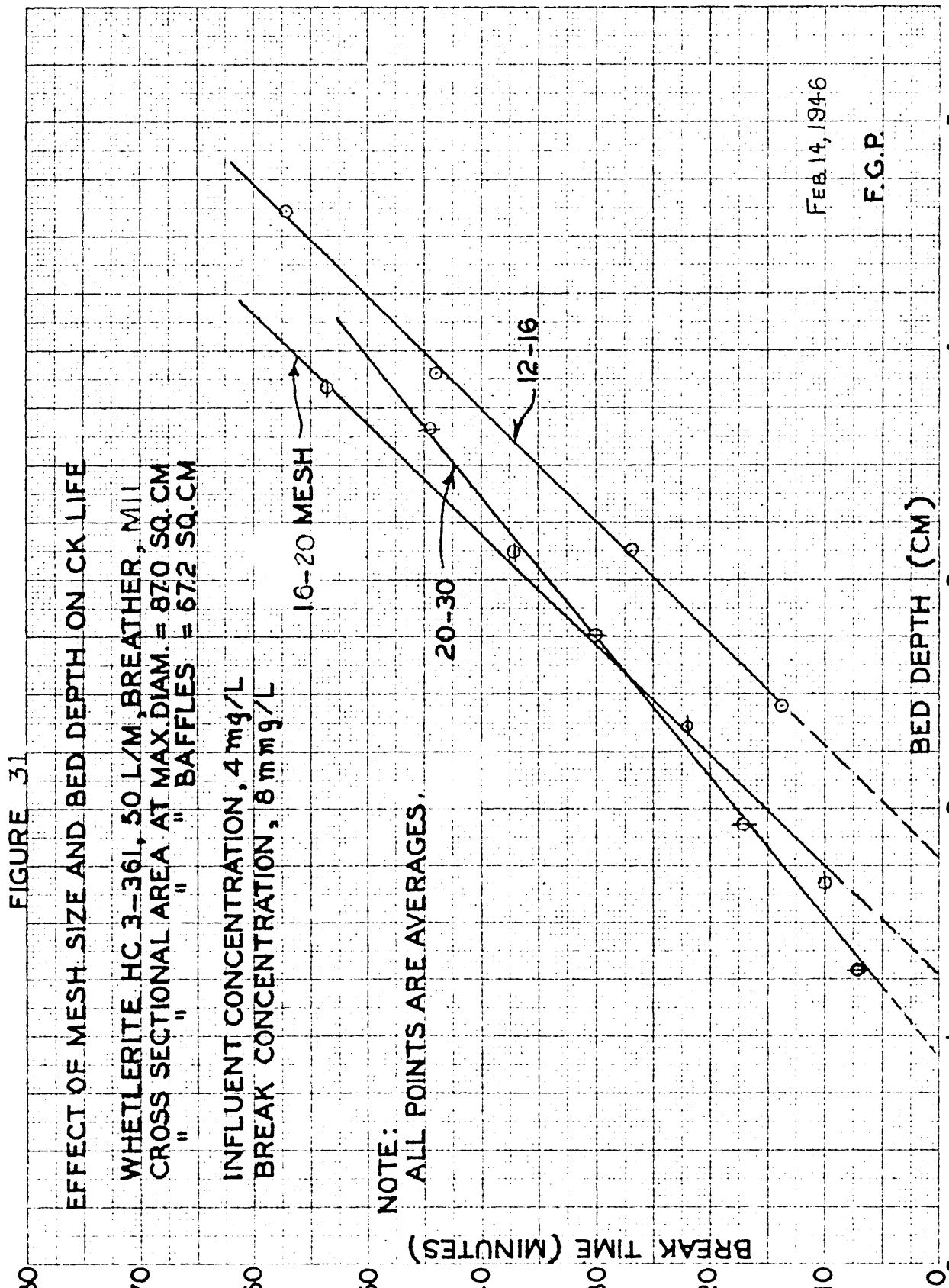

FIGURE 31

DECLASSIFIED

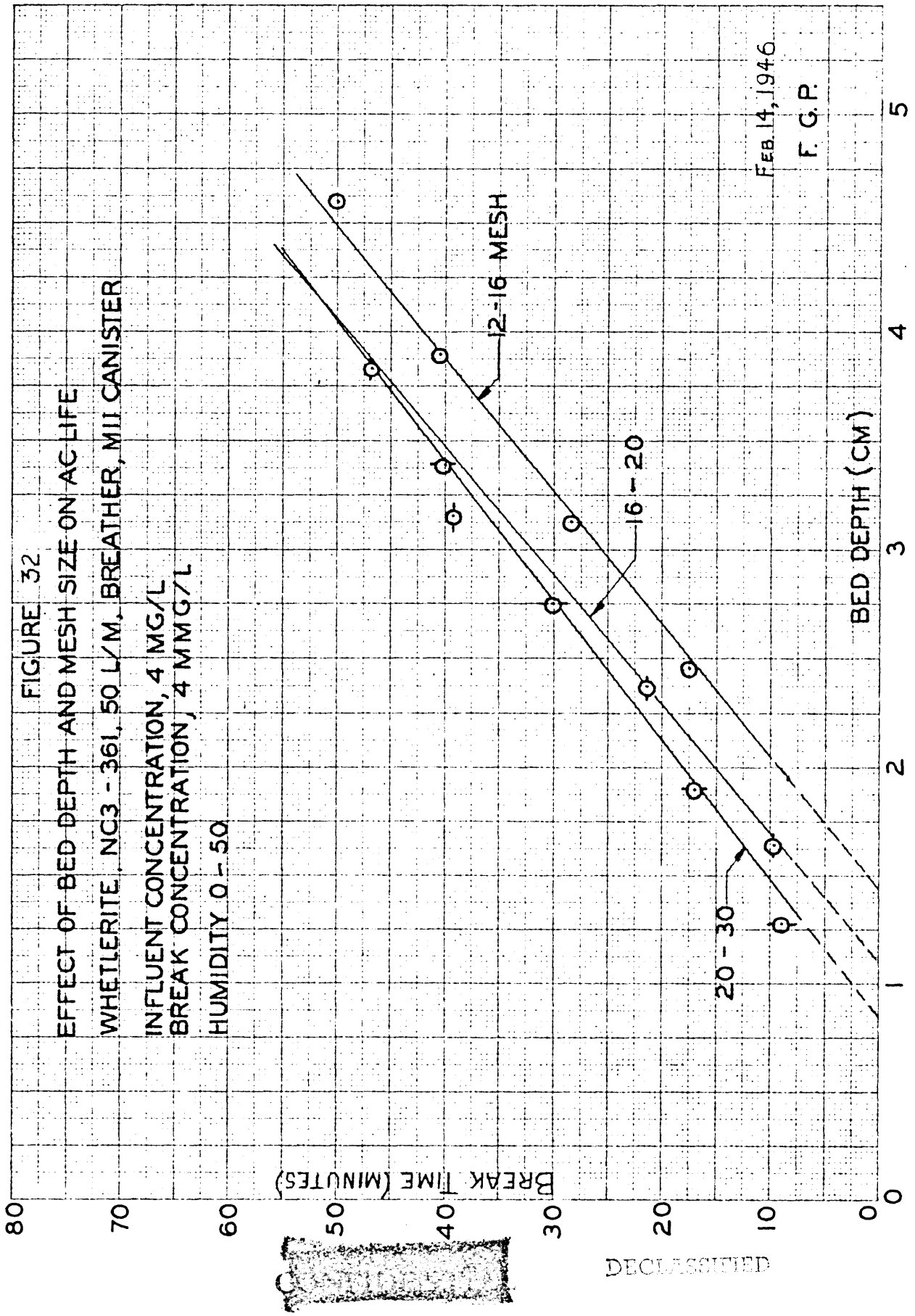

DECLASSIFIED

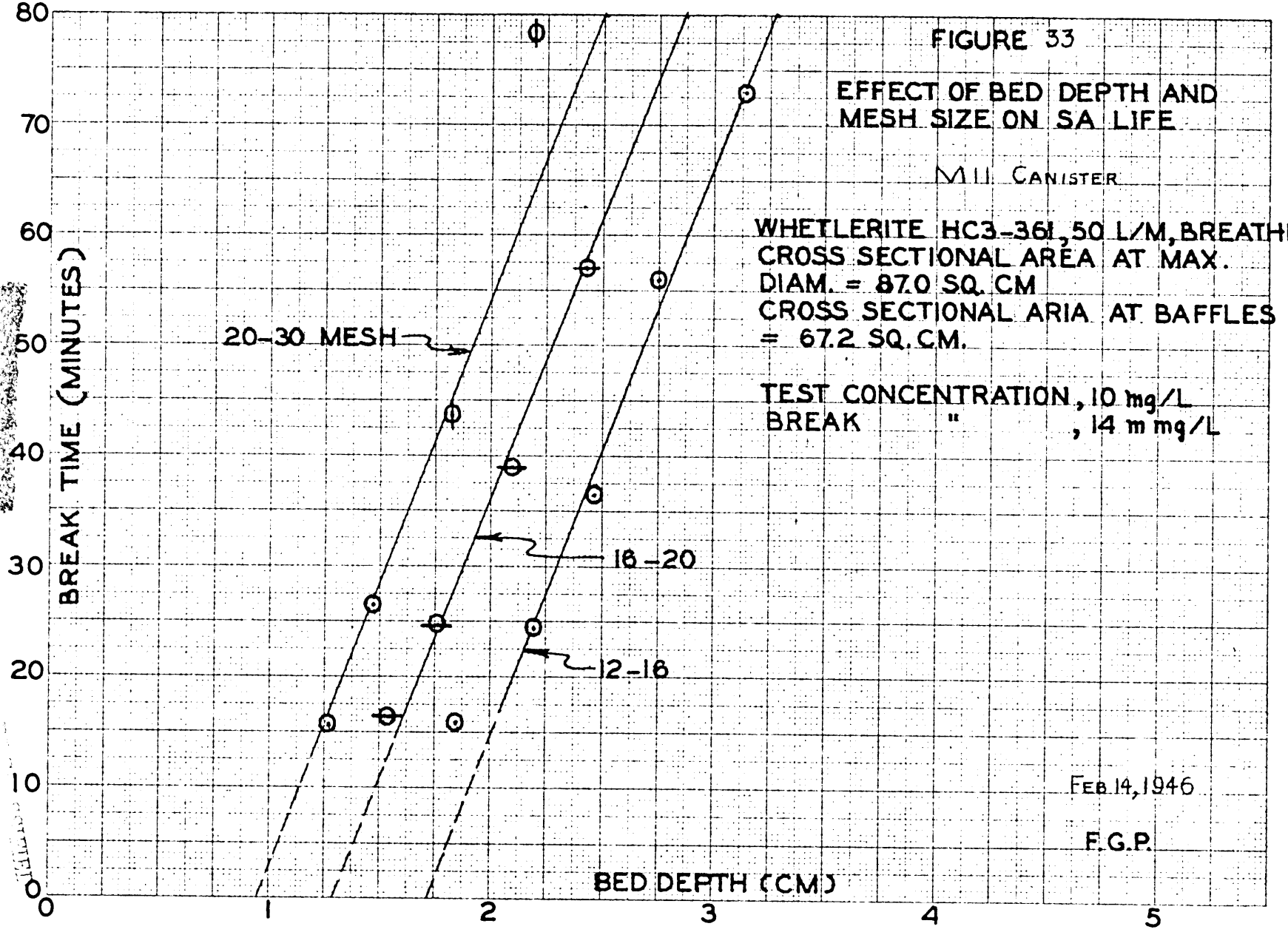

DECLASSIFIED

FIGURE 34

BED DEPTH VS. CG LIFE FOR MESH SIZE BLENDS

50 L/M, BREATHER, M11
CROSS SECTIONAL AREA AT MAX. DIAM. = 87.0 SQ. CM.
" " " " BAFFLES = 67.2 " "

INFLUENT CONCENTRATION, 10 MG/L
BREAK " , 8 MMG/L

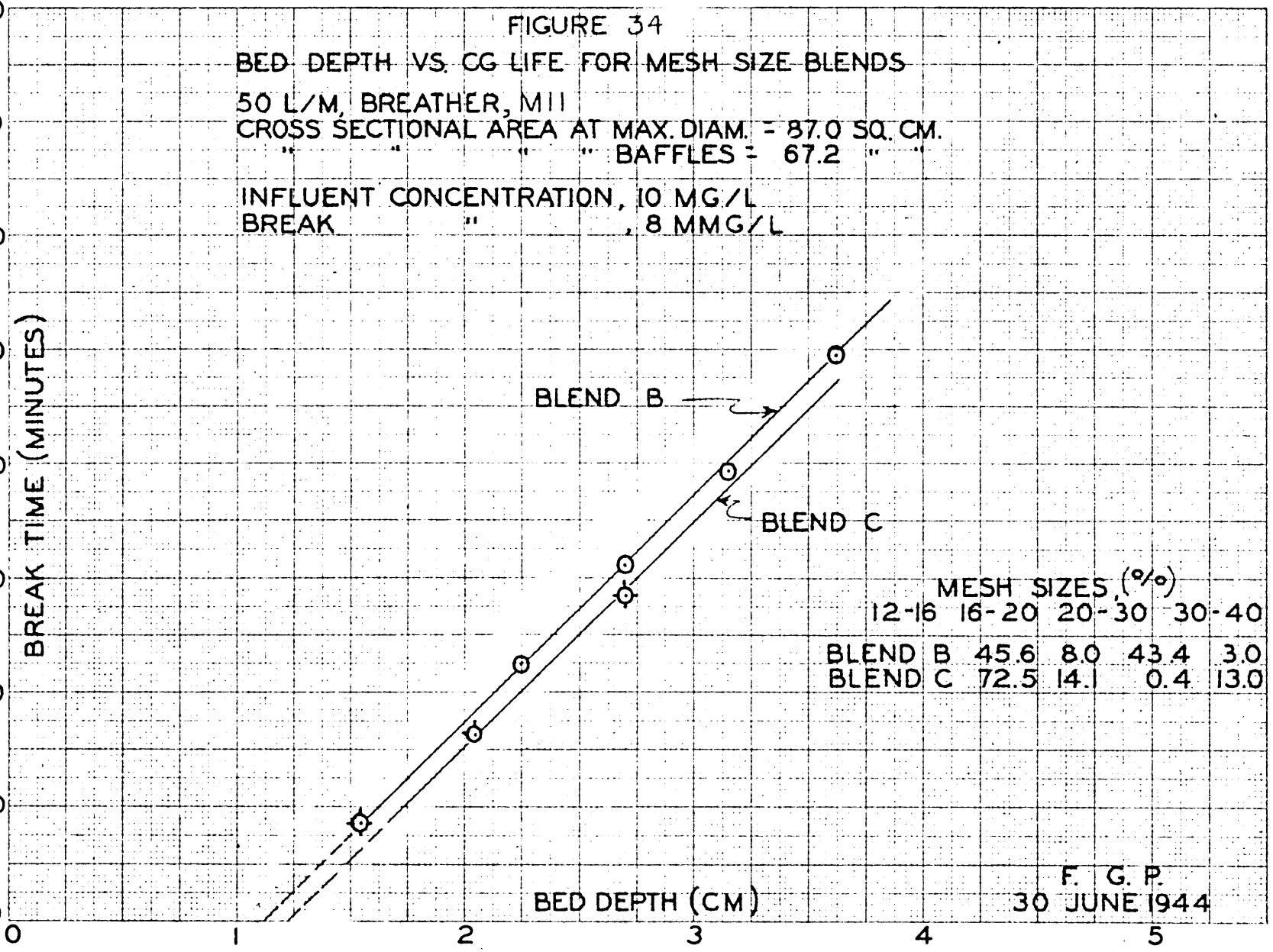

MESH SIZES, (%)	12-16	16-20	20-30	30-40
BLEND B	45.6	8.0	43.4	3.0
BLEND C	72.5	14.1	0.4	13.0

F. G. P.
30 JUNE 1944

DECLASSIFIED

FIGURE 35

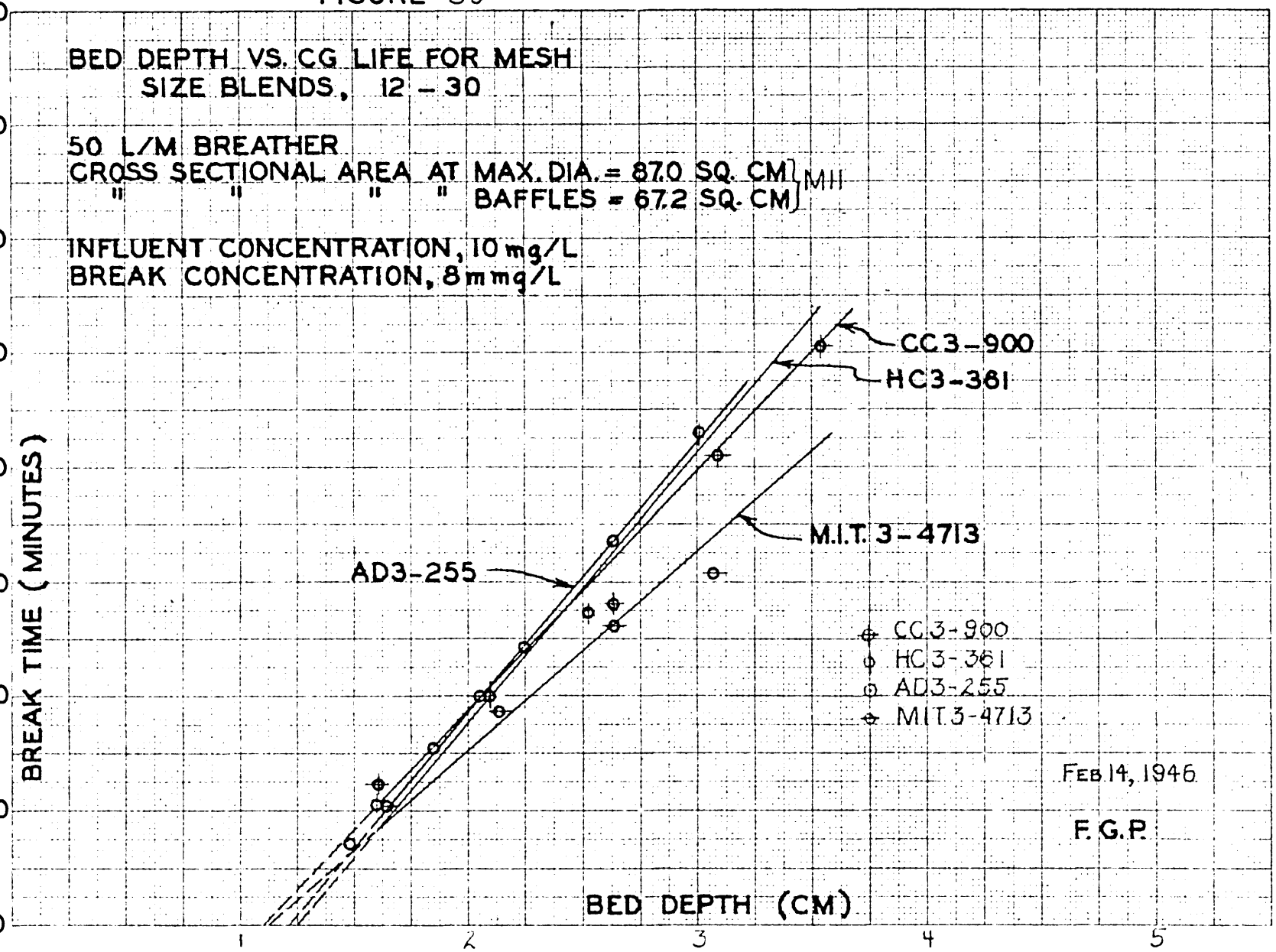

DECLASSIFIED

FIGURE 36

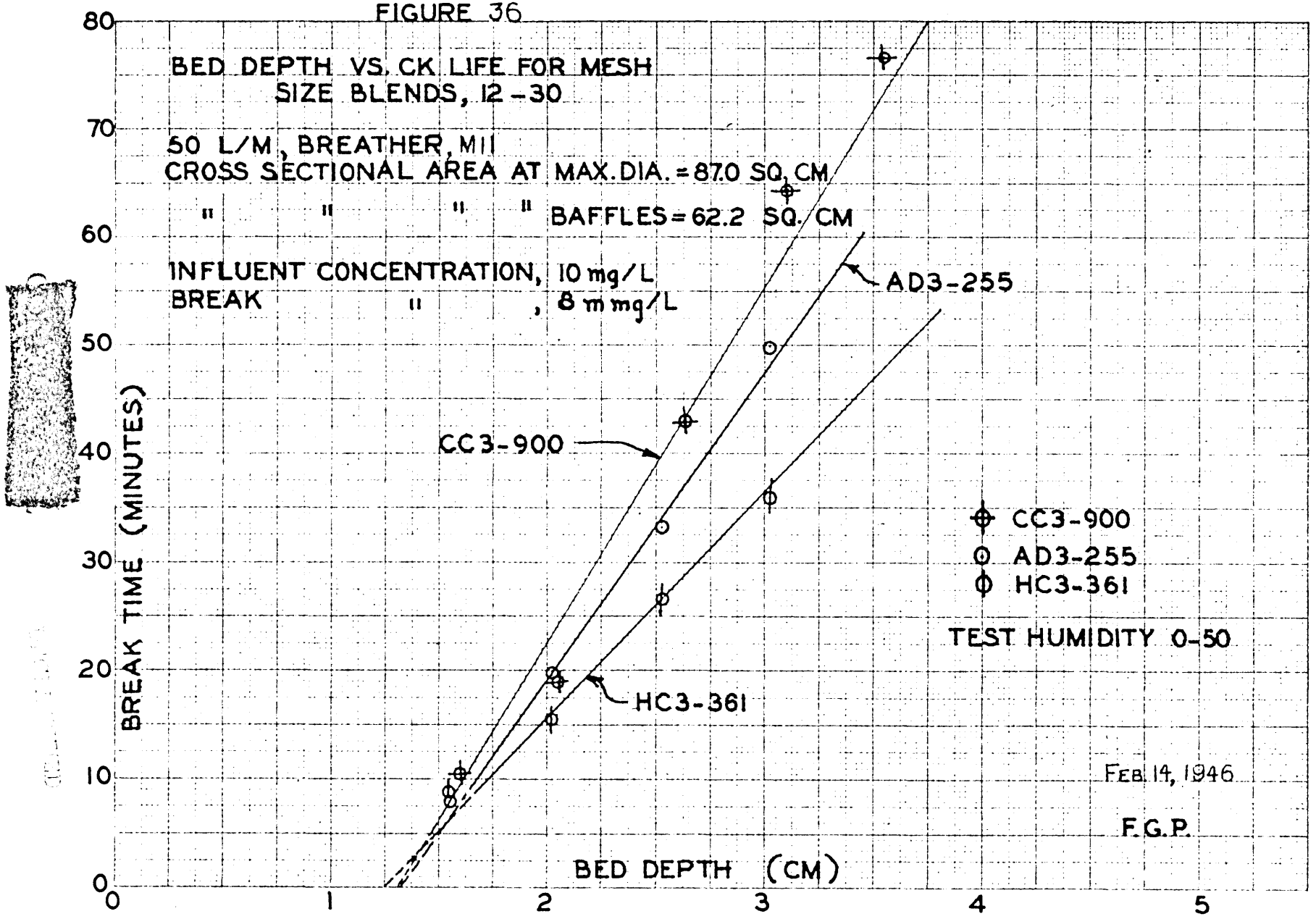

DECLASSIFIED

FIGURE 37

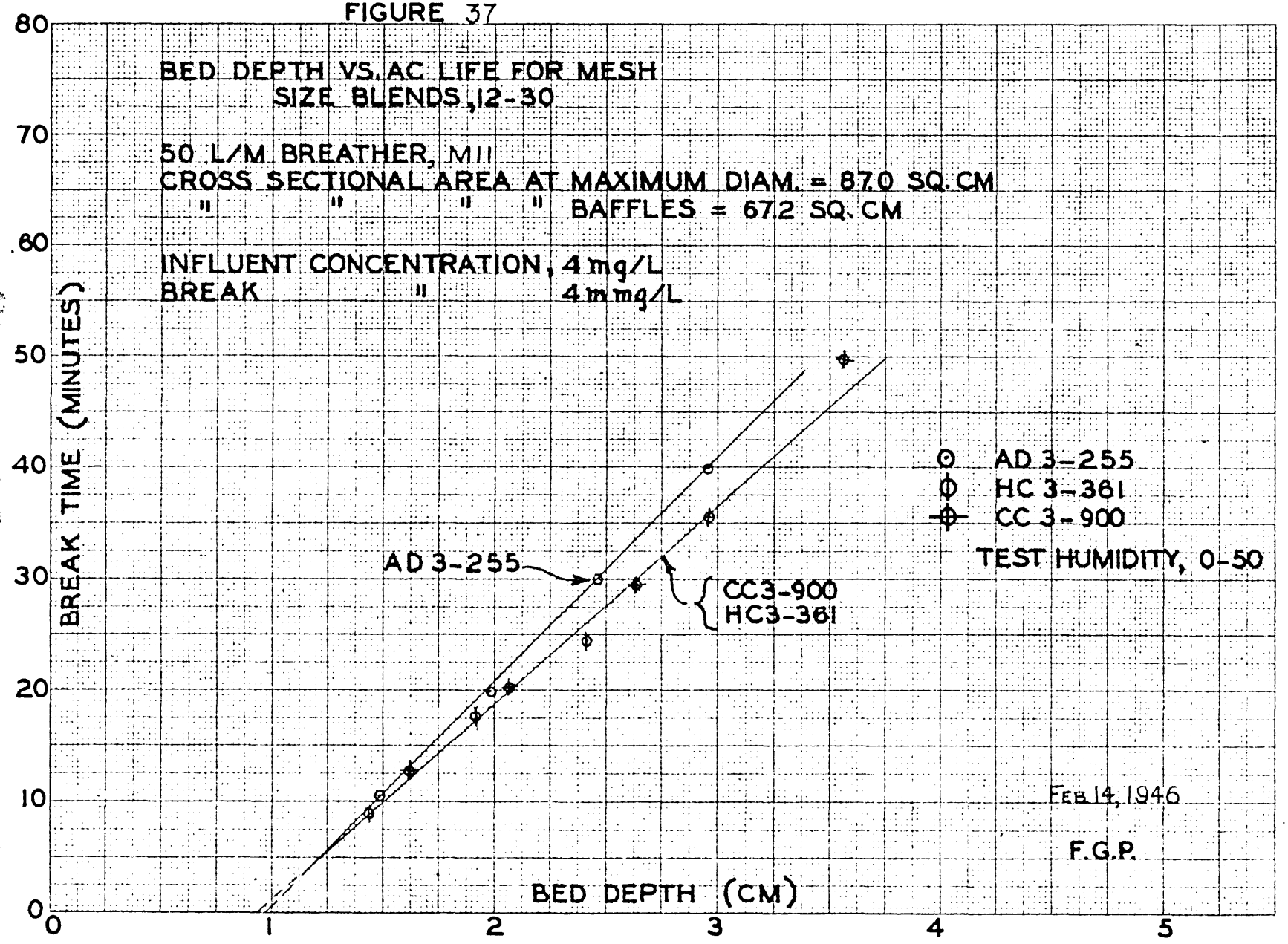
BED DEPTH VS. AC LIFE FOR MESH SIZE BLENDS, 12-30
50 L/M BREATHER, M11
CROSS SECTIONAL AREA AT MAXIMUM DIAM. = 87.0 SQ. CM
" " " " BAFFLES = 67.2 SQ. CM
INFLUENT CONCENTRATION, 4 mg/L
BREAK " 4 mmg/L
AD 3-255
HC 3-361
CC 3-900
TEST HUMIDITY, 0-50
AD 3-255
CC3-900
HC3-361
BREAK TIME (MINUTES)
BED DEPTH (CM)
0
10
20
30
40
50
60
70
80
1
2
3
4
5
FEB 14, 1946
F.G.P.

DECLASSIFIED

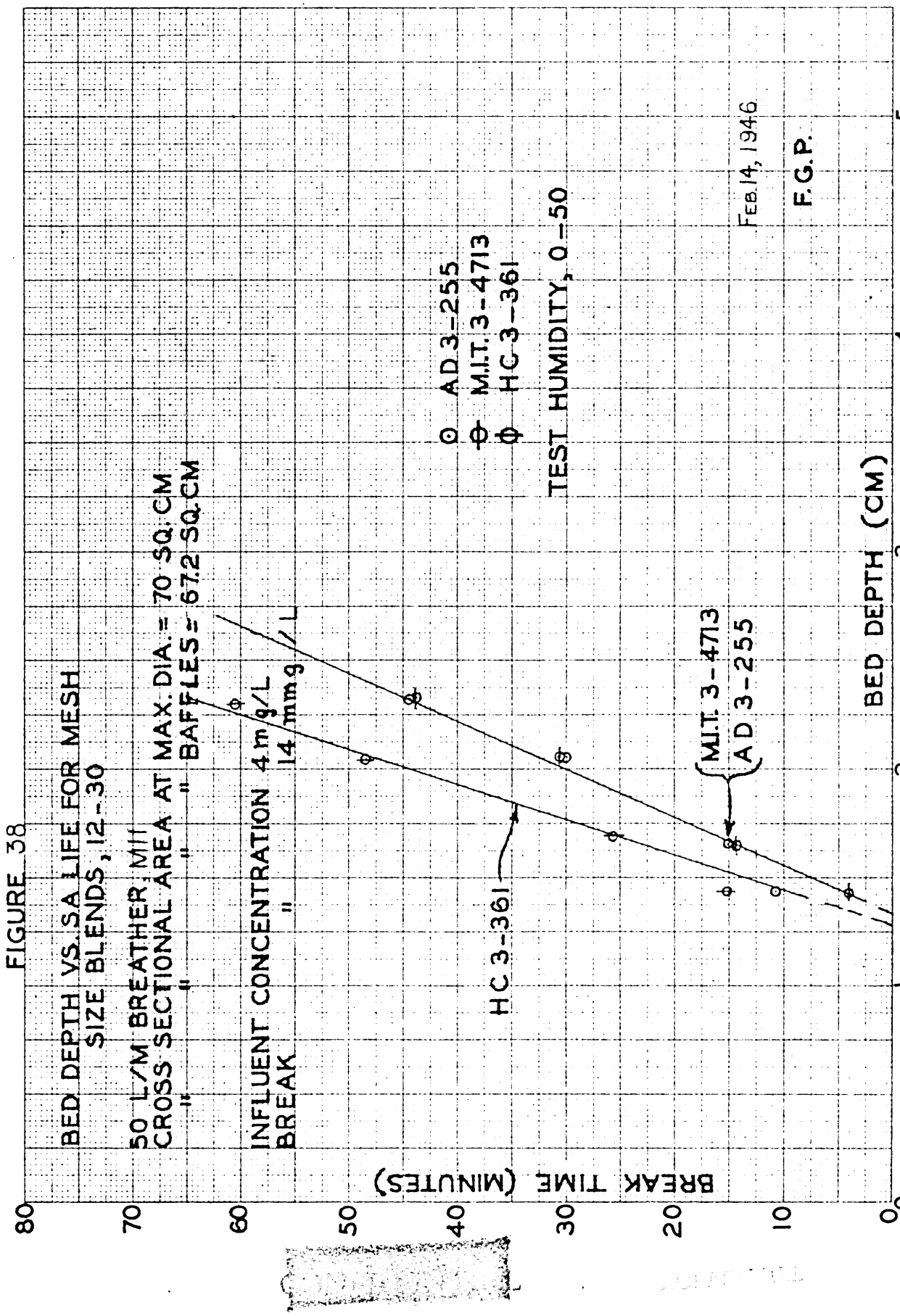

FIGURE 39

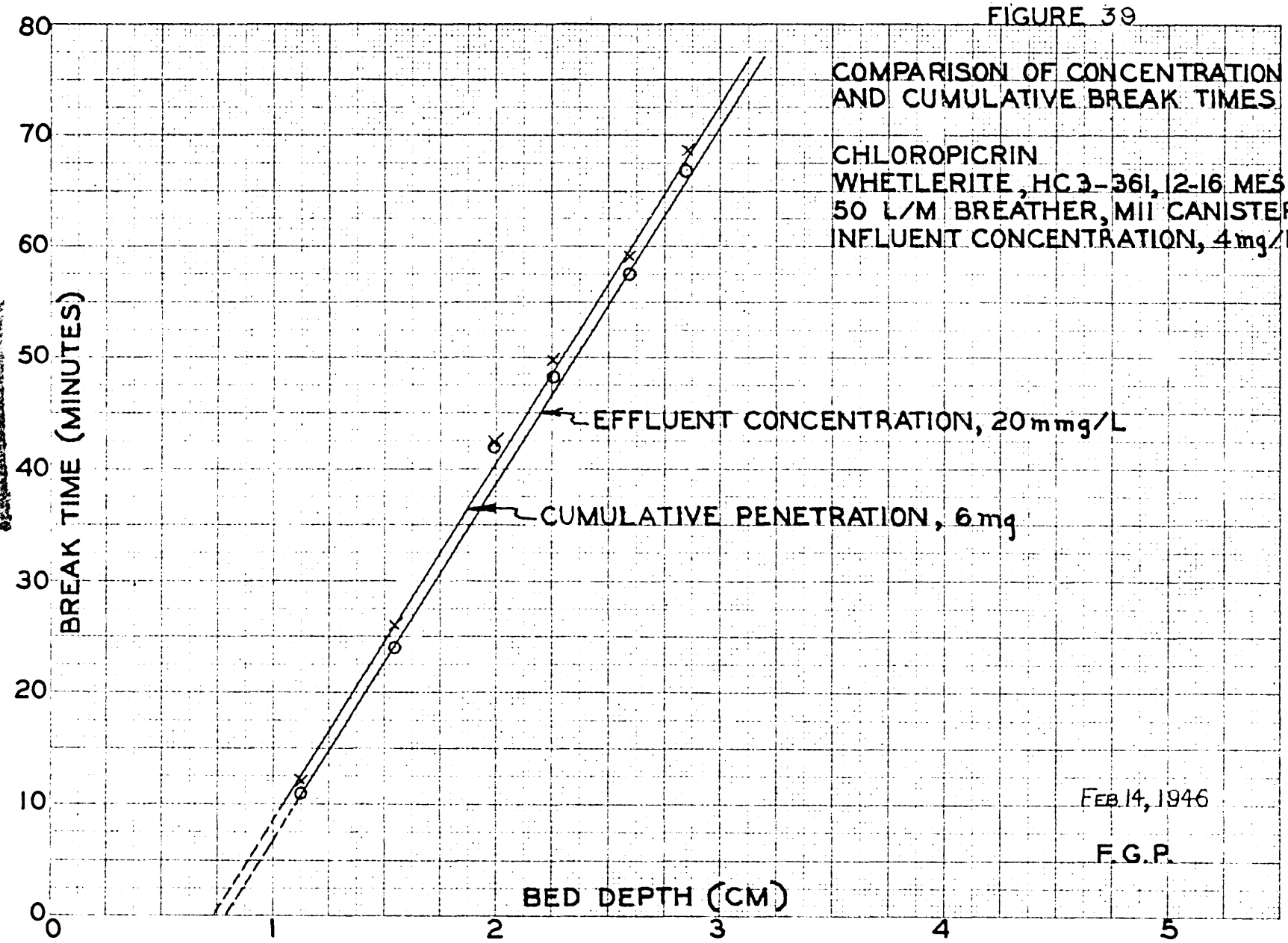

DECLASSIFIED

DECLASSIFIED

FIGURE 40

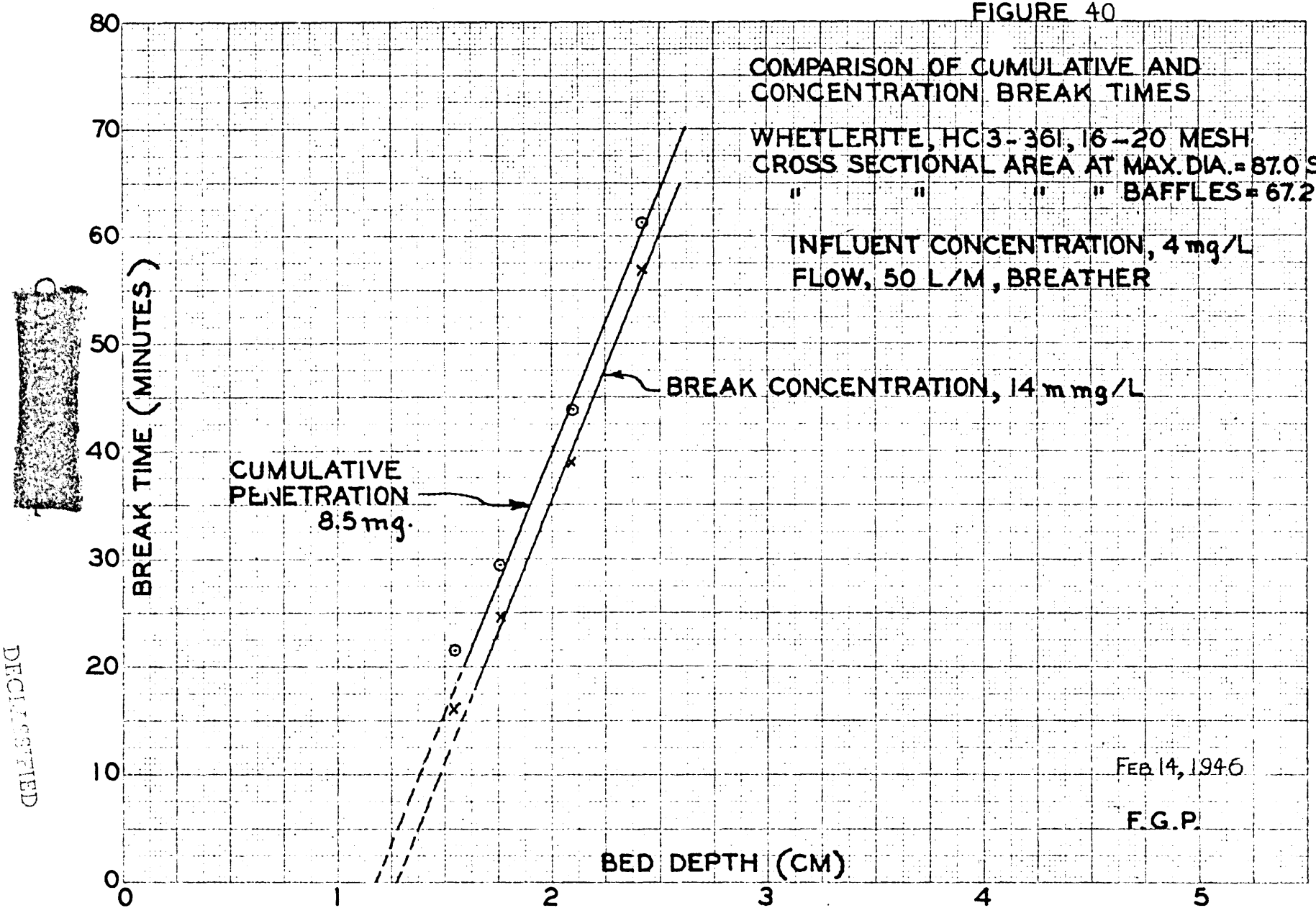

DECLASSIFIED

DECLASSIFIED

FIGURE 41

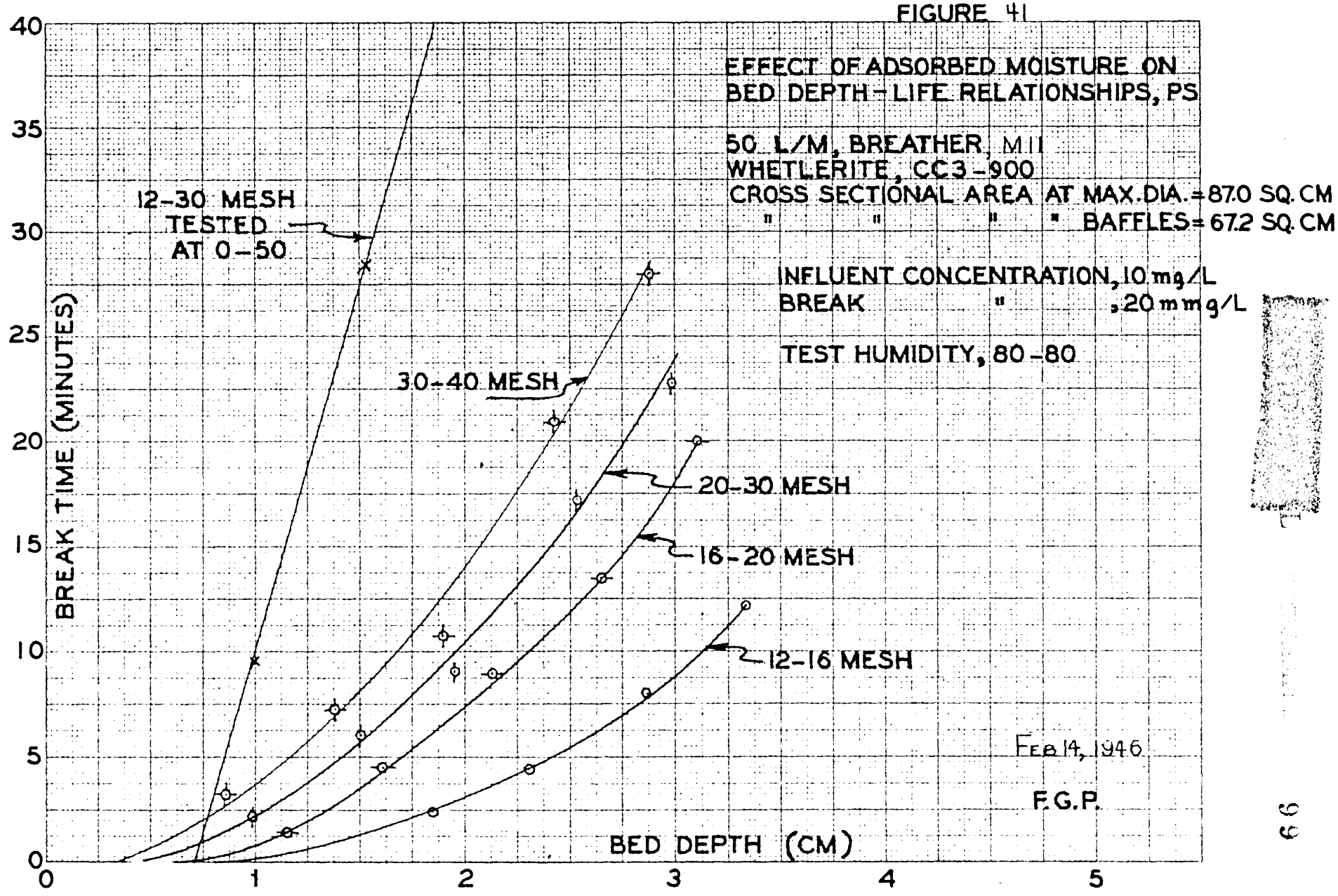

DECLASSIFIED

FIGURE 42

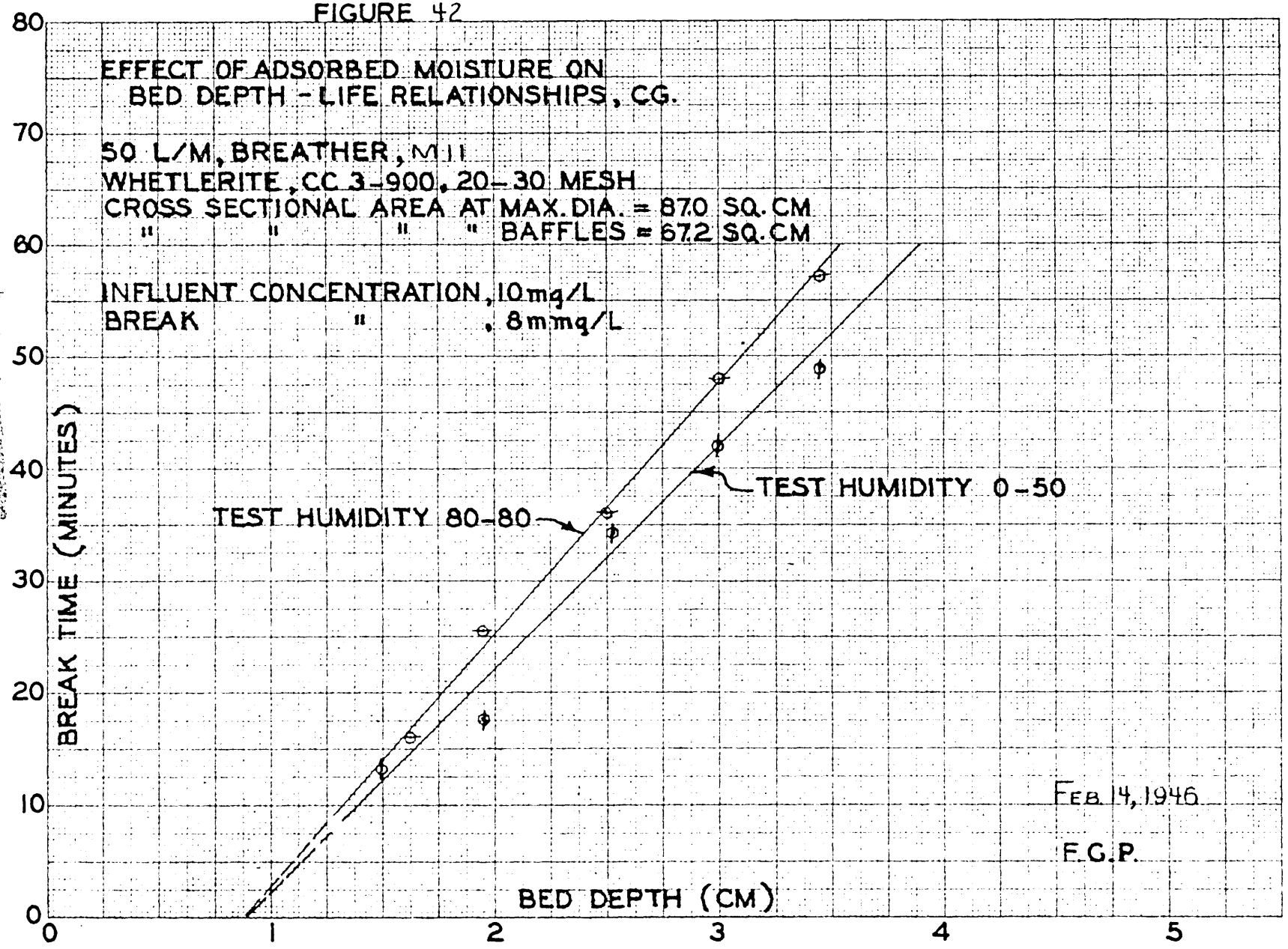

DECLASSIFIED

FIGURE 43

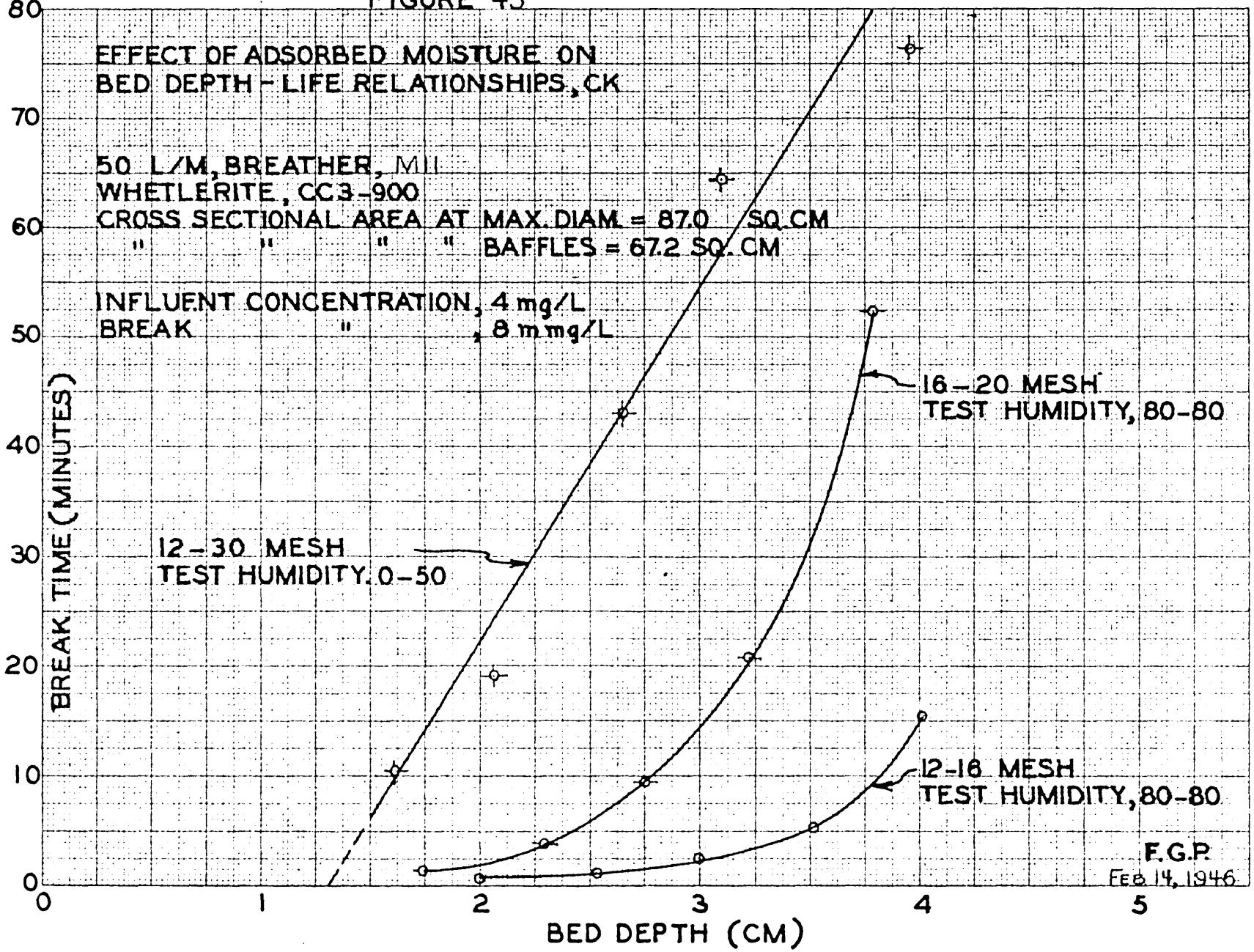

DECLASS. FILE 101

FIGURE 44

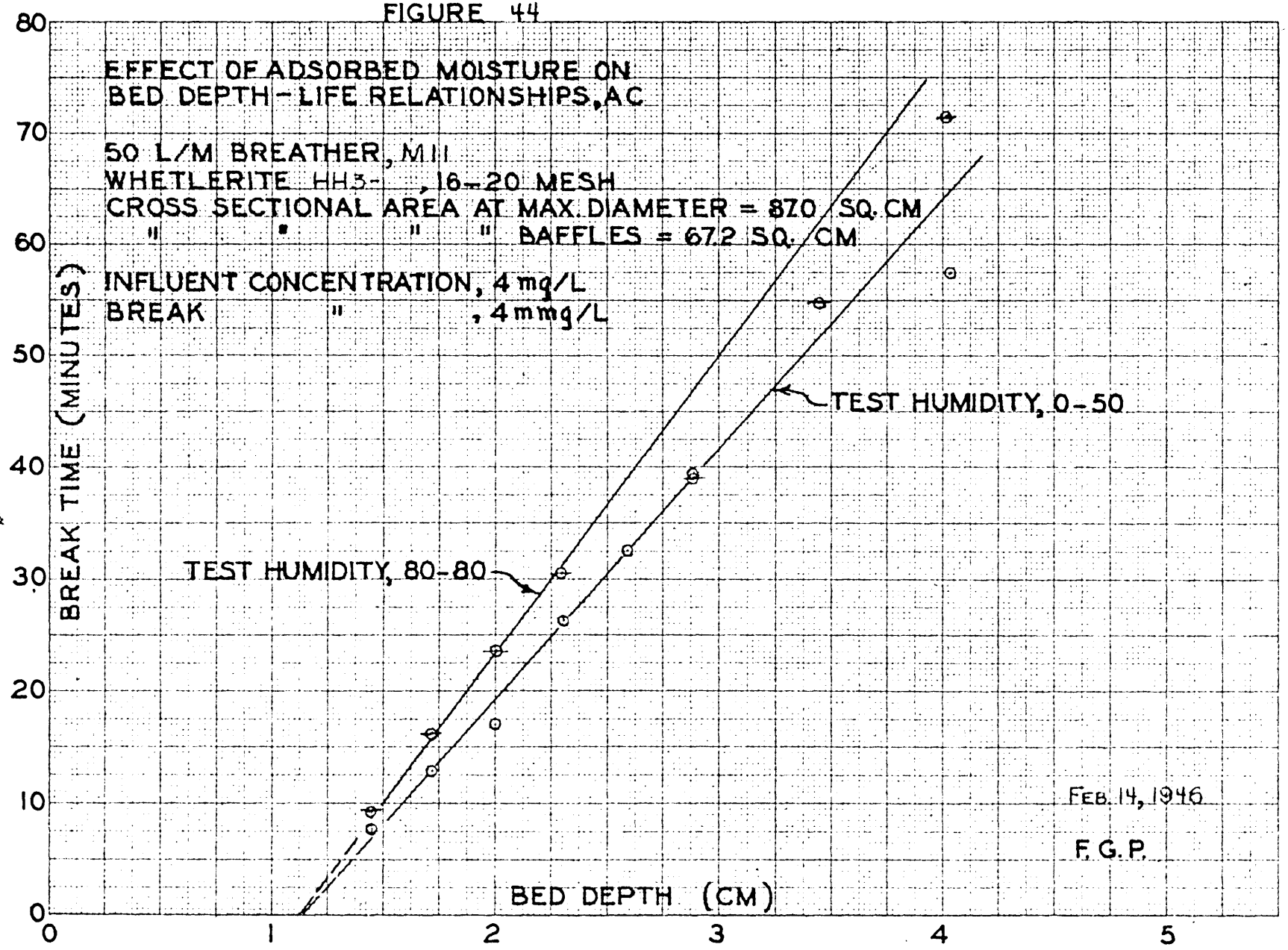

DECLASSIFIED

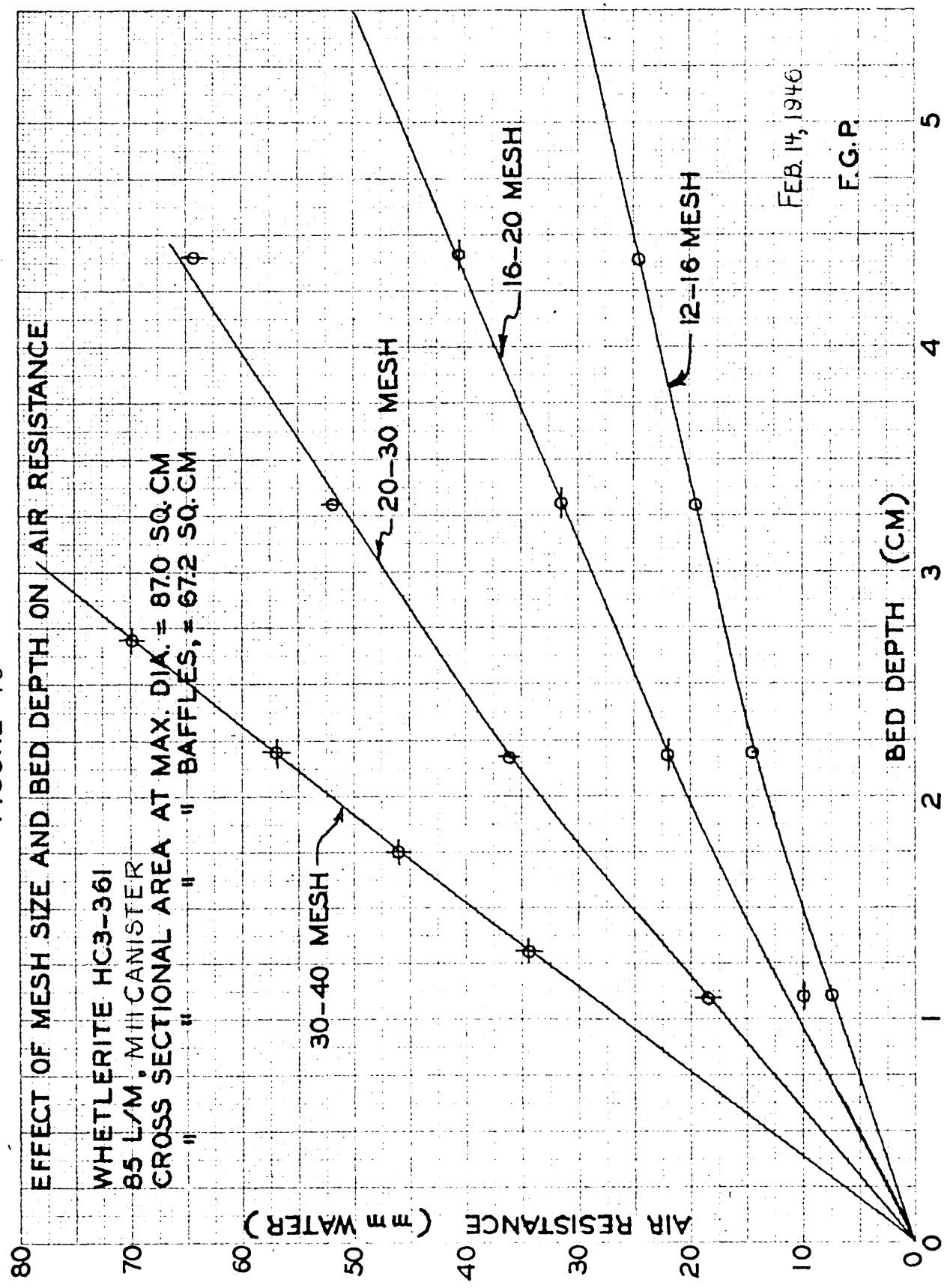
EFFECT OF MESH SIZE AND BED DEPTH ON AIR RESISTANCE
WHETLERITE HC3-361
85 L/M, MII CANISTER
CROSS SECTIONAL AREA AT MAX. DIA. = 87.0 SQ. CM
" " BAFFLES, = 67.2 SQ. CM
" "
FEB. 14, 1946
E.G.P.
30-40 MESH
20-30 MESH
16-20 MESH
12-16 MESH
AIR RESISTANCE (m m WATER)
BED DEPTH (CM)
80
70
60
50
40
30
20
10
0
0
1
2
3
4
5

FIGURE 45

FIGURE 46

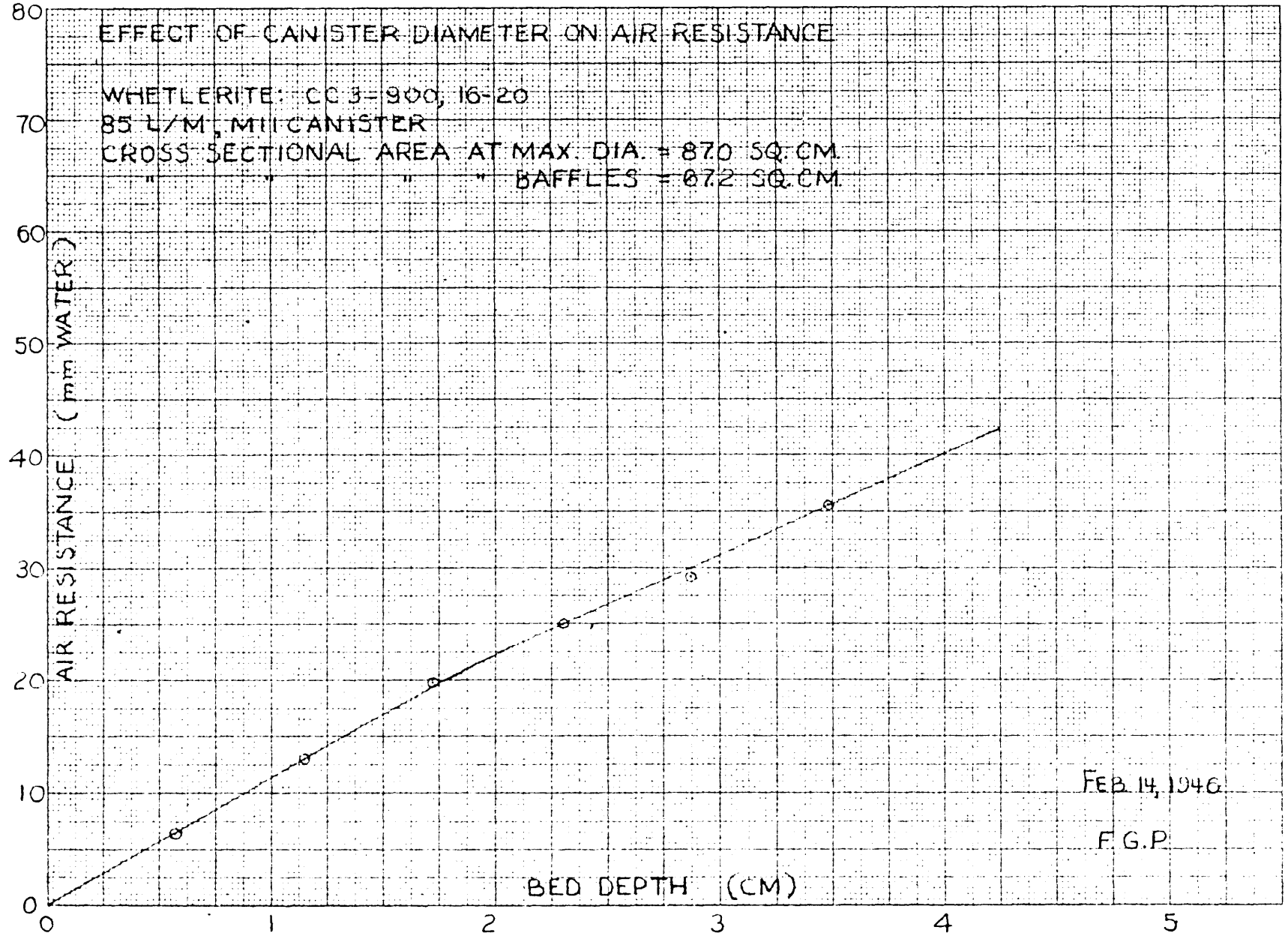

DECLASSIFIED

FIGURE 47

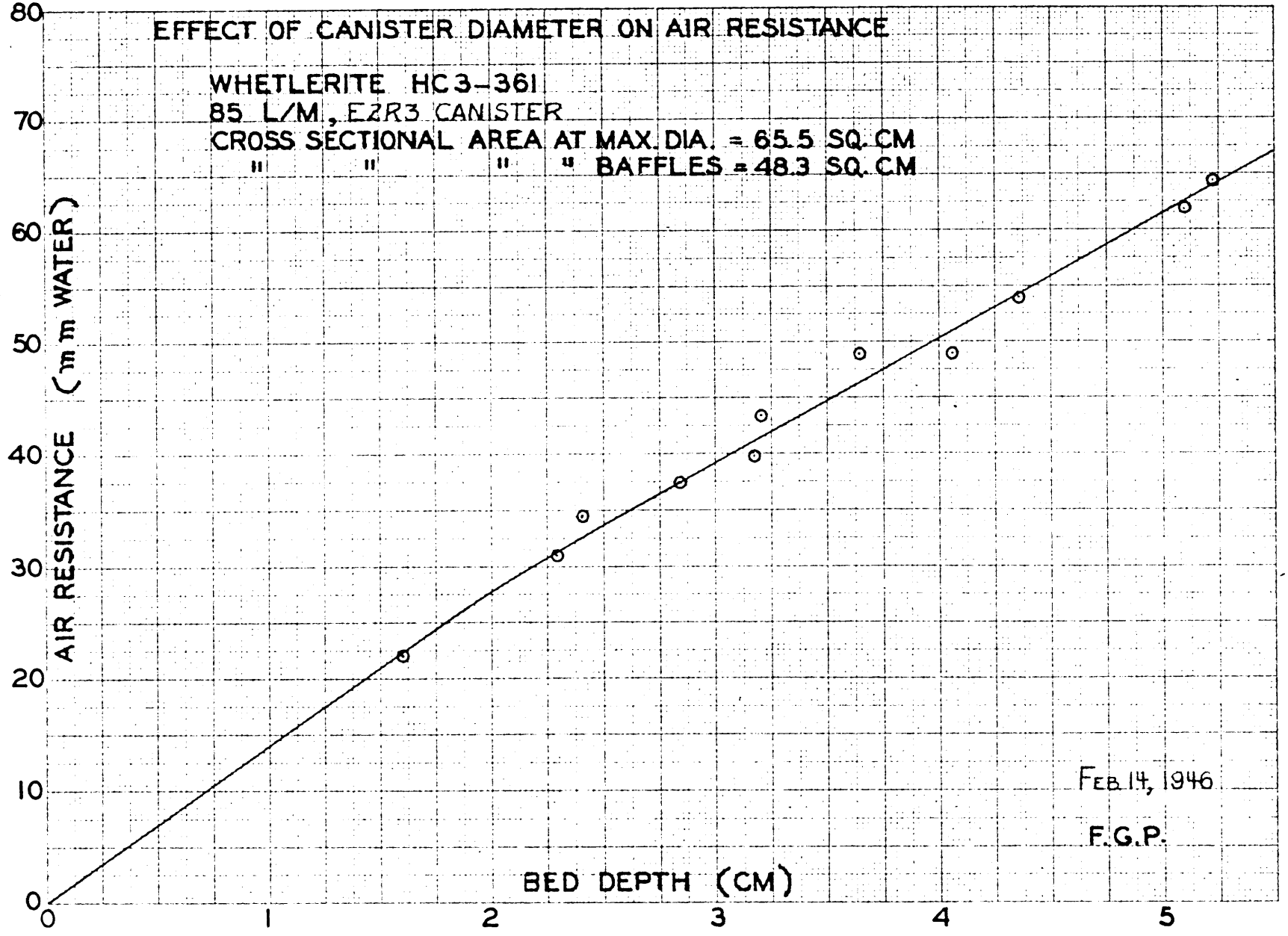

DECLASSIFIED

DECLASSIFIED

FIG. 48

AIR RESISTANCE VS. VELOCITY

WHETLERITE: HC3-361, 390 ml

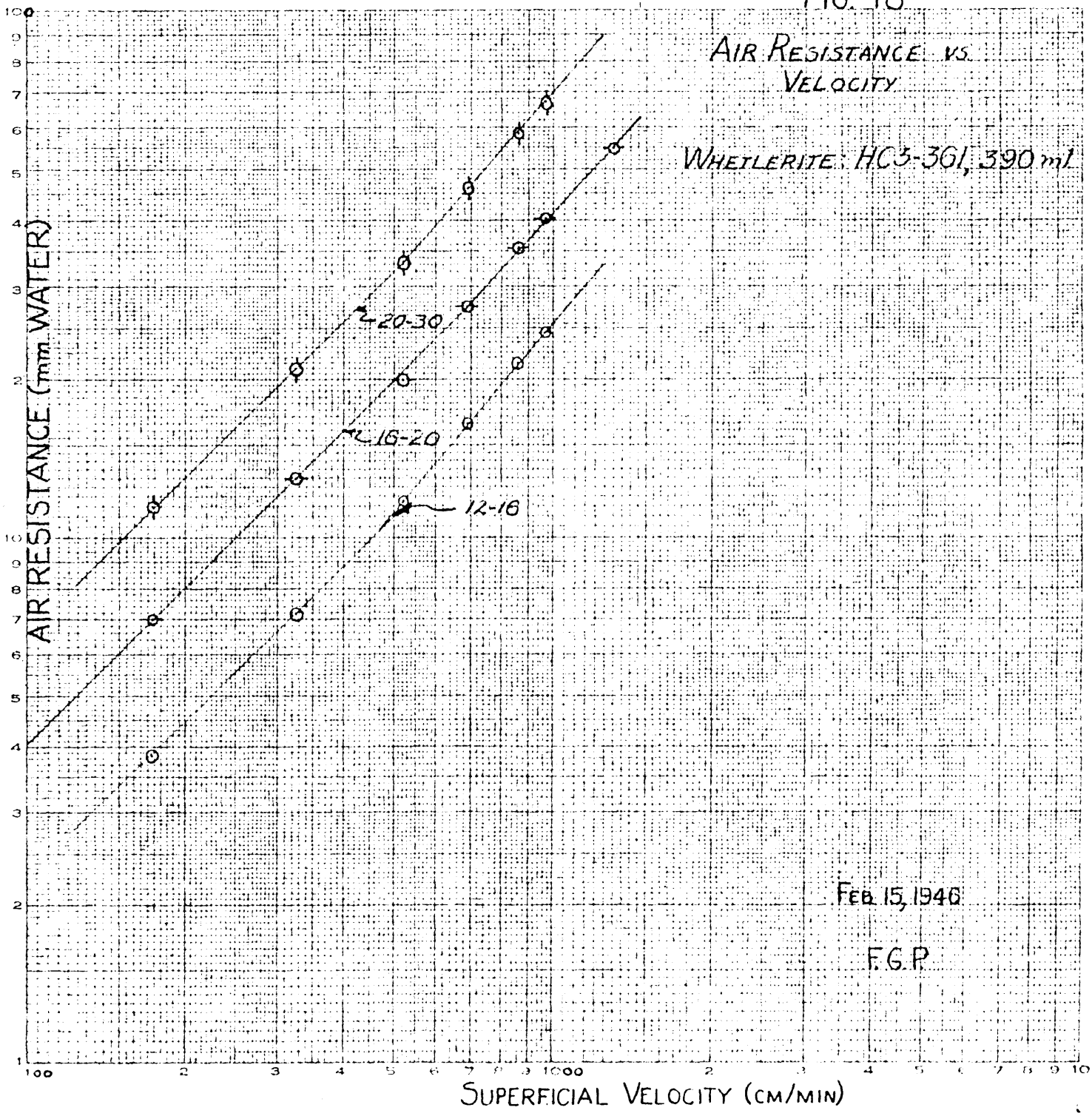

FEB. 15, 1946

F.G.P.

DECLASSIFIED

VII. Discussion of Results

A. Experimental Results

1. Axial Flow Adsorbent Beds

The experimental results of this thesis have been presented in 34 figures and three tables, illustrating the effects of the mechanism of removal, saturation capacity, air flow rate, particle diameter, and break concentration on the performance of an adsorbent bed through which gas-contaminated air is drawn. The points which are plotted in these figures have been corrected by a linear scaling for minor variations in concentration and are, for the most part, averages of two or more duplicate tests. The original data points, as calculated, are tabulated in Appendix G.

The results are discussed in the order which it is believed will result in the most complete and readily grasped understanding of the factors affecting the performance of the adsorbent sections of gas mask canisters.

a. Mechanism of Removal of the Five Standard Agents by Type ASC Impregnated Whetlerite

It was stated previously that the five standard non-persistent Chemical Warfare Service agents are: (1) chloropicrin (PS), (2) phosgene (CG), (3) cyanogen chloride (CK), (4) hydrocyanic acid (AC), and (5) arsine (SA). In order to establish the mechanism by which each of these agents is removed by Type ASC impregnated whetlerite, tests were conducted in which bed depth-break time curves were

obtained for (a) an unimpregnated whetlerite and (b) a Type ASC impregnated whetlerite.

The tests with the unimpregnated whetlerite were conducted using a carrier air stream at a relative humidity of 30 per cent; whereas, the tests with the Type ASC impregnated whetlerite were conducted using a carrier air stream at a relative humidity of 50 per cent. The reason for the use of a low relative humidity for the unimpregnated charcoal tests was to preclude the complication of chemical reaction between adsorbed agent and adsorbed water and to limit the mechanism of removal to reversible, physical adsorption. This was done as a safeguard although it was shown that the moisture gain of adsorbent beds during performance tests is negligible even at relative humidities as high as 50 per cent(43). A previous report by the writer and others (42) showed that only very small amounts of water are adsorbed by charcoal in equilibrium with air at 30 per cent relative humidity. The nature of the water adsorption isotherm is illustrated in Fig. 49.

The tests with the Type ASC impregnated whetlerite were conducted at 50 per cent relative humidity because that is the standard test humidity for the evaluation of adsorbent beds.

The results of these tests are shown in Figs. 15, 16, 17, 18, and 19.

It was shown in Appendix A that the slope of the bed depth-break time curve, for reversible ad-

DECLASSIFIED

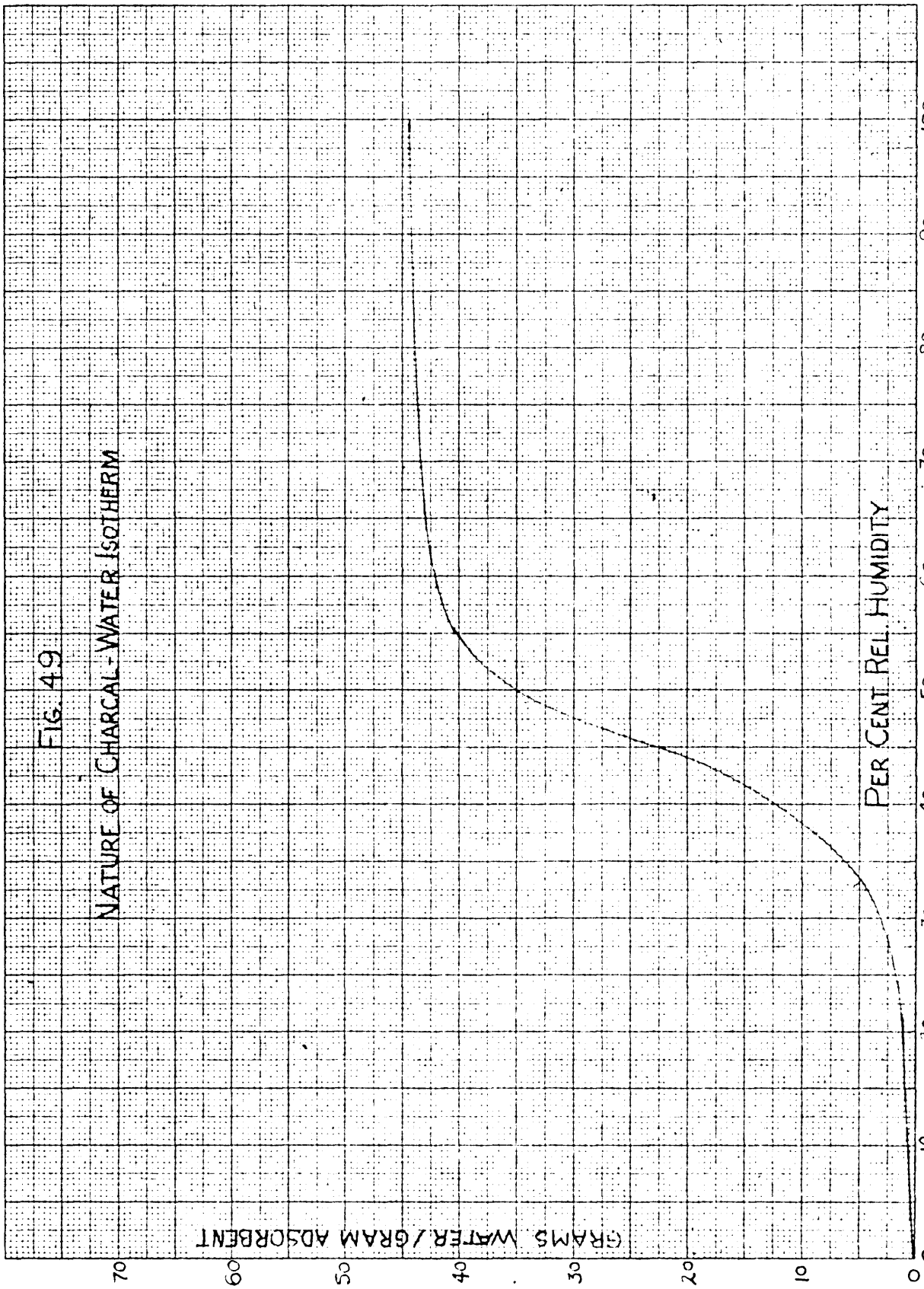

FIG. 49
NATURE OF CHARCAL-WATER ISOTHERM

sorption, should be proportional to the saturation capacity of the adsorbent at the test concentration. Although the saturation capacity varies to some extent with the degree of activation of the base charcoal, the great differences in the slopes (comparison of slope of unimpregnated and impregnated charcoal curves) of the bed depth-break time curves for phosgene, cyanogen chloride, hydrocyanic acid, and arsine indicate that these agents are removed to a large extent by chemical reaction with the impregnants. The slopes of the chloropicrin bed depth-break time curves, however, are practically identical indicating that this agent is removed by both types of adsorbent by physical adsorption.

Another method of distinguishing between the two general mechanisms of removal (physical adsorption and chemical reaction) is the analysis of the intercept of the linear portion of the bed depth-break time plot on the bed depth axis. Although the extrapolation of these plots for phosgene, cyanogen chloride, hydrocyanic acid, and arsine removal by the unimpregnated charcoal are not highly accurate, they are sufficiently accurate to establish the fact that, for these four agents, the intercept (apparent critical bed depth) is much smaller for the unimpregnated charcoal than for the Type ASC impregnated whetlerite. This is definite proof that some rate other than the rate of transfer through the stagnant air film surrounding the granules controls the rate of removal of these agents from the air stream.

The apparent critical bed depths are identical for chloropicrin. This substantiates the conclusion that the mechanism of removal of chloropicrin by Type ASC impregnated whetlerite is by physical adsorption and that the rate of diffusion through the stagnant air film surrounding the granules controls the rate.

b. Chloropicrin Performance

(1) Slope of Bed Depth-Break Time Curve

It is shown in Appendix A that, for Type I kinetics, the slope of the bed depth-break time curve is related to the saturation capacity of the adsorbent at the test concentration by the following equation for those cases when n in Freundlich's isotherm effectively exceeds two:

$$N_o = \frac{C_1 Q S}{A} \qquad (36)$$

The adsorption isotherm was determined for a particular, unimpregnated charcoal and chloropicrin in order to establish the validity of this theoretical equation. The results are shown in Fig. 20. For this particular adsorbent, n in Freundlich's equation varies from six to eleven. Equation 1 should be valid for these high values of n, for the criterion is not that n shall be constant and exceed two but that the isotherm shall at all points be such that the equilibrium concentration at any particular adsorbate content shall be less than it would be were n to equal two.

A bed depth-break time curve was determined for this particular charcoal. This curve is shown in Fig. 21. These tests were conducted at a test concentration of 65 mg./L. Under these conditions, the saturation capacity is obtained from Fig. 20 to be 400 mg./ml. The saturation capacity, calculated from the slope of the bed depth-break time curve and Equation 36, is 356 mg./ml. which is 90 per cent of the actual value. This ten per cent discrepency may be caused by (1) the presence of the influent and effluent baffles, (2) the heat of adsorption, or (3) the slowness of the final stages of adsorption on the granules.

(2) Effect of Velocity on Slope of Bed Depth-Break Time Curve

A series of tests was made to determine the effect of velocity on the chloropicrin bed depth-break time relationships. The dependent variables under investigation were the slope of the bed depth-break time curve and the apparent critical bed depth. These tests were conducted in the M11 canister at 32 L./min, constant flow, 64 L./min, constant flow, and 50 L./min., breather flow. The results of these tests are shown in Fig. 22.

The breather data were analyzed by the method proposed in Appendix C.

The following tabulation shows that N_o , as obtained from the slope of the bed depth-break time plots, is constant as predicted by Equation 1.

Table VII

Constancy of N_o for Chloropicrin Adsorption

Flow Rate (L./min.)	Slope (min./cm.)	C_1 (mg./L.)	A (sq.cm.)	N_o (mg./ml.)
32 C.F.	46.5	10.0	87.0	171
64 C.F.	23.9	10.0	87.0	176
50 B.	31.7	10.0	87.0	182
			Average	176

(3) Effect of Ratio of Test to Break Concentration on Apparent Critical Bed Depth

No data were obtained in this thesis to determine the relationship between the ratio of the test to the break concentration and the apparent critical bed depth, for the work of Dole and Klotz (41) showed that Equation 40, derived in Appendix A, was valid. Their results are shown in Fig. 50. They are plotted as the apparent critical bed depth vs. the natural logarithm of the ratio of the test to the break concentration. The straight line relationship which is obtained is in agreement with Equation 40 which is as follows:

$$\lambda_c = H_t \left(\ln \frac{C_1}{C_2} - \beta\right) \qquad (40)$$

The intercept of this straight line on the concentration ratio axis is equal to β and, in this particular instance, is approximately 0.5. The accuracy of the measurements is not sufficient to warrant a precise

FIGURE 50

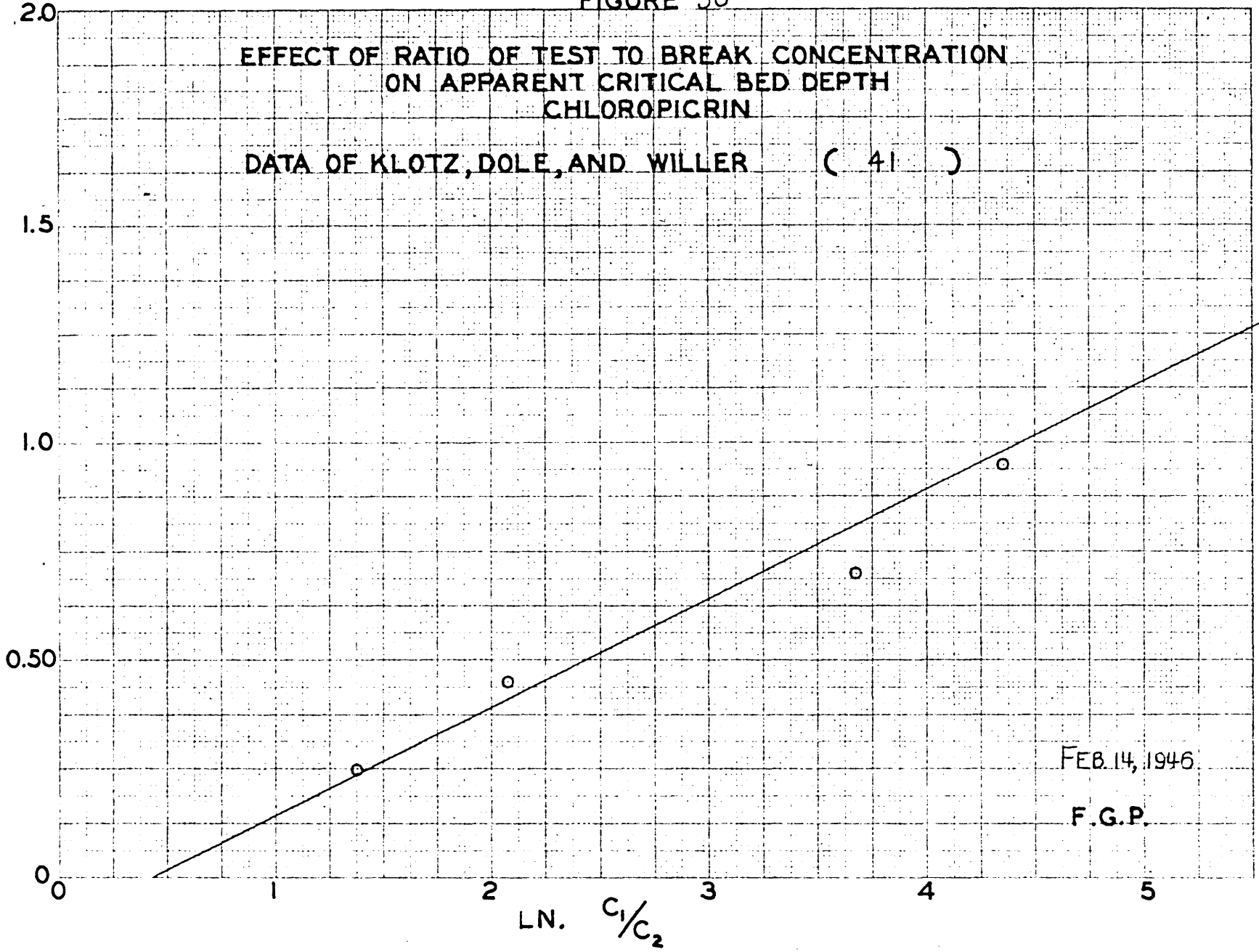

DECLASSIFIED 1 1 4

evaluation of β, but it is sufficiently accurate to indicate a value between zero and unity. This, also, is in complete agreement with the conclusions of Appendix A. Throughout this thesis, β is considered as unity for chloropicrin because n in Freundlich's isotherm is large for chloropicrin-whetlerite and because a small variation in β does not affect the result appreciably when the value of $\ln \frac{C_1}{C_2}$ is large.

The slope of the straight line of Fig. 50 is equal to H_t and, in this particular instance, is equal to 0.25 cm. Unfortunately, the mesh size and flow rate were not specified so that a comparison between the results depicted by Fig. 50 and those obtained in this thesis is impossible.

(4) Effect of Velocity of Flow on H_t

The apparent critical bed depths at each of the test velocities (Fig. 22) are tabulated below with the derived values of H_t calculated by Equation 40.

Table VIII

Variation of λ_c and H_t with Velocity
Chloropicrin; 16-20 Mesh Whetlerite

Q (L./min.)	λ_c (cm.)	C_1 (mg./L.)	C_2 (mg./L/)	H_t (cm.)
32, C.F.	0.42	10.0	.020	.0798
64, C.F.	0.51	10.0	.020	.0970
50, B.	0.62	10.0	.020	.118

These values of H_t are plotted as a function of velocity on logarithmic paper in Fig. 51. The velocities equivalent to the volume flow rates were determined by dividing the volumetric rate by the open area at the effluent baffle, for the critical layer (portion of bed corresponding to the critical bed depth) is obviously located at the effluent end of the canister and it is shown in Table VIII that it is less than one cm. in depth. The results of bed depth-air resistance measurements show that the air flow follows the baffled area for approximately one centimeter into the bed (see Figs. 46 and 47) after which it spreads out over the entire area of the canister. Therefore, the area at the effluent baffle is the logical one to use for correlation of the apparent critical bed depth with velocity.

The air flow rate equivalent to 50 L./min, breather, was obtained by reference to Fig. 92, Appendix C. An estimate of the value of x, the exponent in the equation relating H_t to velocity, is necessary, and this approximation is checked by the conformity of the point so plotted with the line formed by the other two points. Practically, there is very small error in the first approximation, for the steady flow rate equivalent to breather flow is a very shallow function of x. The value of x, the slope of the plot of the logarithm of H_t vs. the logarithm of velocity, is obtained from Fig. 51 to be 0.285. It is not believed that the extent of these measurements validates the enumeration of such a precise

DECLASSIFIED

FIGURE 51

EFFECT OF AIR VELOCITY ON H_T, PS
WHETLERITE HC 3-361, 16 - 20 MESH

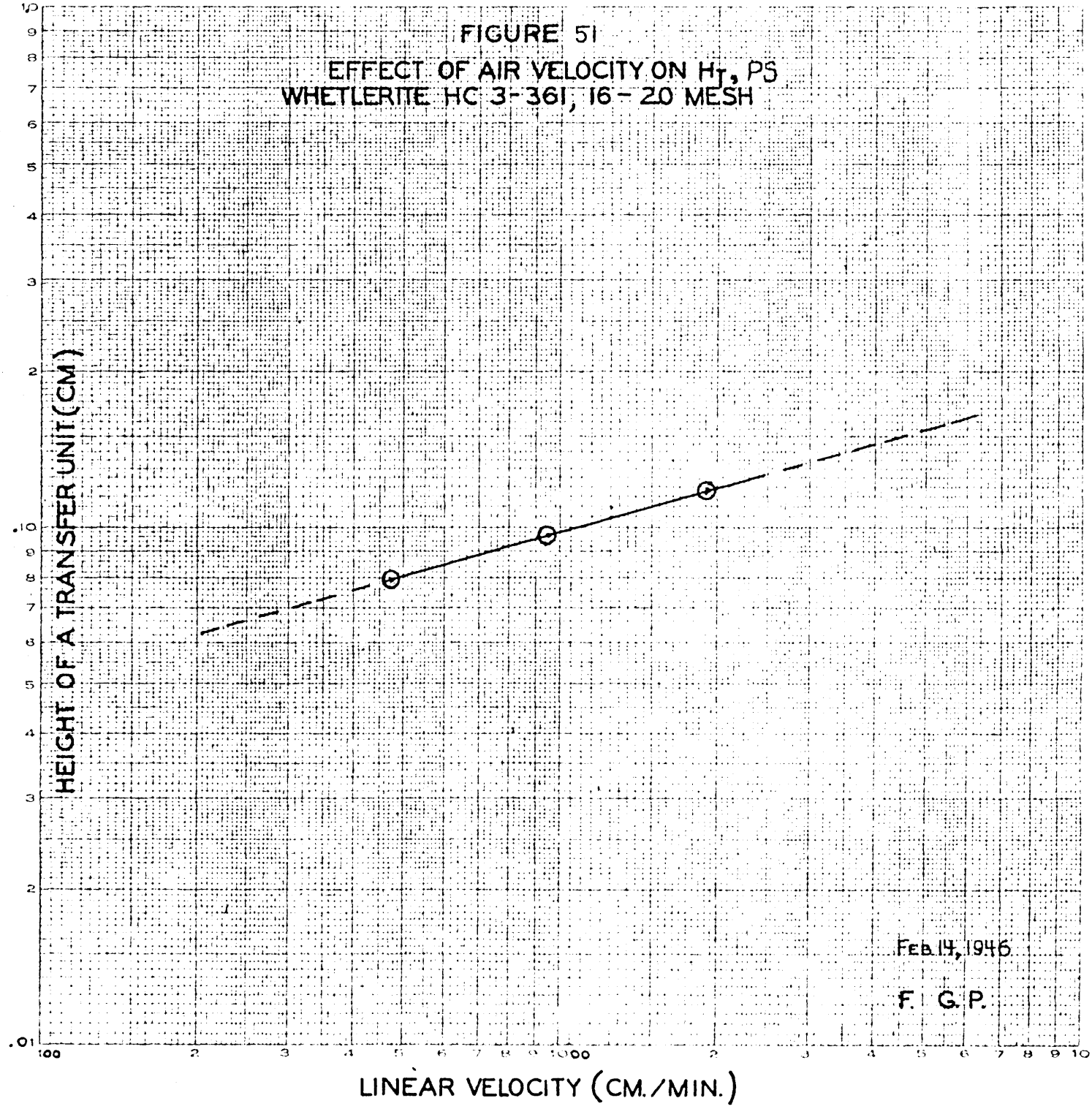

DECLASSIFIED

figure; therefore, in all future applications, it will be rounded off to 0.30.

The fact that the breather data correlated so well proves that the theoretical argument of Appendix C for adaptation of the steady flow equations to breather testing is correct.

(5) Effect of Particle Size on Critical Bed Depth and H_t

A series of tests was made to determine the chloropicrin bed depth-break time relationships for the three mesh size fractions predominant in Type ASC impregnated whetlerite as produced for U. S. gas mask canisters. These tests were made at 50 L./min., breather, in the M11 canister. The results are shown in Fig. 23.

Since it has previously been established that the height of a transfer unit varies as the 0.3 power of the air velocity, the apparent critical bed depths obtained are representative of those which would be obtained at a steady flow rate of 127 L./min. (see Fig. 92, Appendix C).

The slopes of the bed depth-break time plots are practically identical which is as predicted by theoretical considerations. The apparent critical bed depths differ, however, and they and the derived H_t values are given in Table IX.

The derived H_t values are plotted as a function of average particle diameter (average of limits of sieve openings) in Fig. 52 on logarithmic paper.

CONFIDENTIAL

DECLASSIFIED

FIGURE 52

EFFECT OF MESH SIZE (PARTICLE DIAMETER) ON H_t FOR CHLOROPICRIN ADSORPTION

WHETLERITE, HC 3-361
MII CANISTER, 50L/M, BREATHER

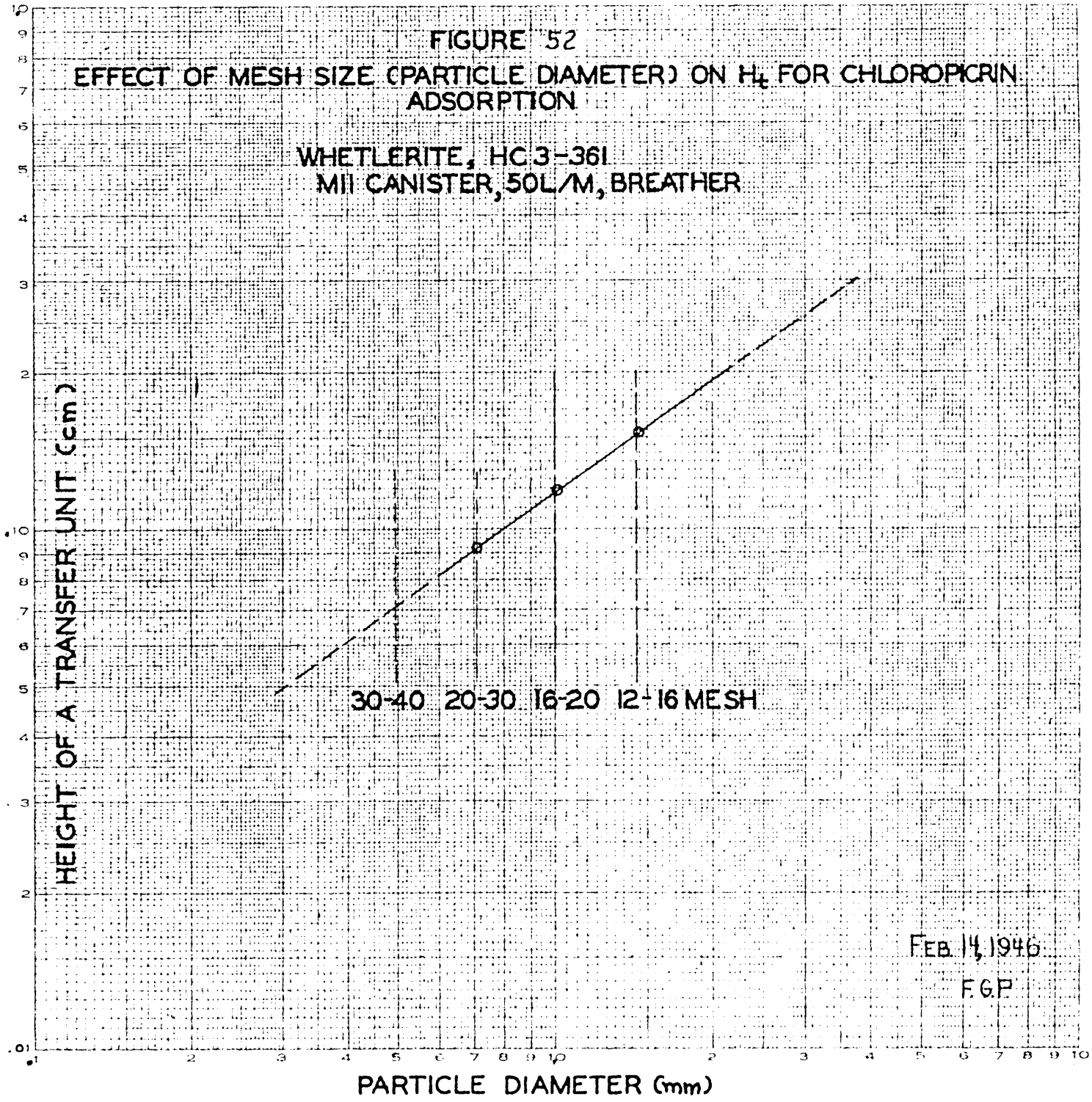

CONFIDENTIAL

The slope of the straight line relationship obtained was measured to be 0.71. This figure is "rounded off" in this thesis to 0.70. It indicates that, over the range investigated, H_t varies as the 0.7 power of the particle diameter as calculated from the average sieve openings.

Table IX

Variation of λ_c and H_t with Sieve Size
Chloropicrin Adsorption

Sieve Size	λ_c (cm.)	C_1 (mg./L.)	C_2 (mg./L.)	H_t (cm.)
12-16	0.79	10.0	.020	.152
16-20	0.62	10.0	.020	.119
20-30	0.48	10.0	.020	.092

(6) Constancy of Ht for Several Whetlerites and Correlation of H_t with Blends of Several Sieve Sizes

Several series of tests were made to determine the chloropicrin bed depth-break time relationships for blends of the predominant sieve sizes. These tests were conducted at 50 L./min., breather, in the M11 canister; four different whetlerites were tested. The results of these tests are shown in Fig. 24, and the blends employed are shown in Table VI.

These plots show that the variation in the saturation capacity for the four whetlerites tested, as reflected by the slope of the bed depth-break time curves, is not great. This is indicative of a relatively uniform activation.

The apparent critical bed depths and the derived values of H_t are given in Table X as are the calculated values of $\bar{H}_t$. The calculated values were obtained from the sieve analyis, the values of H_t for the pure sieve fractions, and Equation 128 which is derived in Appendix F.

Table X

Effect of Sieve Size Blends and Type Whetlerite on H_t Chloropicrin Adsorption

Whetlerite	λ_c (cm.)	H_t (cm.)	Calculated H_t (cm.)	Dev. (%)
HC3-361	0.58	.111	.115	+ 3.6
AD3-255	0.68	.130	.120	- 7.7
CC3-900	0.69	.132	.112	- 15.2
MIT 3-4713	0.57	.109	.116	+ 6.4
			Root mean square of deviations	± 9.3

The best agreement between the calculated and measured values of H_t was obtained for the particular whetlerite with which the values of H_t were determined for the pure sieve fractions (HC3-361), and it is believed that the agreement is within the limits of accuracy of the measurements. Although the other deviations are not large, they are believed to be outside the limits of experimental accuracy and are probably the result of the non-spherical nature of the granules and the non-similarity of the shape of the particles for the different whetlerites. That such non-similarities in particle shape do exist is shown by the differences

in air resistance which will be discussed in a later section.

c. Phosgene, Cyanogen Chloride, Hydrocyanic Acid, and Arsine

(1) Classification of Type of Kinetics

It is quite important that the type of kinetics governing the removal of each of these agents be known, for, as discussed in Appendix E, "Removal of Agents by Chemical Reaction with Impregnants", with all types except Type III-B (1) there is no upper limit on the straight line relationship between bed depth and break time, (2) the slope of this straight line relationship is directly proportional to $N_o + N_r$, (3) the apparent critical bed depth is a true function of H_t and H_r , and (4) the effects of the influent and break concentrations on the apparent critical bed depth are known.

The possibility that the rate of removal of these agents is governed by Type II kinetics (removal by chemical reaction when the rate of chemical reaction is much greater than the rate of diffusion to the surface of the granule) is immediately eliminated by the results shown in Figs. 15-19, for, under identical conditions, the apparent critical bed depths are greater for the Type ASC impregnated whetlerites than for the unimpregnated base charcoal. Therefore, the classifications possible are reduced to Types III-A and III-B (chemical reaction rate important).

The apparent critical bed depth for

those agents for which Type III-A kinetics apply is expressed by the following equation which is derived in Appendix E:

$$\lambda_c = (H_t + H_r)(\ln \frac{C_1}{C_2} - 1) \qquad (42)$$

Obviously C_1 and C_2 are fixed by the test conditions and are known variables. There are two possible methods of determing H_t : (1) by measurement of the intercepts of the bed depth-break time curves for an unimpregnated whetlerite and (2) by calculation from the values of H_t for chloropicrin.

The values of H_t for the unimpregnated whetlerite as calculated from the apparent critical bed depths of Figs. 15-19 are given in Table XI. These values are not as accurate as desired because of the low accuracy of the critical bed depths obtained by extrapolation of the bed depth-break time curves of exceedingly low slope.

In Section III, "Previous Work", it was shown by the analogy of mass transfer in packed adsorbent beds to mass transfer in wetted-wall columns that H_t should be proportional to the diffusivity of the gas being transferred to the -0.56 power. The data of Gamson, Thodos, and Hougen and the data of Hurt show that H_t varies as the -0.67 power of the agent diffusivity.

It is well known that the diffusivity of a gas varies inversely as the square root of the molecular weight. Therefore, the equation relating the value

of H_t for any given agent in terms of that for any other agent, all other test conditions remaining constant, is as follows:

$$(H_t)_x = \frac{(H_t)_y}{\left(\frac{(M.W.)_y}{(M.W.)_x}\right)^{.33}} \qquad (43)$$

At 50 L./min., breather, 16-20 sieve fraction, the value of H_t for chloropicrin at the flow rate obtained in the M11 canister is obtained from Table VIII to be 0.119 cm. The values of H_t for the other agents at these same test conditions, calculated by Equation 43, are shown in Table XI

Table XI

Calculated and Measured Values of H_t
16-20 Sieve, M11 Canister, 50 L./min., Breather

Agent	C_1 (mg./L.)	C_2 (mg./L.)	λ_c (cm.)	H_t (cm.)	M.W.	Calc. H_t (cm.)
CG	10.0	.008	.58	.095	99	.100
CK	4.0	.008	.52	.100	61	.086
AC	4.0	.004	.37	.063	27	.066
SA	4.0	.014	.42	.090	78	.093

If Type III-A kinetics apply, the total critical bed depth should be represented by Equation 42, and the values of $H_t + H_r$ can be calculated from the test conditions and the measured values of the apparent critical bed depths. These calculations were made

for the results represented by Figs. 25, 26, and 27, and the results are given in Table XII.

Table XII

Calculation of $H_t + H_r$
CG, CK, and AC
HC3-361 Whetlerite, 16-20 Sieve
Calculated from Apparent Critical Bed Depths

Agent	Canister	Q (L./min.)	V (cm./min.)	C_1 (mg./L.)	C_2 (mg./L.)	λ_c (cm.)	$H_t + H_r$ (cm.)
CG	M11	32 C.F.	476	10.0	.008	.64	.105
CG	E2R3	32 C.F.	660	10.0	.008	.76	.124
CG	M11	64 C.F.	952	10.0	.008	.97	.159
CG	E2R3	64 C.F.	1320	10.0	.008	1.08	.177
CG	M11	50 B.	1980	10.0	.008	1.24	.202
CG	E2R3	50 B.	2740	10.0	.008	1.48	.242
CK	M11	32 C.F.	476	4.0	.008	.85	.164
CK	M11	64 C.F.	952	4.0	.008	1.04	.200
CK	M11	50 B.	1900	4.0	.008	1.26	.243
AC	M11	32 C.F.	476	4.0	.004	.78	.132
AC	M11	64 C.F.	952	4.0	.004	.94	.159
AC	M11	50 B.	1900	4.0	.004	1.10	.187

It is shown in Appendix E that H_r varies as the first power of the linear flow rate. From the values of H_t and $H_t + H_r$ at 50 L./min., breather, M11 canister, the values of H_r may be obtained by difference. Since H_t has been shown to vary as the 0.30 power of velocity and since H_r has been shown to vary as the first power of velocity, the values of H_t and H_r at any other test velocity can be calculated and the sum can be obtained to compare with the experimentally determined value. The results of these calculations are given in Table XIII.

Table XIII

Variation of $H_t + H_r$ with Velocity
CG, CK, and AC
Calculated vs. Observed Values

Agent	V (cm./min.)	Calculated H_t (cm.)	Calculated H_r (cm.)	Calc. $H_t + H_r$ (cm.)	Obs. $H_t + H_r$ (cm.)
CG	476	.065	.024	.089	.105
CG	660	.072	.034	.106	.124
CG	952	.080	.049	.129	.159
CG	1320	.088	.068	.166	.177
CG	1980	.100	.102	(.202)	.202
CG	2740	.110	.141	.251	.242
CK	476	.057	.039	.096	.164
CK	952	.070	.079	.149	.200
CK	1900	.086	.157	(.243)	.243
AC	476	.044	.030	.074	.132
AC	952	.054	.061	.115	.159
AC	1900	.066	.121	(.187)	.187

These results are plotted in Figs. 53, 54, and 55; the disagreement between the calculated and measured values of $H_t + H_r$ is apparent. Therefore, the removal of phosgene, cyanogen chloride, and hydrocyanic acid by Type ASC impregnated whetlerite does not fall into Type III-A kinetics. This leaves only Type III-B kinetics, the general classification for agents which react with the impregnants.

Another method of distinguishing between Types III-A and III-B kinetics, as discussed in Appendix E, is the nature of the plot of the logarithm of the concentration ratio vs. the apparent critical bed depth. For all types of kinetics, except Type III-B, a straight line relationship is obtained with a positive intercept on the concentration ratio axis between zero

CONFIDENTIAL

FIGURE 53

VARIATION OF H (ANALAGOUS TO H_T FOR DIFFUSION) WITH AIR VELOCITY FOR PHOSGENE REMOVAL

WHETLERITE, HC3-361, 16-20 MESH

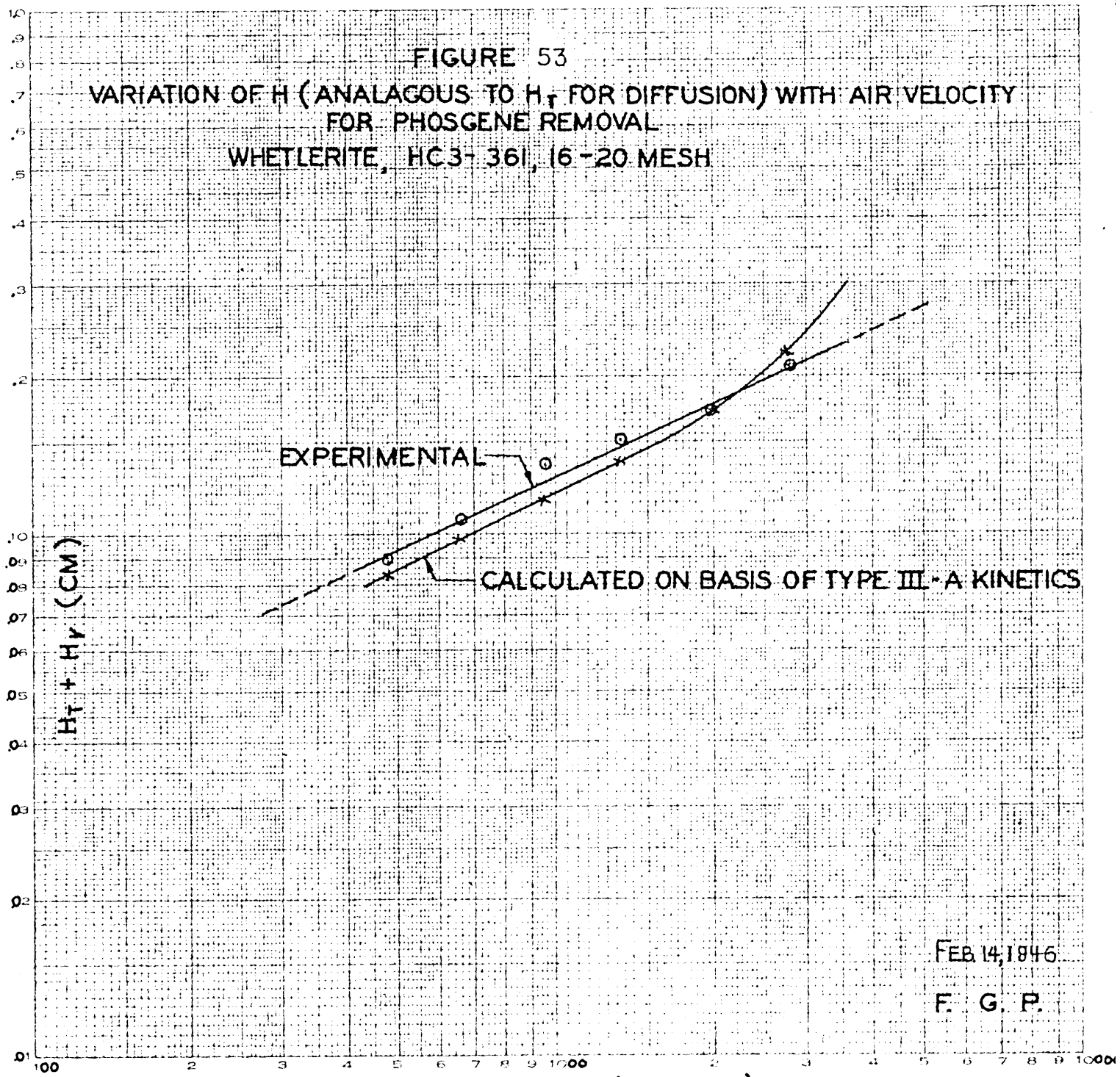

EUGENE DIETZGEN CO.

CONFIDENTIAL

DECLASSIFIED

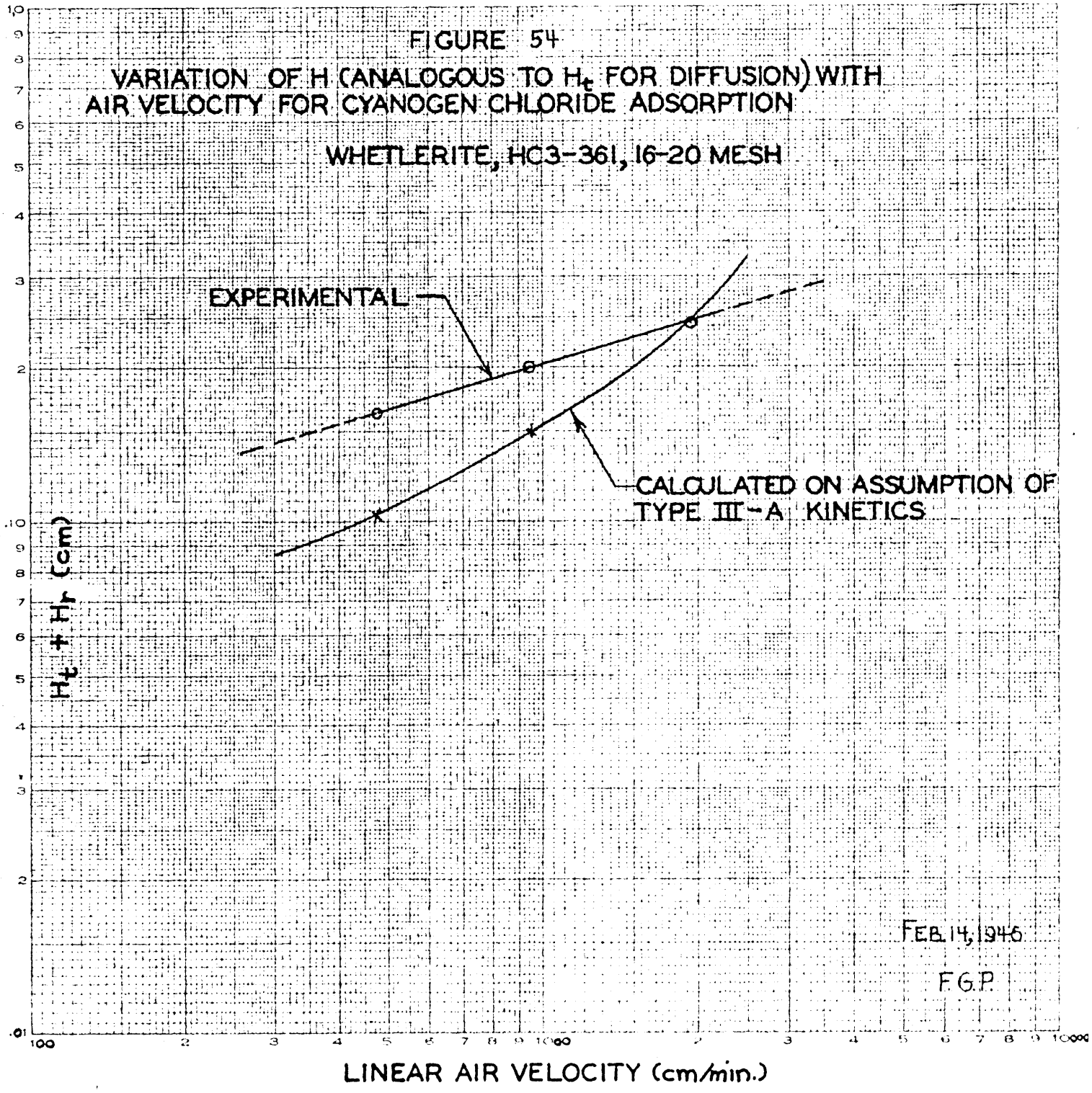

EUGENE DIETZGEN CO.
NO. 340-L22 DIETZGEN GRAPH PAPER
LOGARITHMIC 2 CYCLES X 2 CYCLES

CONFIDENTIAL

DECLASSIFIED

DECLASSIFIED

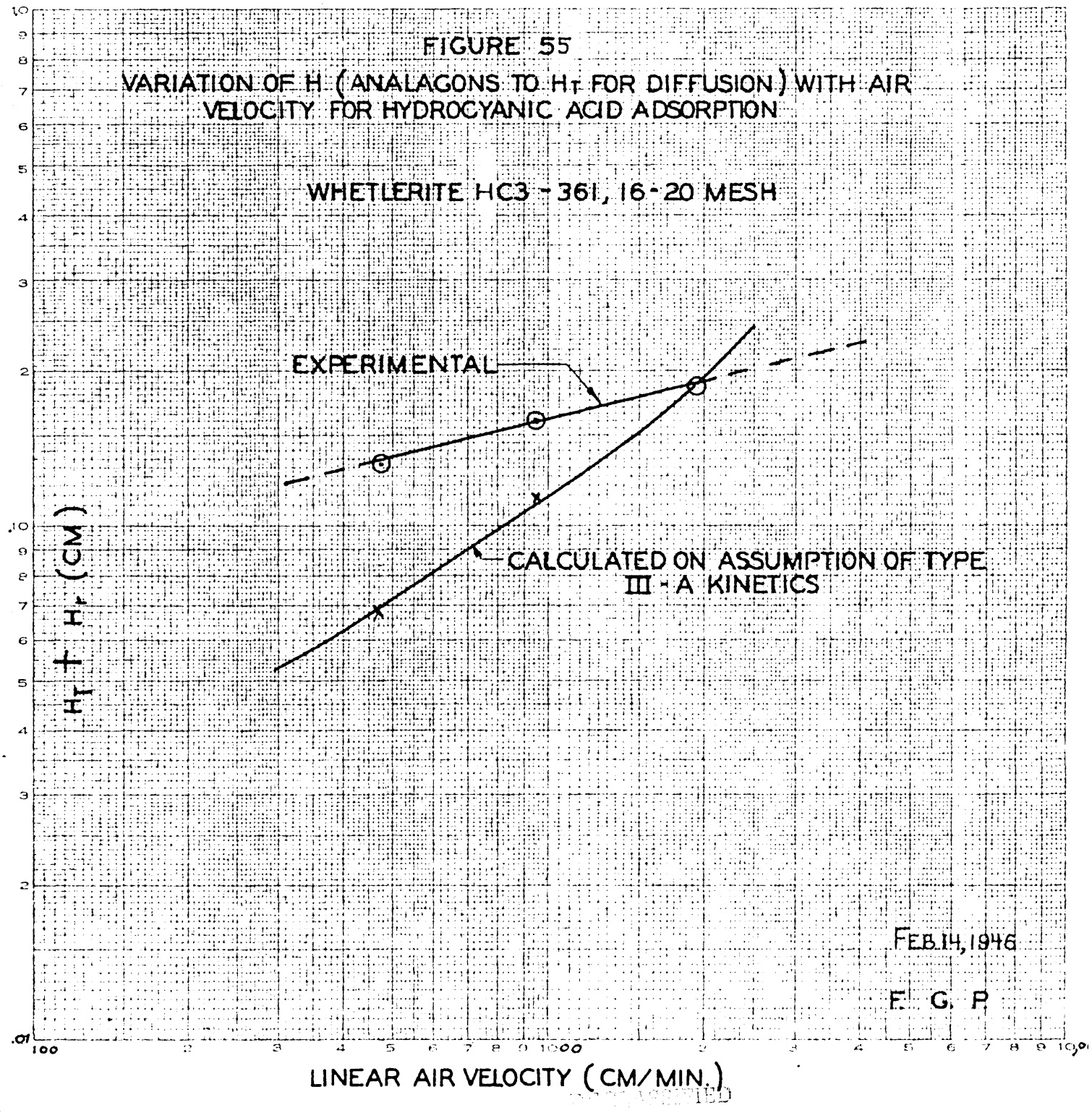

EUGENE DIETZGEN CO.
NO. 340-L22 DIETZGEN GRAPH PAPER
LOGARITHMIC 2 CYCLES X 2 CYCLES

DECLASSIFIED

and unity. For Type III-B kinetics, an apparent straight line relationship is also obtained, but the intercept on the concentration ratio axis is negative. To further substantiate the belief that these agents are removed in accordance with Type III-B kinetics, a series of tests was made in which the cyanogen chloride effluent concentration was measured as a function of time for several adsorbent bed depths. The results of these tests are plotted in Fig. 28.

These data are replotted in Fig. 56 as bed depth vs. break time for several values of the break concentration. It is apparent that the slope of the bed depth-break time plot increases as the break concentration approaches the test concentration. This is indicative of Type III-B kinetics, for, in all other types, the slope is constant for values of the effluent concentration as high as one-tenth of the influent concentration.

The apparent critical bed depths of Fig. 56 are plotted in Fig. 57 as a function of the natural logarithm of the concentration ratio. A straight line correlation is obtained which intersects the concentration ratio axis at -5.0.

Yost (44) conducted similar tests for the removal of arsine by Type ASC impregnated whetlerite. Effluent concentrations were measured by the radio-active tracer technique. His data are replotted in Fig. 58 as effluent concentration as a function of time.

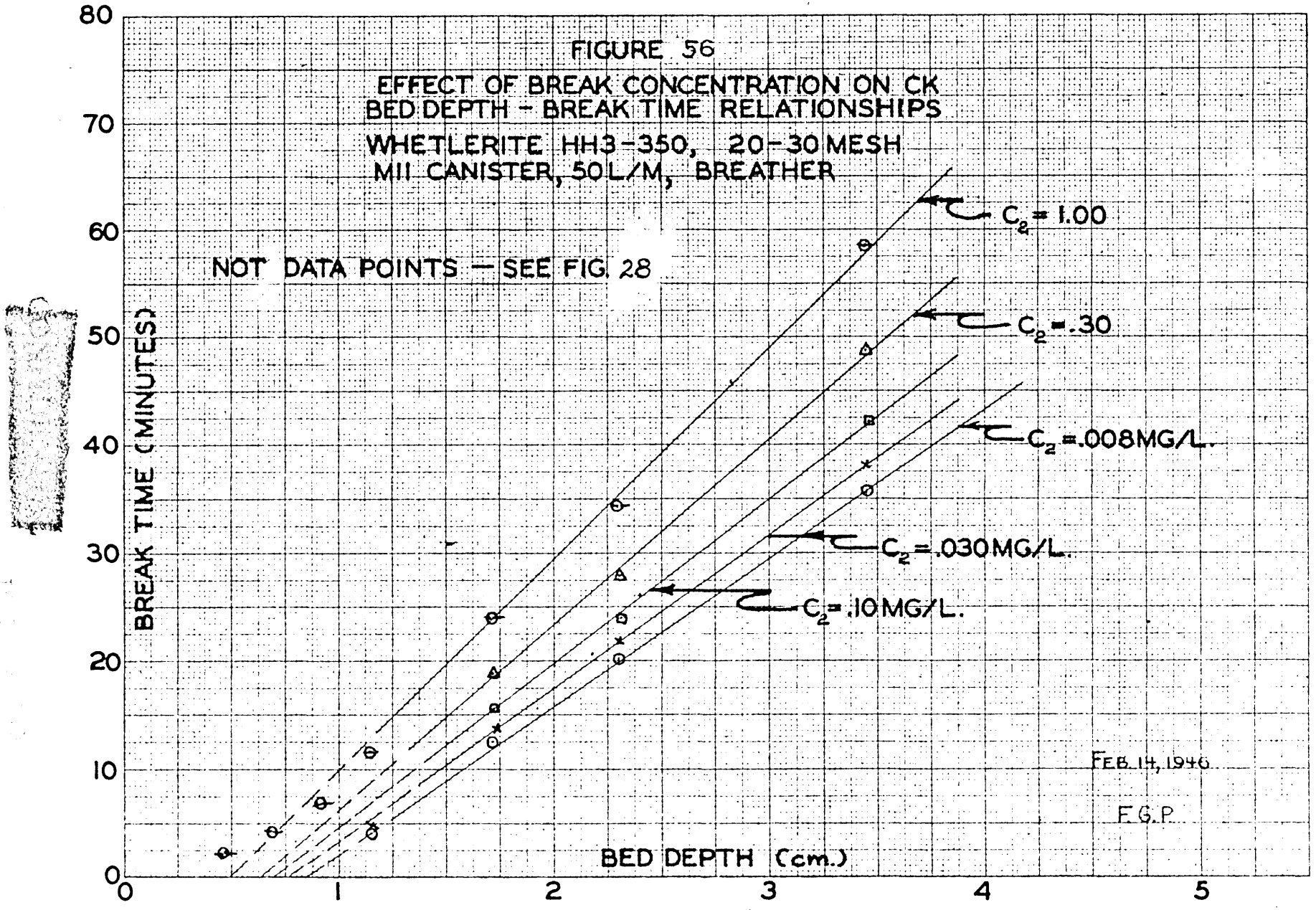

DECLASSIFIED

FIGURE 57

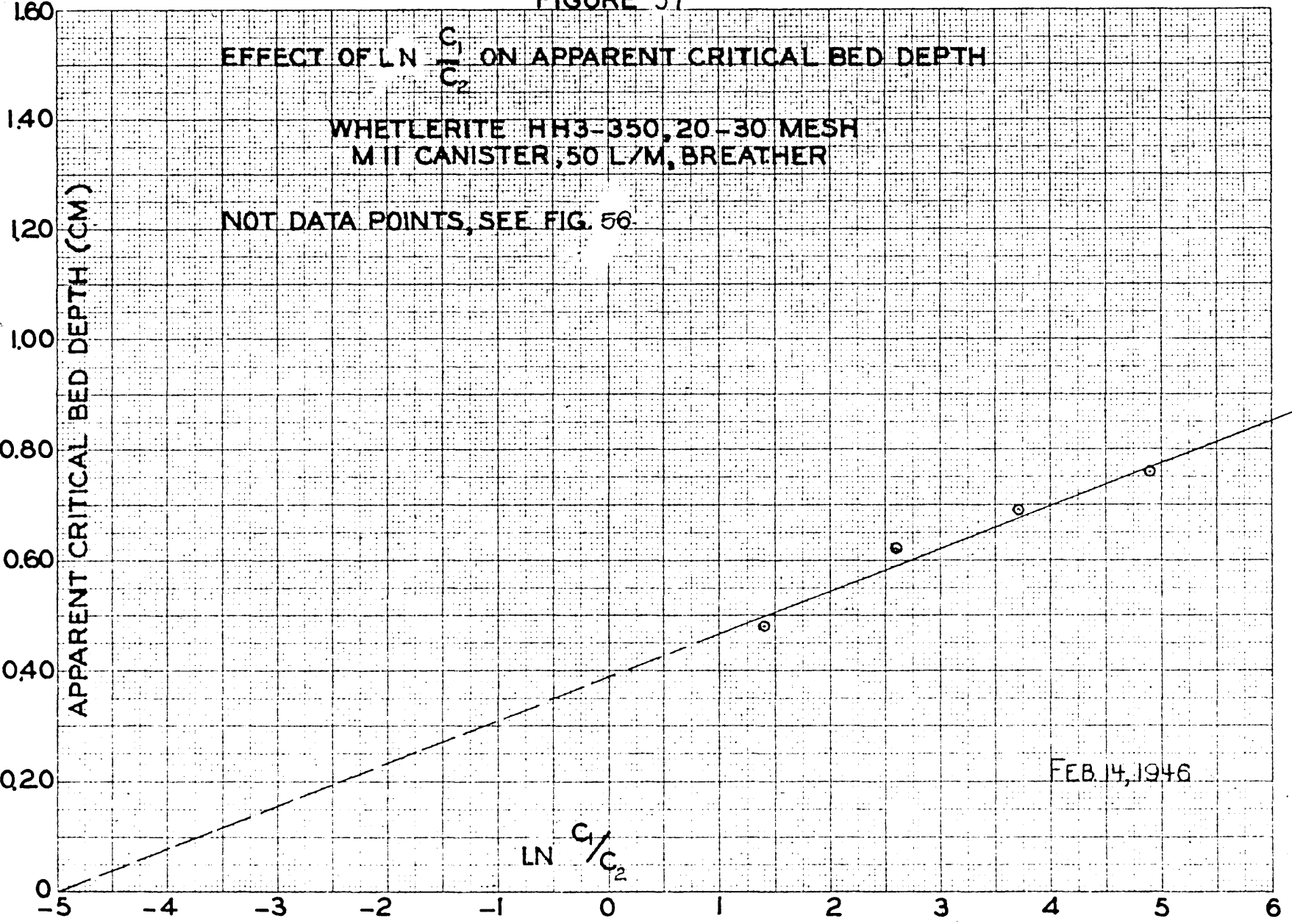

CONFIDENTIAL
DECLASSIFIED

DECLASSIFIED

FIGURE 58

EFFLUENT CONC. VS. TIME, SA.

WHETLERITE CWSN19 TU8
LINEAR VELOCITY 550 cm/min.
INFLUENT CONCENTRATION 7.8 MG/L
HUMIDITY, 0 - 0

DATA OF YOST (44)

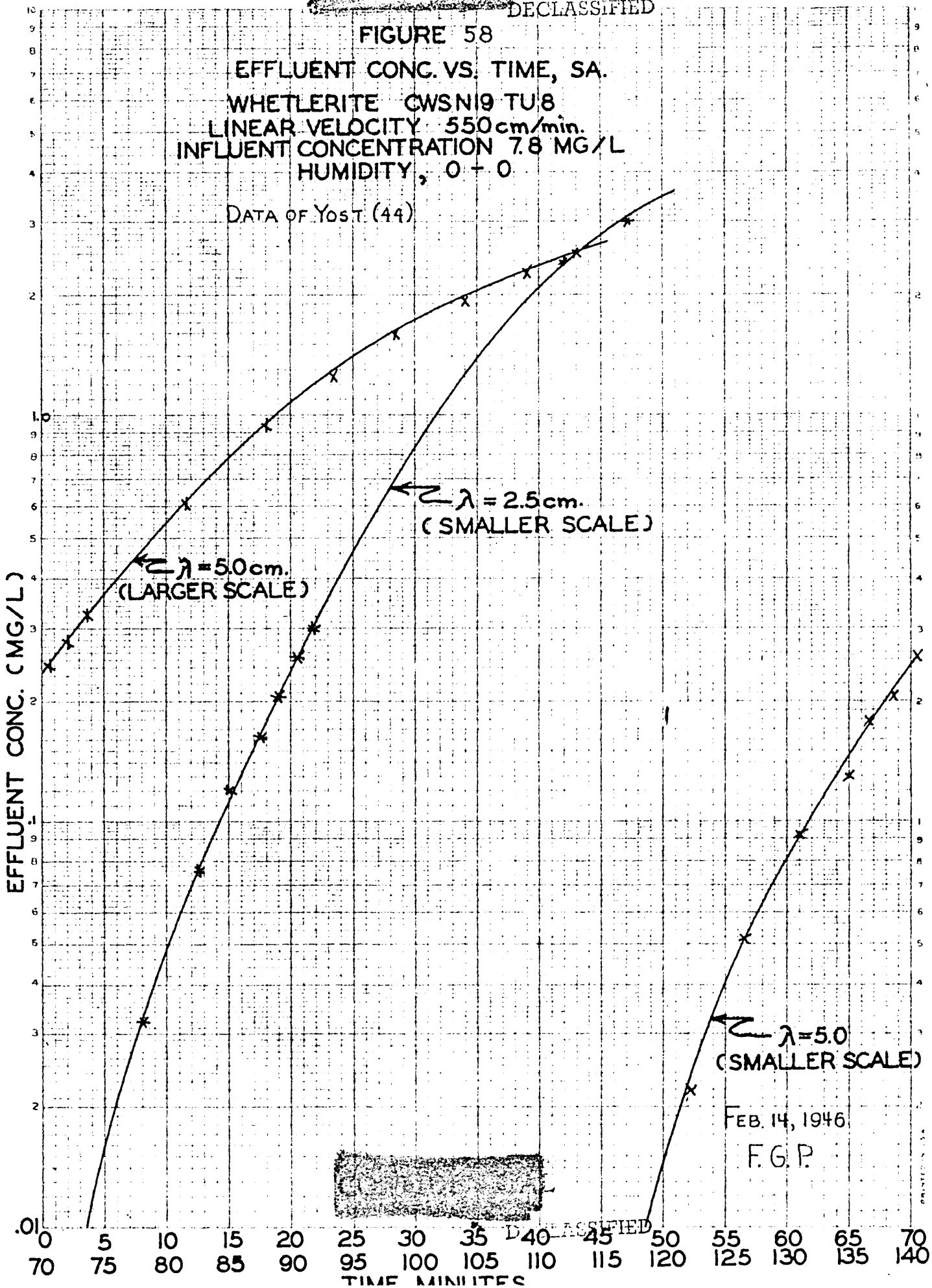

FEB. 14, 1946

F. G. P.

DECLASSIFIED

336-3 SEMI-LOGARITHMIC—3 CYCLES X 70 DIVISIONS THE FREDERICK POST CO. CHICAGO, ILL.

These data are replotted in Fig. 59 as break time vs. bed depth for several values of the break concentration. It is again apparent that the slope of the bed depth-break time curves increases as the break concentration approaches the test concentration. The apparent critical bed depths of Fig. 59 are replotted in Fig. 60 as a function of the logarithm of the concentration ratio. A straight line relationahip is obtained intersecting the concentration ratio axis at -2.5. This indicates that the removal of arsine by Type ASC impregnated whetlerite is also governed by Type III-B kinetics.

The conclusion from these tests is that the rate of removal of phosgene, cyanogen chloride, hydrocyanic acid, and arsine is controlled by Type III-B kinetics. Since this is the case, the simplified equation which was derived for all other types of kinetics is not strictly applicable. However, it has been shown that the apparent critical bed depth for Type III-B kinetics is directly proportional to the logarithm of the concentration ratio and can be represented by the following equation:

$$\lambda_c = k(\ln \frac{C_1}{C_2} - \beta) \qquad (44)$$

Since this equation is very similar to that for the other types of kinetics, the constant, k, is designated as H and termed the "apparent height of an overall transfer unit". Since the exact calculations in

FIGURE 59

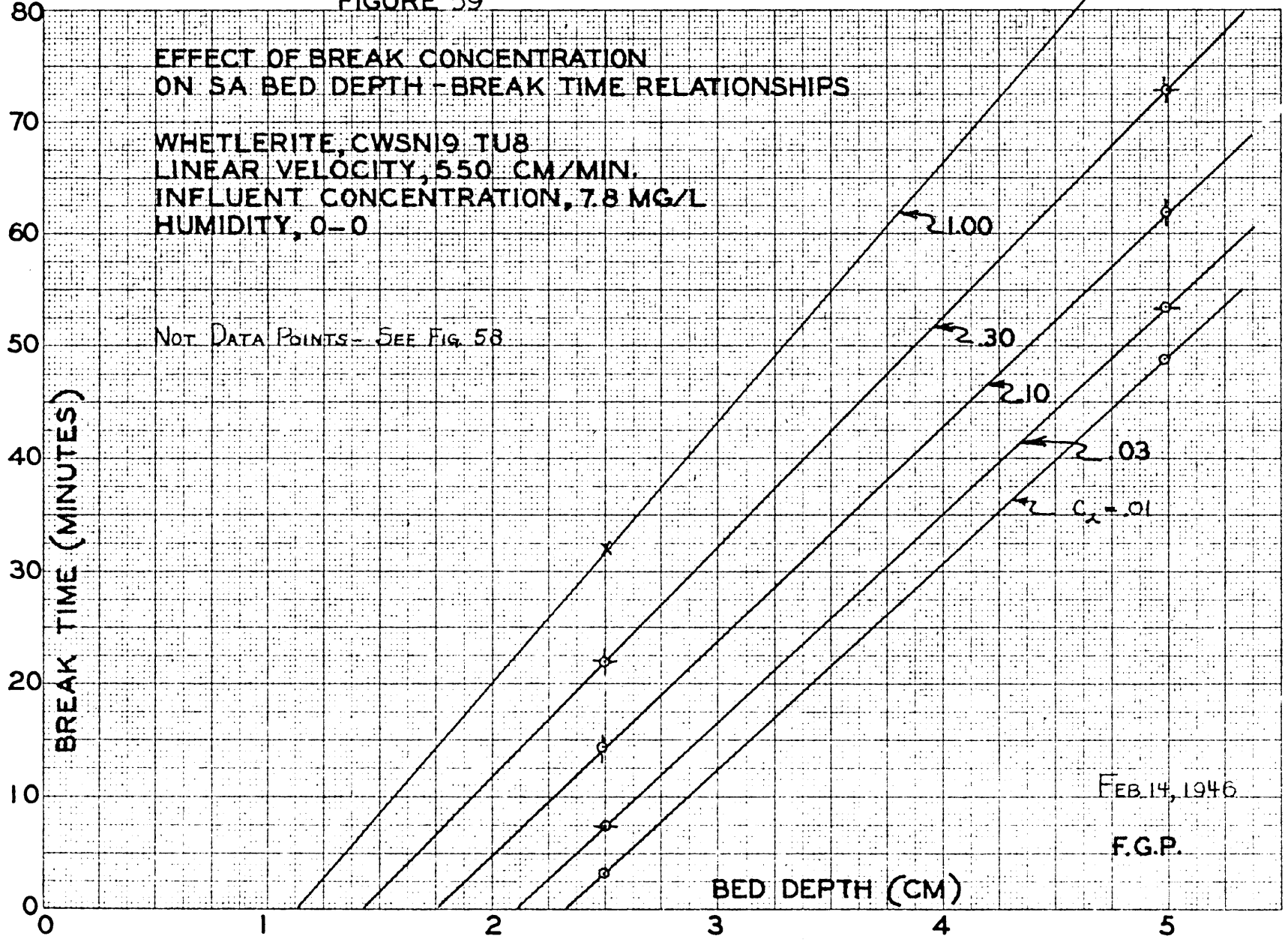

FEB. 14, 1946

F.G.P.

DECLASSIFIED

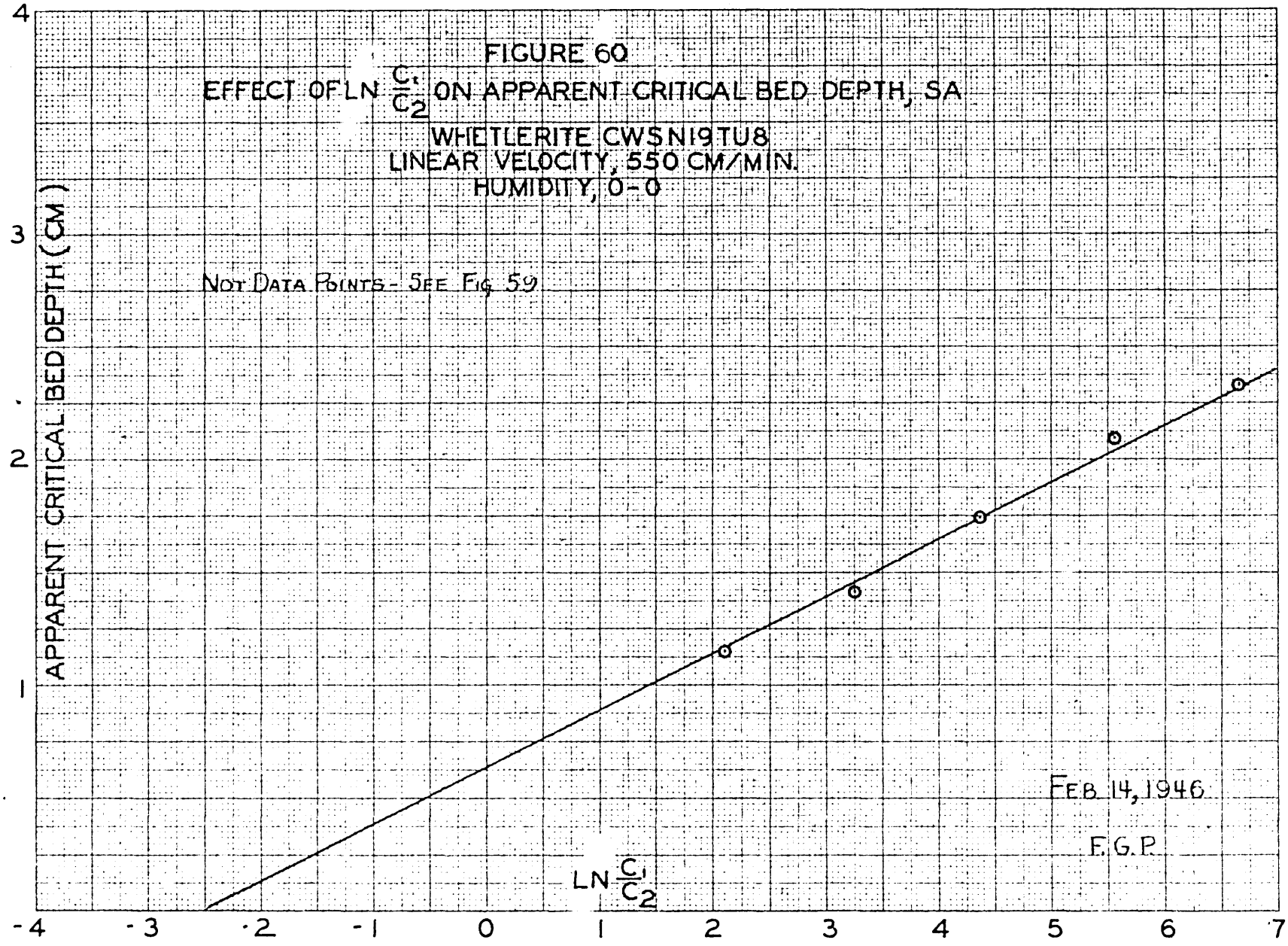

DECLASSIFIED

[redacted] DECLASSIFIED

Appendix E show that β should be equal to -3 and since the arsine tests gave an experimental value of -2.5, a very good agreement, the more exact value of -3 will be used hereafter in this thesis. The cyanogen chloride results, which gave a value of -5 for β are not highly accurate, for the effluent concentrations were measured by the bubbler method and were intended to give only qualitative results to distinguish between Types III-A and III-B kinetics. Therefore, in this thesis the following equation will be used to relate the apparent critical bed depth to H and the concentration ratio:

$$\lambda_c = H(\ln \frac{C_1}{C_2} + 3) \qquad (45)$$

(2) Effect of Velocity on Slope of Bed Depth-Break Time Curves for CG, CK, and AC

Tests were conducted to determine the effect of velocity on the bed depth-break time curves for CG, CK, and AC. These data were obtained with 16-20 sieve fraction Type ASC impregnated whetlerite in the M11 canister at 50 L./min., breather. The results are shown in Figs. 25, 26, and 27. Since the removal of these agents is governed by Type III-B kinetics, there is no known theoretical relationship between the saturation capacity, cross-sectional area, flow rate, and the slope of the bed depth-break time curve; and there is no guarantee that a substantially straight line relationship will result.

The experimental data show, however,

DECLASSIFIED [redacted]

that a substantially straight line relationship is obtained except for lives of less than 15 minutes. The slopes of these curves were analyzed by the same manner as for Type I kinetics, and an experimental constant, N, analogous to N_o or N_r, was determined. The computed values of N for the several conditions of test are shown in Table XIV.

Table XIV

Determination of N for CG, CK, and AC
Whetlerite: HC3-361, 16-20 Mesh

Agent	Q $\frac{L.}{min.}$	Canister	A (sq.cm.)	C_1 $\frac{mg.}{L.}$	S $\frac{min.}{cm.}$	N $\frac{mg.}{ml.}$
CG	32 C.F.	M11	87.0	10.0	29.5	109
CG	32 C.F.	E2R3	65.5	10.0	21.2	104
CG	64 C.F.	M11	87.0	10.0	16.8	124
CG	64 C.F.	E2R3	65.5	10.0	11.2	110
CG	50 B.	M11	87.0	10.0	19.5	112
CG	50 B.	E2R3	65.5	10.0	13.0	100
					Average	110
CK	32 C.F.	M11	87.0	4.0	33.7	48.1
CK	64 C.F.	M11	87.0	4.0	16.1	47.3
CK	50 B.	M11	87.0	4.0	20.7	47.6
					Average	47.7
AC	32 C.F.	M11	87.0	4.0	28.0	41.2
AC	64 C.F.	M11	87.0	4.0	13.3	39.2
AC	50 B.	M11	87.0	4.0	17.0	39.1
					Average	39.8

These data show that N is a constant over the range of variables investigated and may be used in a manner analogous to N_o for reversible, physical adsorption (Type I kinetics).

(3) Effect of Velocity on Apparent Critical Bed Depth and H for CG, CK, and AC

The apparent critical bed depths for

the several agents and test velocities, as determined from Figs. 25, 26, and 27, were listed previously in Table XIII. The derived values of H (obtained by application of Equation 45) are listed in Table XV.

Table XV

Variation of H with Velocity and Agent
Whetlerite: HC3-361, 16-20 Mesh

Agent	V (cm./min.)	λ_c (cm.)	C_1 (mg./L.)	C_2 (mg./L.)	H (cm.)
CG	476	.64	10.0	.008	.063
CG	660	.76	10.0	.008	.075
CG	952	.97	10.0	.008	.096
CG	1320	1.08	10.0	.008	.109
CG	1980	1.24	10.0	.008	.123
CG	2740	1.48	10.0	.008	.146
CK	476	.85	4.00	.008	.092
CK	952	1.04	4.00	.008	.113
CK	1900	1.26	4.00	.008	.137
AC	476	.78	4.00	.004	.079
AC	952	.94	4.00	.004	.095
AC	1900	1.10	4.00	.004	.111

These values of H are plotted as a function of velocity in Fig. 61, and it is apparent that a linear relationship is obtained on logarithmic paper. The slopes of these straight lines were measured, and it was established that H varies as a power of the linear air velocity. These powers are listed in Table XVI.

This correlation for agents known to fall into Type III-B kinetics classification is strikingly analogous to the correlation obtained for Type I kinetics as exemplified by the chloropicrin data.

[redacted] DECLASSIFIED

FIGURE 61

VARIATION OF H WITH VELOCITY AND AGENT
WHETLERITE HC 3-361, 16-20 MESH

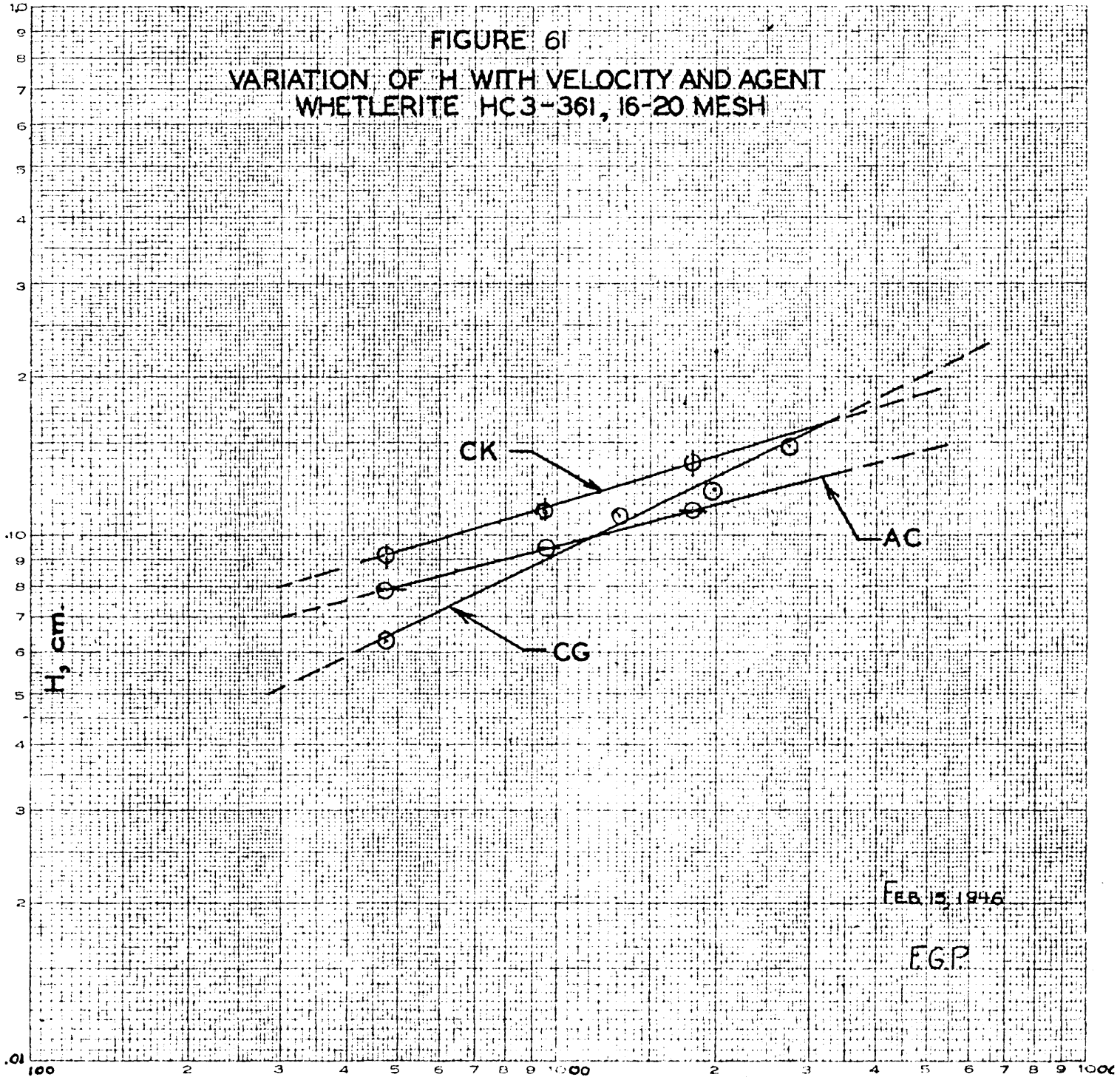

DECLASSIFIED

[redacted]

DECLASSIFIED

Table XVI

Variation of H with Linear Air Velocity
($H = k_1 V^x$)

Agent	x
CG	0.48
CK	0.32
AC	0.26

(4) Variation of Apparent Critical Bed Depth and H with Sieve Fraction

Tests were conducted to determine the effect of sieve size on the bed depth-break time relationships for CG, CK, AC, and SA. The results of these tests are shown in Figs. 29, 30, 31, 32, and 33.

The data show that for 12-16 and 16-20 sieve fractions the slopes of the bed depth-break time curves are identical. For the finer sieve sizes, (20-30 and 30-40), there is a decided tendency for the slope to decrease with the HC3-361 impregnated whetlerite.

In conference with personnel interested in whetlerite production and impregnation, it was learned that considerable difficulty had been experienced in the early stages of production of Type ASC impregnated whetlerite in obtaining uniform activation and impregnation of the finer sieve fractions. Since the HC3-361 whetlerite was an early production lot, a repeat series of tests was made with CC3-900 Type ASC impregnated whetlerite which was a later production lot. The results of these tests are shown in Fig. 30; there is no tendency for the slope of the bed depth-break time curve to de-

DECLASSIFIED

crease with decreasing particle diameter. Therefore, it is concluded that N is a constant for all sieve sizes for those agents the removal of which is governed by Type III-B kinetics with currently produced Type ASC impregnated whetlerite.

The values of the apparent critical bed depths for the standars sieve fractions and the derived H and k_1 ($H = k_1 V^x$) values are listed in the following table:

Table XVII

Variation of H and k_1 with Sieve Size and Agent
M11 Canister, 50 L./min., Breather

Whetlerite	Agent	Sieve Size	λ_c (cm.)	C_1 (mg./L.)	C_2 (mg./L.)	H (cm.)	k_1
HC3-361	CG	12-16	1.86	10.0	.008	.184	.00483
CC3-900	CG	12-16	1.94	10.0	.008	.192	.00504
HC3-361	CG	16-20	1.28	10.0	.008	.127	.00333
CC3-900	CG	16-20	1.31	10.0	.008	.130	.00341
HC3-361	CG	20-30	0.87	10.0	.008	.086	.00226
CC3-900	CG	20-30	0.88	10.0	.008	.087	.00228
HC3-361	CG	30-40	0.54	10.0	.008	.053	.00139
CC3-900	CG	30-40	0.55	10.0	.008	.054	.00142
HC3-361	CK	12-16	1.77	4.00	.008	.192	.0171
HC3-361	CK	16-20	1.26	4.00	.008	.137	.0122
HC3-361	CK	20-30	0.90	4.00	.008	.098	.0088
HC3-361	AC	12-16	1.43	4.00	.004	.145	.0204
HC3-361	AC	16-20	1.10	4.00	.004	.111	.0156
HC3-361	AC	20-30	0.83	4.00	.004	.084	.0118
HC3-361	SA	12-16	1.72	4.00	.014	.199	*.0207
HC3-361	SA	16-20	1.29	4.00	.014	.149	.0155
HC3-361	SA	20-30	0.94	4.00	.014	.108	.0112

*Calculated on assumption that x is equal to 0.30 for SA.

These values of H are plotted in

Fig. 62 as a function of the average particle diameter. It is apparent that a straight line correlation on logarithmic paper is obtained and that H varies as some power of the particle diameter for all four agents. The power for each agent is tabulated below:

Table XVIII

Variation of H with Particle Diameter
($H = k D_p^y$)

Agent	y
CG	1.25
CK	1.00
AC	0.80
SA	0.90

This correlation is again entirely analogous to the correlation for Type I kinetics.

(5) Correlation of H with Sieve Analysis-Independency of H on Adsorbent

Several series of tests were made to determine the relationships between the sieve analysis and the values of H for those agents the removal of which is governed by Type III-B kinetics. These tests were all made in the M11 canister at 50 L./min., breather, and the results are shown in Figs. 34, 35, 36, 37, and 38.

The sieve analyses for the series are shown on Fig. 34 and in Table VI. Since such excellent analogy has been obtained heretofore between the characteristics of Type III-B kinetics and those of Type I kinetics, the same equation as derived in Appendix F (Equation 128) for predicting H_t for blends of several sieve sizes for

[redacted]

FIGURE 62

EFFECT OF MESH SIZE ON H

PHOSGENE - ASC IMPREGNATED WHETLERITE

M11 CANISTER, 50L/M, BREATHER

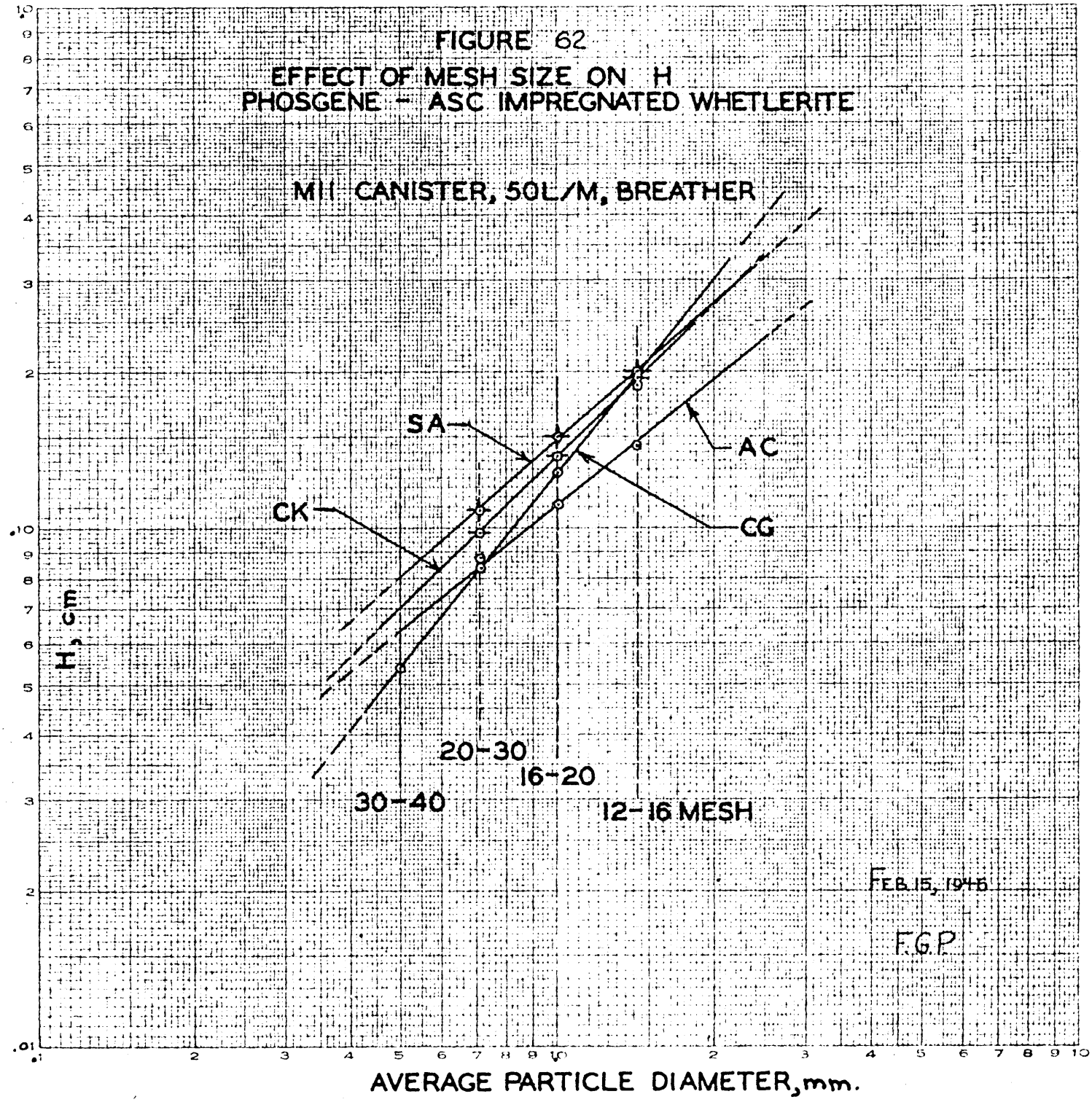

[redacted]

Type I kinetics was tested to determine its applicability in determining H for Type III-B kinetics.

The comparison of the values of H as calculated by this equation and as determined from the apparent critical bed depths is shown in Table XIX

Table XIX

Effect of Sieve Analysis on H, Calculated vs. Measured
M11 Canister, 50 L./min., Breather

Agent	Whetlerite	Sieve Analysis	Observed λ_c (cm.)	Observed H (cm.)	Calc. H (cm.)	Dev. (%)
CG	HC3-361	B, Fig.34	1.13	.112	.115	+ 3
CG	HC3-361	C, Fig.34	1.23	.121	.116	- 4
CG	HC3-361	Table VI	1.26	.124	.119	- 4
CG	CC3-900	Table VI	1.11	.110	.114	+ 4
CG	AD3-255	Table VI	1.22	.120	.128	+ 7
CG	MIT3-4713	Table VI	1.14	.113	.121	+ 7
		Root Mean Square Deviation				± 5
CK	HC3-361	Table VI	1.24	.135	.131	- 3
CK	AD3-255	Table VI	1.32	.143	.128	- 10
CK	CC3-900	Table VI	1.30	.141	.126	- 11
		Root Mean Square Deviation				± 9
AC	HC3-361	Table VI	0.94	.095	.107	+ 13
AC	AD3-255	Table VI	0.97	.098	.112	+ 14
AC	CC3-900	Table VI	0.94	.095	.103	+ 8
		Root Mean Square Deviation				± 12
SA	HC3-361	Table VI	1.28	.148	.143	- 3
SA	AD3-255	Table VI	1.33	.154	.150	- 3
SA	MIT3-4713	Table VI	1.33	.154	.144	- 7
		Root Mean Square Deviation				± 5

These results show that the errors involved in the computation of H from the sieve analysis are small and that, therefore, Equation 128 is equally applicable for Type III-B kinetics and Type I kinetics.

d. Cumulative Penetration

(1) Type I Kinetics, Chloropicrin

All of the previously discussed tests were concerned with the time required for the effluent concentration to reach a specified value (concentration break). The majority of the tests were conducted in this manner because the data are more easily analyzed. However, one series of tests, shown in Fig. 39, was made to determine the validity of the cumulative break equation which is derived in Appendix B. The concentration break points are also shown plotted for comparison.

Fig. 39 shows that the slopes of the concentration and the cumulative break curves are identical as predicted by Equations 1 and 6. The intercept of the cumulative break curve on the bed depth axis is derived in Appendix B to be given by the following equation:

$$\lambda_c = H_t\left(\ln \frac{N_o A H t}{F} - \beta\right) \qquad (46)$$

For these particular test conditions (12-16 sieve whetlerite, M11 canister, 50 L./min., breather), the value of H_t is obtained from Table IX to be 0.152 cm. The value of N_o is shown in Table VII to be 176 mg./ml. The calculated value of the apparent critical bed depth for the cumulative penetration of 6 mg. of chloropicrin is calculated by Equation 46 to be 0.75 cm. This is in exact agreement with the measured value and proves the validity of the cumulative break equations derived in Appendix B.

(2) Type III-B Kinetics, Arsine

The standard test procedure employed with arsine, a cumulative poison, is to measure the elapsed time to the instant that 8.5 mg. of arsine has penetrated the adsorbent bed. Since all other equations, derived for Type I kinetics have applied with slight modifications to Type III-B kinetics, Equation 46 of Appendix B was applied to the cumulative penetration of arsine. Equation 46, when modified in the same manner as Equation 6, takes the following form:

$$\lambda_c = H(\ln \frac{NAH}{F} + 3) \qquad (47)$$

This equation was tested for its applicability to arsine cumulative break relationships by the series of tests shown in Fig. 40. This figure shows the cumulative break and the concentration break bed depth-break time curves for 16-20 sieve whetlerite in the M11 canister at 50 L./min., breather. The slopes of the two curves are identical as predicted by the theoretical consideritions for Type I kinetics.

For these particular test conditions, the value of H is obtained from Table XVII to be 0.149 cm. The value of N, as determined from the slope of the bed depth-break time curves, is 113 mg./ml. The calculated value of the apparent critical bed depth for a cumulative penetration of 8.5 mg. of arsine is 1.21 cm. This is in excellent agreement with the measured value of 1.18 cm.

It is concluded that Equation 6 is equally applicable for Type III-B kinetics and Type I kinetics.

e. Effect of Adsorbed Moisture on Bed Depth-Break Time Relationships

Although it is not the purpose of this thesis to analyze and develop equations for the performance of adsorbent beds of high water content, several tests were made to obtain a qualitative knowledge of the effects of adsorbed water. The results of these tests are shown in Figs. 41, 42, 43, and 44.

These tests were conducted at 50 L./min., breather, in the M11 canister with whetlerites which had been equilibrated with respect to an air stream at 80 per cent relative humidity. Under these conditions, the adsorbent is practically saturated with adsorbed water (see Fig. 49). The equilibrium water content varies with different adsorbents but is approximately 40 per cent of the dry weight of the whetlerite.

This adsorbed water should not affect the equations for the evaluation of the true ~~initial~~ critical bed depth for reversible adsorption except to the extent that counter-diffusion adds additional impedence. The partial pressures of the diffusing gases are so small, however, that this is not a sizeable factor.

The surface available for adsorption, and therefore the adsorption capacity, is tremendously reduced. Therefore, the initial slope of the bed depth-break time curve for those agents which are insoluble and

which are physically adsorbed should be much less with wet than with dry adsorbent. If the agent being adsorbed is very strongly adsorbed, it will slowly displace the more lightly adsorbed water by a process of selective adsorption.

There is always a heat of adsorption involved in the removal of any agent from an air stream. This will tend to raise the temperature of the air stream and consequently reduce the per cent relative humidity. This will, in turn, result in a partial pressure gradient tending to produce vaporization of water from the whetlerite.

The overall effect, in a qualitative sense, is for vaporization of the adsorbed water to occur with a resultant increase in the adsorption capacity for the agent. This would reflect in the bed depth-break time curve by a gradual increase in slope as the bed depth is increased.

The results of Fig. 41 show that this actually occurs for the adsorption of chloropicrin, a relatively water-insoluble compound.

The effect of adsorbed water on the rate of removal of those agents which react chemically with the impregnants would depend upon the accessibility of the impregnant to the diffusing agent. If the agent is water-insoluble, it would be blocked from reaching the impregnant; and a bed depth-break time relationship of the same type as discussed above for reversible, physical

adsorption would be obtained. If, however, the agent is water-soluble, it can reach the impregnant by diffusion through the adsorbed water barrier. This barrier should offer little resistance to transfer because of the extreme "thinness" (several molecular layers) so that, except for complications caused by reaction with the adsorbed water, the bed depth-break time curves should be identical for the wet and dry adsorbent.

The data represented by Figs. 42, 43, and 44 show the bed depth-break time curves for phosgene, hydrocyanic acid, and cyanogen chloride with wet adsorbent. It is apparent that the wet and dry plots are almost identical with phosgene and hydrocyanic acid but are vastly different, and resemble chloropicrin bed depth-break time curves, for cyanogen chloride. Phosgene is decomposed to hydrochloric acid and carbon dioxide by water and the soluble acid can react with the impregnant; hydrocyanic acid is soluble in water in all proportions; cyanogen chloride is only slightly soluble in water. These data substantiate the above arguments.

The slight increase in the slopes of the bed depth-break time curves with wet whetlerite for phosgene and hydrocyanic acid are probably caused by chemical reaction with or physical solution in the adsorbed water.

f. Air Resistance

(1) General

Air resistances were measured for a large number of the adsorbent beds tested to determine the

effect of bed depth, sieve size, and flow rate. The results of these tests are shown in Figs. 45, 46, and 47 and in Tables IV and V.

(2) Effect of Sieve Size on Air Resistance

The results of tests to determine the effect of sieve size on the air resistance of adsorbents are shown in Fig. 45. These tests were conducted with HC3-361 Type ASC impregnated whetlerite in the M11 canister at a flow rate of 85 L./min. It is apparent that, for bed depths above two cm., a linear relationship is obtained, but that, below this bed depth, the slope of the curve increases.

It is to be recalled that the M11 canister has a gross diameter of 4.14 in., but the area is restricted at the influent and effluent ends by a 0.25-inch baffle; this reduces the effective diameter at these points to 3.64 in. The conclusion drawn from Fig. 45 is that the air flow follows the area of the baffles for a distance into the bed and gradually spreads out over the gross area. It must then contract again before it leaves at the effluent end of the canister. Since the straight line relationship starts after the bed depth exceeds two cm., it is assumed that the effects of the baffles extend that distance into the adsorbent bed (one cm. from the influent end and one cm. from the effluent end).

To verify this assumption, a more exact series of measurements was made to determine the

relative slopes of the initial portion of the curve and of the upper portion (above two cm. bed depth). If the above premise is correct, the slope of the initial portion of the curve should be directly proportional to the product of the ratio of the area at the baffles to the gross area and to the slope of that portion of the curve for bed depths in excess of two cm. The results of these tests are shown in Figs. 46 and 47.

The initial slope of the curve shown in Fig. 46 (M11 canister) was measured to be 11.4, and the slope of the portion of the curve above two cm. bed depth was measure to be 8.5 . This is in excellent agreement with the ratio of the gross area to the area at the baffles $(4.19^2/3.69^2)$.

The initial slope of the curve shown in Fig. 47 (E2R3 canister) was measured to be 14.1; the slope of the portion of the curve above two cm. bed depth was measured to be 11.2. This, likewise, is in excellent agreement with the ratio of the gross area to the area at the baffles $(3.625^2/3.125^2)$.

Therefore, it is concluded that the effects of the baffles effectively penetrate one cm. into the adsorbent bed and precede the effluent end of the bed by one cm. These assumptions result in the following general equation for the air resistance of an axial flow canister (streamline flow):

$$\Delta P = k_2 Q \left[\frac{2.00}{A_b} + \frac{\lambda - 2.00}{A}\right] \qquad (48)$$

The constant, k_2, is a function of the sieve fraction. The values of this constant were determined from the data of Fig. 45 and are listed in Table XX.

Table XX

Effect of Sieve Fraction on k_2
Whetlerite: HC3-361

Sieve Fraction	k_2
12-16	5.15
16-20	8.25
20-30	13.4
30-40	21.8

(3) Effect of Specific Whetlerite on k_2

The above tests were made with one specific whetlerite. The principal manufacturers of activated whetlerites during this war were (1) the Pittsburgh Coke and Chemical Co. at Neville Island, Pa. and at Carnegie, Pa., (2) the Barneby-Cheney Engineering Co. at Columbus, Ohio, and (3) the Crown-Zellerbach Corp. at Seattle, Washington. Each of these manufacturers used slightly different raw materials and, therefore, the particle shape might be different from each plant.

There were available at the Chemical Warfare Service Development Laboratory, M.I.T., 30 samples of each of the whetlerites produced in quantity, each sample taken from a day's production. These samples were blended to yield a composite sample which should be re-

presentative of each of the products. These samples were tested to determine the air resistance of the pure sieve fractions in the M11 canister at 85 L./min. with a constant adsorbent volume of 250 ml. The results of these tests are shown in Table IV.

The values of k_2 were calculated from the measured resistances and are shown in Table XXI. In this table (and throughout this thesis) the first letter of the whetlerite designation is code for the manufacturer who produced the activated whetlerite: A or B indicates the Pittsburgh Coke and Chemical Co.; H indicates the Barnebey-Cheney Engineering Co.; and C indicates the Crown-Zellerbach Corp. The second letter indicates the impregnation plant, and the numerals which follow deal with the type of impregnated whetlerite and with the production lot number.

Table XXI

Variation of k_2 with Whetlerite Composite Samples

Composite Whetlerite	Sieve Fraction 12-16	16-20	20-30
HH	5.46	7.76	13.0
AD	6.18	8.18	13.3
CC	7.18	9.13	14.4

These data show that there is considerable variation among the several whetlerites-the variation being the greatest for the courser sieve fractions.

Several specific production samples of these and other whetlerites were tested to determine if the individual lots followed the trends of the composite samples. The results of these tests are shown in Table V. The values of k_2 were calculated from the measured resistances and are shown in Table XXII.

Table XXII

Variation of k_2 with Whetlerite Individual Samples

Whetlerite	Sieve Fraction 12-16	16-20	20-30
AD3-1760	5.61	8.09	12.3
BD3-1750	5.96	7.99	12.8
HH3-465	5.52	7.88	12.1
CC3-1088	5.96	8.76	13.7
CC3-900	5.68	7.99	13.6

These data show that, although exact agreement between the resistance of the specific examples and the resistance of the composite samples is not obtained, the trends remain the same. In order of increasing resistance they may be listed as follows: (1) H, (2) A, and (3) C as exemplified by HH, AD, and CC. Charcoal activated by the Carnegie, Pa. plant of the Pittsburgh Coke and Chemical Co. (designation-B) shows about the same resistance as that manufactured at the Neville, Pa. plant (designation-A).

As an approximating relationship, the values of k_2 as a function of the sieve fraction listed in Table XXI are standardized for H whetlerite.

Resistances calculated using these values of k_2 must be multiplied by a correction factor for other whetlerites. These factors and the standard values of k_2 are shown in Table XXIII

Table XXIII

Values of k_2 for H Whetlerite
and Correction Factors for Other Whetlerites

Activation Designation	k_2 for Sieve Fraction 12-16	16-20	20-30	30-40	Correction Factor
H	5.46	7.76	13.0	21.7	1.00
A	"	"	"	"	1.07
B	"	"	"	"	1.07
C	"	"	"	"	1.15

The maximum deviation between the resistances calculated from these values of k_2 and correction factors and the measured values shown in Tables XX, XXI, and XXII is 13 per cent. Therefore, these values of k_2 and the correction factor are sufficiently accurate for air resistance calculations which need not be precise.

(4) Effect of Sieve Fraction Blends on k_2

Several tests were made to determine the air resistance of blends of the pure sieve fractions. The results of these tests are shown in Table XXIV. It was found that, to calculate the air resistance from the sieve analysis, the values of k_2 for the pure sieve fractions, and the correction factors, a method of weighted

averages must be employed. The assigned weightings are 1.0, 1.2, 1.6, and 2.4 for 12-16, 16-20, 20-30, and 30-40 sieve fractions, respectively.

The values of k_2 , calculated from the values of k_2 for the pure sieve fractions (Table XXIII) and the weighted average, are shown in Table XXIV in comparison with the experimental values.

Table XXIV

Calculated and Observed Values of k_2
Sieve Fraction Blends

Whetlerite	Sieve Analysis 12-16	16-20	20-30	30-40	k_2 Obs.	Calc.	Dev. (%)
HH comp.	23.2	44.6	29.2	3.0	10.5	10.0	- 5
AD comp.	23.2	50.9	23.0	2.9	10.3	11.2	+ 9
CC comp.	16.9	50.6	29.2	3.3	12.0	11.7	- 3
AD3-1760	20.0	50.0	30.0	-	9.44	10.0	+ 6
BD3-1750	20.0	50.0	30.0	-	10.1	10.0	- 1
HH3-465	20.0	50.0	30.0	-	9.35	9.35	0
CC3-1088	20.0	50.0	30.0	-	10.8	10.7	- 1
AD3-1760	19.8	47.9	28.6	4.7	10.4	11.1	+ 7
BD3-1760	19.8	47.9	28.6	4.7	11.2	11.1	- 1
HH3-465	19.8	47.9	28.6	4.7	10.4	10.4	0
CC3-1088	19.8	47.9	28.6	4.7	11.8	11.9	+ 1
CC3-900	30.0	60.0	10.0	-	8.27	8.67	+ 5
CC3-900	30.0	40.0	30.0	-	9.79	10.6	+ 8
CC3-900	30.0	-	70.0	-	12.0	13.2	+ 10
					Root Mean Square Deviation		± 5

The maximum deviation is seen to be ten per cent and the average deviation is five per cent. This agreement between the calculated and observed values of k_2 for sieve fraction blends is as accurate as the agreement between the values of k_2 for the pure sieve fractions, and it establishes the validity of the weighting

schedule.

e. Effect of Velocity on Air Resistance

Several series of tests were made to determine the effect of air velocity on the air resistance of pure sieve fractions in the M11 canister. The results of these tests are shown in Fig. 48 and indicate that, for velocities below 500 cm./min., streamline flow is obtained. Above this velocity, there is a tendency for the air resistance to increase at a rate proportionately greater than the rate at which the velocity increases. This is indicative of a transition stage between streamline and turbulent flow. Since the deviation from streamline flow is not great, the equations for streamline flow have been used throughout in this thesis, bearing in mind that they can not be expected to apply at velocities much in excess of 2000 cm./min.

g. Summarized Results-Axial Flow Beds

(1) Break Time to a Specified Effluent Concentration

It has been shown in this thesis that the following equation, derived in Appendix A, is applicable for Type I kinetics as exemplified by the adsorption of chloropicrin:

$$t = \frac{N_o A}{C_1 Q} \left[\lambda - H_t \left(\ln \frac{C_1}{C_2} - 1 \right) \right] \qquad (1)$$

It has also been shown that, over the range of variables investigated, a similar equation

applies for Type III-B kinetics as exemplified by the removal of phosgene, cyanogen chloride, hydrocyanic acid, and arsine by Type ASC impregnated whetlerite:

$$t = \frac{N\,A}{C_1\,Q}\left[\lambda - H\left(\ln\frac{C_1}{C_2} + 3\right)\right] \qquad (49)$$

N_o and N are functions of the nature of the adsorbent and may vary over wide limits depending upon the activation and impregnation. The only other variable which is not defined by the test procedure is the value of H_t (or H). These functions have been shown to be dependent on the superficial air velocity, the average particle diameter, and the agent.

The variation of H_t (and H) with particle diameter and air velocity for the five standard Chemical Warfare Service non-persistent agents has been established, and the validity of the equation derived in Appendix F for the determination of H_t for sieve fraction blends was shown.

These data may be summarized by the following equation:

$$H_t \text{ (or H)} = k_1 V^x \qquad (50)$$

The values of x were established previously and are tabulated again in Table XXV.

The values of k_1 are a function of the sieve fraction and are directly calculable from the values of H_t (or H) at a particular velocity. The values

of k_1 for a mixture of several sieve fractions may be calculated in a manner analogous to the calculation of H_t (or H) for a blend. Since all commercially produced Type ASC impregnated whetlerites consist essentially of a blend of 12-16, 16-20, and 20-30 sieve fractions with small amounts of 30-40 sieve fraction (0-2.5 per cent), graphs were prepared showing the values of k_1 for any mixture of these sieve sizes. The data represented by by these graphs (Figs. 63, 64, 65, 66, and 67) were calculated from the values of H_t (or H) for the pure sieve fractions obtained from Figs. 52 and 62.

Replacing H_t in Equation 1 by its equal, k_1V^x, the following equations are obtained for Type I and Type III-B kinetics:

$$\text{Type I:} \quad t = \frac{N_o A}{C_1 Q}\left[\lambda - k_1\left(\frac{1000\ Q}{A}\right)^x \left(\ln\frac{C_1}{C_2} - 1\right)\right] \qquad (51)$$

$$\text{Type III-B:} \quad t = \frac{N\ A}{C_1 Q}\left[\lambda - k_1\left(\frac{1000\ Q}{A}\right)^x \left(\ln\frac{C_1}{C_2} + 3\right)\right] \qquad (52)$$

Table XXV

Effect of Velocity on H_t and H

H_t (or H) = k_1V^x

Agent	x
PS	0.30
CG	0.48
CK	0.32
AC	0.26
SA	assumed 0.30

DECLASSIFIED

[redacted]

Fig. 63

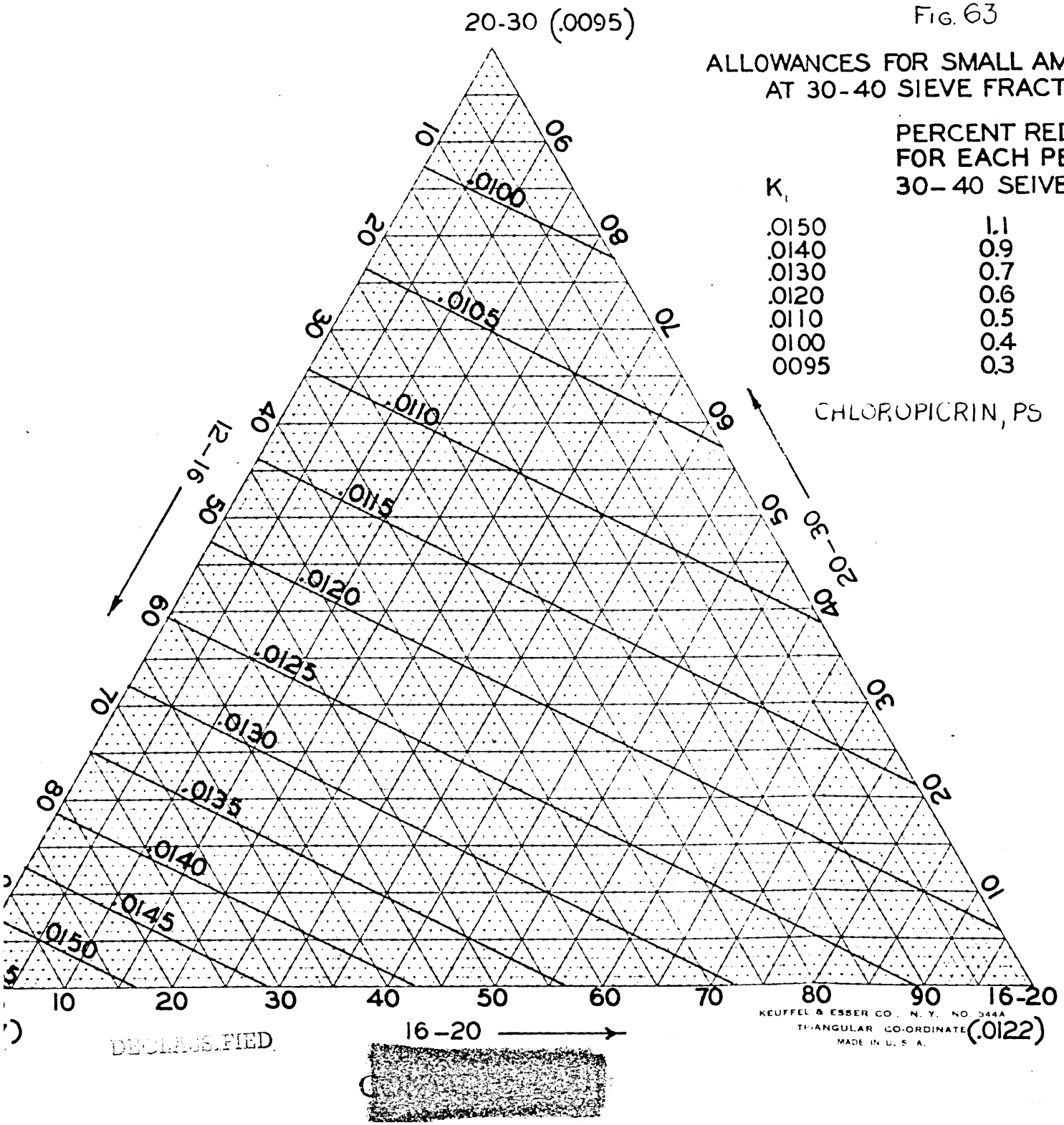

DECLASSIFIED

[redacted]

DECLASSIFIED

CONFIDENTIAL

FIG. 64

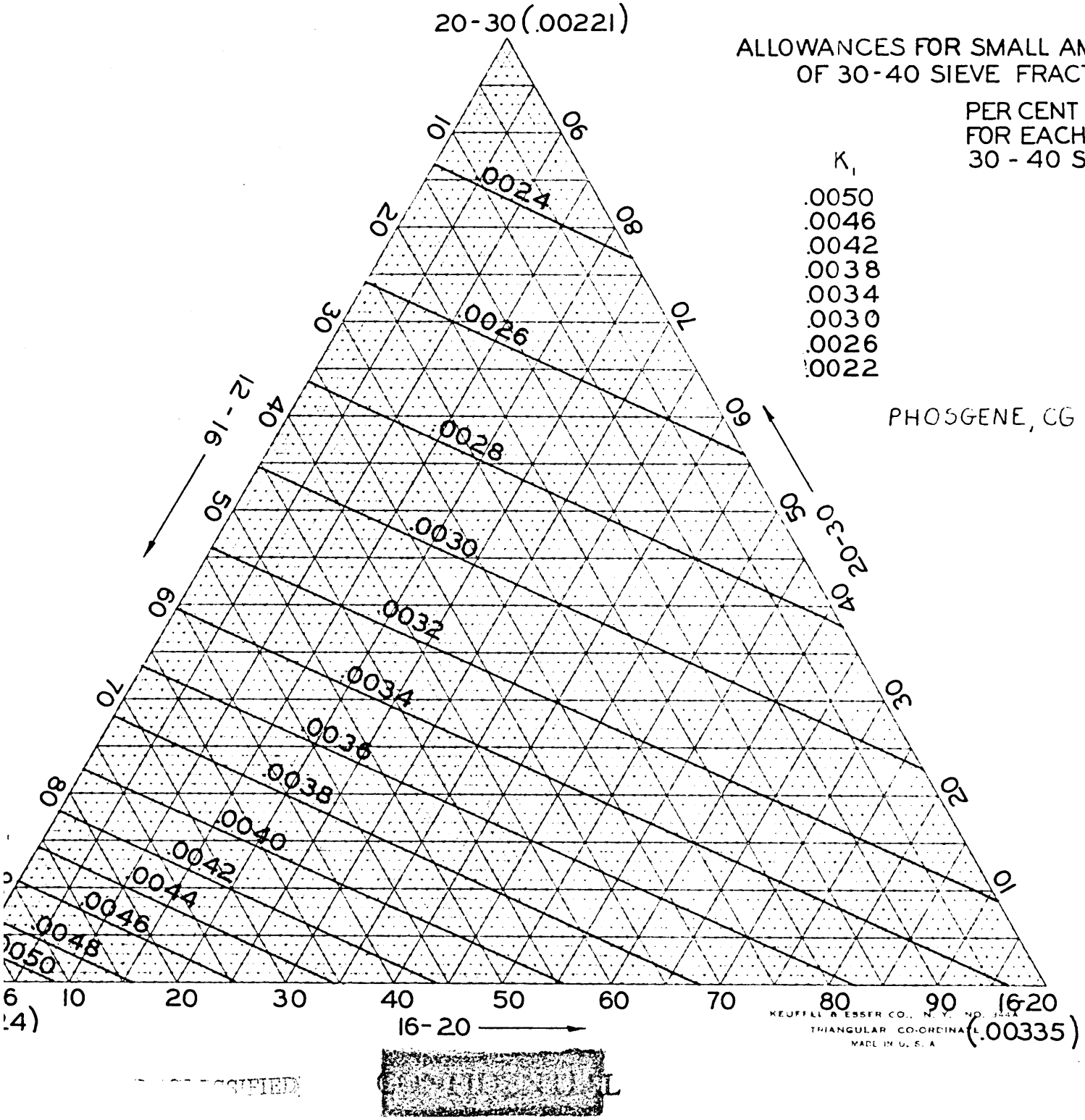

ALLOWANCES FOR SMALL AMOUN
OF 30-40 SIEVE FRACTION

K_1	PER CENT REDU FOR EACH PER 30 - 40 SIEVE
.0050	2.2
.0046	2.0
.0042	1.8
.0038	1.6
.0034	1.4
.0030	1.1
.0026	0.8
.0022	0.5

PHOSGENE, CG

FEB

F

DECLASSIFIED

CONFIDENTIAL

DECLASSIFIED

[redacted]

FIG. 65

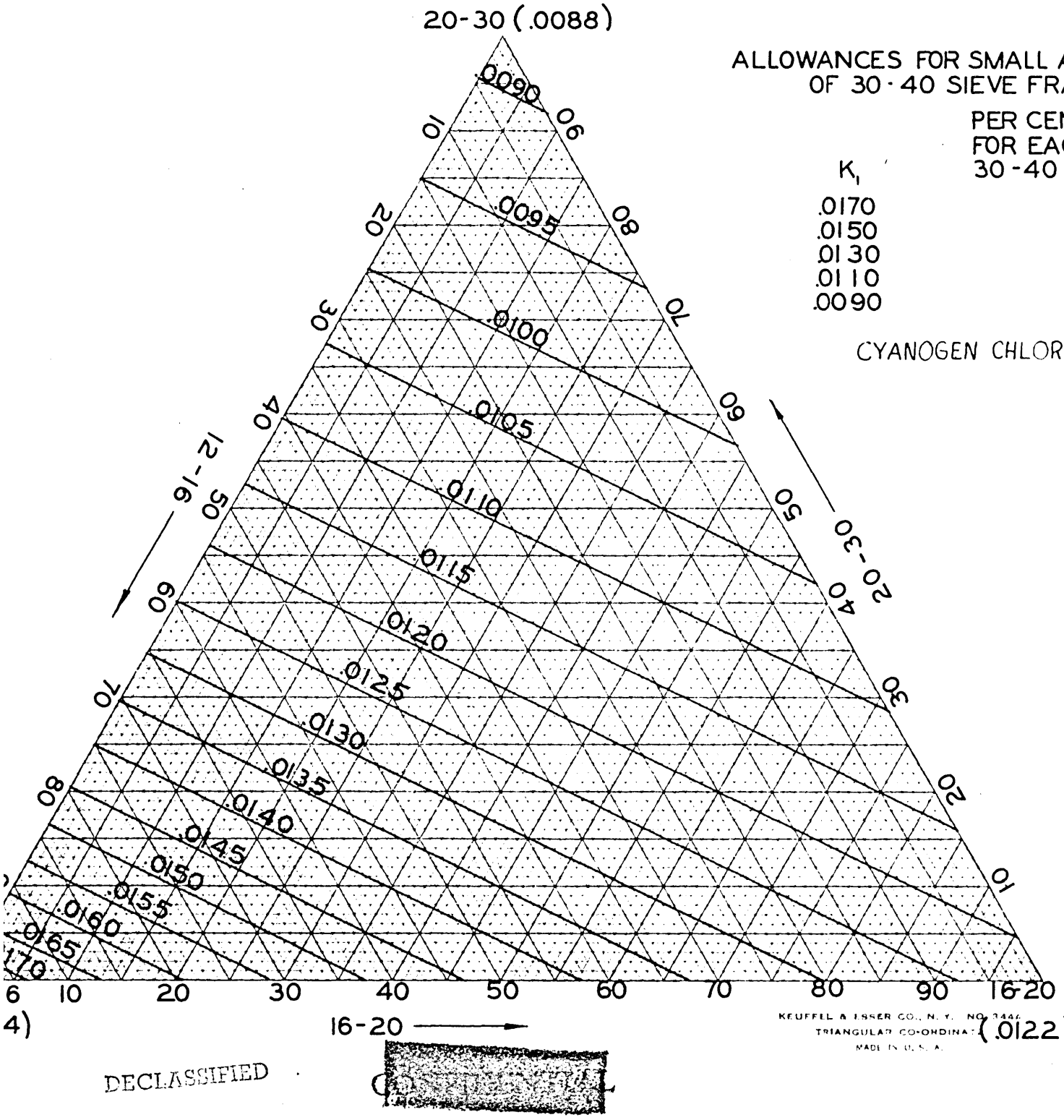

ALLOWANCES FOR SMALL AMOUN
OF 30-40 SIEVE FRACTION

K_1	PER CENT RED FOR EACH PER 30-40 SIEVE
.0170	1.5
.0150	1.3
.0130	1.0
.0110	0.7
.0090	0.5

CYANOGEN CHLORIDE, CK

FEB.

F.

DECLASSIFIED

[redacted]

DECLASSIFIED

CONFIDENTIAL

FIG. 66

ALLOWANCE FOR SMALL PERCEN
OF 30-40 SIEVE FRACTIO

K_1	PERCENT REDU FOR EACH F 30-40 SIEVE I
.0220	1.2
.0200	1.0
.0180	0.8
.0160	0.6
.0140	0.4

HYDROCYANIC ACID, AC

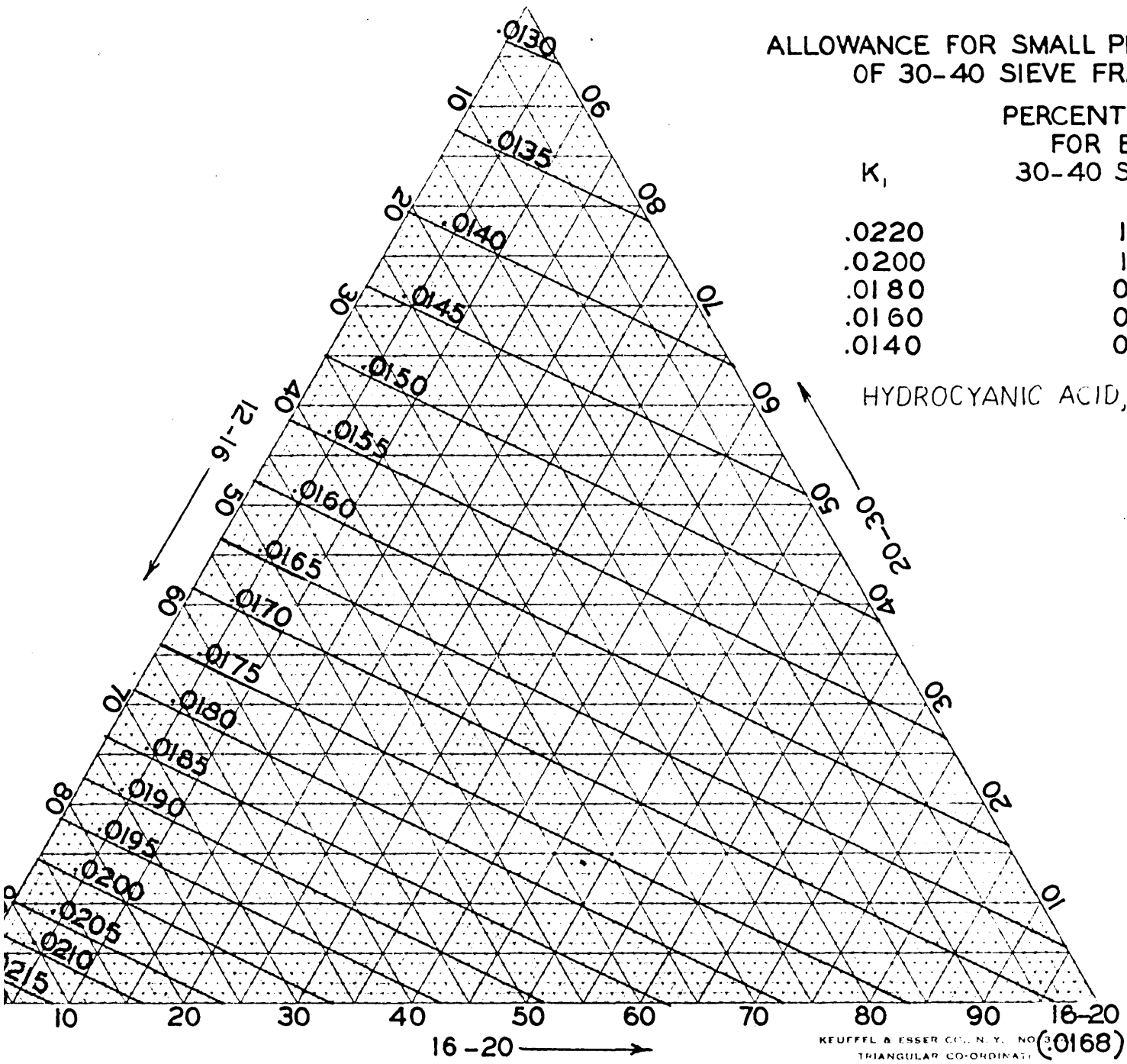

FEB. 15

F. G

DECLASSIFIED

CONFIDENTIAL

DECLASSIFIED

[redacted]

FIG. 67

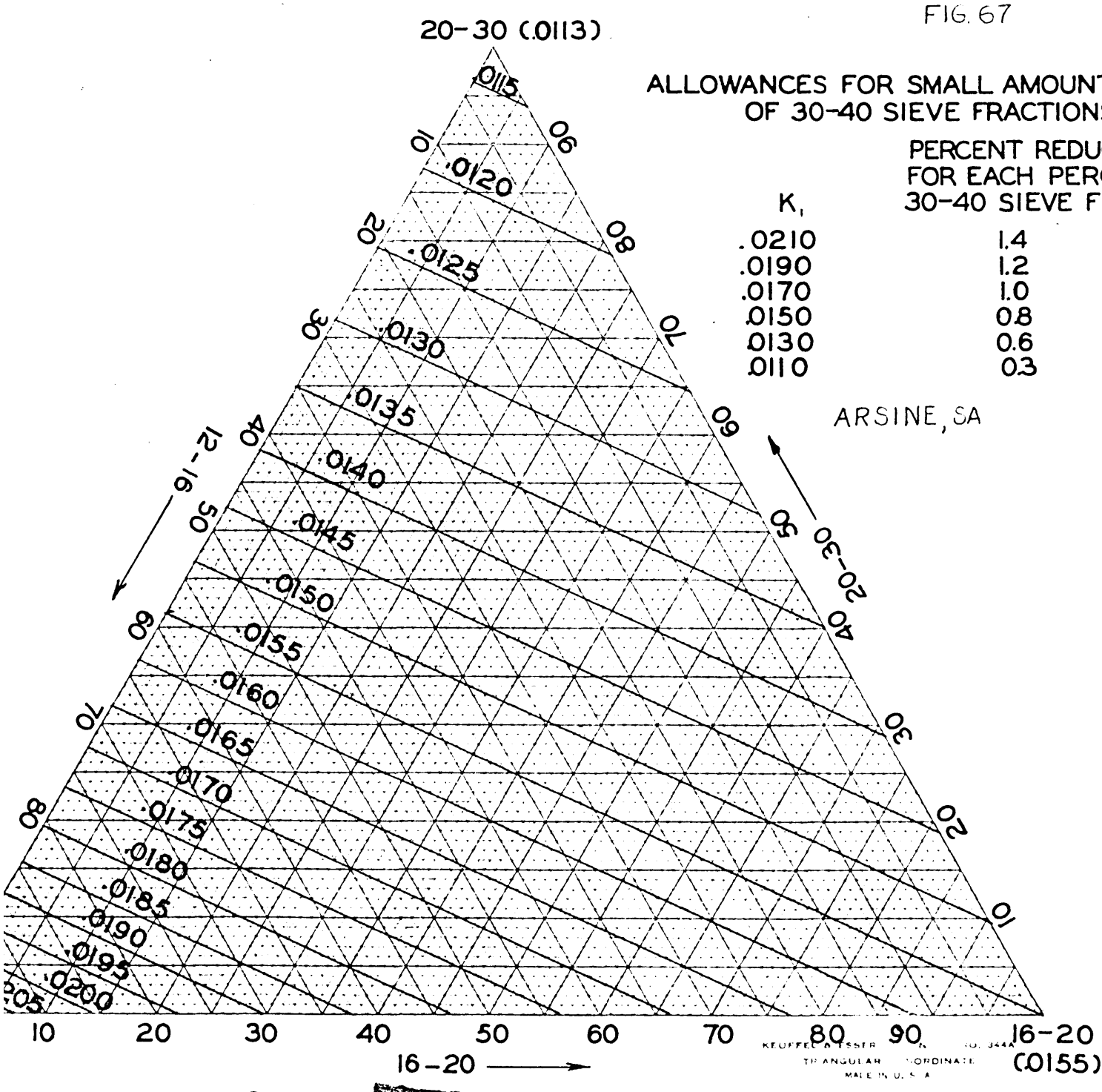

ALLOWANCES FOR SMALL AMOUNTS CO
OF 30-40 SIEVE FRACTIONS

K_1	PERCENT REDUCTION FOR EACH PERCENT 30-40 SIEVE FRACTI
.0210	1.4
.0190	1.2
.0170	1.0
.0150	0.8
.0130	0.6
.0110	0.3

ARSINE, SA

FEB. 15

F.G.

DECLASSIFIED

[redacted]

The effects of the baffles in the canister and of breather testing on the critical bed depths are taken into consideration by the following modifications of these equations, discussed previously:

$$\text{Type I:} \qquad t = \frac{N_o A}{C_1 Q}\left[\lambda - k_1\left(\frac{1000\ Q_e}{A_b}\right)^x\left(\ln\frac{C_1}{C_2} - 1\right)\right] \qquad (53)$$

$$\text{Type III-B:} \qquad t = \frac{N\ A}{C_1 Q}\left[\lambda - k_1\left(\frac{1000\ Q_e}{A_b}\right)^x\left(\ln\frac{C_1}{C_2} + 3\right)\right] \qquad (54)$$

(2) Cumulative Break Time

It has been shown in this thesis that the following equation, derived in Appendix B, is applicable for Type I kinetics, as exemplified by chloropicrin:

$$t = \frac{N_o A}{C_1 Q}\left[\lambda - H_t\left(\ln\frac{N_o H_t A}{F} - 1\right)\right] \qquad (6)$$

It has also been shown that, over the range of variables investigated, a similar equation applies for Type III-B kinetics as exemplified by CG, CK, AC, and SA. The equation is as follows:

$$t = \frac{N\ A}{C_1 Q}\left[\lambda - H\left(\ln\frac{N\ H\ A}{F} + 3\right)\right] \qquad (55)$$

Replacing H and H_t by $k_1 V^x$ and including the effects of baffles and breather test conditions results in the following modifications of these equations,

previously discussed:

$$\text{Type I:} \quad t = \frac{N_o A}{C_1 Q}\left[\lambda - k_1\left(\frac{1000\ Q_e}{A_b}\right)^x\left(\ln \frac{N_o k_1\left(\frac{1000 Q_e}{A_b}\right)^x A_b}{F} - 1\right)\right] \quad (56)$$

$$\text{Type III-B:} \quad t = \frac{N\ A}{C_1 Q}\left[\lambda - k_1\left(\frac{1000\ Q_e}{A_b}\right)^x\left(\ln \frac{N k_1\left(\frac{1000 Q_e}{A_b}\right)^x A_b}{F} + 3\right)\right] \quad (57)$$

(3) Air Resistance

The air resistance of an adsorbent bed is determined by bed depth, air velocity, particle diameter, and the baffles. Minor variations are caused by differences in particle shape. It has been shown that, in the streamline region, the following general equation is applicable for axial flow adsorbent beds:

$$\Delta P = k_2\ Q\left[\frac{2.00}{A_b} + \frac{\lambda - 2.00}{A}\right] \quad (48)$$

The only term in this equation which is not defined by the test conditions is k_2. This term has been shown previously to be a function of the sieve fraction, and it has been shown that it can be calculated for blends of several sieve fractions. These calculations have been made for all blends of 12-16, 16-20, and 20-30 sieve fractions and for mixtures of these sieve fractions containing up to five per cent of 30-40 sieve fraction. The results of these calculations are shown in Fig. 68 which is a plot of k_2 for H whetlerite as a function of

DECLASSIFIED

CONFIDENTIAL

FIG. 68

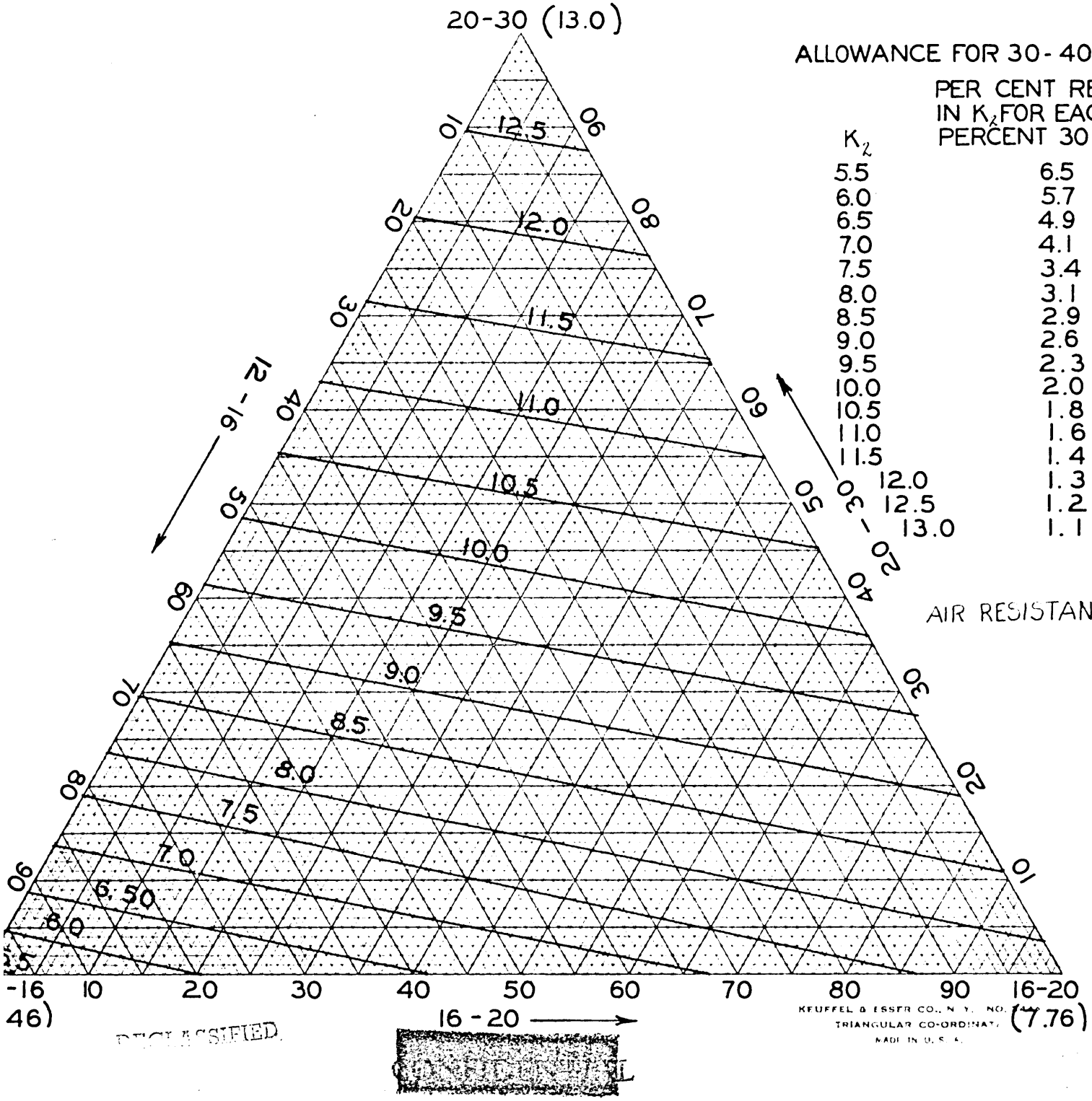

ALLOWANCE FOR 30 - 40 MES

PER CENT REDUC
IN K_2 FOR EACH
PERCENT 30 - 40

K_2	
5.5	6.5
6.0	5.7
6.5	4.9
7.0	4.1
7.5	3.4
8.0	3.1
8.5	2.9
9.0	2.6
9.5	2.3
10.0	2.0
10.5	1.8
11.0	1.6
11.5	1.4
12.0	1.3
12.5	1.2
13.0	1.1

FEB.

F

DECLASSIFIED

CONFIDENTIAL

the sieve analysis. The correction factors (for particle shape) for other whetlerites are shown in Table XXIII.

2. Radial Flow Adsorbent Beds

The applicable equations for reversible, physical adsorption are derived in Appendix D. These equations are as follows:

$$D_c = \left[D_i^{x+1} + 2(x+1)k_1\left(\frac{1000\ Q}{\pi\ L}\right)^x \ln \frac{C_1}{C_2} \right]^{\frac{1}{x+1}} \qquad (4)$$

$$t = \frac{\pi\ L\ N_o}{4\ Q\ C_1} \left[D_2^2 - D_c^2 + 4\ D_c k_1 \beta \left(\frac{1000Q}{\pi\ D_c L}\right)^x \right] \qquad (5)$$

No modification of these equations is necessary for adaptation to Type III-B kinetics if it is recalled that the value of β becomes -3 instead of +1. Substituting the values of β for Type I and for Type III-B kinetics into Equation 5, the following equations are obtained:

$$\text{Type I:} \quad t = \frac{\pi\ L\ N_o}{4\ Q\ C_1} \left[D_2^2 - D_c^2 + 4\ D_c k_1 \left(\frac{1000Q}{\pi\ D_c L}\right)^x \right] \qquad (57)$$

$$\text{Type III-B:} \quad t = \frac{\pi\ L\ N_o}{4\ Q\ C_1} \left[D_2^2 - D_c^2 - 12\ D_c k_1 \left(\frac{1000Q}{\pi\ D_c L}\right)^x \right] \qquad (58)$$

If a portion of the inner tube length, L, is baffled, any term involving the determination of the rate of transfer must be concerned with the free length at the baffles. This is analogous to the use of the open area at the baffles in axial flow canisters for the determination of the critical bed depth. Thus, in the above equa-

tions, any term involving L to the xth power actually involves the free length at the baffle, L_b.

For breather test conditions, the air flow rate for those portions of the equations pertaining to the effects of velocity on the rate of transfer must be replaced by the steady flow rate equivalent to breather flow.

Modifications of the above equations to allow for these two considerations results in the following equations:

$$D_c = \left[D_i^{x+1} + 2(x+1)k_1 \left(\frac{1000Q_e}{\pi L_b} \right)^x \ln \frac{C_1}{C_2} \right]^{\frac{1}{x+1}} \quad (59)$$

$$\text{Type I:} \quad t = \frac{\pi L N_o}{4 Q C_1} \left[D_2^2 - D_c^2 + 4 D_c k_1 \left(\frac{1000Q_e}{\pi D_c L_b} \right)^x \right] \quad (60)$$

$$\text{Type III-B:} \quad t = \frac{\pi L N_o}{4 Q C_1} \left[D_2^2 - D_c^2 - 12 D_c k_1 \left(\frac{1000Q_e}{\pi D_c L_b} \right)^x \right] \quad (61)$$

For those particular tests wherein cumulative penetration break times are determined, Equation 59 must be modified in the following manner which is analogous to the modification of the equations for axial flow beds:

$$D_c = \left[D_i^{x+1} + 2(x+1)k_1 \left(\frac{1000Q_e}{\pi Lb} \right)^x \ln \frac{NA_b k_1 \left(\frac{1000Q_e}{A_b} \right)^x}{F} \right]^{\frac{1}{x+1}} \quad (62)$$

In this equation, A_b must be taken at the average values at D_c and at D_i. Therefore, the solution of Equation 62 involves the method of successive approximations.

During the course of investigations at the Chemical Warfare Service Development Laboratory, M.I.T., tests were conducted to determine the relative performance of the standard U.S.Army gas mask canisters. The canisters which were tested were: M10A1, M10, M1 Training, and the M11, combat. All of these canisters except the M11 are of the radial flow design. These results were reported in Weekly Progress Report, Project D1.1-1b11 (Service Canisters) for the week ending Feb. 19, 1944. The results of these tests are shown in Table XXVI.

The sieve analyses of the whetlerites employed for these tests are shown in Table XXVII.

Table XXVII

Sieve Analyses of Whetlerites
Test Results: Table XXVI

Whetlerite	Sieve Analysis 12-16	16-20	20-30	30-40
HH2-	28.0	44.0	27.0	1.0
HC3-361	31.1	40.0	25.7	3.0
AD3-255	37.4	40.6	20.7	1.2

The dimensions of the radial flow canisters are shown in Table XXVIII.

The validity of the radial flow equations can be determined by testing the equations with these data. This was done by determing k_1 from the sieve analysis and N_o (or N) from the gas life of any one of the canisters. The gas life of any of the other canisters can

Table XXVI

Comparison of Performance of Service Canisters

Type Canister	Whetlerite Designation	CG		CK		AC		PS		SA	
		Calc.	Obs.	Calc.	Obs.	Calc.	Obs.	Calc.	Obs.	Calc.	Obs.
		*Break Times (Minutes)									
M10	HH-2	31	30	46	48	36	31	72	69	71	75
	HC3-361	35	36	33	32	28	32	94	84	86	81
	AD3-255	36	36	43	39	36	34	71	67	76	80
M10A1	HH-2	-	42	-	65	-	52	-	91	97	113
	HC3-361	-	47	-	47	-	39	-	119	118	133
	AD3-255	-	50	-	62	-	51	-	91	105	117
M1 Training	HH-2	20	20	31	25	26	21	53	51	48	43
	HC3-361	23	25	23	21	20	19	70	71	58	56
	AD3-255	23	24	29	23	25	23	54	58	48	40
M11 250 ml.	HH-2	31	32	52	51	43	37	73	81	-	77
	HC3-361	35	39	38	37	32	32	96	105	-	92
	AD3-255	37	43	51	48	43	39	73	72	-	81

* Each datum is average of two to five individual tests.

Test Conditions

Agent	Flow Rate	Humidity	C_1 (mg./L.)	C_2 (mg./L.)	F (mg.)
CG	50 L./min., B.	AR-50	10.0	.008	-
CK	"	"	4.0	.008	-
AC	"	"	4.0	.004	-
PS	"	"	10.0	.020	-
SA	"	"	4.0	-	8.5

DECLASSIFIED

DECLASSIFIED

then be computed by application of Equations 53, 54, 56, 57, 59, 60, 61, and 62.

Table XXVIII

Dimensions of Radial Flow Canisters
All Dimensions in cm.

Dimension	Canister M1 Training	M10	M10A1
Diameter, Inner Tube	3.17	3.17	3.17
Diameter, Outer Tube	6.35	6.35	6.79
Total Tube Length	8.89	11.42	11.42
Open Tube Length at Baffle	7.62	10.15	10.15

N_o (or N) was calculated from the M10A1 life (for all cases except the SA results) because the longest lives were obtained with this canister and the constant errors are minimized. The M11 canister life was used to determine N for SA because this eliminated the necessity of a double trial and error calculation which would be required were the M10A1 life to be used (SA lives were measured to a cumulative break).

The results of these computations are shown in comparison with the observed lives in Table XXVI. The agreement is seen to be very good indicating the validity of the radial flow equations, breather flow adaptation to radial flow equations, and cumulative penetration adaptation to the radial flow equations. The detailed calculation procedure is described in Appendix I.

B. Practical Canister Design

A gas mask canister is composed of two fundamental parts: the smoke or particulate filter and the gas filter. Neither section of the canister can be designed without consideration of the other.

The two basic designs have been described previously as the radial and axial flow types. The axial flow canister, for canisters of reasonable diameter, is a high velocity canister as compared to a radial flow type, for the latter type can be made longer to reduce the linear velocity. Prior to this war the quality of the particulate filter was such that the use of axial flow canisters was obviated because of excessive resistance of this filter. During this war, however, all of the major powers so improved the quality of their filter media that an axial flow canister of reasonable diameter became feasible. Here we have an example of the adsorbent bed design being controlled by the filter media available.

The advantages of the axial flow canister rest in its compactness. There are no void spaces such as the inner tube and the annular spaces between the canister body and the chemical container. Also, the axial flow canister can be designed to be much shorter so that direct attachment of the canister to the facepiece can be accomplished without excessive pendulum action when the head is moved. Attachment of the canister to the facepiece has the obvious advantages of compactness and elimination of the hose tubes which might interfere with

combat activities.

For these reasons the United States, Great Britain, Canada, and Germany adopted the axial flow canister. The Japanese had an axial flow adsorbent bed and a radial flow filter.

In an axial flow canister, gas life, air resistance, canister diameter, charcoal volume, adsorbent particle size, and many other variables are inter-related. A qualitative representation of this inter-dependency is shown in Figs. 69 and 70. These figures were calculated on the basis of the phosgene performance of the CC3-900 Type ASC impregnated whetlerite previously discussed. Similar relationships would result for any of the other agents.

Fig. 69 shows that at a fixed gas life (dotted line) and canister diameter, the air resistance increases with decreasing particle diameter. It also shows that the charcoal volume required decreases with decreasing particle diameter. Since a low resistance and volume of adsorbent are both desired, a balance must be made.

The factors which control the choice of the of the balance among air resistance, sieve size, canister diameter, charcoal volume, and break time are beyond the scope of this thesis. It involves such abstract factors as physical comfort, impedance of motion, design of the facepiece, etc. The exact balance is still a controversial point in the Chemical Warfare Service although certain standards have been adopted.

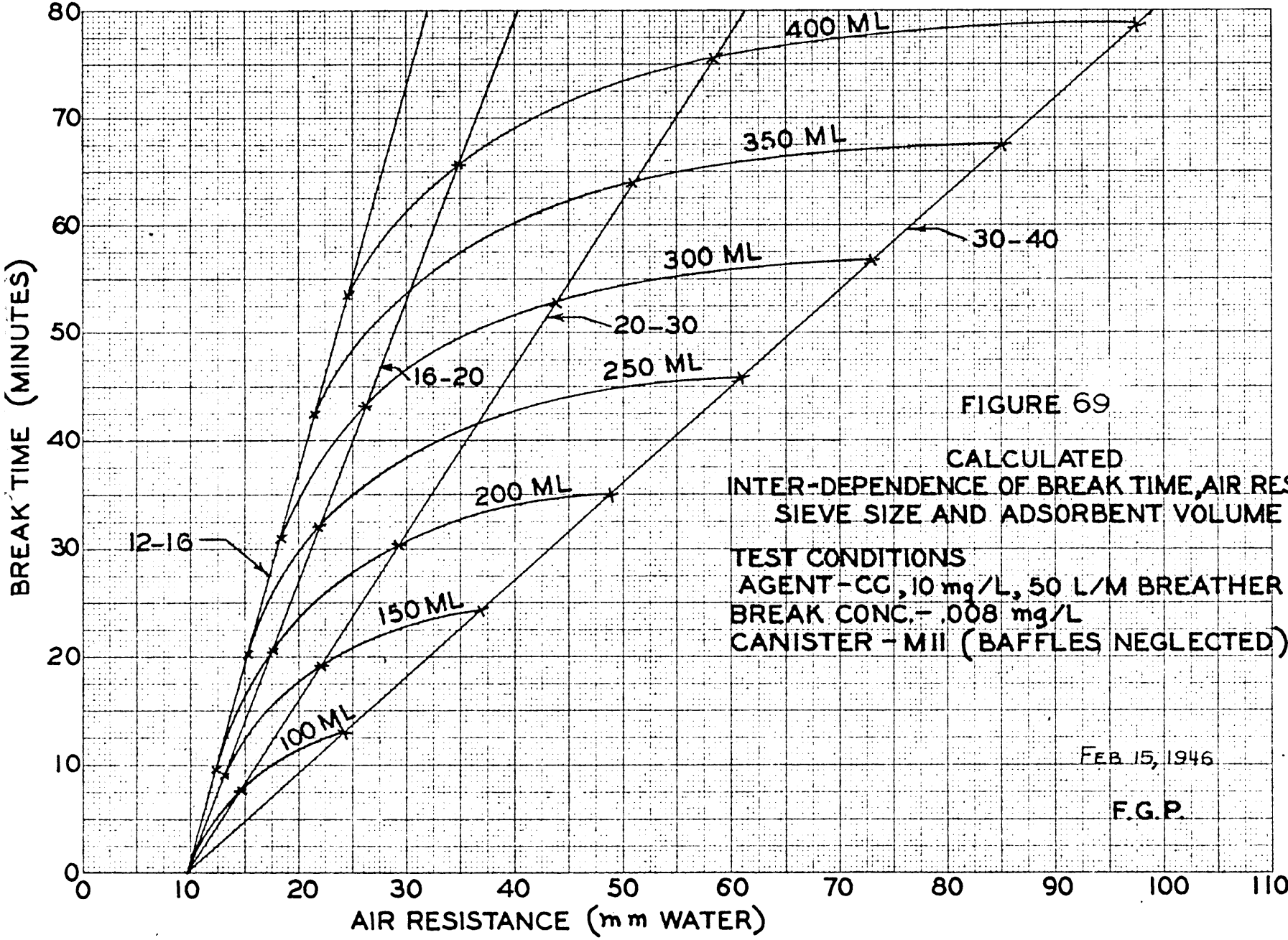

DECLASSIFIED

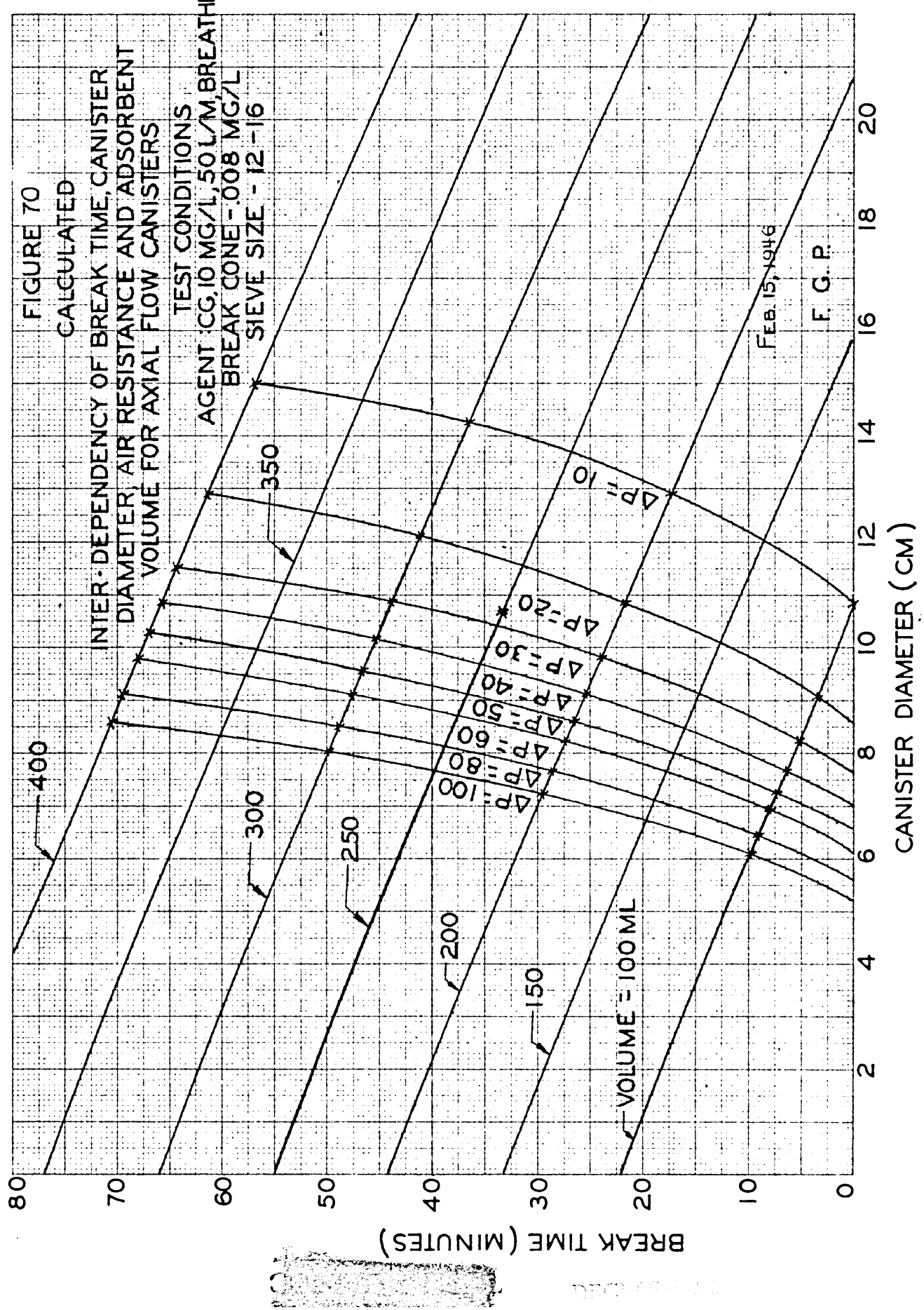
FIGURE 70
CALCULATED
INTER-DEPENDENCY OF BREAK TIME, CANISTER DIAMETER, AIR RESISTANCE AND ADSORBENT VOLUME FOR AXIAL FLOW CANISTERS
TEST CONDITIONS
AGENT: CG, 10 MG/L, 50 L/M, BREATHER
BREAK CONE - .008 MG/L
SIEVE SIZE - 12-16
FEB. 15, 1946
F. G. P.
ΔP = 10
ΔP = 20
ΔP = 30
ΔP = 40
ΔP = 50
ΔP = 60
ΔP = 80
ΔP = 100
400
350
300
250
200
150
VOLUME = 100 ML
BREAK TIME (MINUTES)
CANISTER DIAMETER (CM)
0
10
20
30
40
50
60
70
80
2
4
6
8
10
12
14
16
18
20

VIII. CONCLUSIONS

It is concluded that:

1. The following equation adequately defines the relationship beteeen bed depth of axial flow adsorbent beds, break time, air flow, cross sectional area, sieve fraction, influent concentration, and effluent concentration for those agents which are physically adsorbed and for which n in Freundlich's adsorption isotherm is effectively greater than two and for which Type I kinetics apply:

$$t = \frac{N_o A}{C_1 Q}\left[\lambda - k_1\left(\frac{1000\,Q}{A}\right)^x\left(\ln\frac{C_1}{C_2} - \beta\right)\right] \qquad (51)$$

2. All the other standard Chemical Warfare Service non-persistent agents (CG, CK, AC, and SA) are removed by Type ASC impregnated whetlerite by a combination of physical adsorption and chemical reaction with the impregnants. Furthermore, the kinetics of removal is the most involved type, Type III-B, for which the rate of chemical reaction with the impregnants is an involved function of the amount of unreacted impregnant remaining (the impregnant is not uniformly active).

3. For Type III-B kinetics, there is no exact linear relationship between break time to a specified effluent concentration and bed depth for axial flow canisters, but the following semi-empirical equation

accurately predicts the performance of beds of Type ASC impregnated whetlerite for those agents which are removed by Type III-B kinetics over the range of variables investigated:

$$t = \frac{N\,A}{C_1 Q}\left[\lambda - k_1\left(\frac{1000\,Q}{A}\right)^x\left(\ln\frac{C_1}{C_2} + 3\right)\right] \qquad (52)$$

4. The values of k_1 in the above equations have been shown to be a function of sieve size, and it has been shown that they are relatively constant for different Type ASC impregnated whetlerites of the same sieve fraction.

5. The value of k_1 for a mixture of several sieve fractions can be calculated accurately for both Type I and Type III-B kinetics by the following equation:

$$k_1 = \frac{1}{\frac{f_a}{(k_1)_a} + \frac{f_b}{(k_1)_b} + \cdots \frac{f_x}{(k_1)_x}} \qquad (63)$$

6. The above equations are equally applicable for breather flow test conditions and for baffled adsorbent beds if all the terms which contain the air flow rate or the cross sectional area and which affect the critical bed depth are modified so that the air flow rate is replaced by the air flow rate equivalent to the breather flow and the cross sectional area is replaced by the cross sectional area at the baffles.

7. The time to a specified cumulative penetration is accurately obtained by the following equations for an axial flow adsorbent bed:

$$\text{Type I:} \quad t = \frac{N_o A}{C_1 Q}\left[\lambda - k_1\left(\frac{1000\ Q_e}{A_b}\right)^x\left(\ln\frac{N_o A_b k_1\left(\frac{1000 Q_e}{A_b}\right)^x}{F} - 1\right)\right] \tag{56}$$

$$\text{Type III-B:} \quad t = \frac{N\ A}{C_1 Q}\left[\lambda - k_1\left(\frac{1000\ Q_e}{A_b}\right)^x\left(\ln\frac{NA_b k_1\left(\frac{1000 Q_e}{A_b}\right)^x}{F} + 3\right)\right] \tag{57}$$

8. The air resistance of an axial flow canister, for air velocities below 2000 cm./min., can be represented by the following equation:

$$\Delta P = k_2 Q\left[\frac{2.00}{A_b} + \frac{\lambda - 2.00}{A}\right] \tag{48}$$

9. The performance of a radial flow adsorbent bed is accurately predicted by the following equations for Type I and Type III-B kinetics:

$$D_c = \left[D_i^{x+1} + 2(x+1)k_1\left(\frac{1000 Q_e}{\pi\ L_b}\right)^x\left(\ln\frac{C_1}{C_2}\right)\right]^{\frac{1}{x+1}} \tag{59}$$

$$\text{Type I:} \quad t = \frac{\pi L N_o}{4QC_1}\left[D_2^2 - D_c^2 + 4D_c k_1\left(\frac{1000 Q_e}{\pi\ D_c L_b}\right)^x\right] \tag{60}$$

$$\text{Type III-B:} \quad t = \frac{\pi L N}{4QC_1}\left[D_2^2 - D_c^2 - 12D_c k_1\left(\frac{1000 Q_e}{\pi\ D_c L_b}\right)^x\right] \tag{61}$$

10. The time to a specified cumulative penetration for a radial flow adsorbent bed can be represented

by the following equations:

$$\text{Type I:} \qquad D_c = \left[D_i^{x+1} + 2(x+1)k_1 \left(\frac{1000Q_e}{\pi L_b} \right)^x \left(\ln \frac{N_o A_b k_1 \left(\frac{1000Q_e}{A_b} \right)^x}{F} \right) \right]^{\frac{1}{x+1}} \tag{62}$$

$$\text{Type III-B:} \quad D_c = \left[D_i^{x+1} + 2(x+1)k_1 \left(\frac{1000Q_e}{\pi L_b} \right)^x \left(\ln \frac{NA_b k_1 \left(\frac{1000Q_e}{A_b} \right)^x}{F} \right) \right]^{\frac{1}{x+1}} \tag{63}$$

The values of D_c , calculated from these equations, can be substituted into Equation 60 or 61 to determine the break time. The value of A_b must be taken as the average at D_c and at D_i.

IX. RECOMMENDATIONS

It is recommended that:

1. The equations which are derived in Appdx. A of this thesis for reversible, physical adsorption be tested further with other physically adsorbed gases and that the value of β be accurately determined as a function of the strength of adsorption.

2. Further research be done with strongly adsorbed gases ($\beta = 1$) so that the values of H_t may be correlated accurately with such variables as diffusivity, viscosity, density, temperature, pressure, etc. in the form of dimensionless groups covering a wide range of the variables.

3. Work be conducted to determine the effects of packing density on the values of H_t. This variable was not studied during this investigation because all canisters were filled by the standard free-fall technique. It was found, however, in other work at the C.W.S. Development Laboratory, M.I.T., that higher packing densities can be obtained by vibration of the adsorbent bed when held under a high pressure. Qualitatively, this resulted in a higher resistance and a shorter break time for a constant volume of adsorbent.

4. Additional work be done within the Chemical Warfare Service to increase the activity (rate of reaction) of the impregnants on Type ASC impregnated whetlerite and that this work be analyzed and directed in an attempt to

decrease the critical bed depths to as near the critical bed depths inherent with diffusional resistance as practical.

5. The principles developed in this thesis be adopted to research on such industrial processes as purification of gases, elimination of noxious waste gases, solvent recovery, separation of mixtures of gases, and gas-solid catalysis.

6. These same principles be applied to the concentration of components of solutions.

X. APPENDIX

GROUP - 4
Downgraded at 3 year intervals;
declassified after 12 years.
PER D.L. ADDERLEY

Classification Changed
TO: UNCLASSIFIED
By Authority of:
DAVID L.
ADDERLEY 1 NOV 68
Name Date
EDGEWOOD ARSENAL
MARYLAND

APPENDIX A

DERIVATION OF EQUATION FOR CASES OF PHYSICAL ADSORPTION

A. Derivation of Differential Equation

Consider a differential thickness of an adsorbent bed with a constant cross-sectional area. The quantities of adsorbable gas in the voids surrounding the adsorbent particles at times t and t+dt, respectively, are:

$$\frac{C\ A\ \alpha\ d\lambda}{1000} \quad \text{and} \quad \frac{A\ \alpha\ d\lambda}{1000}\left(C + \frac{\partial C}{\partial t}\ dt\right)$$

The amounts of adsorbate entering and leaving this differential thickness in time interval, dt, are:

$$\frac{V\ A\ C}{1000}\ dt \text{ and } \frac{V\ A}{1000}\ \left(C + \frac{\partial C}{\partial \lambda}\right)dt$$

In the above expressions, the linear velocity is considered to be constant although it actually decreases slightly because of adsorption. In all Chemical Warfare Service application, however, the change never exceeds two per cent and the assumption is justified. The normal test concentrations, converted to volume percentages at 70°F., are tabulated below to show the validity of this simplification (Table XXIX).

The difference between the quantities entering and leaving must, by a material balance, be equal to the sum

of the accumulation in the voids between the charcoal granules and the accumulation on the adsorbent. From diffusion rate considerations, the latter quantity is equal to $k_g a(C-C^*)Ad\lambda dt$. This equality may be expressed by the following equation:

$$k_g a(C^* - C) = \left(\frac{a}{1000}\right)\frac{\partial C}{\partial t} - \left(\frac{V}{1000}\right)\frac{\partial C}{\partial \lambda} \qquad (64)$$

Table XXIX

Normal and Maximum Test Concentrations

Agent	Normal Test Concentration (mg./L.)	Normal Test Concentration (Volume Per Cent at 70°F.)	Maximum Test Concentration (mg./L.)	Maximum Test Concentration (Volume Per Cent at 70°F.)
CG	10.0	0.24	40	0.99
PS	10.0	0.15	50	0.74
AC	4.0	0.36	20	1.81
SA	10.0	0.32	20	0.64
CK	4.0	0.16	20	0.81

By similar reasoning, the following equation, relating C, t, and m, may be derived:

$$k_g a\ (C - C^*) = \frac{\partial m}{\partial t} \qquad (65)$$

Equations 64 and 65 govern the relationships among C, t, λ, and m; it is the solution of these equations which is desired. The value of C^*, the equilibrium concentration,

is a function of the amount of adsorbate on the adsorbent and the temperature. For isothermal conditions, it is a function of m only, the function reverting to the adsorption isotherm.

Eliminiating C between equations 64 and 65 and substituting f(m) for C^*, the following general differential equation is obtained:

$$\frac{\alpha}{1000k_ga}\frac{\partial^2 m}{\partial t^2} + \frac{V}{1000k_ga}\frac{\partial^2 m}{\partial \lambda \partial t} + \frac{\partial m}{\partial t} + \frac{\alpha}{1000}\frac{\partial f(m)}{\partial t} + \frac{V}{1000}\frac{\partial f(m)}{\partial \lambda} = 0 \qquad (11)$$

The solubility of this equation depends on the nature of f(m). The only conditions for which solutions are known are when f(m) is constant and when f(m) is directly proportional to m. Unfortunately, neither of these relationships is valid for the adsorption of vapors by charcoal although the latter, which represents Freundlich's adsorption isotherm when n is equal to zero, is a limiting case which applies for the adsorption of gases at temperatures far above their condensation temperature. Therefore, no general analytical relationship of C and m as a function of λ and t can be obtained.

B. Apparent and True Critical Bed Depth

Two concepts, the apparent and the true critical bed depths, will be referred to frequently in the following discussion. Therefore, they are defined at this point for clarity.

The "true critical bed depth" is defined as that bed

depth which, at the test conditions, will result in an effluent concentration, at the instant the test starts (taking into consideration the time required for the air stream to penetrate the bed) equal to the previously established break concentration.

The "apparent critical bed depth" is herein defined as that bed depth at which the extrapolation of the linear portion of the bed depth-break time curve strikes the bed depth axis (if such a linear portion exists).

C. Solution of Equations 64 and 65 for Definite Values of the Variables

Although Equation 11 cannot be solved by any known method to give an algebraic relationship between the variables, Equations 64 and 65 can be solved for particular, specified values of the constants by a tedious, step-wise process of successive approximations (trial and error).

When this was attempted, it was found that the term $\frac{\alpha}{1000}\frac{\partial C}{\partial t}$ in Equation 64 was always inconsequential as compared to the term $\frac{V}{1000}\frac{\partial C}{\partial \lambda}$ and may be neglected (this is exemplified in Table XXX). Elimination of this term results in the following equation:

$$k_g a(C^* - C) = \frac{V}{1000}\frac{\partial C}{\partial \lambda} \qquad (66)$$

Although this equation can be handled in this form, the method of transfer units results in simpler relationships and is employed throughout. Substituting the equation for the transfer unit in terms of $k_g a$ and V, the following equation is obtained:

UNCLASSIFIED

CONFIDENTIAL

Table XXX

Comparison of $\frac{\alpha}{1000}\frac{\partial C}{\partial t}$ and $\frac{V}{1000}\frac{\partial C}{\partial \lambda}$

Taken from Results of Calc. No. 1, Table XXXI
Bed Depth: 0.32 Cm.

t (min.)	C (mg./L.)	$\frac{\partial C}{\partial \lambda}$	$\frac{\partial C}{\partial t}$	$\frac{V}{1000}\frac{\partial C}{\partial \lambda}$	$\frac{*\alpha}{1000}\frac{\partial C}{\partial t}$
0	0.18	2.3	0	1.31	0
2	0.19	2.4	.01	1.36	.00001
4	0.32	4.0	.11	2.30	.00011
6	0.60	7.5	.20	4.31	.00020
8	1.12	14.0	.39	8.06	.00039
10	2.13	26.6	.72	15.4	.00072
12	4.05	50.6	1.38	29.2	.0014
14	7.10	88.6	2.41	51.0	.0024
16	9.25	58.7	.70	33.8	.0007
18	10.-	10.0	0 +	5.8	.0000 +

*α assumed at maximum value of unity.

UNCLASSIFIED

CONFIDENTIAL

$$\frac{C^* - C}{Ht} = \frac{\partial C}{\partial \lambda} \qquad (67)$$

If a very small bed depth increment and time increment are taken so that C^* may be taken as constant at its average value, the partial differentials may be replaced by total differentials and the equation may be integrated. This results in the following equation:

$$C_2 = C^* + \frac{C_1 - C^*}{e^{\frac{\Delta \lambda}{Ht}}} \qquad (68)$$

The other relationship which is necessary for the solution of the general case is obtained by equating Equations 65 and 66. This results in the following equation:

$$\frac{\partial m}{\partial t} = - \frac{V}{1000} \frac{\partial C}{\partial \lambda} \qquad (69)$$

For a very small time interval and bed depth increment, this equation may be rewritten as follows:

$$\Delta m = - \frac{V}{1000} \frac{\Delta C}{\Delta \lambda} \Delta t \qquad (70)$$

The solution is obtained by a series of successive approximations which are started with an increment of bed depth at the influent end of the adsorbent bed and proceed through the bed by successive steps and which are checked by Equations 68 and 70 and the adsorption isotherm.

The method of solution is exemplified in Table XLIII, Appendix I.

Those variables which affect the relationships among C, t, λ, and m (the dependent variables) are V, H_t, and the adsorption isotherm. If Freundlich's isotherm is employed, the two constants in his correlation, k and n, carry the burden of reflecting the influence of the adsorption isotherm.

The above type of calculations were carried through for the values of the independent variables shown in Table XXXI.

Table XXXI

Values of Independent Variables Employed in Numerical Solution of Equations 64 and 65

Calculation Number	C_1 (mg./L.)	V (cm./min.)	H_t (cm.)	[1]Constants in Freundlich's Isotherm k	n
1	10.0	575	.080	$5.00(10)^{-8}$	4.0
2	10.0	575	.140	$5.00(10)^{-8}$	4.0
3	10.0	368	.055	$5.00(10)^{-8}$	4.0
4	10.0	575	.080	$2.22(10)^{-4}$	2.0
5	10.0	575	.080	$4.71(10)^{-2}$	1.0
6	10.0	575	.080	0	infinity[2]
7	4.0	575	.145	$.755(10)^{-6}$	4.0

1. Freundlich's isotherm is herein expressed as $C^* = km^n$; C^* is in mg./L.; m is in mg./ml.
2. This results in an indeterminate value of C^* at any value of m. It is further stipulated that when C^* is equal to 10.0 m is equal to 212.

The results of these calculations showing the relationships among concentration in the air stream, bed depth, and time are given in Figs. 71, 72, 73, 74, 75, 76, and 77.

D. Interpretation of Particular Solutions and Development of General Equation for Axial Flow Adsorbent Beds

1. Particular Case When n in Freundlich's Isotherm is Equal to or Greater than Two

a. Interpretation of Computations

The results of the computations were replotted as bed depth vs. the time to a specified effluent concentration for several values of the effluent concentration. These plots are shown in Figs. 78, 79, 80, 81, 82, 83, and 84. It is apparent, from these figures, that, for all values of n equal to or greater than two, a straight line relationship is obtained except at bed depths near the critical bed depth. For a given set of independent variables, the slopes of these curves are constant: i.e., the slope is not a function of the break concentration.

This linear relationship which resulted from the solution of the non-integrable differential equations governing the performance of adsorbent beds suggested the possibility of a simplified, approximating relationship. A straight line is defined by the slope and the intercept on one of the coordinate axes. Therefore, if some relationship could be obtained among the independent variables and the slope and the intercept, an approximating solution of the differential equations would be obtained.

CONFIDENTIAL

DECLASS.

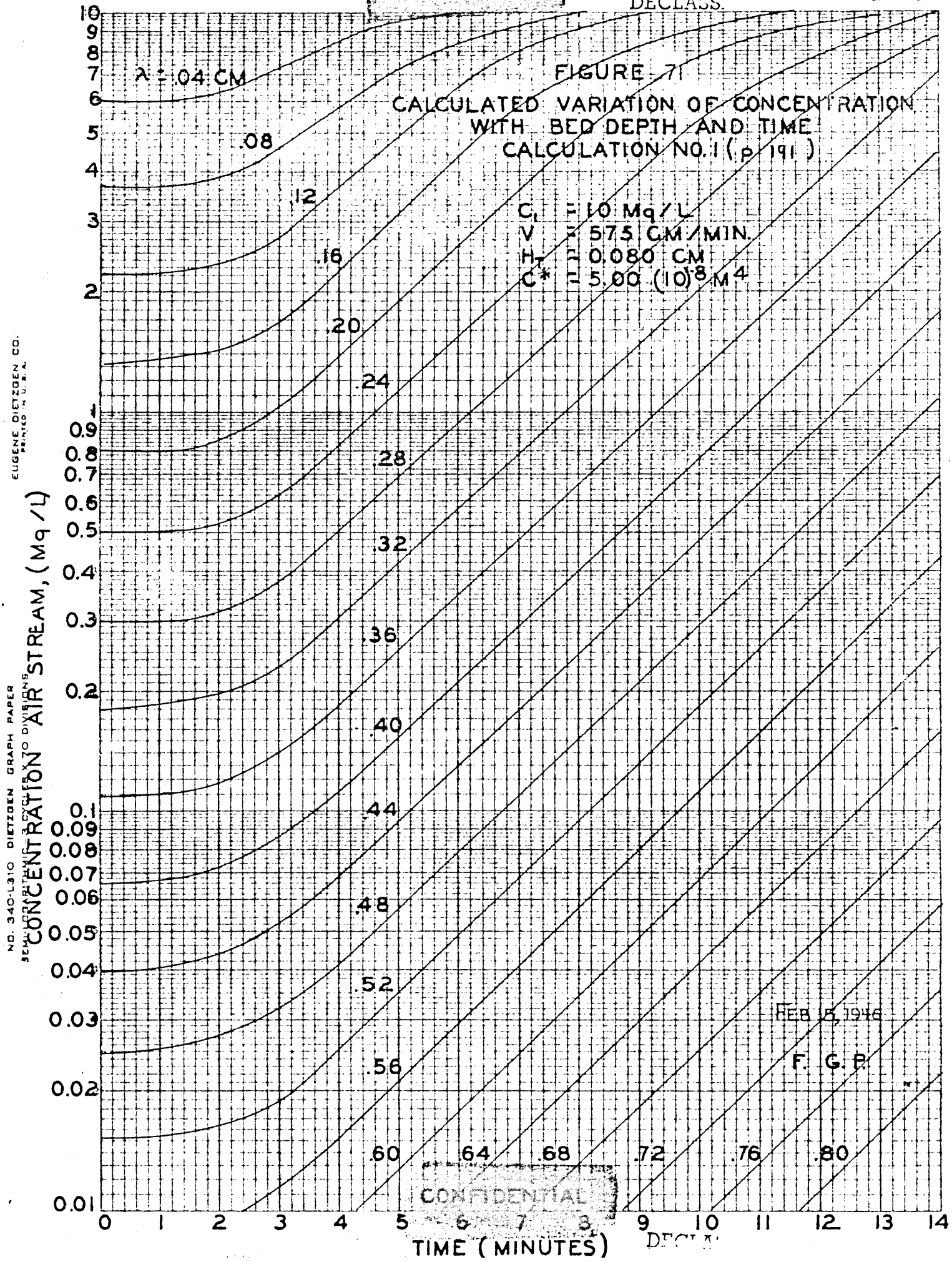

FIGURE 71

CALCULATED VARIATION OF CONCENTRATION WITH BED DEPTH AND TIME

CALCULATION NO. 1 (p 191)

FEB 15, 1946

F. G. P.

EUGENE DIETZGEN CO. PRINTED IN U.S.A.
NO. 340-L310 DIETZGEN GRAPH PAPER
SEMI-LOGARITHMIC 10 DIVISIONS

CONFIDENTIAL

DECLASS.

CONFIDENTIAL DECLASSIFIED

FIGURE 72

CALCULATED VARIATION OF CONCENTRATION WITH BED DEPTH AND TIME

CALCULATION NO. 2 (p 191)

C_1 = 1.0 Mq/L

V = 575 CM./MIN.

N_Z = 0.140 CM.

C^* = 5.00 (10)$^{-8}$ M^4

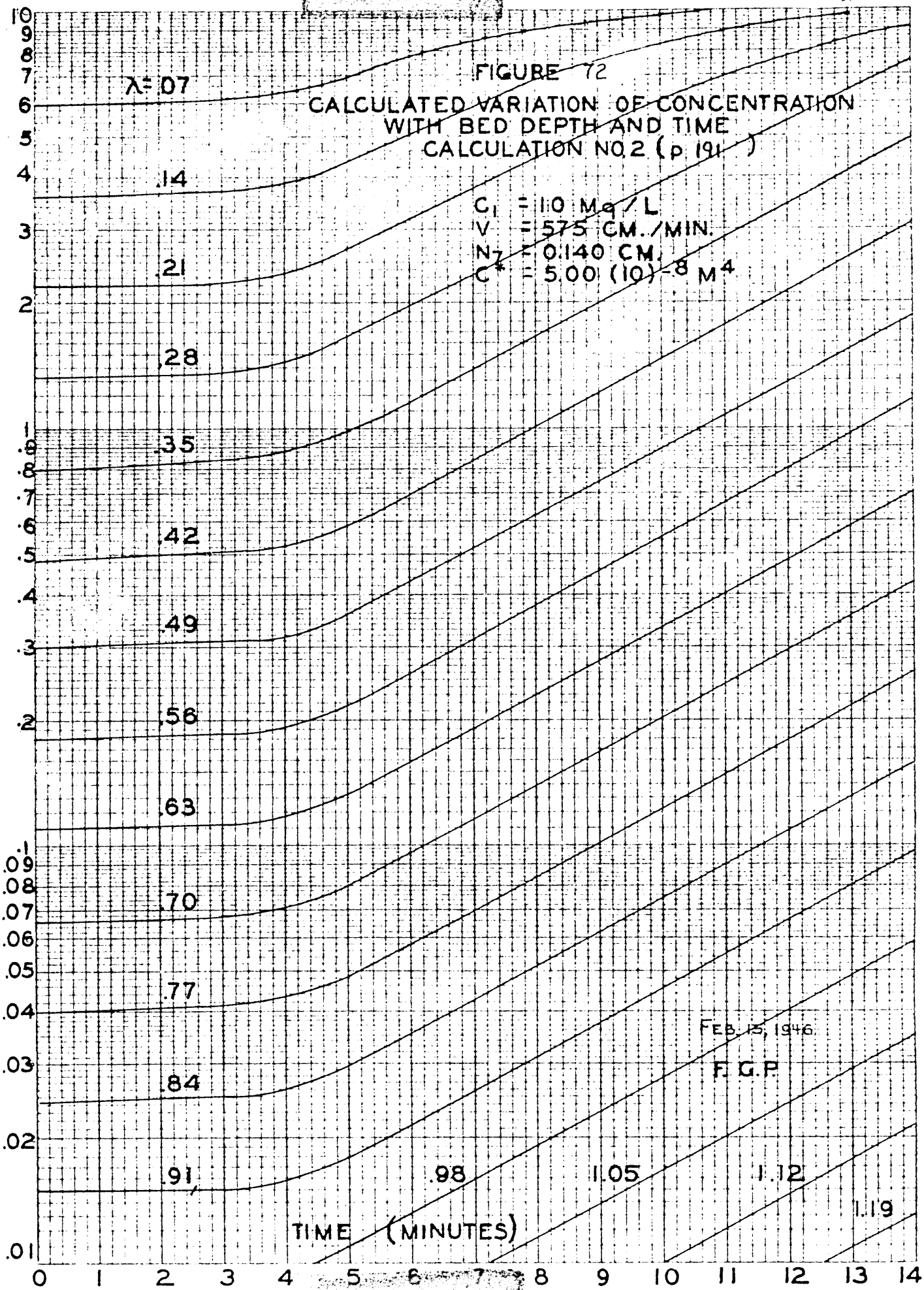

FEB. 15, 1946

F. G. P.

EUGENE DIETZGEN CO. PRINTED IN U.S.A.

NO. 340-L310 DIETZGEN GRAPH PAPER SEMI-LOGARITHMIC—3 CYCLES X 70 DIVISIONS

CONFIDENTIAL DECLASSIFIED

CONFIDENTIAL

DECL

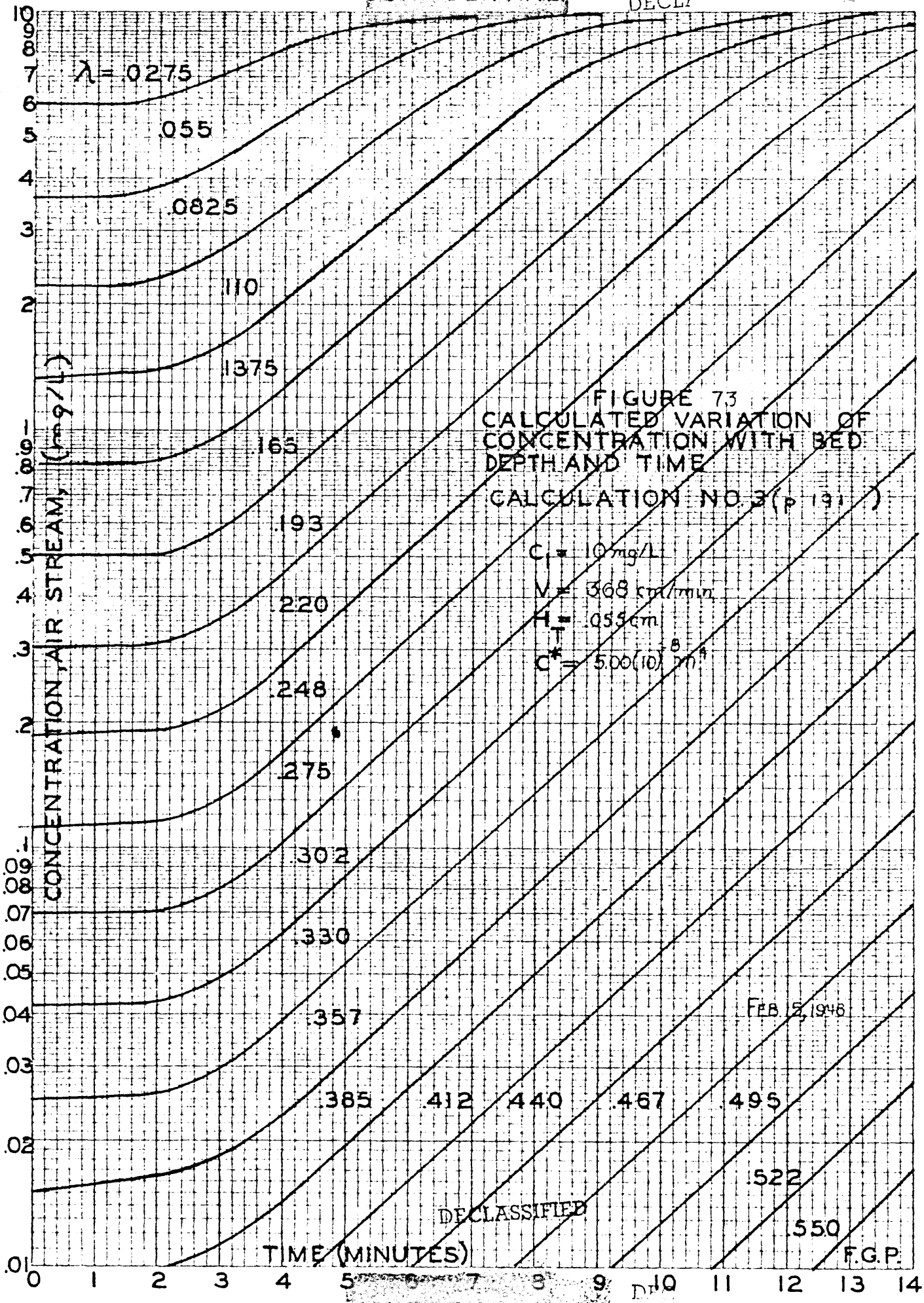

FIGURE 73
CALCULATED VARIATION OF CONCENTRATION WITH BED DEPTH AND TIME
CALCULATION NO 3 (P 191)

C_1 = 10 mg/L
V = 368 cm/min
H = .055 cm
T
$C^* = 5.00(10)^{-8}$ mg/L

FEB 15, 1946

DECLASSIFIED

F.G.P.

DP

CONFIDENTIAL

EUGENE DIETZGEN CO.
PRINTED IN U.S.A.

NO. 340-L310 DIETZGEN GRAPH PAPER
SEMI-LOGARITHMIC - 3 CYCLES X 70 DIVISIONS

CONFIDENTIAL DECLASSIFIED

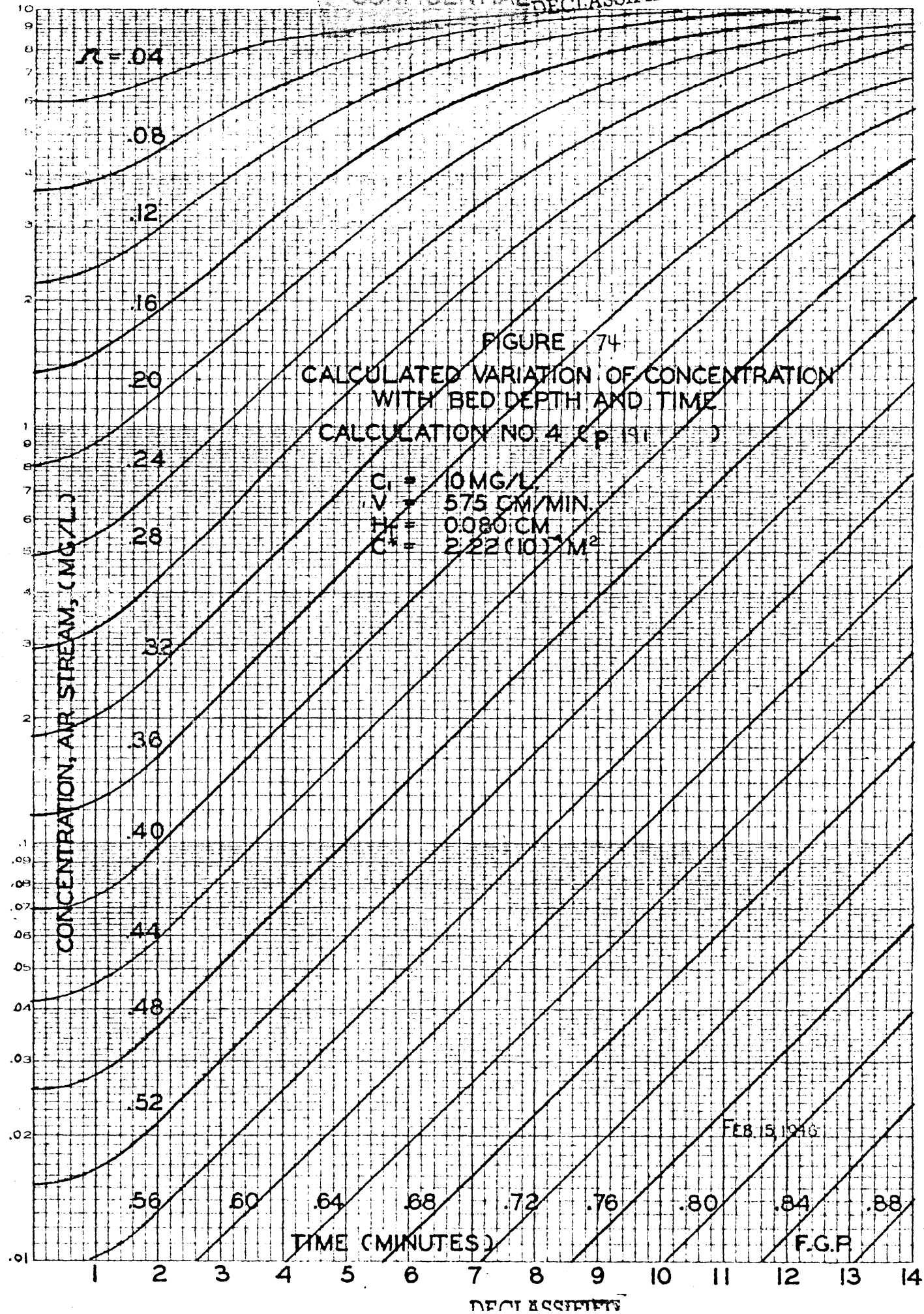

FIGURE 74

CALCULATED VARIATION OF CONCENTRATION WITH BED DEPTH AND TIME

CALCULATION NO. 4 (P 191)

EUGENE DIETZGEN CO. PRINTED IN U.S.A.

NO. 340-L310 DIETZGEN GRAPH PAPER SEMI-LOGARITHMIC—3 CYCLES X 70 DIVISIONS

DECLASSIFIED

FIGURE 75

CALCULATED VARIATION OF CONCENTRATION WITH BED DEPTH AND TIME
CALCULATION NO. 5, (p 191)

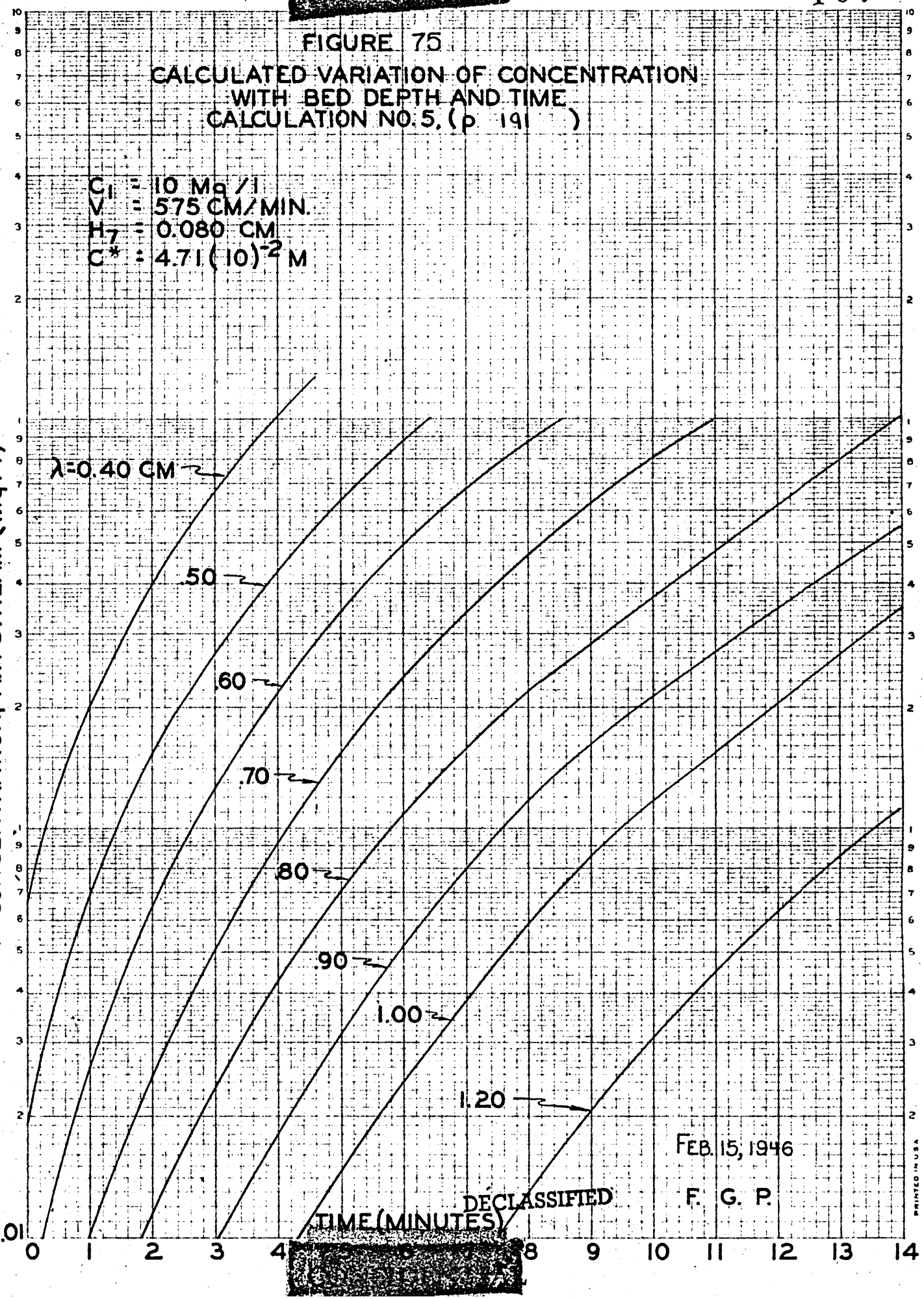

FEB. 15, 1946

F. G. P.

DECLASSIFIED [redacted]

336-3 SEMI-LOGARITHMIC—3 CYCLES X 70 DIVISIONS THE FREDERICK POST CO., CHICAGO, ILL.
PRINTED IN U.S.A.

[redacted]

DECLASSIFIED

FIGURE 76
CALCULATED VARIATION OF CONCENTRATION WITH BED DEPTH AND TIME CALCULATION NO. 6, (p 191)

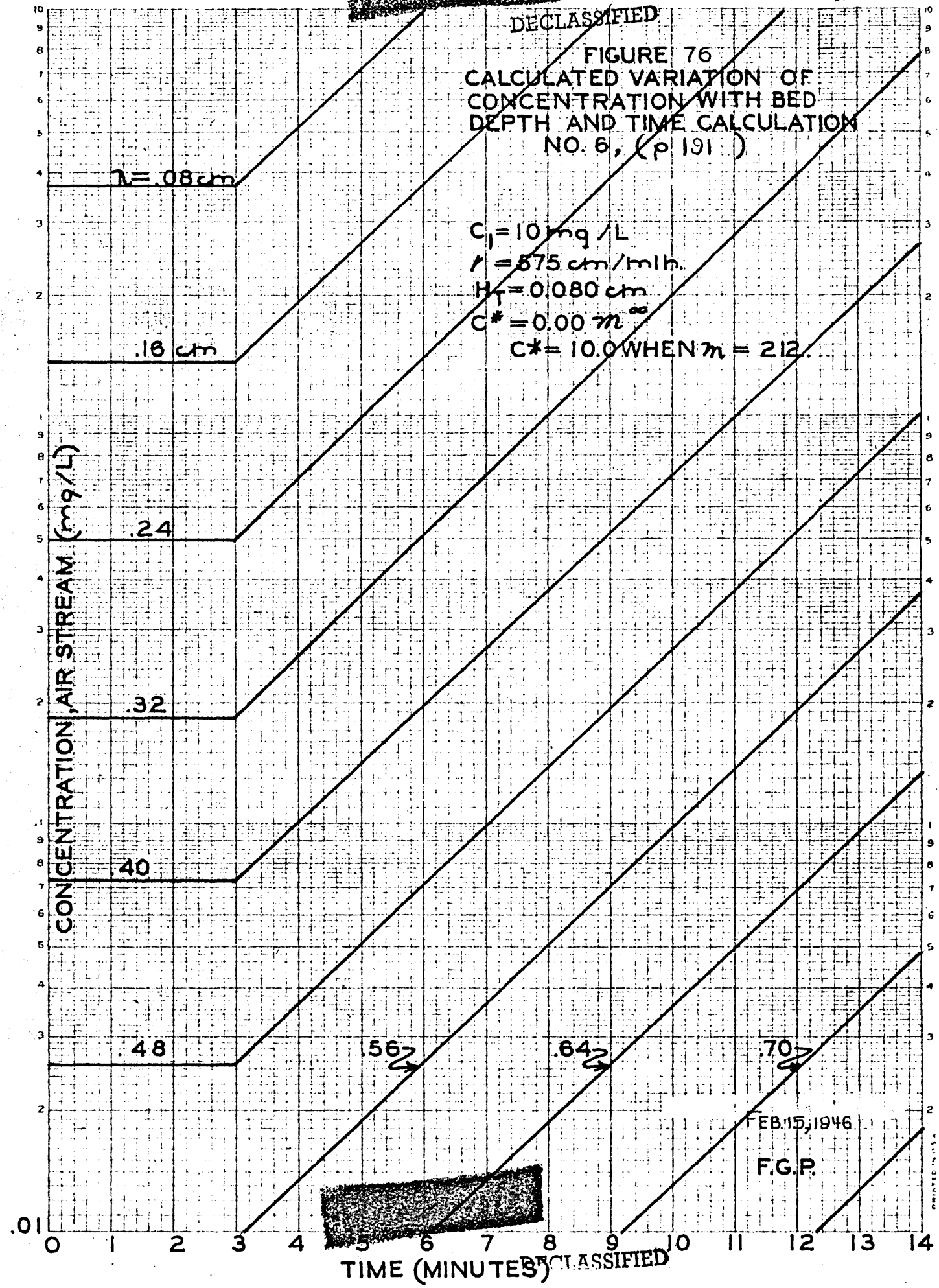

FEB. 15, 1946

F.G.P.

[redacted]

DECLASSIFIED

336-3 SEMI-LOGARITHMIC—3 CYCLES X 70 DIVISIONS THE FREDERICK POST CO. CHICAGO ILL.

[redacted] DECLASSIFIED

FIGURE 77

CALCULATED VARIATION OF CONCENTRATION WITH BED DEPTH AND TIME

CALCULATION NO. 7 (p 191)

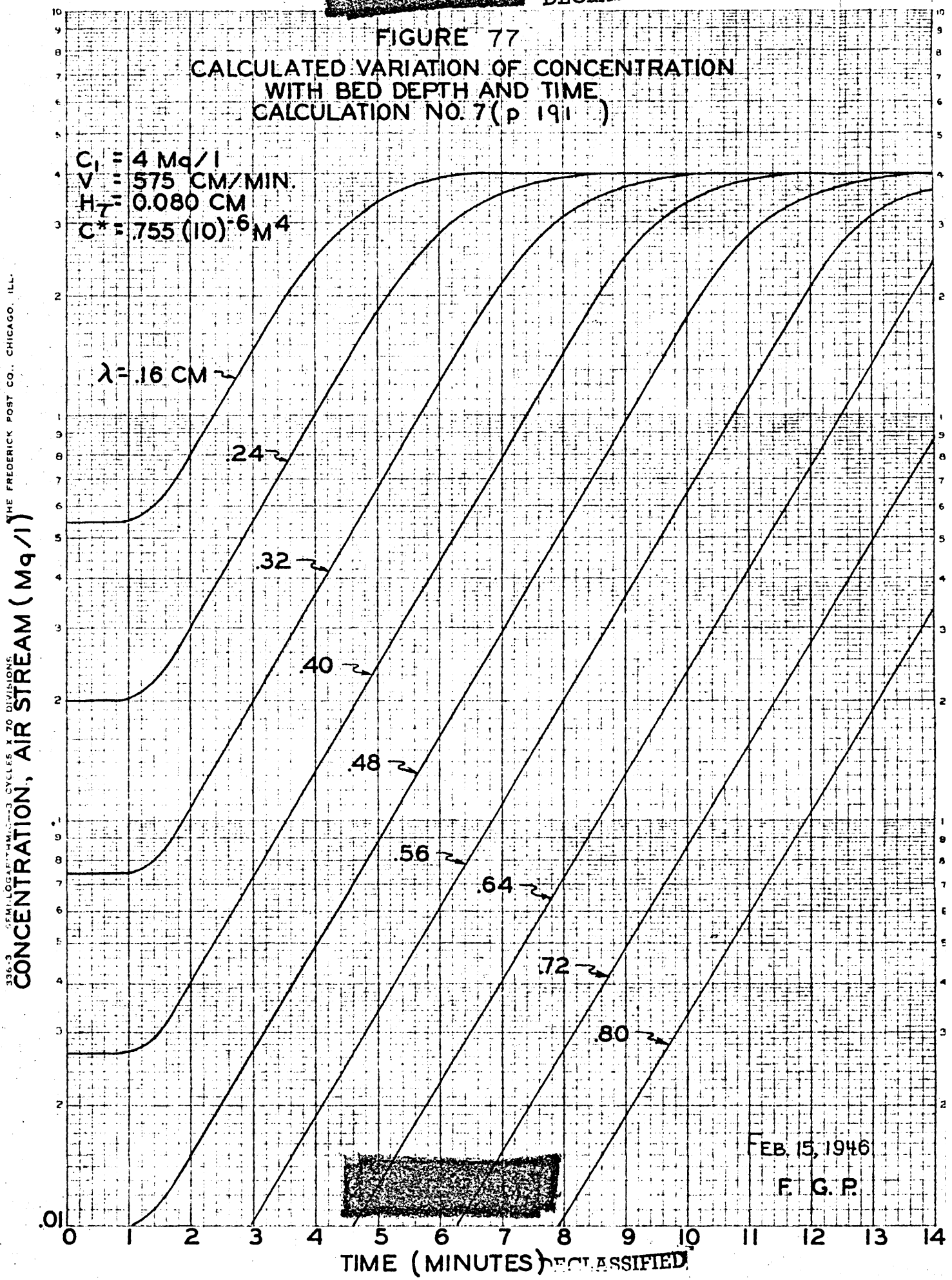

[redacted]

FEB. 15, 1946

F. G. P.

DECLASSIFIED

FIGURE 78

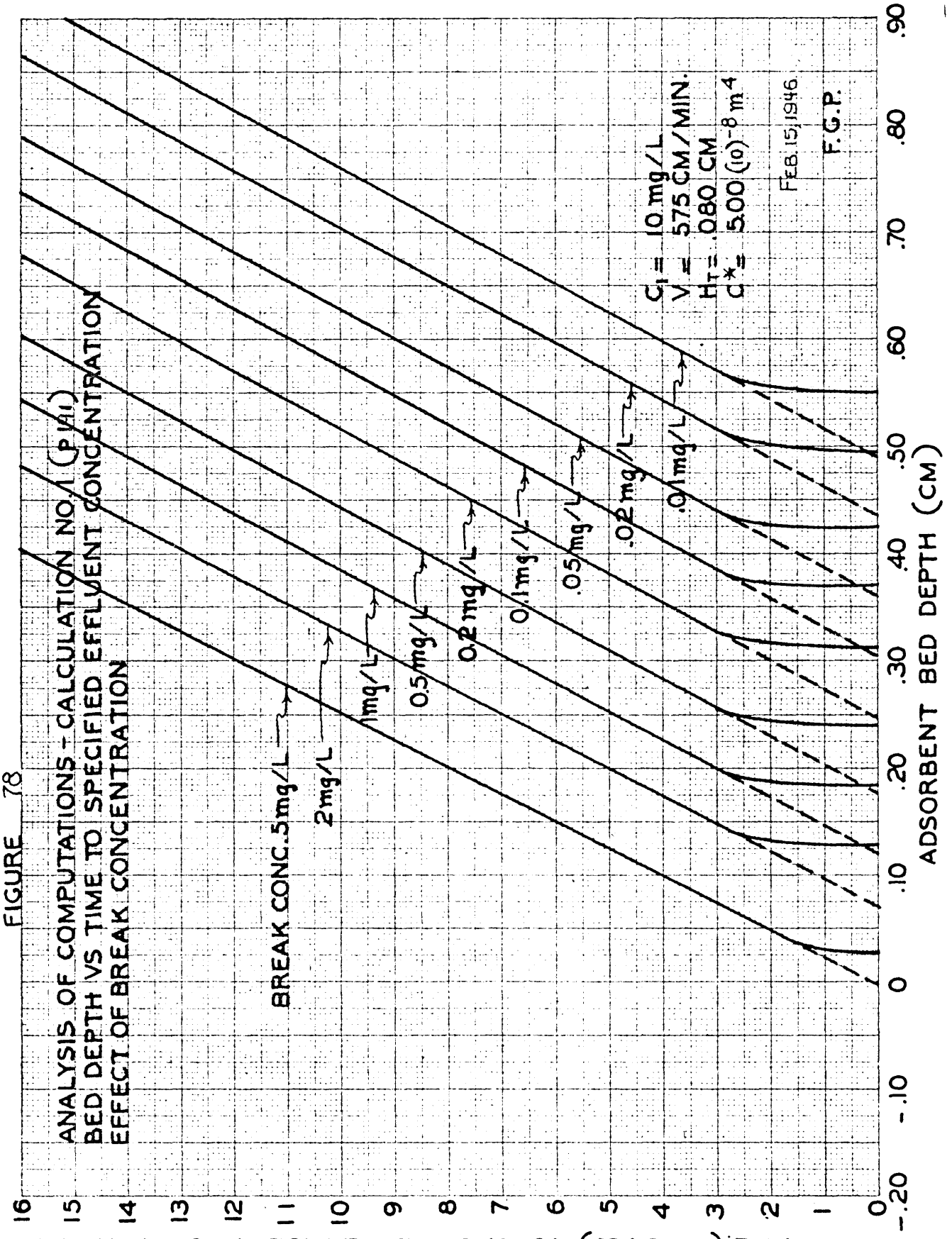
ANALYSIS OF COMPUTATIONS - CALCULATION NO. 1 (P 141)
BED DEPTH VS TIME TO SPECIFIED EFFLUENT CONCENTRATION
EFFECT OF BREAK CONCENTRATION
BREAK CONC. .5 mg/L
2 mg/L
1 mg/L
0.5 mg/L
0.2 mg/L
0.1 mg/L
.05 mg/L
.02 mg/L
.01 mg/L
C_1 = 10 mg/L
V = 575 CM/MIN.
H_T = .080 CM
C^* = 5.00 $(10)^{-8}$ m^4
FEB. 15, 1946
F.G.P.
TIME (MINUTES) TO SPECIFIED EFFLUENT CONCENTRATION
ADSORBENT BED DEPTH (CM)
16
15
14
13
12
11
10
9
8
7
6
5
4
3
2
1
0
-.20
-.10
0
.10
.20
.30
.40
.50
.60
.70
.80
.90

DECLASSIFIED

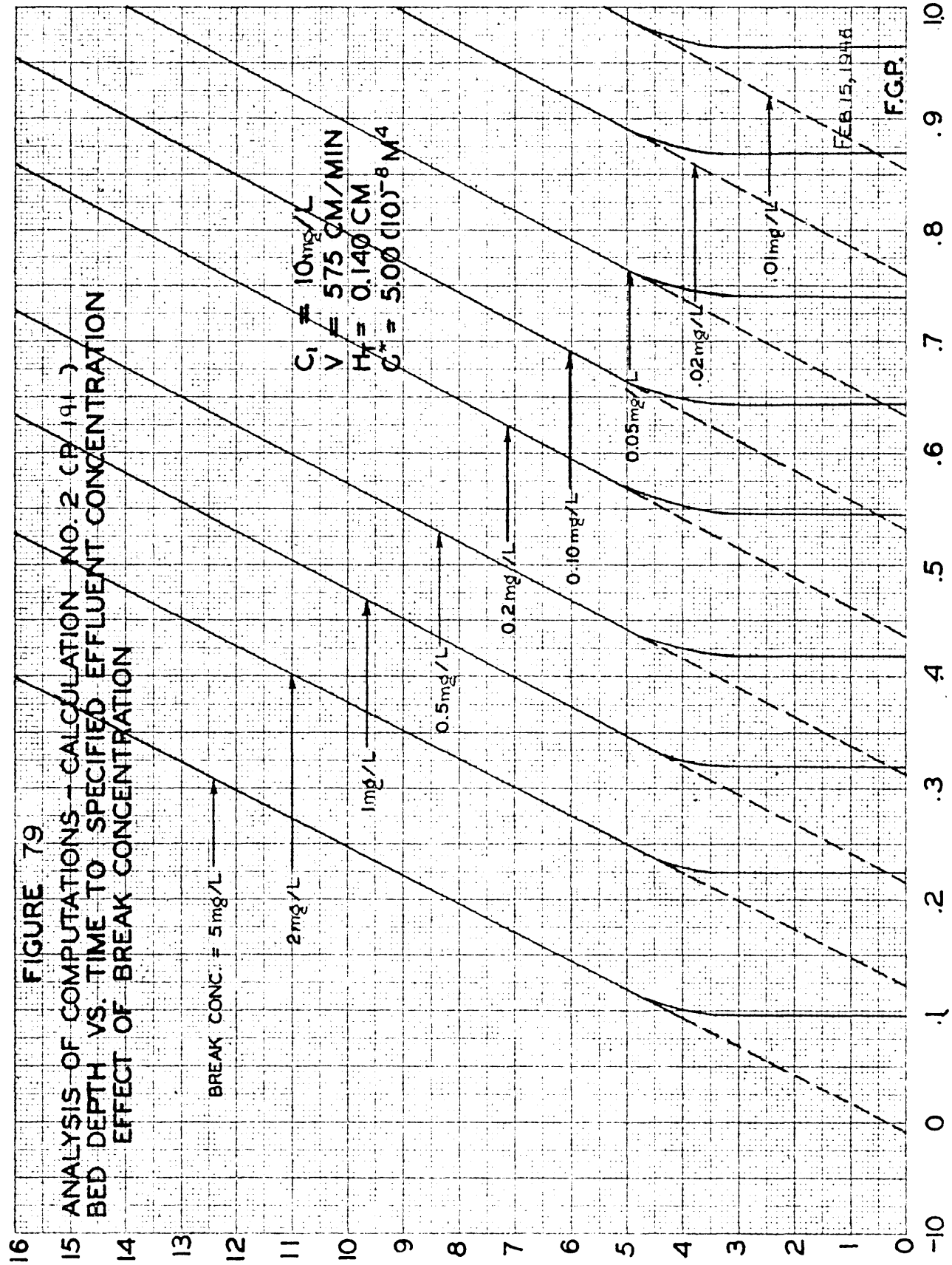

DECLASSIFIED

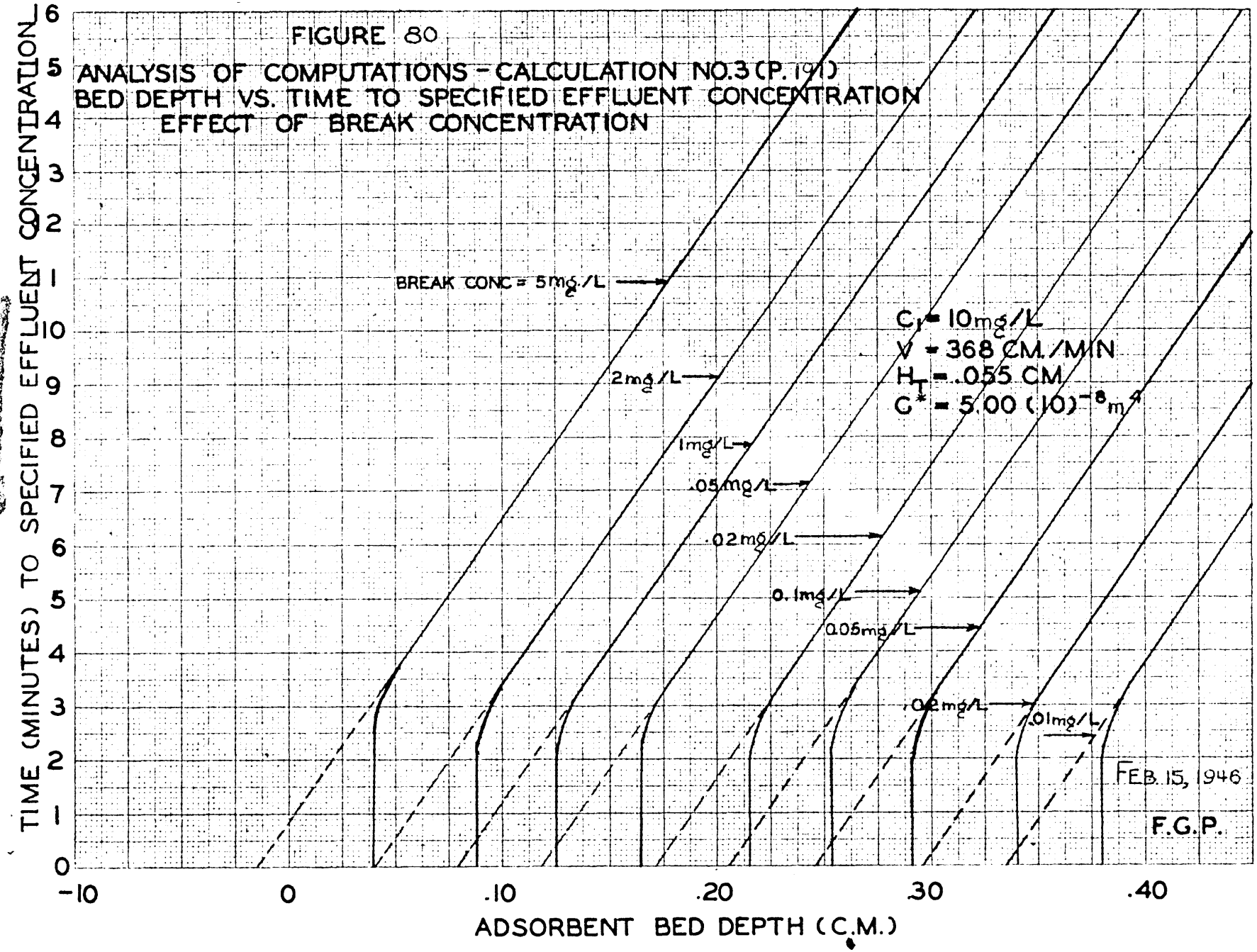

DECLASSIFIED

DECLASSIFIED

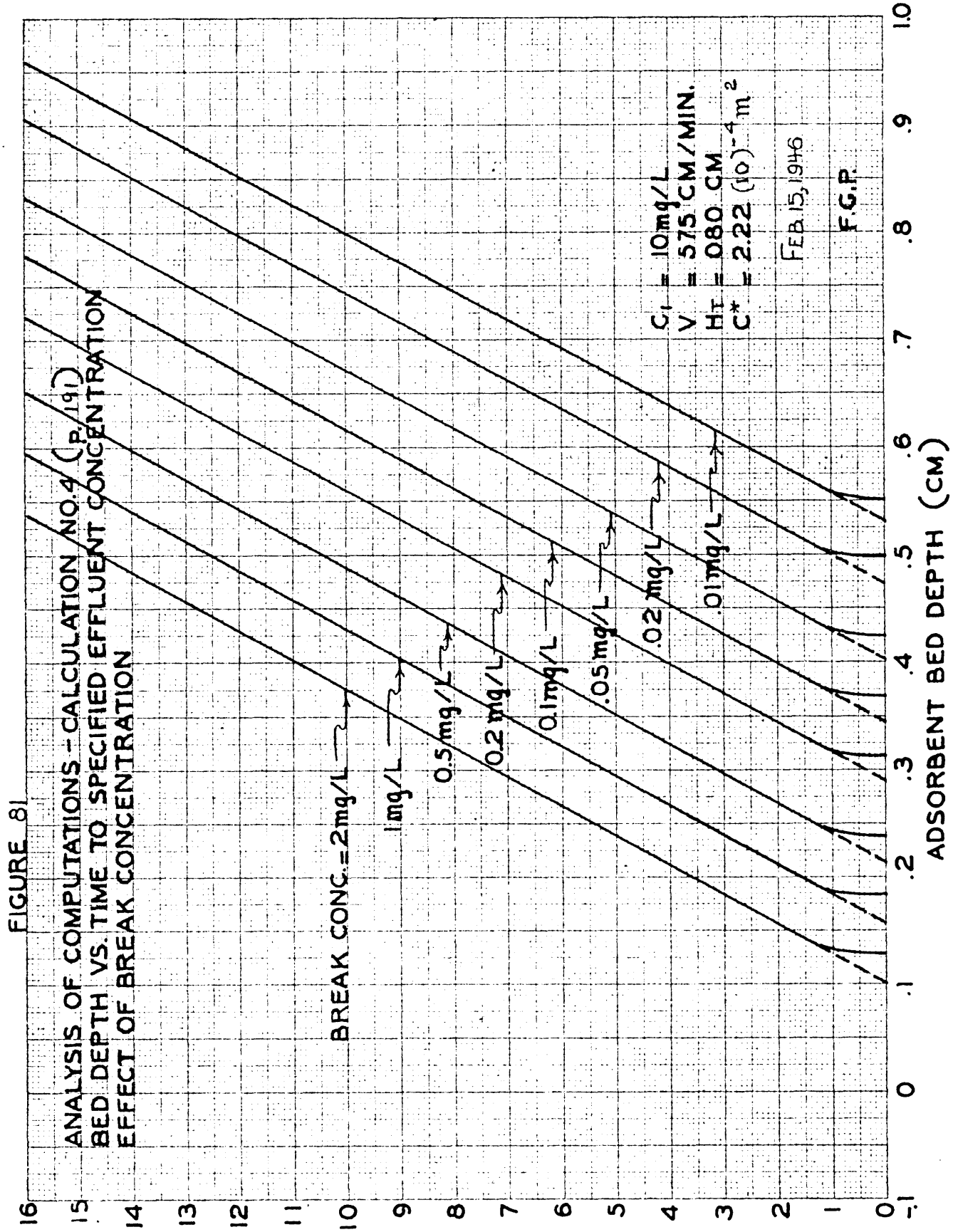
ANALYSIS OF COMPUTATIONS - CALCULATION NO.4 (P.191)
BED DEPTH VS. TIME TO SPECIFIED EFFLUENT CONCENTRATION
EFFECT OF BREAK CONCENTRATION
BREAK CONC.=2mg/L
1mg/L
0.5mg/L
0.2 mg/L
0.1mg/L
.05mg/L
.02 mg/L
.01mg/L
C_1 = 10mg/L
V = 575 CM/MIN.
H = 080 CM
C^* = 2.22 $(10)^{-4}$ m^2
FEB.15,1946
F.G.P.
TIME (MINUTES) TO SPECIFIED EFFLUENT CONCENTRATION
ADSORBENT BED DEPTH (CM)

FIGURE 81

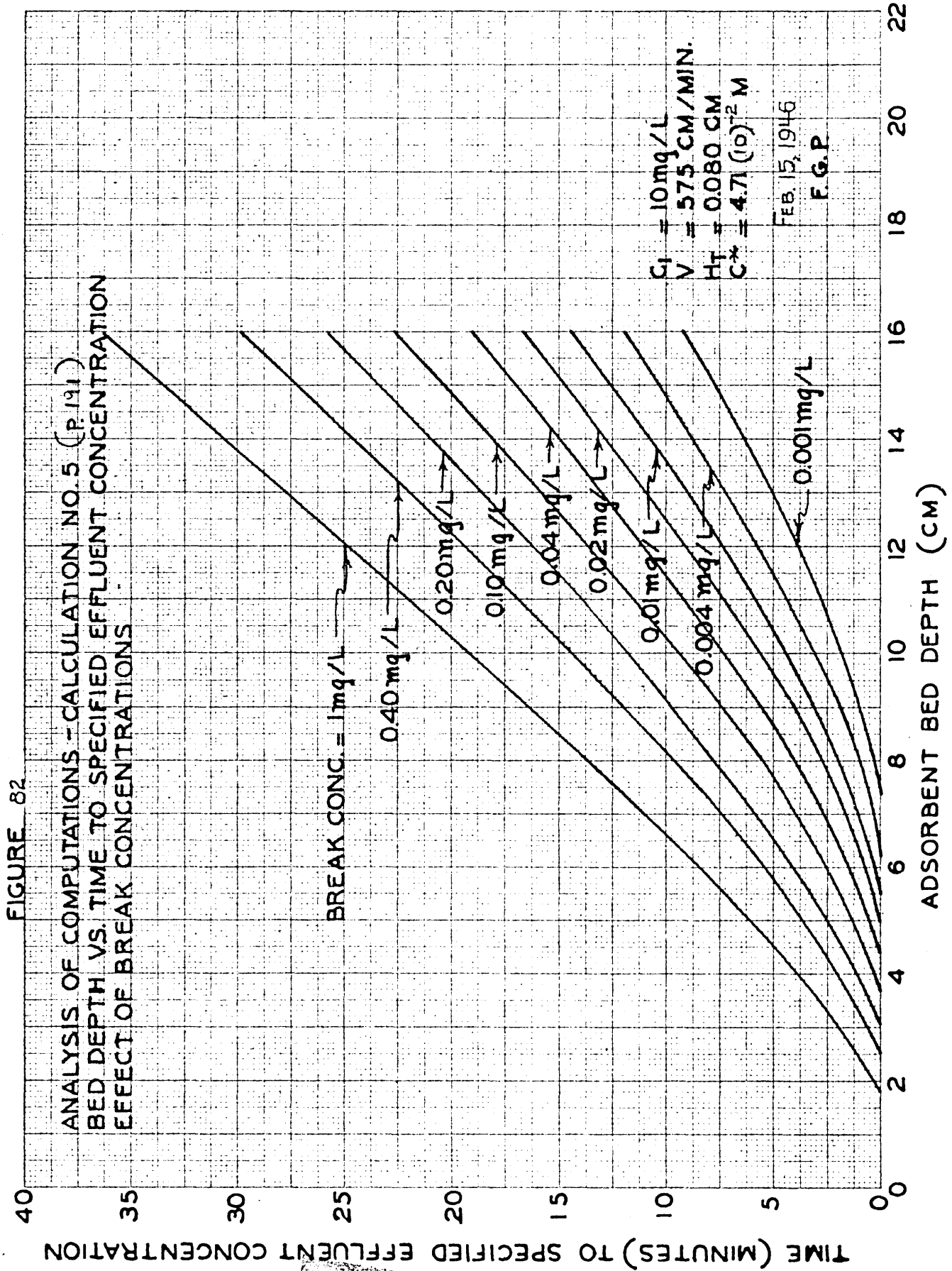
ANALYSIS OF COMPUTATIONS - CALCULATION NO. 5 (P. 191)
BED DEPTH VS. TIME TO SPECIFIED EFFLUENT CONCENTRATION
EFFECT OF BREAK CONCENTRATIONS
BREAK CONC. = 1 mg/L
0.40 mg/L
0.20 mg/L
0.10 mg/L
0.04 mg/L
0.02 mg/L
0.01 mg/L
0.004 mg/L
0.001 mg/L
C_1 = 10 mg/L
V = 575 CM/MIN.
H_T = 0.080 CM
$C^* = 4.71 (10)^{-2}$ M
FEB. 15, 1946
F.G.P.
TIME (MINUTES) TO SPECIFIED EFFLUENT CONCENTRATION
ADSORBENT BED DEPTH (CM)
0
5
10
15
20
25
30
35
40
2
4
6
8
10
12
14
16
18
20
22

FIGURE 82

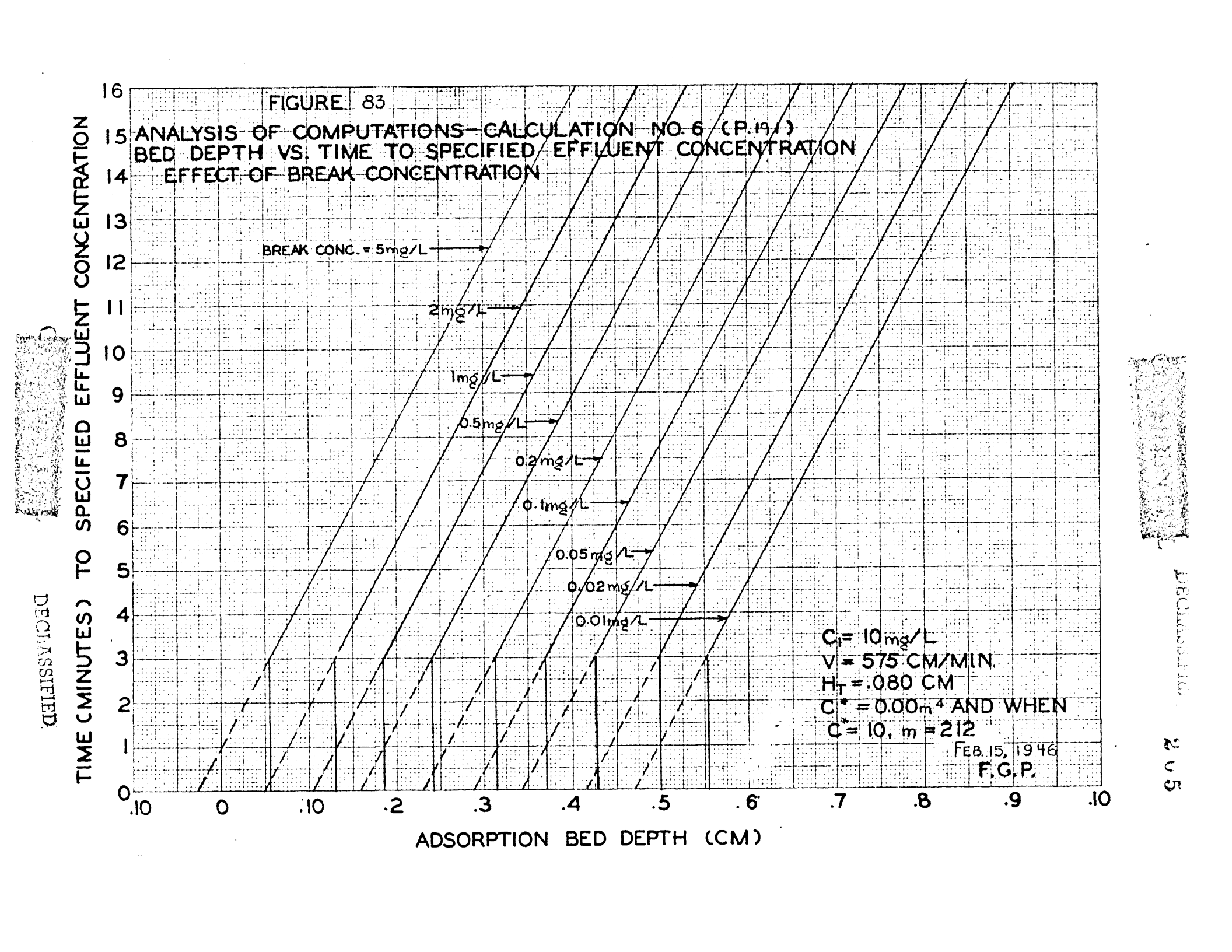

DECLASSIFIED

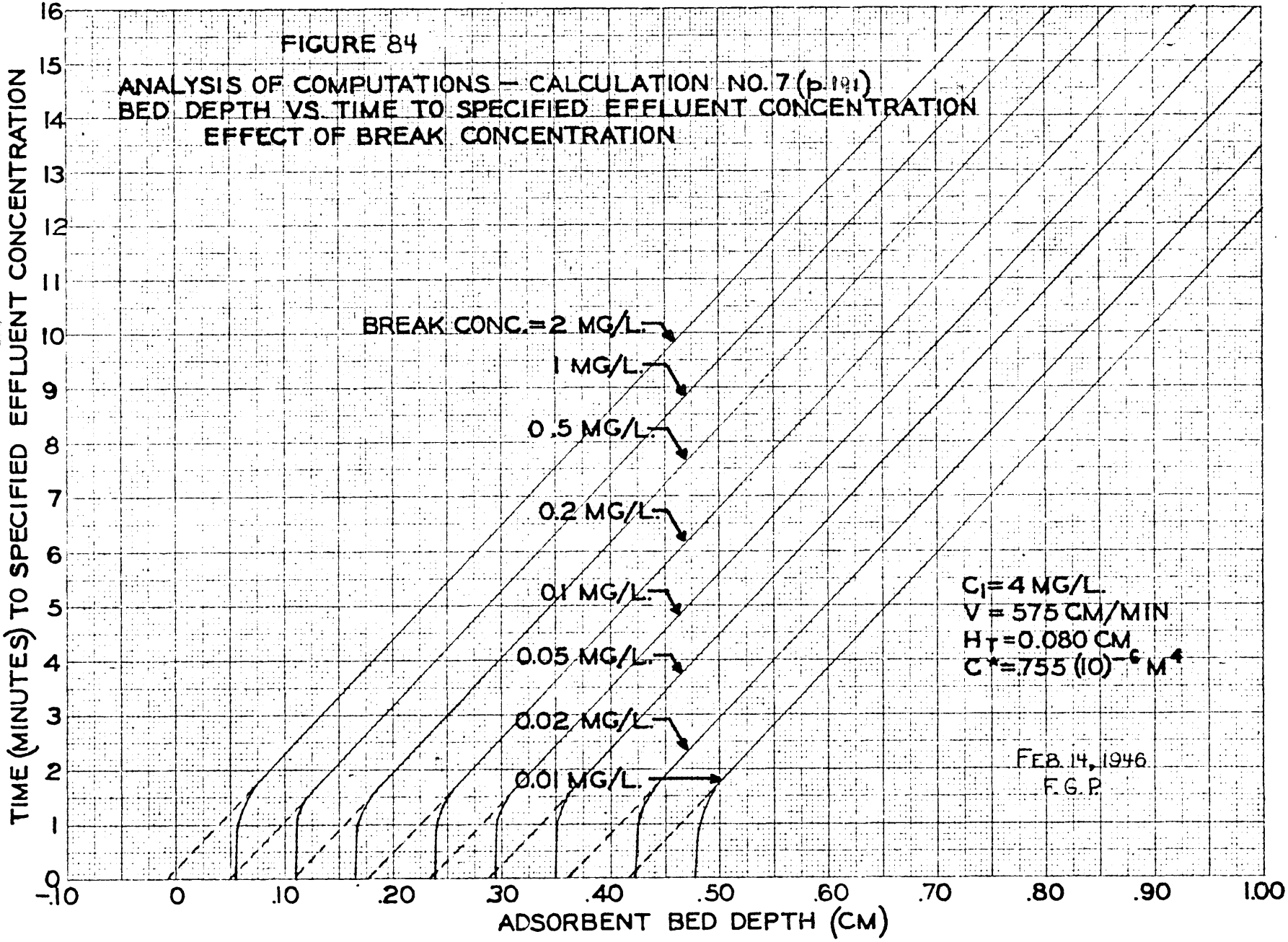

DECLASSIFIED

A clearer insight into the reason for the linear relationship is obtained if Calculation Number 4, the case where n in Freundlich's adsorption isotherm is equal to infinity, is analyzed separately.

For this particular case, the value of C^* is equal to zero until the instant at which the adsorbent becomes saturated. At this instant, adsorption stops, for C^* becomes equal to C_1. Therefore, when the gas-laden air is first introduced into the bed, the concentration decreases with bed depth as predicted by Equation 67 when C^* is equal to zero. As time progresses, the first infinitesimal layer of adsorbent increases in adsorbate content at a constant rate until the saturation capacity is attained. During this period, the effluent concentration remains constant. The time interval required for the saturation of this layer can be calculated from the known test conditions by combining Equations 67 and 69. This results in the following expression:

$$\Delta t_1 = \frac{1000\ H_t\ N_o}{C_1\ V} \qquad (71)$$

The amount of adsorbate which has been adsorbed by the bed at this instant is equal to the product of the time and the quantity entering per unit time (assuming practically complete removal by the bed under consideration). This results in the following equation:

$$M_1 = \left(\frac{1000\ H_t\ N_o}{C_1\ V}\right)\left(\frac{C_1\ V}{1000}\right) = H_t N_o \qquad (72)$$

At the instant that the first layer of adsorbent becomes saturated the influent concentration begins to penetrate into the bed. As time progresses more and more of the bed becomes saturated. At the instant that the specified concentration (assumed to be negligibly small) first penetrates the bed, the bed depth which has become saturated is represented by the following equation and is graphically illustrated in Fig. 85.

$$\lambda_s = \lambda - H_t \ln \frac{C_1}{C_2} \qquad (73)$$

The quantity of adsorbate in this saturated layer is represented by the following equation:

$$M_s = N_o\left(\lambda - H_t \ln \frac{C_1}{C_2}\right) \qquad (74)$$

The amount of adsorbate adsorbed by the effluent layer, which is not saturated, is identical to the quantity transferred to the bed during the time interval required to saturate the first differential bed thickness. Therefore, the total quantity transferred to the bed is equal to the sum of these and is represented by the following equation:

$$M_t = M_1 + M_s = N_o\left(\lambda - H_t \ln\frac{C_1}{C_2}\right) + H_t N_o$$

$$= N_o\left[\lambda - H_t\left(\ln \frac{C_1}{C_2} - 1\right)\right] \qquad (75)$$

[redacted] DECLASSIFIED

FIGURE 85

DIAGRAMATIC REPRESENTATION OF CONCENTRATION GRADIENTS IN AN ADSORBENT BED
(ZERO BACK PRESSURE UNTIL INSTANT OF SATURATION)

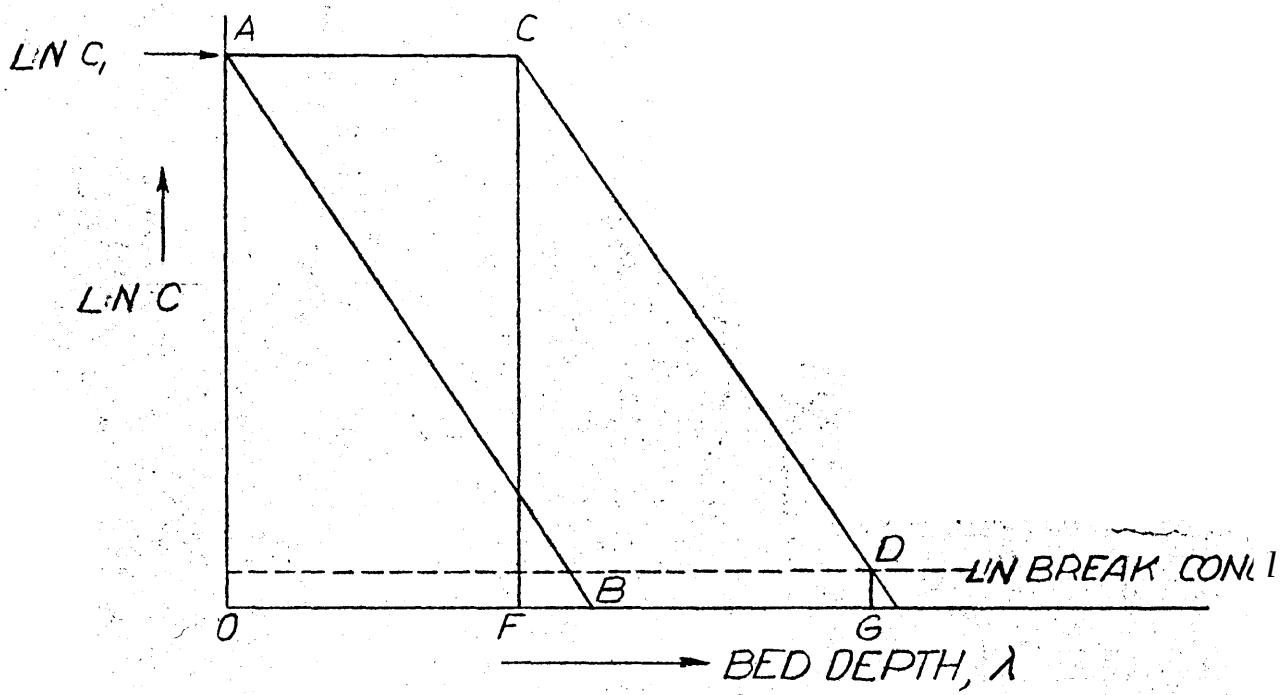

AB REPRESENTS CONC. GRADIENT AT INSTANT FIRST LAYER BECOMES SATURATED (t_1)
ACD REPRESENTS CONC. GRADIENT AT ANY LATER TIME, t
OG = TOTAL BED DEPTH, λ
OF = SATURATED LAYER AT INSTANT OF BREAK, λ_s
FG = NON - SATURATED LAYER AT INSTANT OF BREAK

FEB. 15, 1946

DECLASSIFIED G.P.
[redacted] DECLASSIFIED

This must, by a material balance, be equal to the quantity of material which entered the bed. This equality is represented by the following equation:

$$\frac{C_1 V t}{1000} = N_o \left[\lambda - H_t\left(\ln \frac{C_1}{C_2} - 1\right)\right] \quad (76)$$

$$t = \frac{1000 N_o}{C_1 V}\left[\lambda - H_t\left(\ln \frac{C_1}{C_2} - 1\right)\right] \quad (77)$$

$$t = \frac{N_o A}{C_1 Q}\left[\lambda - H_t\left(\ln \frac{C_1}{C_2} - 1\right)\right] \quad (78)$$

These equations relate the variables in an analytical expression which is exact if the bed depth is greater than the true critical bed depth (the true critical bed depth is equal to $H_t \ln \frac{C_1}{C_2}$) with the obvious limitation that C_2 shall not exceed C_1. For reasons of simplicity, this equation was derived on the assumption that the effluent concentration at break was negligible as compared to the influent concentration. However, this is not a necessary stipulation; it was made only to simplify the argument.

The important features of this equation are as follows:

1. It stipulates that the slope of the bed depth-break time curve is equal to $\frac{N_o A}{C_1 Q}$.

2. It stipulates that the intercept of the linear portion of the bed depth-break time curve

on the bed depth axis (the apparent critical bed depth) is equal to $H_t(\ln \frac{C_1}{C_2} - 1)$.

These relationships may be expressed by the following equations:

$$S = \frac{1000\ N_o}{C_1 V} = \frac{N_o A}{C_1 Q} \qquad (35)$$

$$\lambda_c = H_t\ (\ln \frac{C_1}{C_2} - 1) \qquad (79)$$

The true critical bed depth is, of course, expressed by the following equation:

$$\lambda_c' = H_t \ln \frac{C_1}{C_2} \qquad (16)$$

These relationships were derived for the particular case when the back pressure, C^*, is zero except at the instant at which saturation is attained: (i.e., n in Freundlich's adsorption isotherm is equal to infinity).

b. Correlation of Slope with Independent Variables

It has been shown that when n in Freundlich's isotherm is equal to infinity the slope of the bed depth-break time curve is equal to $\frac{1000 N_o}{C_1 V}$. The validity of this relationship for other values of n (equal to or greater than two) is shown by the calculated data of Table XXXII.

This tabulation shows that, for values of n of Freundlich's isotherm of two or greater, the slope of

the linear portion of the bed depth-break time curve is equal to $\frac{1000N_o}{C_1V}$. The slight discrepencies are within the accuracy of the calculations.

Table XXXII

Correlation of Slope of Bed Depth-Break Time Curve with Independent Variables

Calculation Number	C_1 mg./L.	V cm./min.	N_o (m when $C = C_1$) mg./ml.	n	$\frac{1000N_o}{C_1V}$ min./cm.	Slope from Figure min./cm.
1	10.0	575	212	4.0	36.9	38.1
2	10.0	575	212	4.0	36.9	39.0
3	10.0	368	212	4.0	57.6	57.0
4	10.0	575	212	2.0	36.9	36.7
6	10.0	575	212	inf.	36.9	36.9
7	4.0	575	48	4.0	20.9	21.0

c. Correlation of Apparent Critical Bed Depth with Independent Variables

It has been shown that, for those instances where the value of n in Freundlich's isotherm is equal to infinity, the apparent critical bed depth can be represented by the following equation:

$$\lambda_c = H_t \left(\ln \frac{C_1}{C_2} - 1\right) \qquad (79)$$

If the dimensionless ratio, λ_c/H_t, is plotted on coordinate paper vs. the logarithm of the concentration

[redacted] DECLASSIFIED

ratio, a straight line should result represented by the following expression:

$$\frac{\lambda_c}{H_t} = \ln \frac{C_1}{C_2} - 1 \qquad (81)$$

This straight line has a slope of unity and an intercept on the logarithm of the concentration ratio axis of unity. Fig. 86 shows the plot of these two functions for other values of n than infinity. The points on the curves were obtained from Figs. 78, 79, 80, 81, 83, and 84.

Fig. 86 shows that, for all values of n equal to or greater than two, a straight line relationship is obtained with a slope of unity. The intercept of these straight lines on the concentration ratio axis, however, changes and is a function of n. The following tabulation shows the value of the intercept, β, as a function of the value of n in Freundlich's adsorption isotherm. This relationship is represented graphically in Fig. 87.

Table XXXIII

Correlation of β with n

$$\frac{\lambda_c}{H_t} = \ln \frac{C_1}{C_2} - \beta \qquad (41)$$

Calculation Number	n	β
1	4.0	0.78
2	4.0	0.78
3	4.0	0.78
4	2.0	0.36
6	infinity	1.00
7	4.0	0.78

[redacted] DECLASSIFIED

DECLASSIFIED

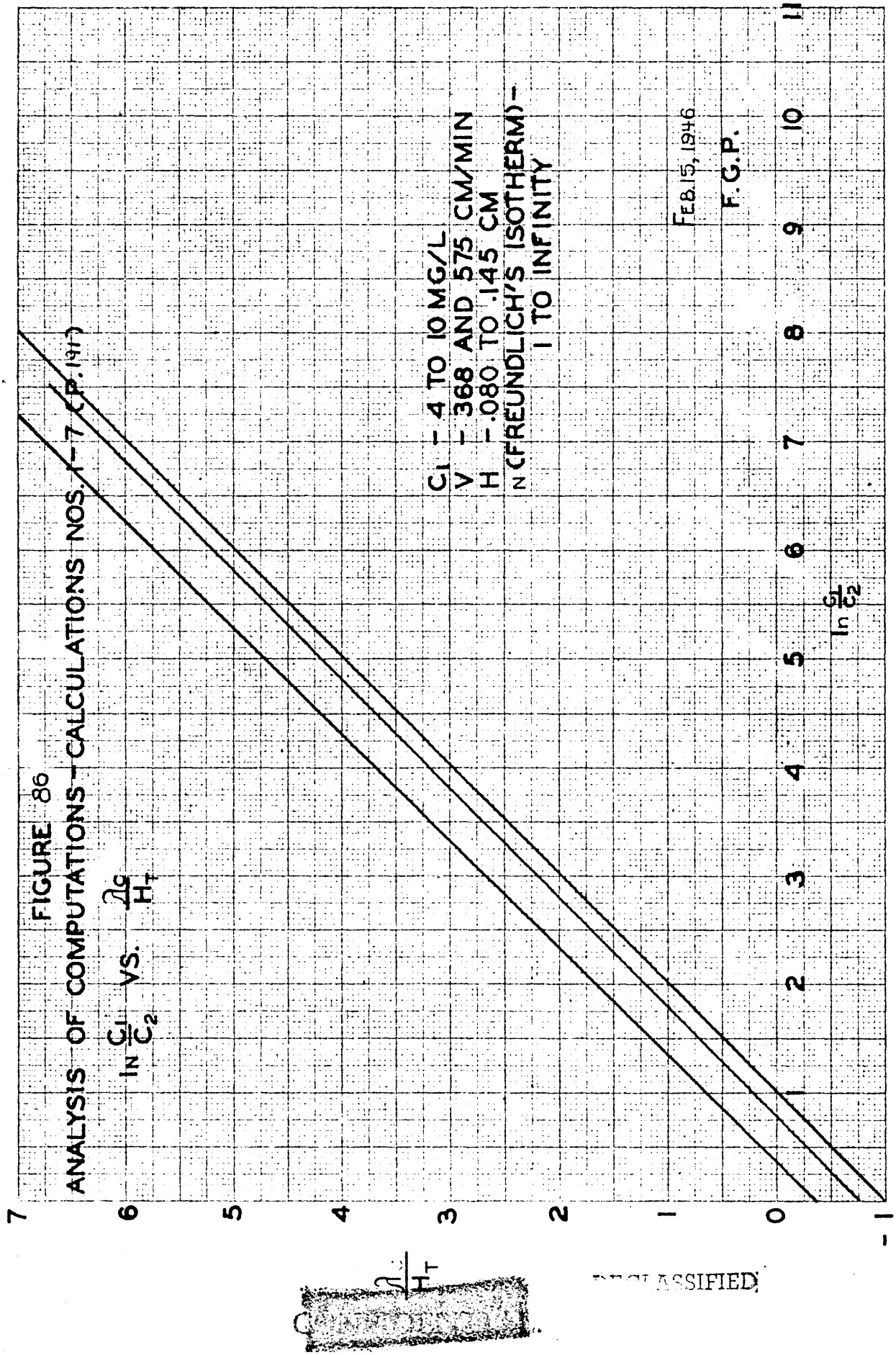

DECLASSIFIED

DECLASSIFIED

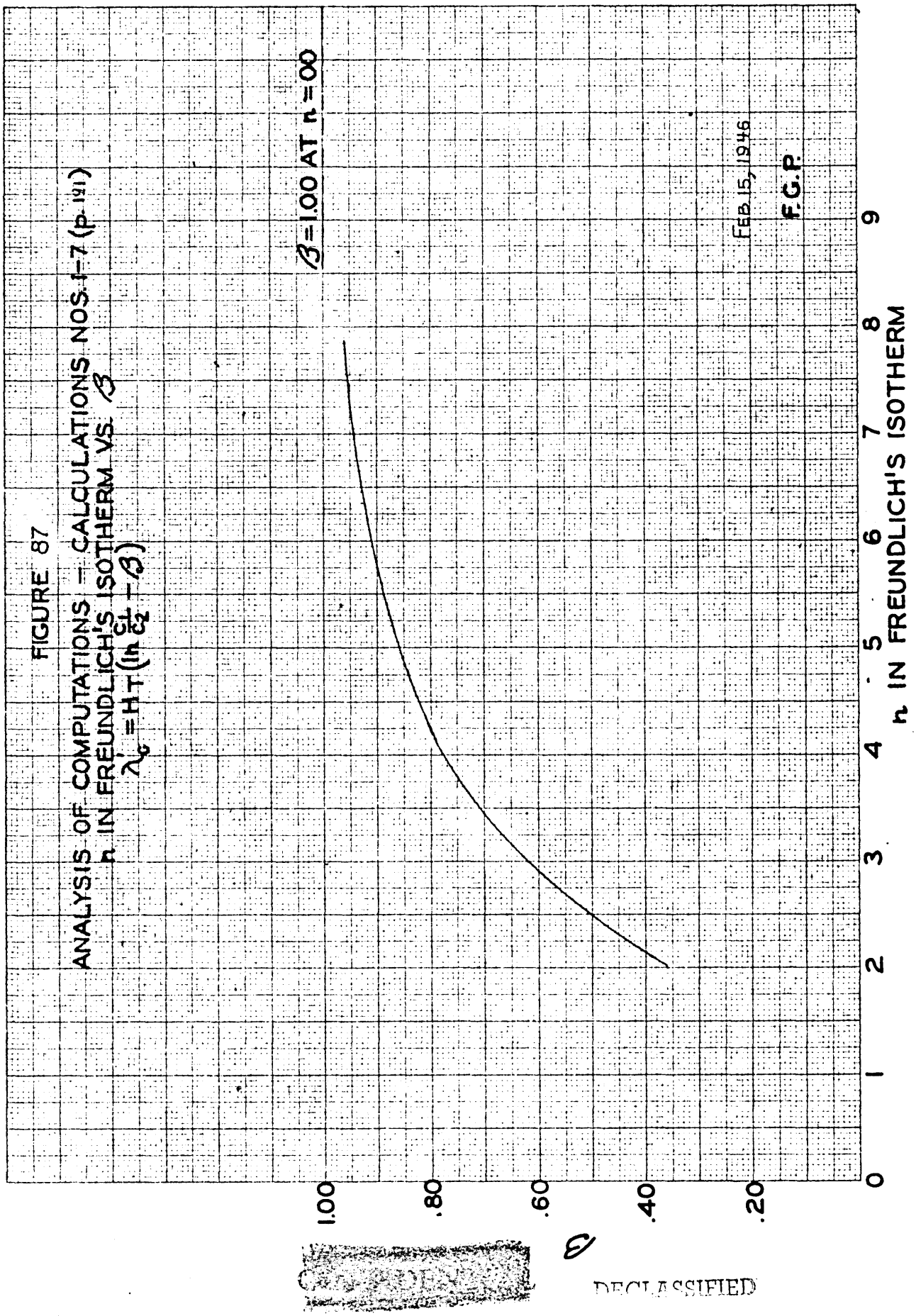

DECLASSIFIED

d. General Equation

It has been established herein that, for values of n in Freundlich's adsorption isotherm equal to or greater than two, the slope of the straight line relating bed depth and break time is equal to $\frac{1000\ N_o}{C_1 V}$ and the intercept on the bed depth axis is equal to $H_t(\ln \frac{C_1}{C_2} - \beta)$. Therefore, the complete relationship may be represented by the following equation:

$$t = \frac{1000\ N_o}{C_1 V}\left[\lambda - H_t\ (\ln \frac{C_1}{C_2} - \beta)\right]$$

$$t = \frac{N_o\ A}{C_1\ Q}\left[\lambda - H_t\ (\ln \frac{C_1}{C_2} - \beta)\right] \qquad (1)$$

In this equation, β is a function of n varying from 0.36 to unity as n increases from two to infinity.

2. Particular Case When n in Freundlich's Isotherm is Equal to Unity

It was stated previously that a solution of the general differential equation (Equation 11) was known for the particular case when n in Freundlich's isotherm is equal to unity. This particular case was originally solved by Angelius (45) who obtained differential equations similar to Equations 64 and 65 for heat transfer to porous beds by a flowing gas stream. The general solution is given by the following equation:

$$\frac{C}{C_1} = 1 - e^{-k(k_g a)t} \int_0^{\lambda/H_t} I_o\ 2\sqrt{k(k_g a)t\ s}\ \ e^{-s} ds \qquad (82)$$

In this equation, $I_o(z)$ denotes the modified Besel function, $J_o(iz)$. Precisely, this is represented by the following equation:

$$I_o(2\sqrt{s}) = 1 + s + \frac{s^2}{(2!)^2} + \cdots\cdots + \frac{s^n}{(n!)^2} \quad (83)$$

The integral represented by Equation 82 has been solved for various values of the independent groups, and the solutions have been published by Furnas (46) and expanded by Drew, Spooner, and Douglas (47) for very small values of C/C_1. The solutions were published in the form of graphs.

Calculation No. 5 was computed by the use of these graphical representations of the general solution of Equation 82. The resulting bed depth-break time relationships are shown in Fig. 82 for low values of the bed depth and in Fig. 88 for large values of the bed depth.

These figures show that there is a very definite curvature in the bed depth-break time relationships, the curvature increasing as the break concentration is decreased. Even at a break concentration of 1 mg./ml., the curvature does not cease until a life of approximately 400 minutes is attained.

Therefore, it is apparent that Equation 1 does not apply for the adsorption of those agents, the adsorption isotherm of which is linear: i.e., n in Freundlich's isotherm is equal to unity.

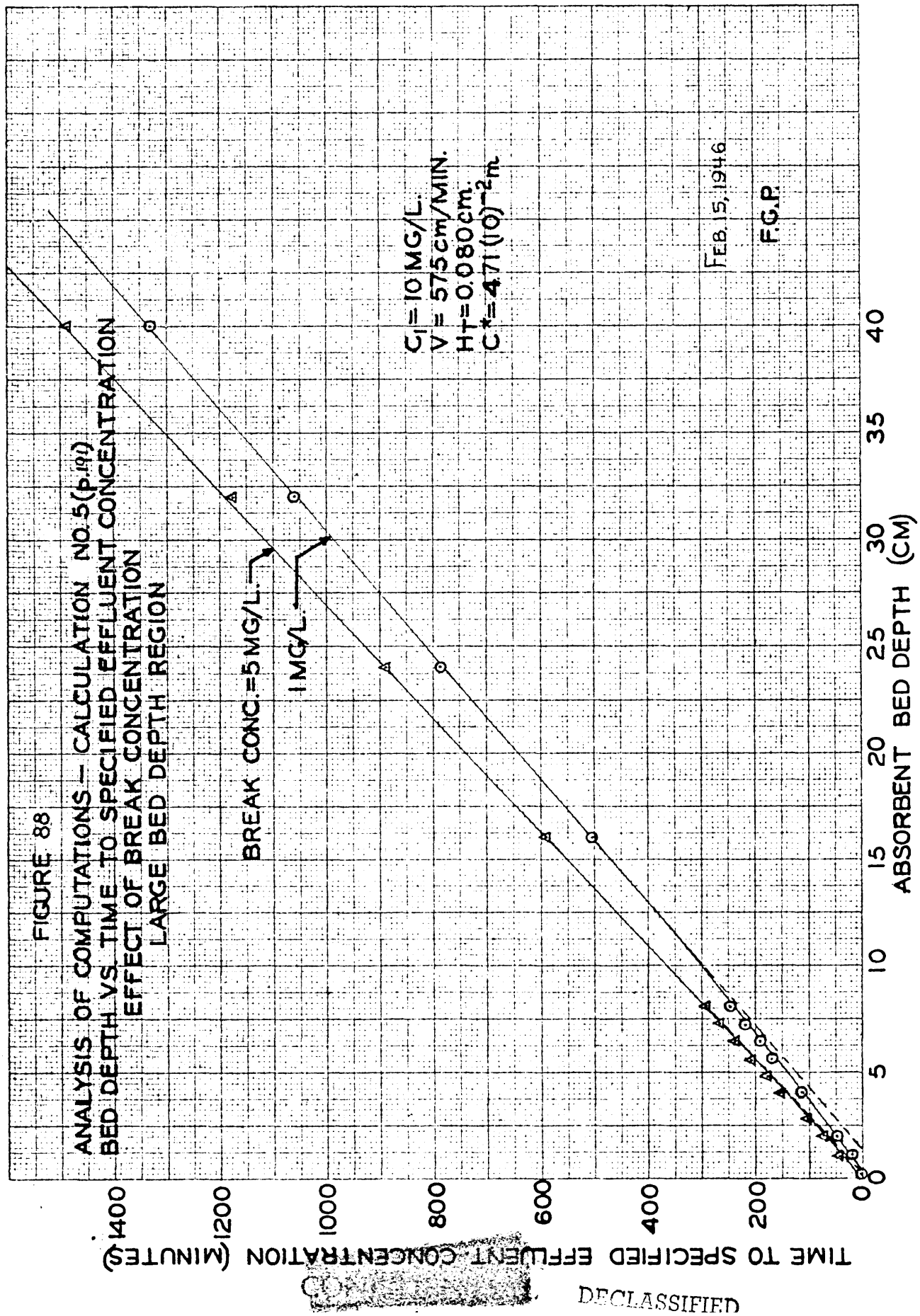
FIGURE 88
ANALYSIS OF COMPUTATIONS — CALCULATION NO. 5 (p. 191)
BED DEPTH VS. TIME TO SPECIFIED EFFLUENT CONCENTRATION
EFFECT OF BREAK CONCENTRATION
LARGE BED DEPTH REGION
BREAK CONC. = 5 MG/L.
1 MG/L.
C_1 = 10 MG/L.
V = 575 cm/MIN.
HT = 0.080 cm.
$C^* = 4.71 (10)^{-2} m$
FEB. 15, 1946
F.G.P.
TIME TO SPECIFIED EFFLUENT CONCENTRATION (MINUTES)
0
200
400
600
800
1000
1200
1400
ABSORBENT BED DEPTH (CM)
0
5
10
15
20
25
30
35
40

E. Limitations of General Equation

1. Assumption of Isothermal Valid

Equation 1 was derived to fit the calculated relationship between bed depth and break time for the linear portion of the curve relating these variables. However, it has been pointed out that this equation does not apply for bed depths near the critical value.

It has not been specifically pointed out that this equation does not apply if the break concentration is too near the influent concentration. This range of inaccuracy increases with decreasing values of n in Freundlich's isotherm. Fig. 89 shows the inaccuracy which can be expected at high break concentrations with n equal to two. This figure shows the calculated values of C as a function of time at a particular bed depth as compared with the values calculated from Equation 1.

It is evident that, even with this low value of n, disagreement between the exact relationships and the relationships predicted by Equation 1 does not occur until effluent concentrations exceeding ten per cent of the influent concentration are attained. In all Chemical Warfare Service standard test procedures, the break concentration never exceeds one per cent of the influent concentration; therefore, no discrepency is to be expected.

2. Non-Isothermal Considerations

The previously derived equations were derived on the assumption of isothermal adsorption. Actually, heat is liberated when a material is adsorbed, the quan-

DECLASSIFIED

Fig. 89

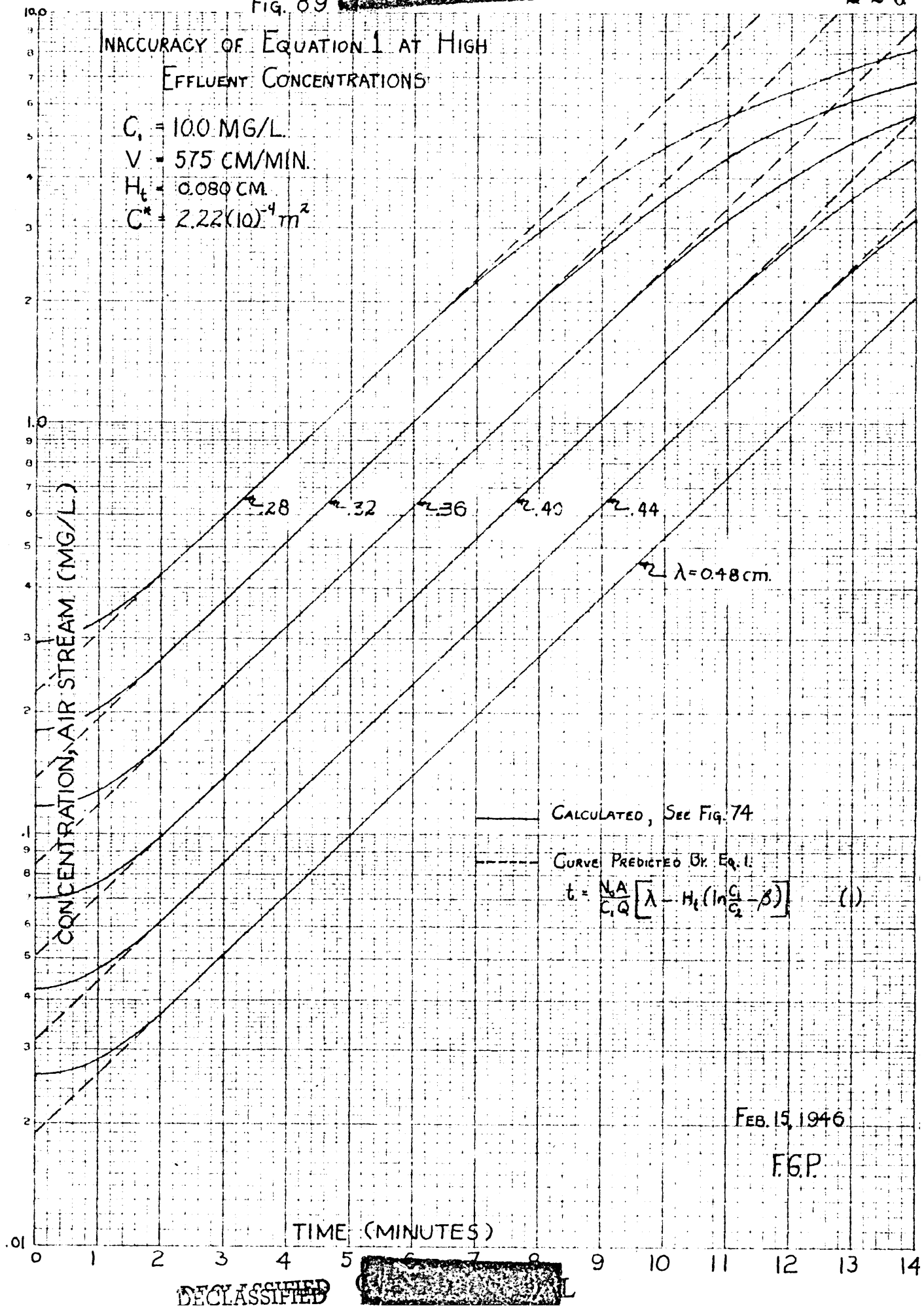

THE FREDERICK POST CO. CHICAGO, ILL.
336-3 SEMI-LOGARITHMIC—3 CYCLES X 70 DIVISIONS

DECLASSIFIED

tity of heat increasing with increasing adsorbate concentration. The heat which is released is transferred partially to the adsorbent and partially to the air stream; so the temperature of both increases. An increase in the temperature of the air stream has little effect, for the partial pressure of the adsorbate is not affected and the mass transfer coefficient is not materially affected by a change in temperature.

An increase in the temperature of the adsorbent, however, does have an appreciable effect. For a given adsorbent content of the granules, increasing the temperature increases the equilibrium partial pressure which decreases the rate of mass transfer.

If a particular point in the bed is studied, the following temperature history is obtained (graphically illustrated in Fig. 90). Initially the temperature rises sharply because of adsorption and heat liberation at a point in the bed ahead of the specified point. After this initial, sharp rise, the temperature gradually increases as the adsorption wave approaches the chosen location. As material is adsorbed at the designated point, the rate of adsorption decreases because of the increasing back pressure. This decrease in the adsorption rate decreases the rate of heat liberation which, in turn, allows the temperature of the adsorbent to drop. As the temperature of the adsorbent drops, the partial pressure decreases and further adsorption occurs. This process is repeated until saturation at the influent temperature is attained.

CODEX BOOK COMPANY, INC. NORWOOD, MASSACHUSETTS

Fig. 90

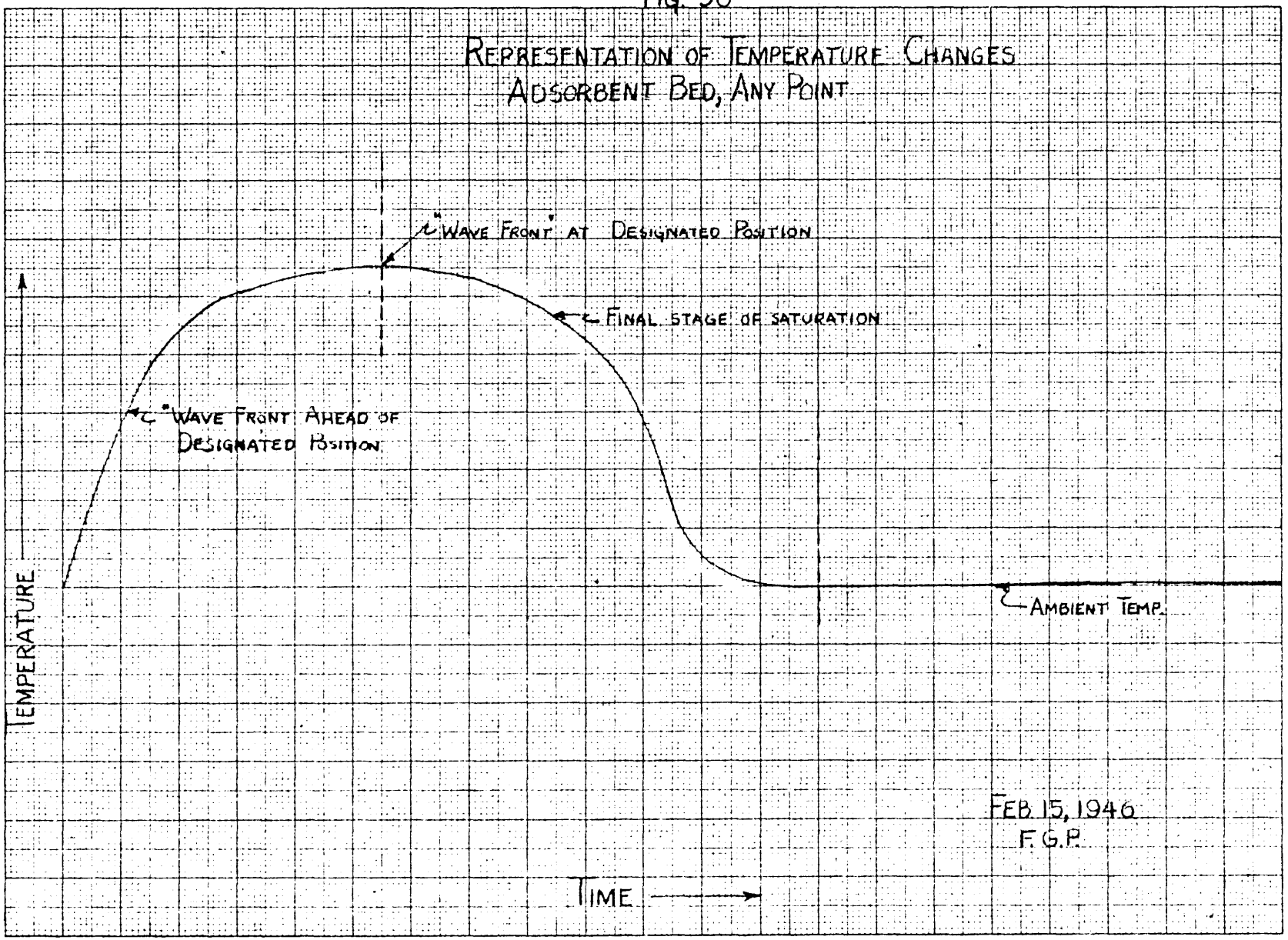

DECLASSIFIED

It is, of course, a gradual process and does not occur in steps as indicated above.

Qualitatively, this entire process is analogous to the isothermal adsorption of a gas for which n in Freundlich's isotherm is decreased, for both the heat liberation and the decrease in n retard the rate of adsorption during the final stages of saturation by increasing the back pressure from the adsorbent. Therefore, the interpretation of data and the correlation of data with the results predicted by Equation 1 must take cognizance of the heat of adsorption.

Practically, the normal agent concentrations are quite low so that large temperature rises are not obtained and the effect of this variable is minimized. This is especially true for those agents for which n in Freundlich's isotherm is large. The major discrepencies are to be expected with those agents for which the value of n is low (around two), for, if the temperature rise is sufficient to reduce the effective value of n to near unity, it has been shown previously that Equation 1 will no longer apply.

APPENDIX B

DERIVATION OF EQUATIONS FOR CUMULATIVE PENETRATION BREAK

A. General

The usual practice in the evaluation of adsorbent beds is to measure the time to a specified effluent concentration which is chosen to approximate the minimum physiologically detectable concentration. However, certain agents (e.g., arsine) are cumulative poisons and, therefore, the time to a specified cumulative penetration is more nearly representative of the protection afforded by an adsorbent bed. Since this method of canister evaluation is standard practice for particular agents, it is important to modify the equations to cover this test method.

B. Derivation of Equation for Axial Flow Adsorbent Beds

The general equation relating the variables was derived in Appendix A and is as follows:

$$t = \frac{N_o A}{C_1 Q}\left[\lambda - H_t\left(\ln\frac{C_1}{C_2} - \beta\right)\right] \qquad (1)$$

Solution of this equation for the effluent concentration results in the following equation:

$$C_2 = \frac{C_1}{e^{\left(\frac{C_1 Q\, t}{N_o A\, H_t} - \frac{\lambda}{H_t} - \beta\right)}} \qquad (84)$$

This equation relates the effluent concentration with time for fixed values of the independent variables.

The cumulative quantity penetrating the bed is represented by the following equation:

$$F = \int_o^t Q\, C_2\, dt \qquad (85)$$

Substituting the value of C expressed by Equation 84 into Equation 85 and integrating, the following expression is obtained:

$$F = -N_o A\, H_t \left[e^{\left(-\frac{C_1 Q\, t}{N_o A\, H_t} + \frac{\lambda}{H_t} + \beta \right)} - e^{\left(\frac{\lambda}{H_t} + \beta \right)} \right] \qquad (86)$$

Rearrangement of this equation results in the following relationship:

$$F = -N_o A H_t e^{\left(\frac{\lambda}{H_t} + \beta \right)} \left[e^{-\frac{C_1 Q\, t}{N_o A H_t}} - 1 \right] \qquad (87)$$

For such values of time that the first term inside the brackets is much greater than unity, the following equation is derived by rearrangement and taking logarithms:

$$t = \frac{N_o\, A}{C_1\, Q} \left[\lambda - H_t \left(\ln \frac{N_o A\, H_t}{F} - \beta \right) \right] \qquad (6)$$

This equation is strikingly similar to Equation 1 and represents a straight line with the same slope but with a different intercept on the bed depth axis.

It should be borne in mind that Equation 84 is not exact for very short time intervals. This was explained in Appendix A. For a short time after the start of the

test, the effluent concentration remains constant and is represented by the following equation:

$$C_2 = \frac{C_1}{e^{\frac{\lambda}{H_t}}} \tag{68}$$

Solving for the cumulative penetration as before, the following equation is obtained:

$$t = \frac{F\, e^{\frac{\lambda}{H_t}}}{C_1 Q} \tag{88}$$

Therefore, the entire curve of cumulative break time vs. bed depth is represented, in parts, by three separate equations. For very short break times, Equation 88 applies; for relatively large break times, Equation 6 applies; and for intermediate values of the break time, Equation 87 applies.

It is to be observed that there is no true critical bed depth for a cumulative penetration test, for a finite time interval is required for a finite quantity of agent to pass through the bed even at zero bed depth. This time interval is obtained from Equation 88 to be as follows:

$$t_{\lambda = 0} = \frac{F}{C_1 Q} \tag{89}$$

APPENDIX C

ADAPTATION OF EQUATIONS FOR BREATHER FLOW

A. Need for Adaptation

The equation which was derived in Appendix A for the removal of agents from carrier air streams by passage through granular adsorbent beds is limited to conditions of steady flow. In the past three years, the "sine wave breather tester" has been developed. This machine simulates the breathing cycle of the average person under conditions of heavy exercise. Gas-laden air is drawn through the canister under examination at a variable flow rate which approximates a sine wave. The "minute-volume" (integrated volume of gas drawn through the canister in one minute) is held at 50 L./min. for the standard test although this can be varied by regulating the number of cycles per minute. The sine wave flow has a duration of one-half of a complete cycle (simulating inspiration), and no flow occurs during the second half of the cycle (simulating expiration). The standard test procedure employs 33 cycles per minute. These flow conditions are represented graphically in Fig. 91.

Since this test procedure has become standard for the evaluation of adsorbents, the modification of the equations to this test condition is important.

B. Derivation of Equation

It was shown in Appendix A that, if n in Freundlich's isotherm is equal to infinity, the axial flow

FIG. 91

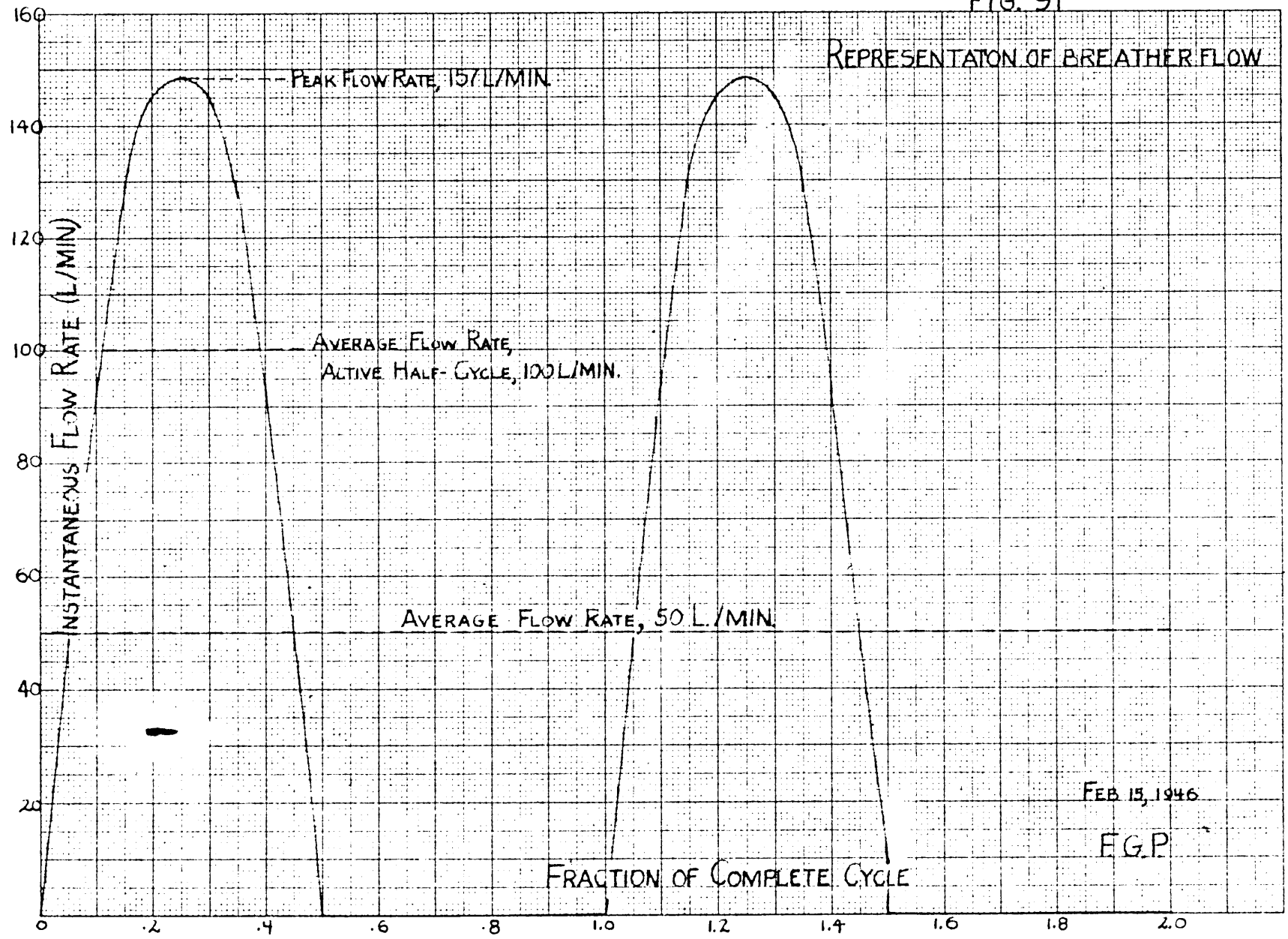

FEB 15, 1946

E.G.P.

DECLASSIFIED

DECLASSIFIED

bed could be divided into two parts: (1) that portion of the bed which is saturated with respect to the influent concentration and in which the concentration in the air stream is constant at the influent concentration and (2) that portion which is not saturated and in which the relationship between concentration and bed depth is represented by the following equation:

$$\ln \frac{C_1}{C_2} = \frac{\lambda'_c}{H_t} \tag{80}$$

Solving this equation for C_2, the following expression is obtained:

$$C_2 = \frac{C_1}{e^{\frac{\lambda'_c}{H_t}}} \tag{90}$$

For a given set of test conditions, it is known that H_t varies with velocity as expressed by the following equation:

$$H_t = k_1 V^x \tag{50}$$

Substituting this value of H_t into Equation 90, the following equation is obtained:

$$C_2 = \frac{C_1}{e^{\frac{\lambda'_c}{k_1 V^x}}} \tag{91}$$

For the sine wave breather, the flow rate during the

inspiration half of the cycle is represented by the following equation:

$$Q = 157 \sin(2 \pi f_r t) \tag{92}$$

$$\text{Let } s = 2 f_r t \tag{93}$$

$$\text{Then: } Q = 157 \sin(\pi s) \tag{94}$$

Dividing the flow rate by the cross-sectional area of the adsorbent bed and multiplying by 1000, the following equation is obtained:

$$V = \frac{157{,}000 \sin(\pi s)}{A} \tag{95}$$

Substituting the value of V from Equation 95 into Equation 91, the following equation is obtained:

$$C_2 = \frac{C_1}{e^{\left[\frac{\lambda_c/k_1}{\left(\frac{157{,}000}{A}\right)^x (\sin \pi s)^x}\right]}} \tag{96}$$

The total quantity of material penetrating the adsorbent bed over a single half cycle may be represented by the following equation:

$$F = \int_0^{\frac{1}{2f_r}} Q\, C_2 dt \tag{97}$$

$$= \frac{157\, C_1}{2 f_r} \int_0^{'} \frac{(\sin \pi s)\, ds}{e^{\left[\frac{\lambda_c/k_1}{\left(\frac{157{,}000}{A}\right)^x (\sin \pi s)^x}\right]}} \tag{98}$$

The average concentration penetrating during this cycle is equal to the total amount penetrating divided by the integrated air flow during the period. This equality is represented by the following equation:

$$(C_2)_{avg.} = \frac{\frac{157\ C_1}{2\ f_r}\int_0^1 \frac{(\sin \pi s)\ ds}{e^{\left[\frac{\lambda'_c/k_1}{\left(\frac{157,000}{A}\right)^x (\sin \pi s)^x}\right]}}}{\frac{157}{2\ f_r}\int_0^1 (\sin \pi s)\ ds} \qquad (99)$$

$$= 1.57\ C_1 \int_0^1 \frac{(\sin \pi s)\ ds}{e^{\left[\frac{\lambda'_c/k_1}{\left(\frac{157,000}{A}\right)^x (\sin \pi s)^x}\right]}} \qquad (100)$$

Rearrangement of this equation results in the following expression:

$$\ln \frac{C_1}{C_2} = \ln \frac{1}{1.57\int_0^1 \frac{(\sin \pi s)\ ds}{e^{\left[\frac{\lambda'_c/k_1}{\left(\frac{157,000}{A}\right)^x (\sin \pi s)^x}\right]}}} \qquad (101)$$

It is apparent from this differential equation that the following equation is applicable:

$$\frac{\lambda'_c/k_1}{\left(\frac{157,000}{A}\right)^x} = f\left(x, \ln \frac{C_1}{C_2}\right) \qquad (102)$$

Designating this function by the symbol, B, the following simplification results:

$$\lambda'_c = k_1\left(\frac{157,000}{A}\right)^x B \qquad (103)$$

For steady flow conditions, λ'_c is given by the following equation previously derived:

$$\lambda'_c = H_t \ln \frac{C_1}{C_2} \qquad (80)$$

Substituting the value of H_t given by Equation 50 into Equation 80, the following equation is obtained:

$$\lambda'_c = k_1 \frac{1000\ Q^{-x}}{A} \ln \frac{C_1}{C_2} \qquad (104)$$

If Q_e is designated as the "steady flow rate equivalent to breather flow" to the extent that it affects the value of λ'_c, Equations 103 and 104 may be set equal to one another. This results in the following relationship:

$$k_1\left(\frac{1000\ Q_e}{A}\right)^x \ln \frac{C_1}{C_2} = k_1\left(\frac{157,000}{A}\right)^x B \qquad (105)$$

Solving this equation for the steady flow rate equivalent to breather flow, Q_e, the following equation is obtained:

$$Q_e = \frac{157}{\left(\frac{\ln \frac{C_1}{C_2}}{B}\right)^{\frac{1}{x}}} \qquad (106)$$

Since, in this equation, B is a function of $\ln \frac{C_1}{C_2}$ and x, Q_e must also be a function of these same variables. Equation 101 was integrated (graphically) and the resulting relationship between Q_e, $\ln \frac{C_1}{C_2}$, and x is shown in Fig. 92.

Thus, it has been shown that the length of the true critical bed depth for the case of breather flow testing may be represented by an equation analogous to the equation applicable for steady flow conditions. These analogous equations are as follows:

a. Steady Flow

$$\lambda_c' = k_1 \left(\frac{1000\ Q}{A}\right)^x \ln \frac{C_1}{C_2} \qquad (104)$$

b. Breather Flow

$$\lambda_c' = k_1 \left(\frac{1000\ Q_e}{A}\right)^x \ln \frac{C_1}{C_2} \qquad (106)$$

The development of the remaining groups in the equation relating break time to the pertinent variables for breather testing is identical to that for steady flow testing. Therefore, the resulting equation relating the variables for breather flow testing (constant cross section adsorbent bed) is as follows:

$$t = \frac{N_o A}{C_1 Q}\left[\lambda - H_t\left(\ln \frac{C_1}{C_2} - \beta\right)\right] \qquad (1)$$

DECLASSIFIED

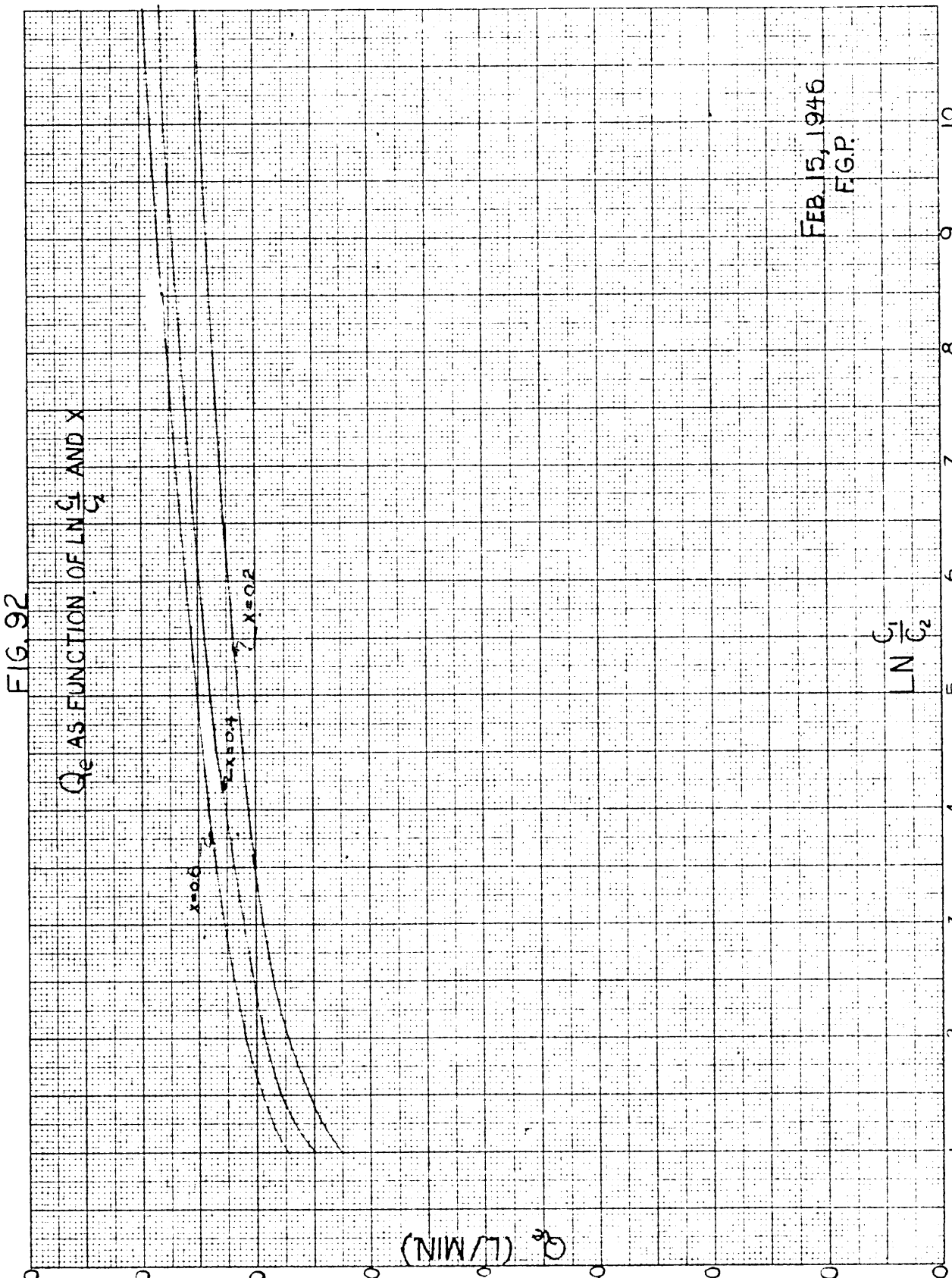

DECLASSIFIED

APPENDIX D

ADAPTATION OF EQUATIONS TO RADIAL FLOW

A. Need for Adaptation

The equation which was developed in Appendix A (Equation 1) for the removal of agents from carrier air streams is limited to axial flow adsorbent beds: i.e., beds of constant cross-sectional area perpendicular to the direction of air flow. This design is the simplest of the many possible designs of adsorbent beds. However, several of the U.S.Army gas mask canisters are of the "radial flow" design. In this construction the adsorbent is retained between two concentric, perforated cylinders. The air stream enters the face of the outer cylinder perpendicular to the axis of the cylinder and leaves through the inner cylinder-commonly called the "inner tube". It is obvious from this description that the air velocity is a function of the position in the bed. Since the radial flow canister is used by the U.S.Army, the adaptation of the previously derived equations to apply for this type of design is important.

B. Derivation of Equation for the Critical Diameter

The critical diameter for a radial flow canister is analogous to the critical bed depth for an axial flow canister. For a particular inner tube diameter, it is defined as the outer tube diameter which will result in an effluent concentration equal to the break concentration at the instant the air first penetrates the bed.

DECLASSIFIED

The general flow characteristics and the nomenclature for the radial flow canister are shown in Fig. 93.

The following equation was developed in Appendix A to express the relationship between bed depth and concentration:

$$\frac{C^* - C}{H_t} = \frac{dC}{d\lambda} \tag{67}$$

This equation is equally applicable to radial flow canisters if it is modified as follows (see Fig. 93):

$$\frac{C^* - C}{H_t} = - \frac{2\,dC}{dD} \tag{107}$$

For the particular case when n in Freundlich's isotherm is equal to infinity, C^* is equal to zero to the instant that saturation occurs. Introduction of this consideration and rearrangement of the terms results in the following equation:

$$\frac{dC}{C} = \frac{dD}{2H_t} \tag{108}$$

It has been shown previously that H_t is a function of velocity and, for a given set of conditions, can be represented by the following equation:

$$H_t = k_1 V^x = k_1 \left(\frac{1000\,Q}{\pi\,D\,L}\right)^x \tag{109}$$

Substituting this value of H_t into Equation 108, the following equation is obtained:

DECLASSIFIED

FIG. 93 237

REPRESENTATION OF RADIAL FLOW CANISTER

DECLASSIFIED

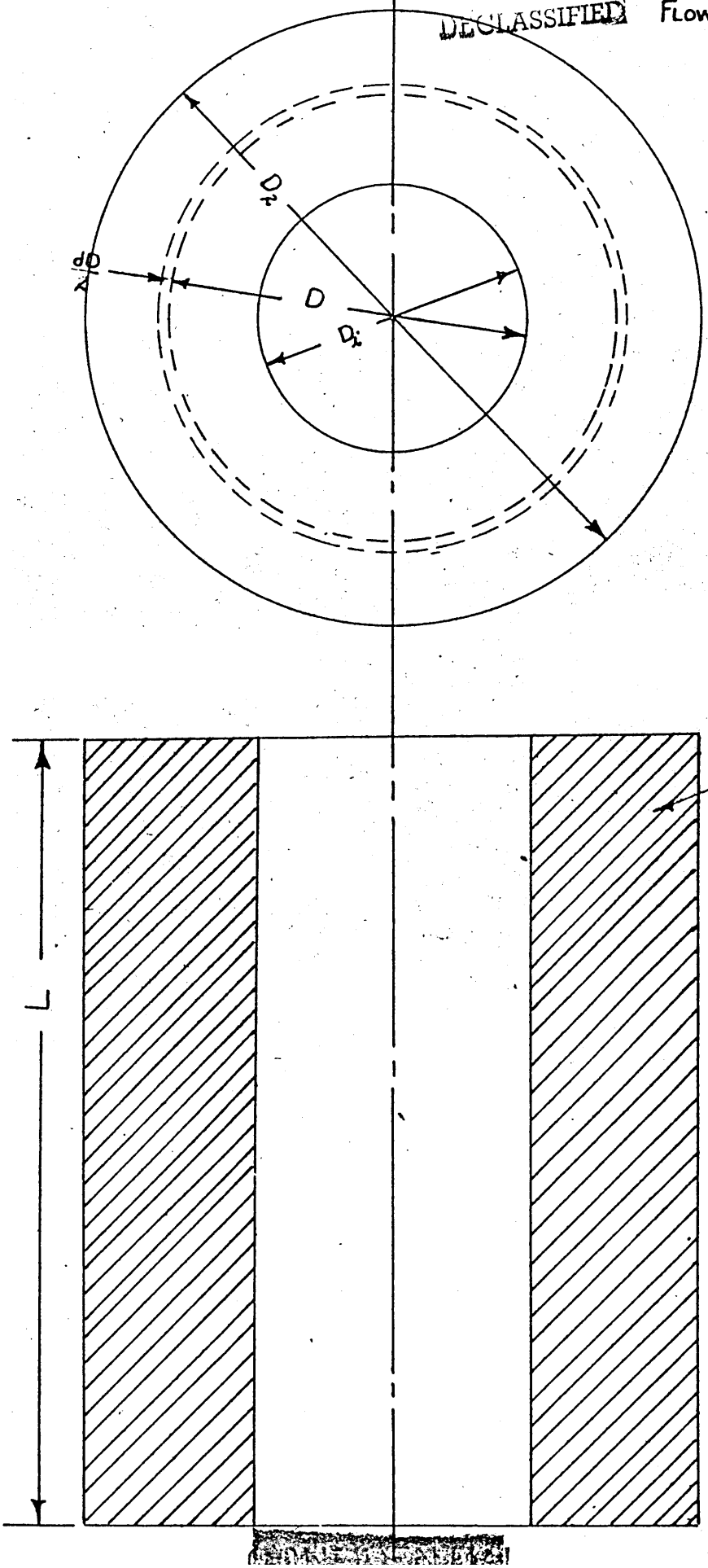

FEB. 18, 1946

F.G.P.

DECLASSIFIED

$$\frac{dC}{C} = \frac{D^x \, dD}{2k_1 \left(\frac{1000\ Q}{\pi\ L}\right)^x} \qquad (110)$$

Integration of this equation from the influent to the effluent concentration and from the critical diameter to the inner tube diameter results in the following equation:

$$\ln \frac{C_1}{C_2} = \frac{D_c^{x+1} - D_i^{x+1}}{2k_1(x+1)\left(\frac{1000\ Q}{\pi\ L}\right)^x} \qquad (111)$$

Solving this equation for the critical diameter, the following equation is obtained:

$$D_c = \left[D_i^{x+1} + 2k_1(x+1)\left(\frac{1000\ Q}{\pi\ L}\right)^x \ln \frac{C_1}{C_2} \right]^{\frac{1}{x+1}} \qquad (4)$$

C. Determination of Time Interval Required for Saturation of Differential Thickness at Critical Diameter

If the canister were constructed to have an outer diameter equal to the critical diameter, the effluent concentration would remain constant at the break concentration until the first differential bed thickness became saturated. The purpose of this section is to determine the time interval required to obtain saturation of this differential thickness.

A material balance across this section results in the following equation:

$$A \, dm \, \frac{dD}{2} = Q \, dC \, dt \qquad (112)$$

DECLASSIFIED

Substituting the value of A as a function D and rearranging and solving for dt, the following equation is obtained:

$$dt = \frac{\pi \ D \ L \ dm}{2 \ Q \ \frac{dC}{dD}} \qquad (113)$$

Substituting into this equation the value of dC/dD obtained from Equation 110 and integrating from m equal to zero and m equal to N_o, the following relationship is obtained:

$$\Delta t_1 = \frac{\pi \ D_c \ L \ N_o \ k_1}{C_1 \ Q} \left(\frac{1000 \ Q}{\pi \ D_c \ L}\right)^x \qquad (114)$$

It is important to note that this equation is identical to the equation for axial flow beds derived in Appendix A, for $\pi D_c L$ is equal to A and the term, $k_1\left(\frac{10000}{\pi \ D_c L}\right)^x$ is equal to the height of a transfer unit at the critical diameter.

Since this is analogous to the equation for axial flow adsorbent beds, it is reasonable to assume that the effect of the isotherm should be analogous. From the treatment of the axial flow adsorbent bed, the effect of n in the Freundlich isotherm is expressed by the following equation:

$$\Delta t_1 = \left(\frac{\beta \pi \ D_c \ L \ N_o}{C_1 \ Q}\right) k_1 \left(\frac{1000 \ Q}{\pi \ D_c L}\right)^x \qquad (115)$$

D. Derivation of Complete Equation

For the particular instance when n in Freundlich's isotherm is equal to infinity, all adsorbent contained in the concentric cylinders bounded by the outer cylinder and the cylinder defined by the critical diameter is saturated with respect to the influent concentration. From a material balance which takes into consideration the quantity of agent entering and the quantity in the saturated and in the unsaturated layers, the following equation was derived for radial flow adsorbent beds:

$$t = \frac{\pi L N_o}{4 C_1 Q}\left[D_2^2 - D_c^2 + 4D_c k_1\left(\frac{1000\ Q}{\pi D_c L}\right)^x\right] \qquad (51)$$

Taking into consideration the effect of n in Freundlich's adsorption isotherm, the following equation was obtained:

$$t = \frac{\pi L N_o}{4 C_1 Q}\left[D_2^2 - D_c^2 + 4D_c k_1 \beta\left(\frac{1000\ Q}{\pi D_c L}\right)^x\right] \qquad (5)$$

APPENDIX E

REMOVAL OF AGENTS BY CHEMICAL REACTION WITH IMPREGNANTS

A. General

The previous appendices were concerned with the removal of agents by reversible, physical adsorption when the rate of mass transfer from the air stream to the surface of the granules controls the overall rate of removal. The more difficult problem is encountered in those instances when the impregnation on the whetlerite contributes towards its capacity, for in such instances another rate, the rate of chemical reaction, must be considered. It is held to be self-evident that such materials must be adsorbed before the impregnation on the adsorbent can function. Therefore, the mass transfer from the air stream to the surface of the adsorbent must be the first step in the removal of any agent.

Consider first the case when the impregnant does aid in the removal of the agent by chemical reaction and the rate of chemical reaction is very rapid as compared to the rate of diffusion to the surface of the adsorbent. As the material is transferred to the surface, it is removed so rapidly that no appreciable "back" pressure of the diffusing material is obtained to retard the rate of transfer until the reactive capacity is completely utilized. This case was analyzed and was found to be entirely analogous to that of reversible, physical adsorption when n in Freundlich's isotherm is equal to infinity. This

analysis revealed that the simplified equation derived in Appendix A (Equation 1) is equally applicable for this mechanism of removal with the modification that N_o must be replaced by the sum of the adsorptive and reactive capacity, $N_o + N_r$. These conditions of gas removal are designated in this thesis as Type II kinetics (Type I classification being reserved for removal by reversible, physical adsorption when the rate of transfer through the stagnant air film surrounding the granules controls the overall rate of removal).

Second, let us consider the case when the impregnant aids in the removal of the agent by chemical reaction but the rate of chemical reaction is of the same order of magnitude as, or much less than, the rate of diffusion to the surface of the granules. For the latter case, the adsorbent will rapidly pick up the quantity of adsorbate which it can physically adsorb. During this saturation period, a very small amount will have reacted and will continue to react slowly tending to reduce the "back" pressure and allowing a small, additional quantity to be transferred by diffusion to the adsorbent surface. This process will continue until the chemical capacity is completely utilized.

This situation is somewhat analogous to an electric condenser with a slight leak, for it is rapidly charged by impressing a voltage across it and then draws a small amount of current, the leakage current, to maintain the charge.

This would correspond very closely to a chemical reaction on the adsorbent which is quite slow but infinite in capacity to remove the agent. This general condition shall be designated in thesis as Type III kinetics.

B. Mathematics of Type III Kinetics

1. General Equation

The rate of chemical reaction between adsorbed molecules and the impregnants on the adsorbent is very probably a function of two variables. These are the concentration of agent physically adsorbed (not reacted) and the quantity of impregnant which has not been consumed by previous reaction. This relationship may be expressed by the following equations:

$$\frac{dM}{dt} = k_r a' f(m) \qquad (12)$$

$$k_r a' = f(I) \qquad (116)$$

The rate of mass transfer to the surface of the adsorbent was shown in Appendix A to be represented by the following equation:

$$\frac{d(M+m)}{dt} = k_g a \ (C - C^*) \quad \text{or}$$

$$d(M+m) = k_g a \ (C - C^*) \, dt \qquad (8)$$

From a material balance, the amount of agent which is transferred to a differential bed thickness, axial flow bed, must be equal to the rate of mass transfer mul-

tiplied by the time, the area, and the differential bed thickness. This results in the following equation:

$$Q\, dC\, dt = k_g a\, (C^* - C)\, A\, d\lambda\, dt$$

$$dC = (C^* - C)\, \frac{d\lambda}{H_t} \qquad (67)$$

This must, in turn, be equal to the sum of the amount which has reacted chemically, the accumulation of unreacted material on the surface of the adsorbent, and the accumulation of unreacted agent in the voids surrounding the granules. This may be represented by the following equation:

$$-Q\, dC\, dt = k_r a'\, f(m)\, A\, d\lambda\, dt + A\, dm\, d\lambda + \frac{A\, \alpha}{1000}\, d\lambda\, dC$$

$$dC = \left[\frac{k_r a'\, A\, f(m)}{Q} + \frac{A}{Q}\frac{dm}{dt} + \frac{A\, \alpha}{1000}\frac{dC}{dt}\right] d\lambda \qquad (117)$$

It was shown in Appendix A that, for reversible adsorption, the term representing accumulating in the voids surrounding the adsorbent granules was negligible. This will be shown to be equally true for the removal of agents by chemical reaction later in this thesis. Elimination of that term results in the following simplification:

$$dC = -\left[\frac{k_r a'\, A\, f(m)}{Q} + \frac{A}{Q}\frac{dm}{dt}\right] d\lambda \qquad (118)$$

The height of a reaction unit, which is analogous to the height of a transfer unit, is defined by the

DECLASSIFIED

following equation:

$$H_r = \frac{V}{1000\ k_r a'} = \frac{Q}{A\ k_r a'} \qquad (119)$$

Substituting this relationship into Equation 118, the following equation is obtained:

$$dC = -\left(\frac{1}{H_r} f(m) + \frac{1000}{V}\frac{dm}{dt}\right) d\lambda \qquad (120)$$

If the functions H_r, $f(m)$, and H_t were known for a particular set of test conditions, the relationship among the variables bed depth, concentration, and time could be computed by a tedious, step-wise integration involving trial and error computations at each step checked by Equations 67 and 120 and by the adsorption isotherm.

2. Particular Solutions

a. Type III-A Kinetics

It was assumed by Hurt (34) that, for catalytic reactions on the surface of granular solids, $f(m)$ is equal to the partial pressure of the reacting material on the surface of the adsorbent. It was further assumed that the rate of reaction is independent of the previous utilization of the impregnant. These assumptions lead to the following modification of Equation 120:

$$dC = -\left(\frac{C^*}{H_r} + \frac{1000}{V}\frac{dm}{dt}\right) d\lambda \qquad (121)$$

This particular type of kinetics has been solved for the values of the independent variables shown in Table XXXIV by a tedious, step-wise integration:

DECLASSIFIED

[redacted] DECLASSIFIED

Table XXXIV

Test Conditions for Computation of Type III-A Kinetics

Test Concentration, C_1	4.0 mg./L.
Flow Rate, Q(1000)/A = V	1000 cm./min.
H_t	.050 cm.
H_r	.235 cm.
Indicator Break Conc., C_2	.008 mg./L.
Equilibrium Relationship	$C^* = .0178\ m^2$
Reactive Capacity	89 mg./ml.

The results of these computations are shown in Figs. 94, 95, and 96. The method of calculation is exemplified in Table XLIV , Appendix I.

Fig. 94 shows that the plot of the logarithm of the effluent concentration vs. time consists of two straight lines joined by a transition curve. Fig. 95 shows the plot of the logarithm of m vs. bed depth and is of the same general type. Fig. 96 shows the plot of time to a specified effluent concentration vs. bed depth and is also in the form of two connecting straight lines.

Table XXXV shows the analysis of Fig. 96 as correlated with the equation relating bed depth and break time for reversible, physical adsorption (Type I kinetics-Equation 1)

The comparisons of Table XXXV show that, for the upper portion of the bed depth-break time curve, the following equation applies:

$$t = \frac{1000(N_o + N_r)}{C_1 V}\left[\lambda - (H_t + H_r)\left(\ln \frac{C_1}{C_2} - 1\right)\right] \quad (2)$$

[redacted] DECLASSIFIED

DECLASSIFIED

FIGURE 94

RELATIONSHIP BETWEEN CONCENTRATION IN AIR STREAM, BED DEPTH, AND TIME FOR TYPE III-A KINETICS

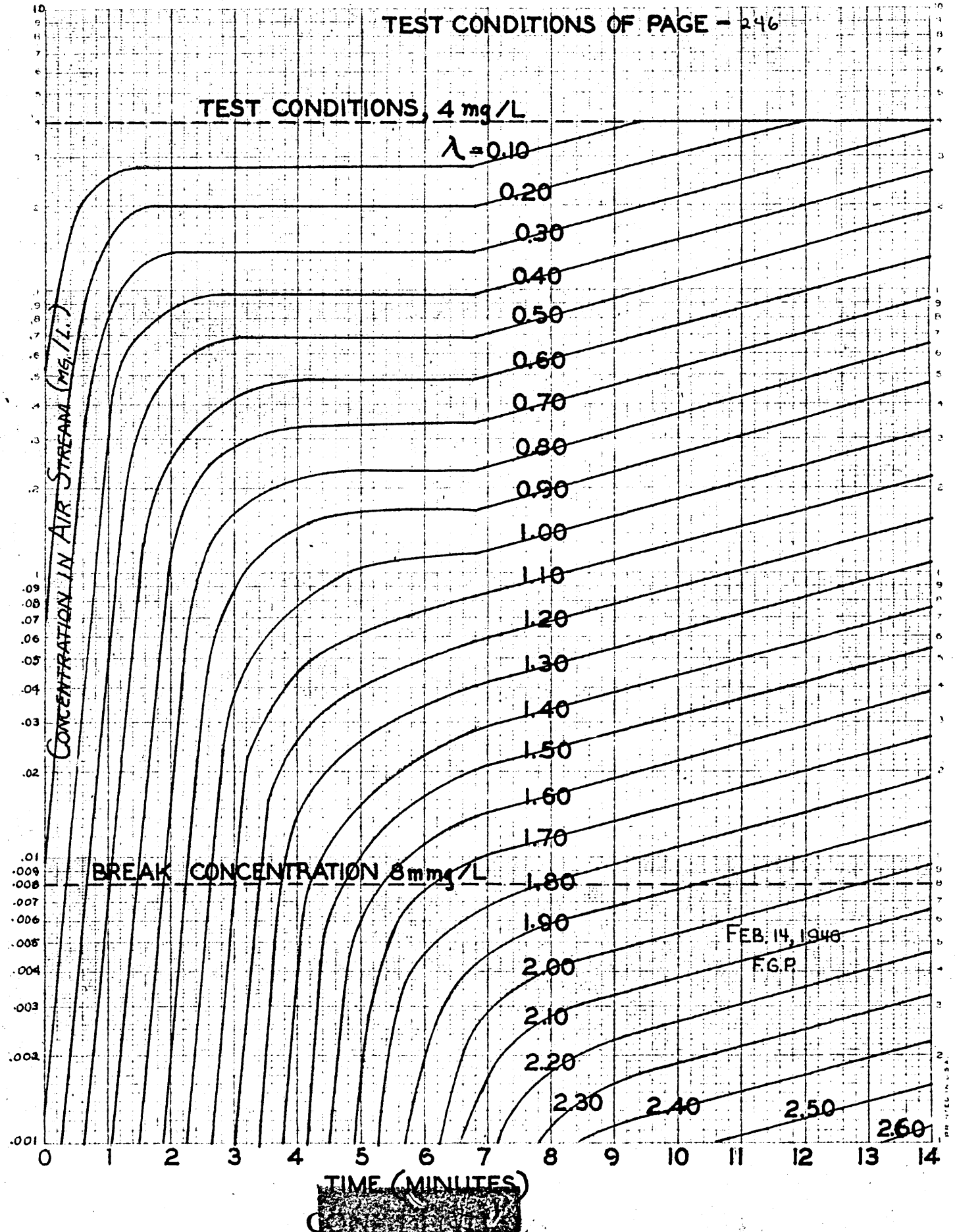

DECLASSIFIED

DECLASSIFIED

CAPACITY - 104 mg/mL

FIGURE 95

RELATIONSHIP BETWEEN BED DEPTH, TIM
AND CONCENTRATION OF AGENT ON
ADSORBENT FOR TYPE III KINETICS

TEST CONDITIONS OF P.

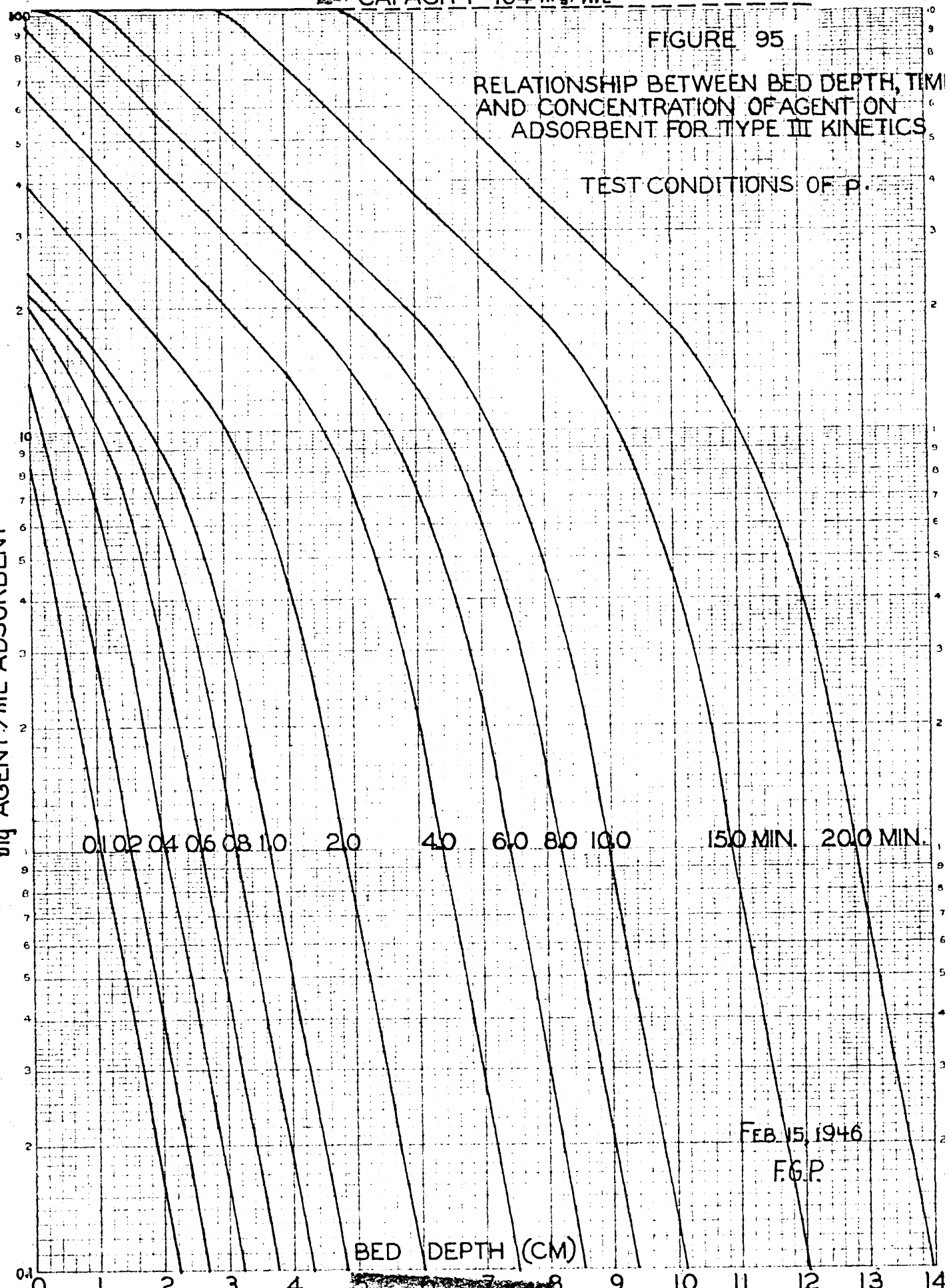

FEB 15, 1946
F.G.P.

THE FREDERICK POST CO CHICAGO, ILL.
336-3 SEMI LOGARITHMIC—3 CYCLES X 70 DIVISIONS

DECLASSIFIED

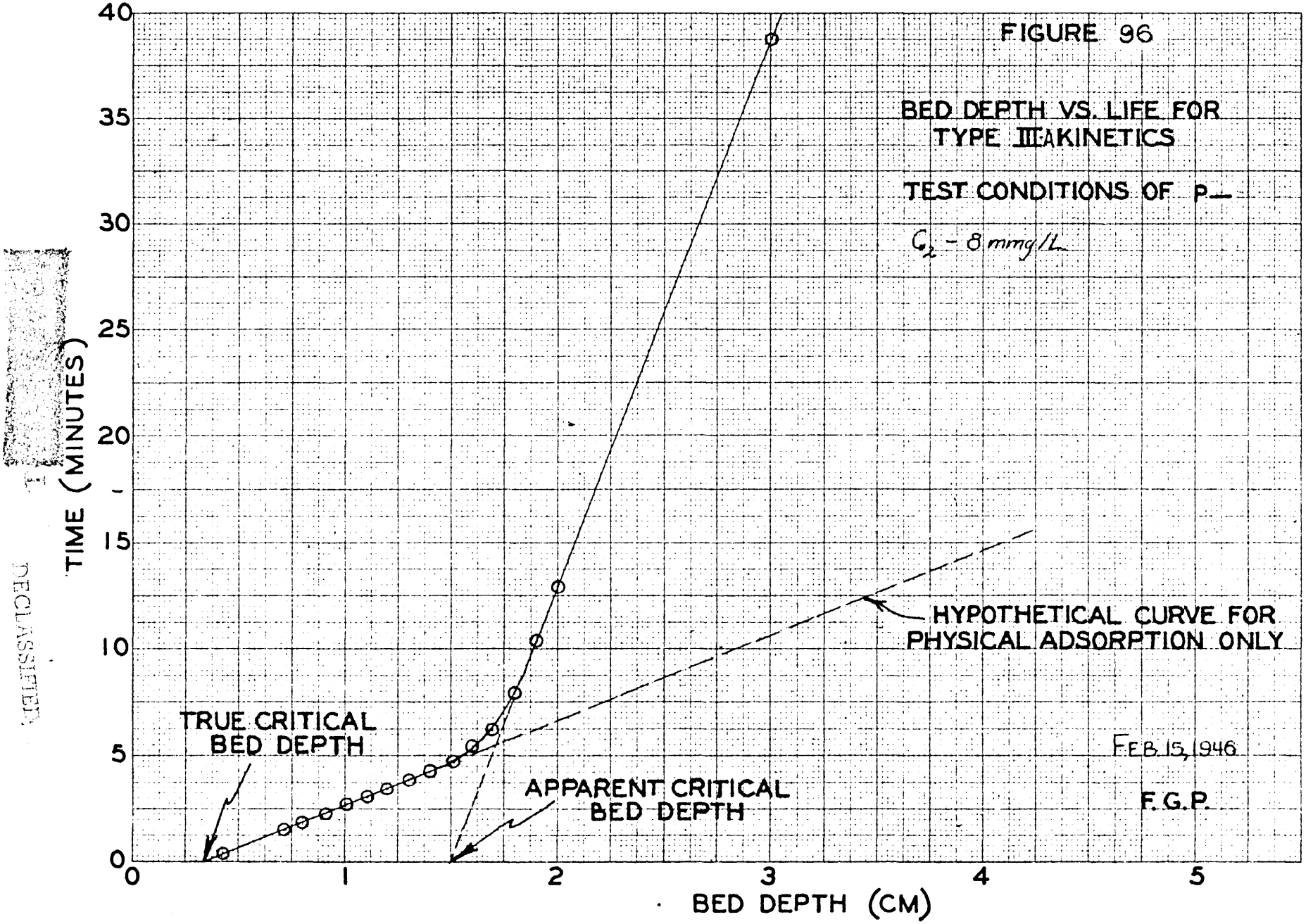

DECLASSIFIED

DECLASSIFIED

Table XXXV

Correlation of Calculations for Type III-A Kinetics

N_o, Physical Adsorption Capacity at C_1	15.0	mg./ml.
$\frac{1000\ N_o}{C_1 V}$	3.75	min./cm.
Slope of Lower, Straight Portion of Curve	3.7	min./cm.
$N_o + N_r$	104	mg./ml.
$\frac{1000(N_o + N_r)}{C_1\ V}$	26.0	min./cm.
Slope of Upper, Straight Portion of Curve	26.0	min./cm.
$(H_t + H_r)(\ln \frac{C_1}{C_2} - 1)$	1.49	cm.
Apparent Critical Bed Depth	1.49	cm.

This equation is entirely analogous to that for Type I kinetics if $N_o + N_r$ is substituted for N_o and $H_t + H_r$ is substituted for H_t and if it is considered that n in Freundlich's isotherm is effectively infinity. The reason for this similarity becomes more apparent if C^* is eliminated between Equations 67 and 121. This elimination results in the following equation:

$$\frac{dC}{\frac{1000}{V}\frac{dm}{dt} - C} = \frac{d\lambda}{H_t + H_r} \qquad (122)$$

If, in this equation, dm/dt is considered to be negligible, the equation may be integrated and results in the following expression:

$$\lambda'_c = (H_t + H_r) \ln \frac{C_1}{C_2} \qquad (123)$$

This equation is likewise identical in form to that applicable for reversible adsorption.

The lower part of the bed depth-break time curve is identical to that which would be obtained if no reaction occurred on the adsorbent, for a certain interval of time is required for the slower chemical reaction to reflect in the bed depth-break time curve.

b. Type III-B Kinetics

Although there is a great lack of data for all the Chemical Warfare agents, it was shown quite conclusively by the data of Wiig (48, 49, 50, 51, 52) that the rate of removal of cyanogen chloride from air streams by Type ASC impregnated whetlerite is influenced by the previous utilization of the impregnant. Wiig conducted tests in which cyanogen chloride-laden air was passed through very thin adsorbent beds and in which the chloride content of the adsorbent was measured as a function of time. Selected results of his experiments are shown in Figs. 97 and 98.

Wiig did not analyze his data for compliance with Equation 12. However, since the rate of attainment of equilibrium was so slow as compared to that predicted by diffusion considerations, it is obvious that practical physical saturation must have been attained relatively rapidly. Therefore, the term, f(m), in Equation 12 is practically constant except for the short, initial part of the test which was required for physical saturation.

FIGURE 97

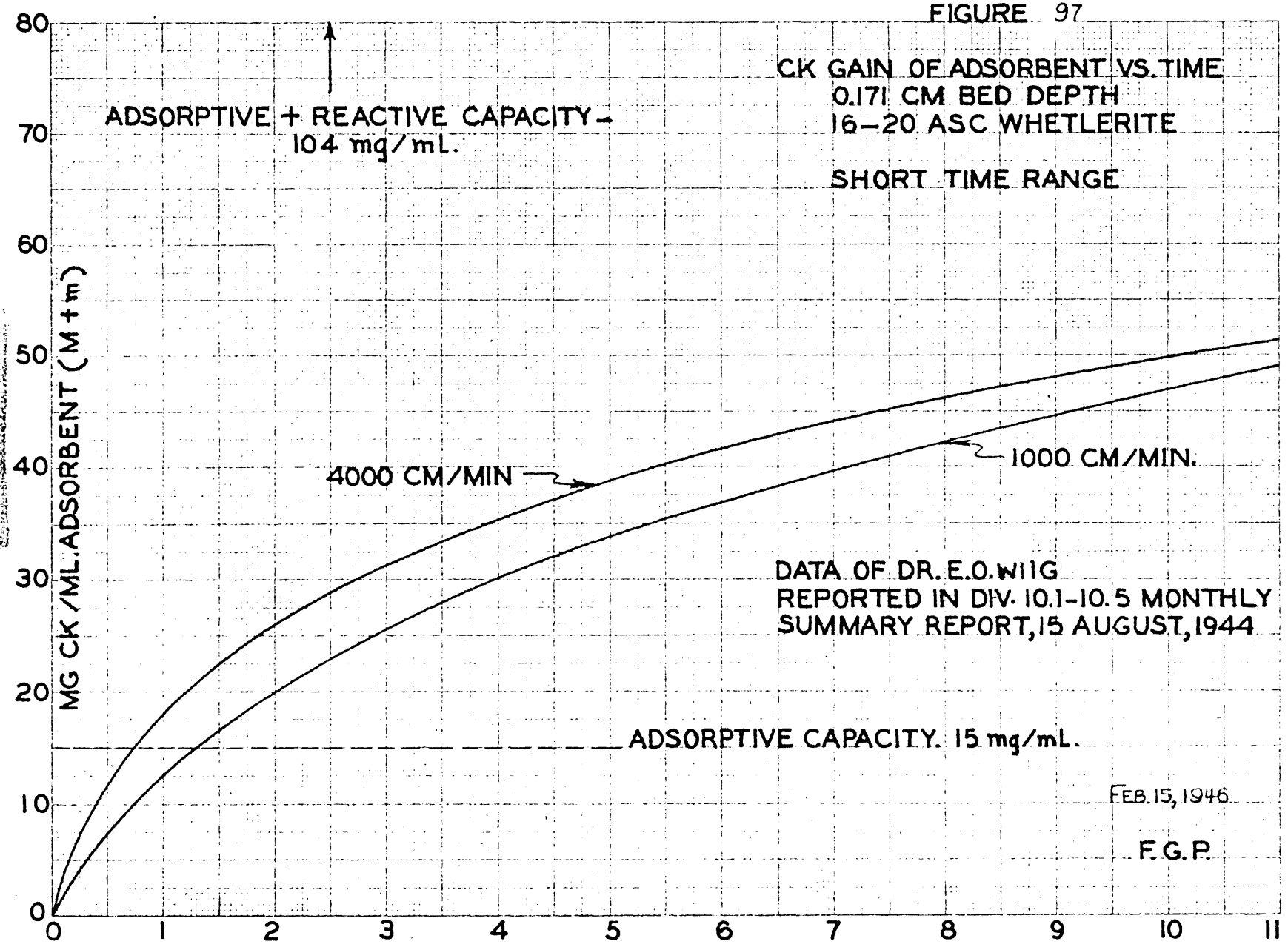

DECLASSIFIED

DECLASSIFIED

FIGURE 98

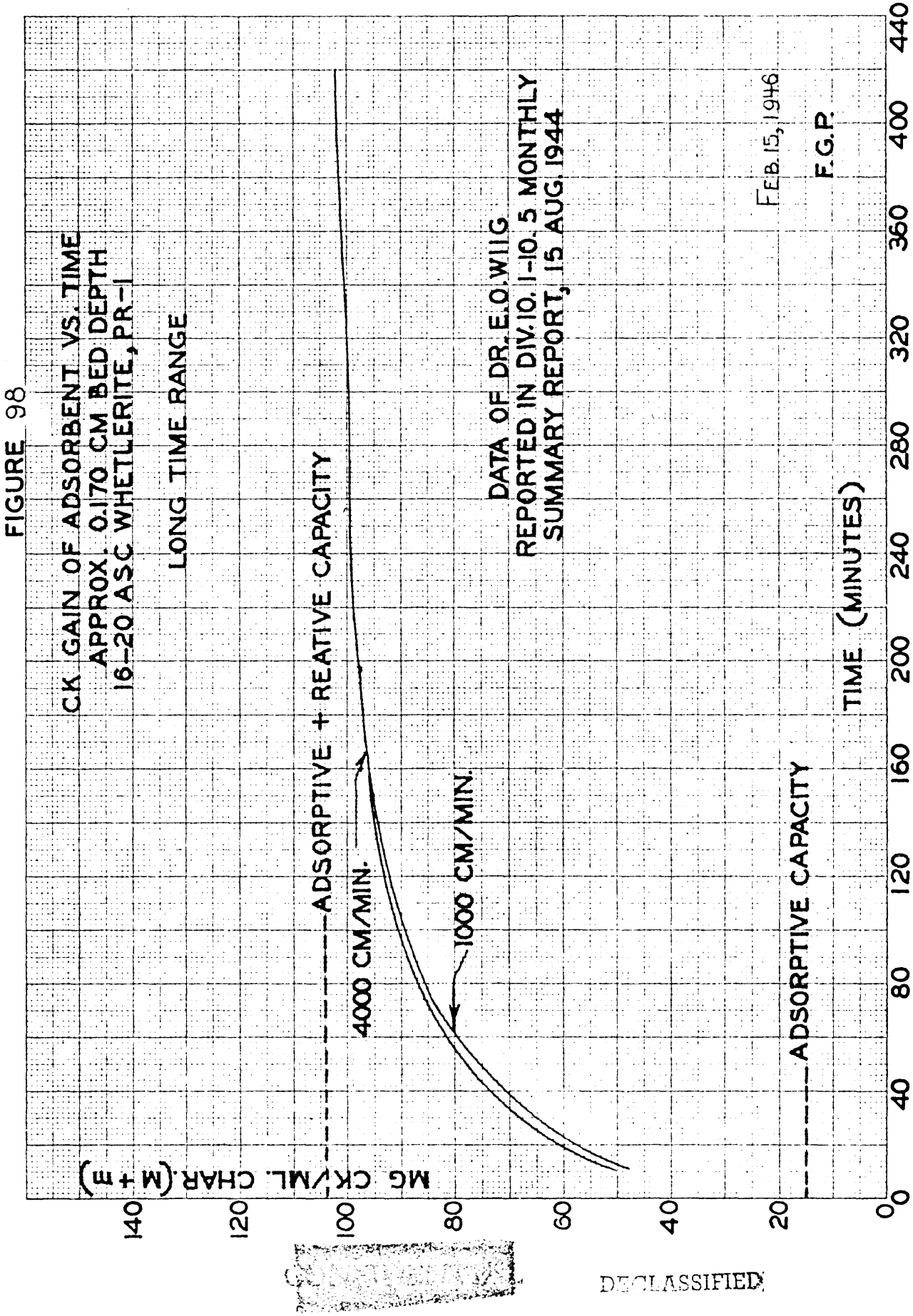

DECLASSIFIED

The slope of the plot of cyanogen chloride content vs. time is, by Equation 12, equal to $k_r a' f(m)$. If it is assumed that f(m) is directly proportional to m, $k_r a'$ can be calculated from the slope of these curves. These calculations were made and the resulting relationship is shown in Fig. 99. It is to be noticed that a unique curve was obtained for the two test velocities employed by Wiig (1000 and 4000 cm./min.). This adds credence to the validity of Equation 12.

Using the values of $k_r a'$ shown in Fig. 99 and employing the assumption that f(m) is equal to m, this particular type of kinetics was solved for the following values of the independent variables by a tedious, stepwise integration similar to that employed for Type III-A kinetics:

Table XXXVI

Test Conditions for Computation of Type III-B Kinetics

Test Concentration, C_1	4.0 mg./L.
Linear Flow Rate, V	4000 cm./min.
H_t	0.36 cm.
Equilibrium Relationship	$C^* = .0178\ m^2$
Reactive Capacity	89 mg./ml.

The reason for the choice of the adsorption isotherm shown in Table XXXVI was that it complies with the adsorption capacity of the unimpregnated whetlerite (15 mg./ml. at a concentration of 4 mg./L. from data of Wiig) and because cyanogen chloride is a lightly

[redacted]

DECLASSIFIED

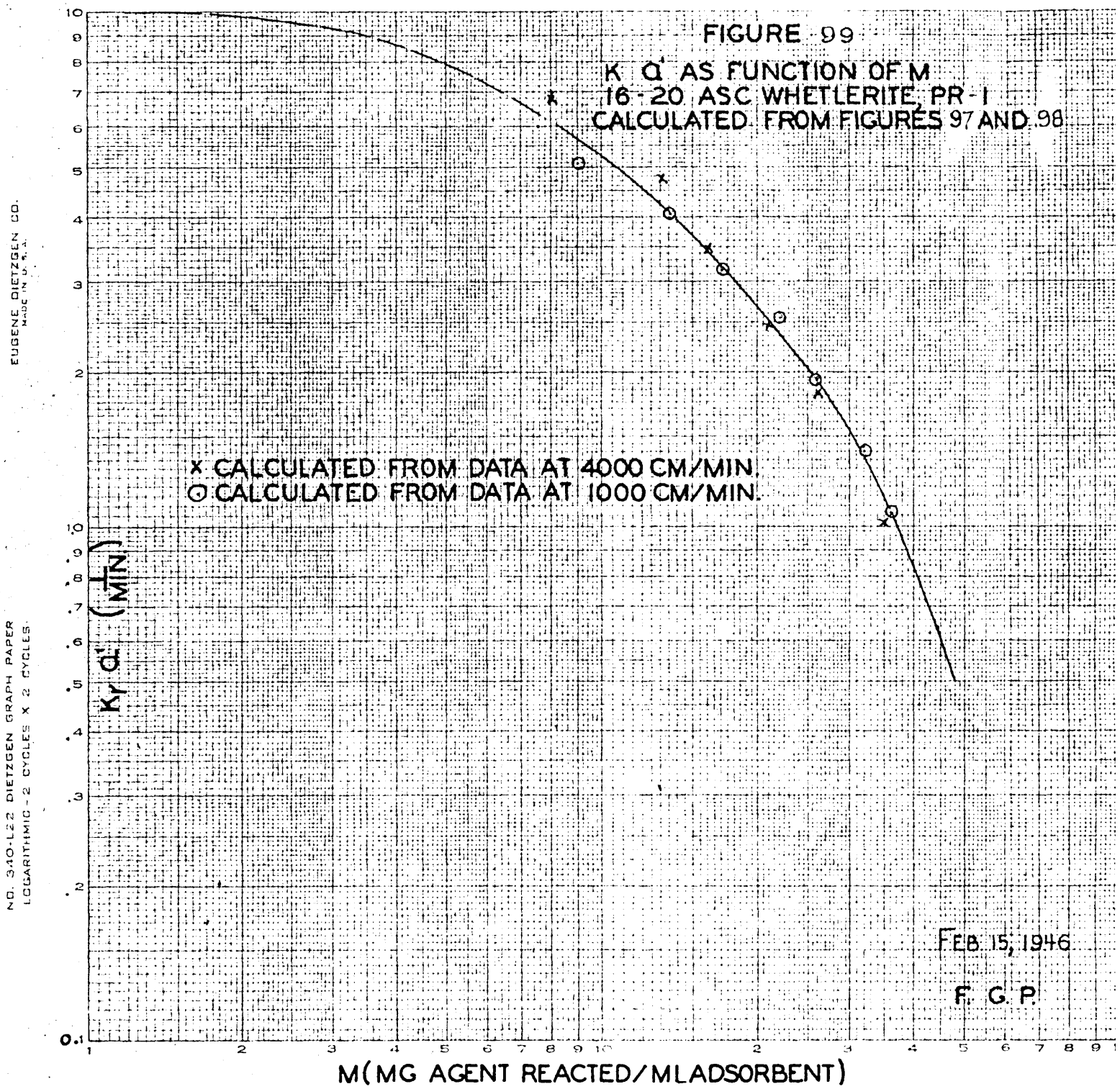

[redacted]

DECLASSIFIED

adsorbed agent and, therefore, should have a fairly small value of n. The value of H_t was purposely chosen at a higher value than theory predicts (H_t should actually be approximately 0.05 cm.) to facilitate the computations and because the value of this variable is not critical in the final analysis (the chemical reaction rate controls).

The results of these calculations are shown in Figs. 100, 101, and 102. Fig. 100 shows that the plot of the logarithm of the effluent concentration vs. time results in a continuous curve with no straight part. Fig. 101 shows that the plot of the logarithm of m+M vs. time results in a curve which degenerates to a straight line at large bed depths. Unlike all other types of kinetics, saturation of the influent layers was not obtained, and it is apparent that the final stages of saturation are quite slow. Fig. 102 shows the plot of the time to a specified effluent concentration vs. bed depth. The initial portion of this curve conforms to the curve anticipated from the adsorptive capacity of the whetlerite in the same manner as for Type III-A kinetics. At larger bed depths, however, the similarity ceases, for although an apparent straight line relationship is obtained, the curvature actually continues to a slight extent; it can be shown that this curvature will continue to persist at all bed depths. For all practical purposes, however, the upper part can be considered to be a straight line. Correlation of the pertinent functions represented

DECLASSIFIED

FIGURE 100

RELATIONSHIP BETWEEN CONCENTRATION IN AIR STREAM, BED DEPTH, AND TIME FOR TYPE III-B KINETICS

TEST CONDITIONS OF P.

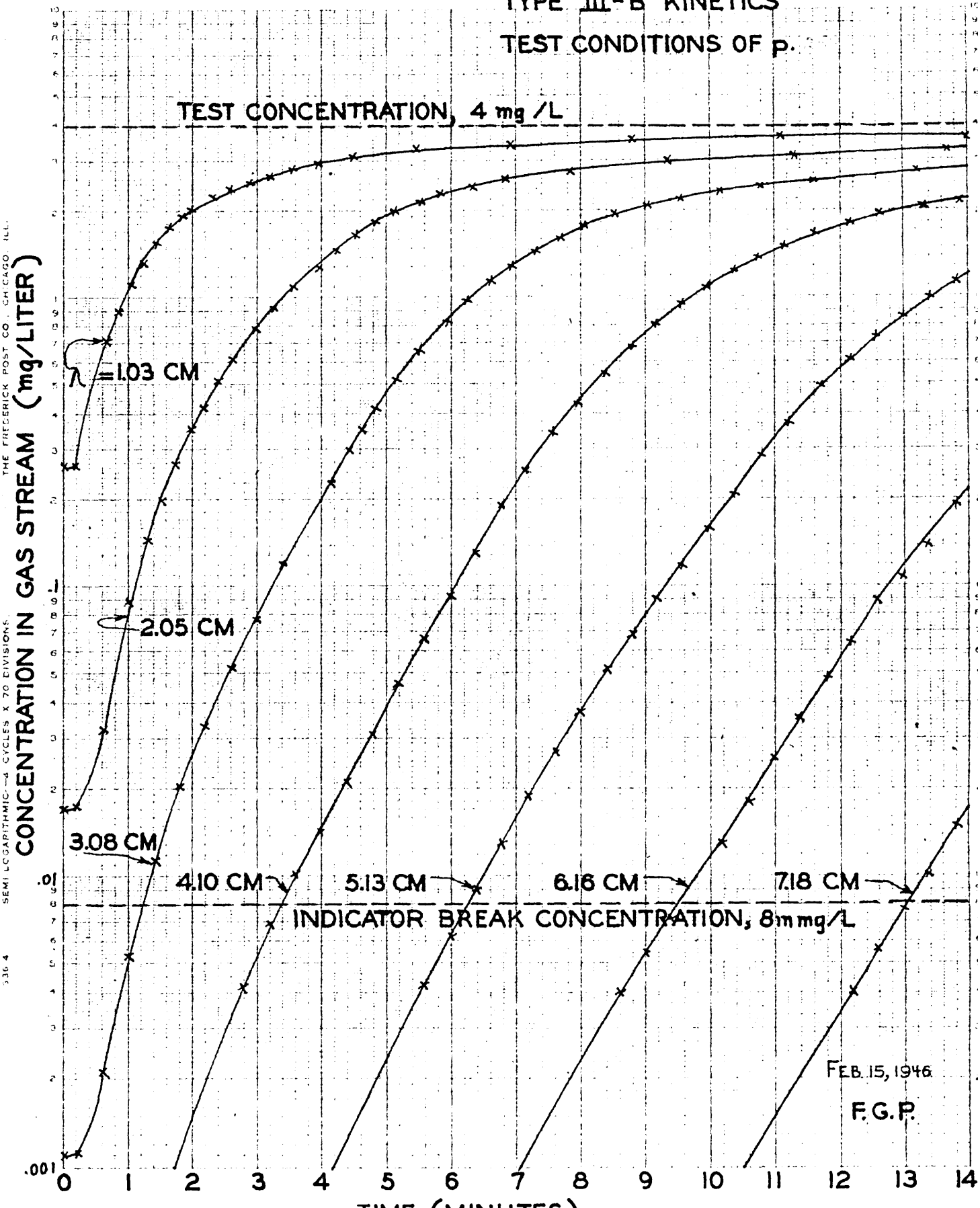

DECLASSIFIED

DECLASSIFIED

FIGURE 101

RELATIONSHIP BETWEEN BED DEPTH, TIME, AND CONCENTRATION OF AGENT ON ADSORBENT FOR TYPE III-B KINETICS

TEST CONDITIONS OF P. 264

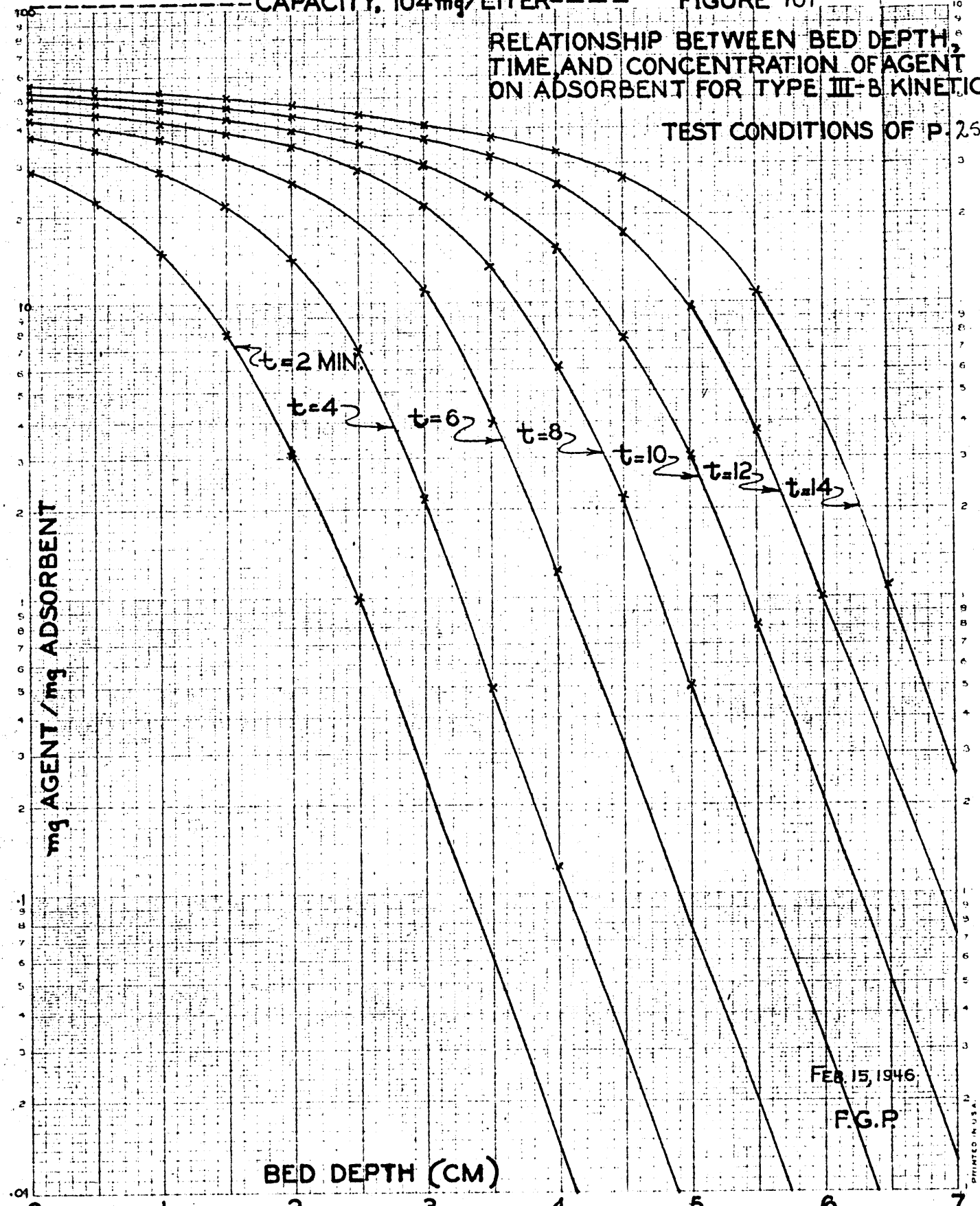

THE FREDERICK POST CO. CHICAGO, ILL.
336-4 SEMI-LOGARITHMIC—4 CYCLES X 70 DIVISIONS
PRINTED IN U.S.A.

CONFIDENTIAL
DECLASSIFIED

DECLASSIFIED

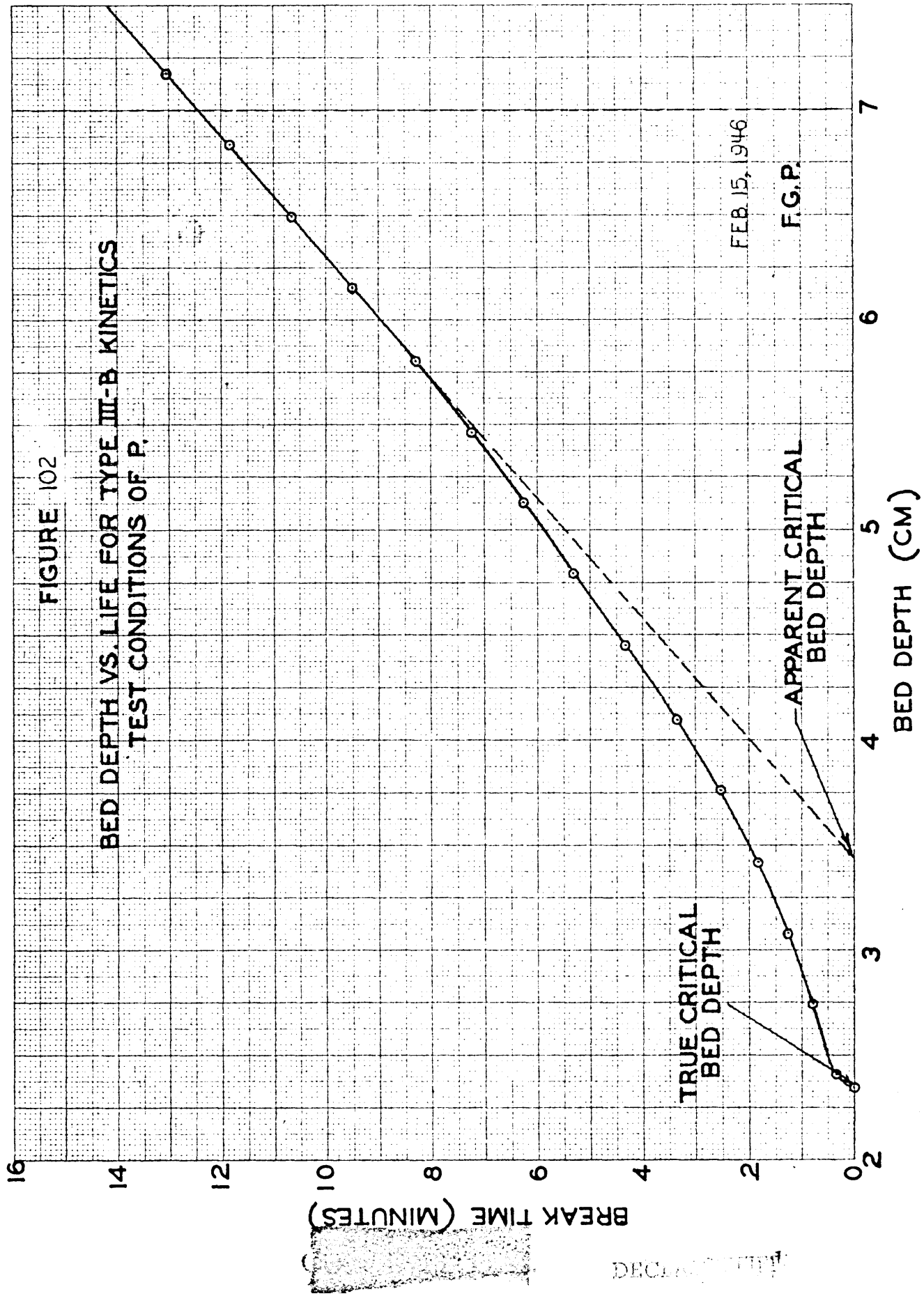

DECLASSIFIED

in Fig. 102 with the relationship predicted for Type I kinetics by Equation 1 is shown in Table XXXVII.

Table XXXVII

Correlation of Calculations for Type III-B Kinetics

N_o, Physical Adsorption Capacity at C_1	15.0	mg./ml.
$\frac{1000\ N_o}{C_1\ V}$	0.94	min./cm.
Slope of Lower, Straight Part of Curve	1.20	min./cm.
$N_o + N_r$	104	mg./ml.
$\frac{1000(N_o + N_r)}{C_1 V}$	6.5	min./cm.
Slope of Upper, Straight Part of Curve	3.5	min./cm.
Apparent Critical Bed Depth	3.45	cm.

It is seen that the slope of the linear, upper part of the bed depth-break time curve does not conform with the slope predicted by either Equation 1 or Equation 2. Since H_r is not a constant, there is no theoretical value for the apparent critical bed depth with which to correlate the observed value.

In summary, no simplified relationship between bed depth and break time was obtained for this type of kinetics. This classification is designated in this thesis as Type III-B kinetics.

A plot was made of the apparent critical bed depth as a function of the logarithm of the ratio of the influent to the effluent concentration from the calculated values of C_2 as a function of time and bed depth shown in Fig. 100. This plot (Fig. 103) shows

DECLASSIFIED

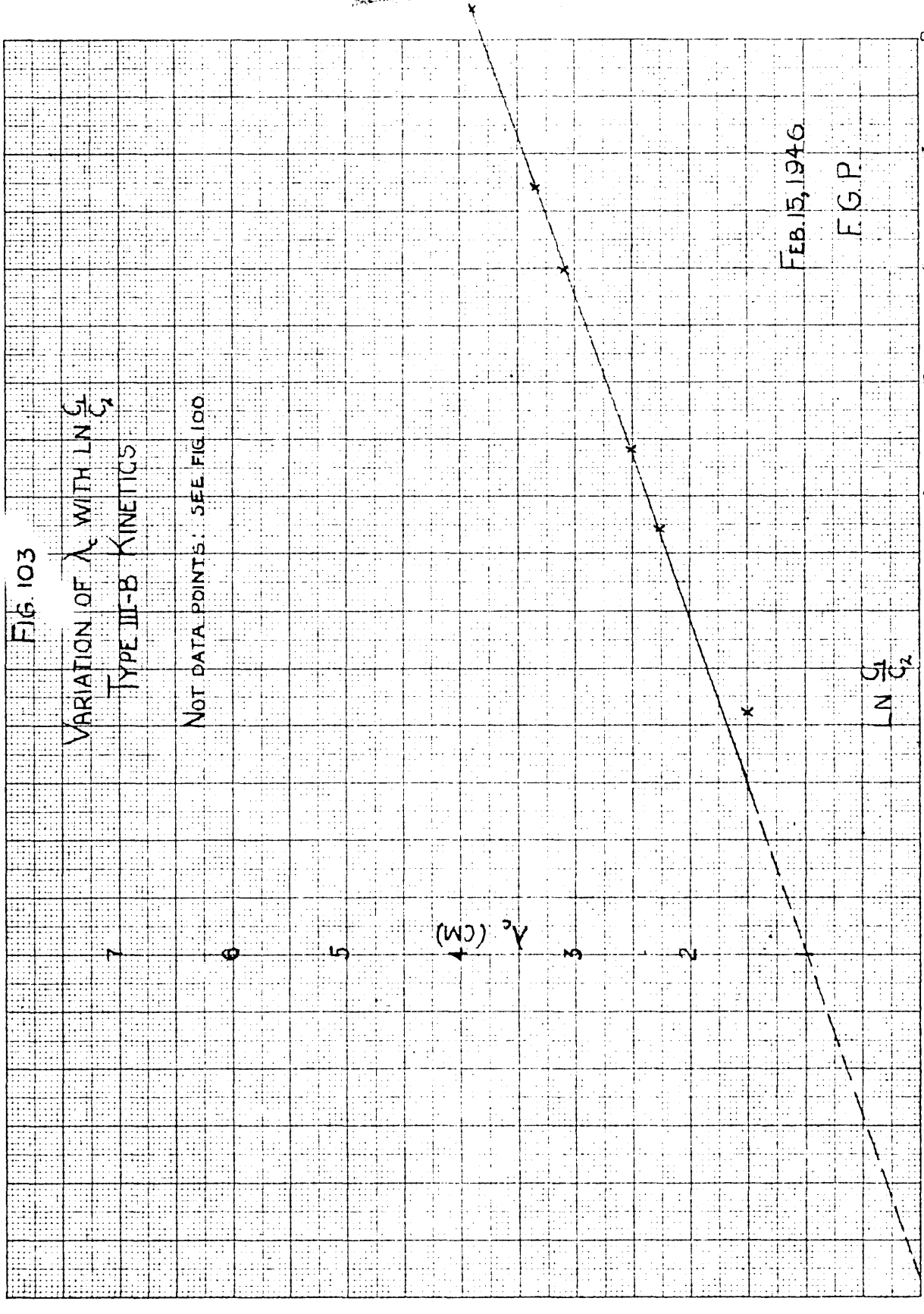

DECLASSIFIED

that a linear relationship exists as with all other types of kinetics but that the intercept lies at a negative value of $\ln \frac{C_1}{C_2}$ of 3.0. It is to be recalled that for all other types of kinetics this intercept falls between zero and unity. Therefore, it may be considered that, for Type III-B kinetics, β is equal to -3.0.

Wiig conducted one test under the conditions for which the foregoing computations were made for an adsorbent bed depth of seven cm. and obtained a break time of 14 minutes to an effluent concentration of eight mmg./L. From Fig. 102, it is seen that a computed life of 12.5 minutes was obtained. This is in excellent agreement and further strengthens the assumptions made to enable the completion of the computations.

After this test, Wiig sectioned the adsorbent bed and analyzed for agent content. His results, as compared with the calculated results, are shown in Fig. 104. Actually, the agreement is believed to be better than indicated, for in this particular case there is an inconsistency in Wiig's data. In the fourteen minutes of test, 224 milligrams of CK were passed into the bed and practically 100 per cent of this was transferred to the adsorbent. The area under the curve representing Wiig's data only accounts for 196 mg. indicating that some error was made and that the ordinates should be greater. The area under the calculated curve accounts for the entire 224 milligrams. This would make the agreement between the experimental and calculated distribution of the

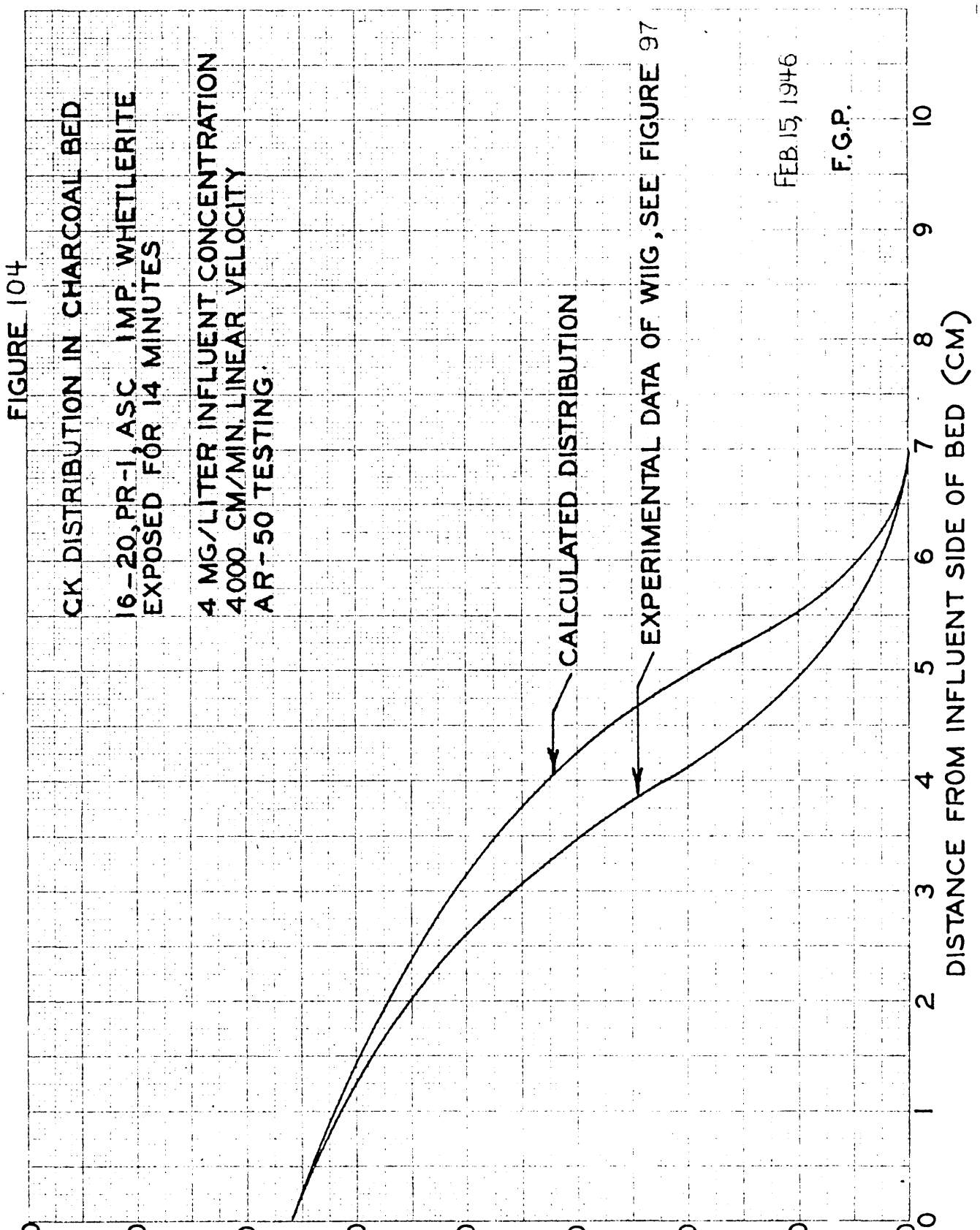

DECLASSIFIED

agent even closer.

This does not indicate that Wiig's data are unreliable, for all other data are remarkably consistent in that the material balances close.

It is interesting to note that if the error were caused by an incorrect, low influent concentration, the correct life would also be lower and would correct (on a linear scaling) to 12.3 minutes. This is almost identical with the calculated life of 12.5 minutes. The difference in the distribution curves is also as would be expected from a slightly low test concentration for the experimental data.

Klotz (53) made a very accurate measurement of break time vs. bed depth for the removal of CK by Type ASC impregnated whetlerite and obtained the data shown in Fig. 105. In these tests, break times were measured with an ultra-violet adsorption meter so that the lag associated with chemical (bubbler type) indicators was not obtained. The qualitative agreement between Figs. 103 and 105 is obvious.

C. Discussion of Computations

It has been shown that the removal of an agent from carrier streams can be segregated into at least three major classifications. These are as follows:

1. Type I Kinetics: Removal by reversible, physical adsorption when the rate of diffusion from the air stream to the surface of the adsorbent controls the overall rate of removal.

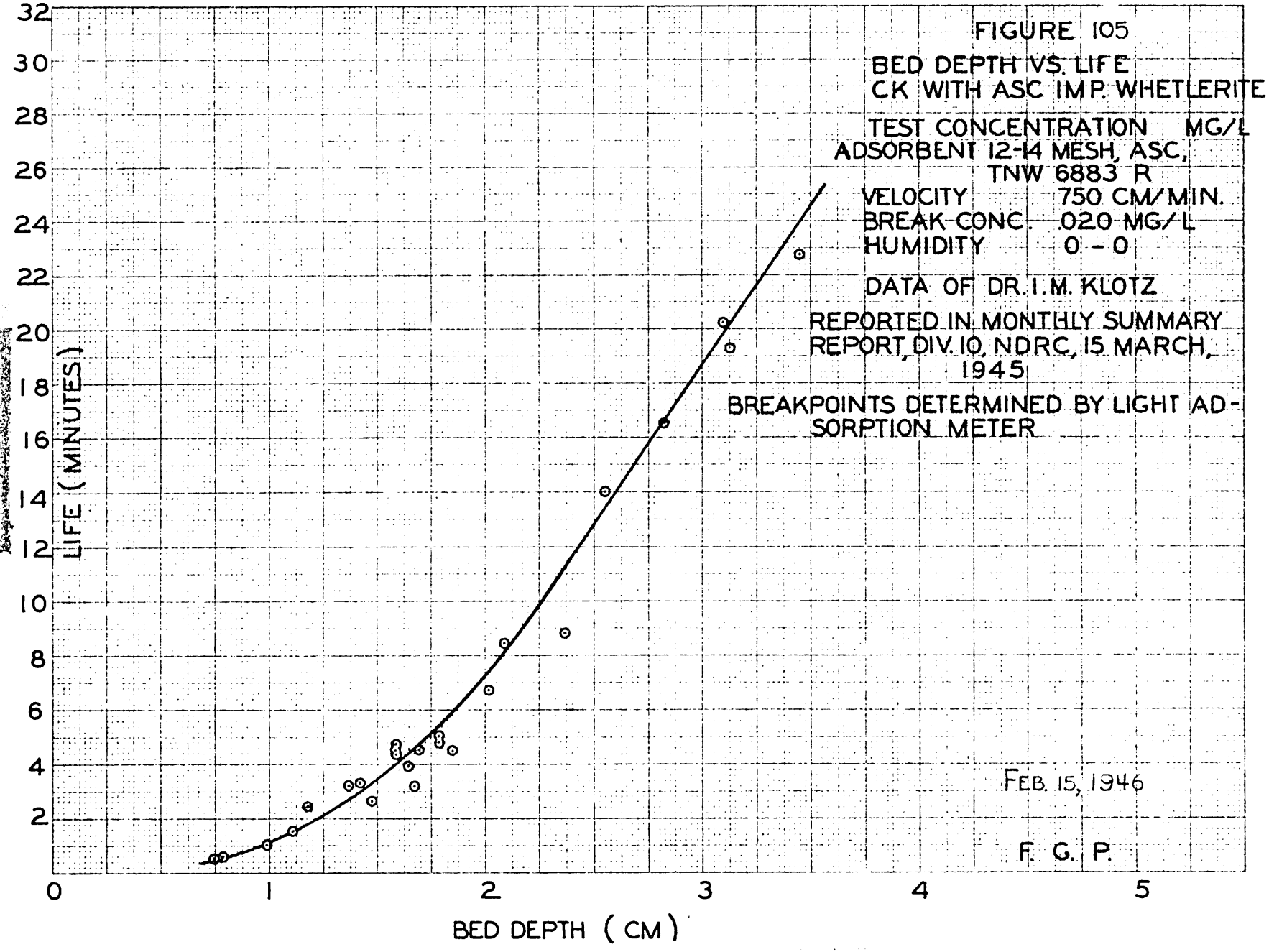

CONFIDENTIAL
DECLASSIFIED

2. Type II Kinetics: Removal by reversible, physical adsorption and by relatively rapid chemical reaction when the rate of diffusion from the air stream to the surface of the adsorbent controls the overall rate of removal.

3. Type III Kinetics: Removal by reversible, physical adsorption and by chemical reaction when the rate of chemical reaction is of the same magnitude as, or much slower than, the rate of diffusion from the air stream to the surface of the adsorbent.

It has been shown further that Type III kinetics may be subdivided into at least two distinct classifications. These are as follows:

1. Type III-A Kinetics: The rate of chemical reaction is independent of the previous utilization and is directly proportional to the partial pressure of the agent at the surface of the adsorbent.

2. Type III-B Kinetics: The rate of chemical reaction is an involved function of both the previous utilization of the adsorbent and the amount of unreacted agent on the adsorbent.

The computations showed that the bed depth-break time relationships are accurately represented for all these classifications, except Type III-B kinetics, by the following equation:

$$t = \frac{(N_o + N_r)}{C_1 V} \left[\lambda - (H_t + H_r)\left(\ln \frac{C_1}{C_2} - \beta\right) \right] \qquad (2)$$

Although Type III-B kinetics can not be correlated by this equation theoretically, the shape of the bed depth-break time curve (Fig. 103) suggests that an empirical equation of the same type might be found which would adequately represent the experimental data over a limited range of the variables. Such an equation might involve the replacement of $N_o + N_r$ by an experimentally determined constant and $H_t + H_r$ by another experimentally determined constant. An equation of this type would be extremely valuable in canister design.

It is interesting to note that, if Type I or Type II kinetics apply, the effects of velocity on the apparent critical bed depth are reflected by the effects of velocity on H_t. Since it was shown in Previous Work, III, that H_t varies as a fractional power of the velocity, λ_c can be expected to vary in the same manner.

However, if Type III-A kinetics apply, the effect of velocity on the apparent critical bed depth is reflected by the changes in both H_t and H_r. Since the chemical reaction rate function, $k_r a'$, can not be expected to change with velocity (verified by Wiig's data, Fig. 99), the velocity effect on H_r is shown directly by Equation 119: i.e., H_r should be directly proportional to velocity. Thus, for Type III kinetics, the apparent critical bed depth is proportional to the sum of (1) a term which varies as a fractional power of velocity and (2) a term which varies linearly with velocity.

DECLASSIFIED

APPENDIX F

THEORETICAL ADAPTATION OF EQUATIONS FOR BLENDS OF SEVERAL SIEVE FRACTIONS

A. General

It is practically impossible to obtain pure sieve fractions in commercial production, for it would entail a large loss of "off-size" material. The Chemical Warfare Service employs a sieve fraction blend which is classified as "12-30 mesh" whetlerite. Practically 100 per cent of the whetlerite passes through a No. 12 U.S. Standard screen and very little passes through a No. 30 screen.

Obviously, it would be impossible to test all the possible blends of the various standard sieve fractions between 12 and 30 sieve fractions (12, 16, 20, and 30 sieve fractions) to obtain the rate functions. The more practical approach is to obtain these functions for the pure sieve fractions and to interpolate, by a suitable equation, for blends of these separate fractions. The following is the derivation of a theoretical equation to allow such interpolation.

B. Derivation of Interpolation Equation for Mass Transfer Functions

The height of a transfer unit has been defined previously by the following equation:

$$Ht = \frac{V}{1000\ kga} \qquad (13)$$

If, in the limited range of the particle sizes em-

DECLASSIFIED

ployed, k_g may be considered to be constant, the only factor which affects the transfer rate is the area per unit volume of adsorbent, a. Therefore, for a blend of sieve fractions, the value of $k_g a$ would be equal to the product of k_g and the sum of the values of a for each pure sieve fraction multiplied by the fraction that sieve size is of the total. Expressed mathematically, this may be represented by the following equation:

$$k_g a = k_g(f_1 a_1 + f_2 a_2 + f_3 a_3 + \cdots f_n a_n) \quad (124)$$

Substituting this function into Equation 13, the following relationship is obtained:

$$H_t = \frac{V}{1000 k_g (f_1 a_1 + f_2 a_2 + \cdots\cdots f_n a_n)} \quad (125)$$

Taking the reciprocal of each side of Equation 125, the following equation is obtained:

$$1/H_t = \frac{1000k\ (f_1 a_1 + f_2 a_2 + \cdots\cdots f_n a_n)}{V} \quad (126)$$

Representing the height of a transfer unit for a particular sieve fraction as $(H_t)x$, Equation 126 resolves to the following expression:

$$1/H_t = f_1 \frac{1}{(H_t)_1} + f_2 \frac{1}{(H_t)_2} + \cdots f_n \frac{1}{(H_t)_n} \quad (127)$$

Taking the reciprocal of this equation, the relation-

ship between H_t for a blend of sieve fractions and the values of H_t for the individual sieve fractions is obtained. This relationship is expressed by the following equation:

$$H_t = \frac{1}{f_1 \frac{1}{(H_t)_1} + f_2 \frac{1}{(H_t)_2} + \ldots . f_n \frac{1}{(H_t)_n}} \qquad (128)$$

C. Effect of Sieve Fraction on Adsorptive Constant

The small amount of experimental data obtained to date (Mecklenberg's results) showed no effect of the sieve fraction on the capacity constant, N_o. This is in agreement with theory, for the small increase in surface area associated with a change in sieve fraction in the normal range is insignificant in comparison with the enormous surface areas of activated charcoals.

APPENDIX G

SUMMARIZED DATA

Table XXXVIII

Summarized Data

Whetlerite Designation	Sieve Fraction	Flow Rate	Type Canister	Char. Volume (ml.)	λ (cm)	Temp. (°F.)	Rel.Hum. (%)	C_1 (mg/L)	Break Times (min)	Std. Break (min)	Corr. Break (min)	Agent	Figure
Unimpreg. PCI Base, Drum No. 1	16-20	50 L./min., B.	M11	100	1.15	82	30	10.10	18,20	18	18	PS	15
	"	"	"	125	1.44	82	30	10.10	28,29	28	28	"	"
	"	"	"	150	1.73	76	30	10.00	40,41	40	40	"	"
	"	"	"	175	2.01	82	30	10.00	49,52,54	52	52	"	"
	"	"	"	200	2.30	80	30	10.00	47,54,57,59	57	57	"	"
	"	"	"	225	2.59	80	30	10.00	60,63,64	63	63	"	"
	"	"	"	250	2.87	79	31	10.00	72,74	72	72	"	"
HC3-361	16-20	50 L./min., B.	M11	115	1.32	81	50	10.00	24,25	24	24	PS	15
	"	"	"	115	1.32	82	50	10.00	23,24	23	23	"	"
	"	"	"	143	1.64	82	50	10.15	34,36	34	34	"	"
	"	"	"	143	1.64	79	50	10.30	31,33	31	32	"	"
	"	"	"	172	1.98	82	50	10.30	42,44	42	43	"	"
	"	"	"	172	1.98	80	50	10.15	41,43	41	42	"	"
	"	"	"	201	2.31	80	50	10.15	50,52	50	51	"	"
	"	"	"	201	2.31	80	50	10.00	51,54	51	51	"	"
	"	"	"	86	.99	82	50	10.15	13,15	13	13	"	"
Unimpreg. PCI Base, Drum No. 1	16-20	50 L./min., B.	M11	125	1.44	80	30	10.00	4,6	4	4	CG	16
	"	"	"	150	1.73	80	30	10.00	6,8	6	6	"	"
	"	"	"	175	2.01	80	30	10.00	5,8,9	8	8	"	"
	"	"	"	200	2.30	80	30	10.00	4,9,11	9	9	"	"
	"	"	"	225	2.59	80	30	10.00	10,12	10	10	"	"
	"	"	"	250	2.88	80	30	10.00	13,15	13	13	"	"
HC3-361	16-20	50 L./min., B.	M11	143	1.64	75	50	9.90	13,14	13	13	CG	16
	"	"	"	143	1.64	78	50	10.10	11,13	11	11	CG	"
	"	"	"	143	1.64	80	50	10.20	11,13	11	11	"	"

DECLASSIFIED
DECLASSIFIED

Table XXXVIII (Continued)

Whetlerite Designation	Sieve Fraction	Flow Rate	Type Canister	Char. Volume (ml)	λ (cm)	Temp. (°F)	Rel.Hum. (%)	C_l (mg/L)	Break Times (min)	Std. Break (min)	Corr. Break (min)	Agent	Figure
HC3-361	16-20	50 L./min., B.	M11	205	2.36	75	50	9.90	21,23	21	21	CG	16
	"	"	"	205	2.36	75	50	10.30	22,24	22	23	"	"
	"	"	"	205	2.36	75	50	10.30	23,24	23	24	"	"
	"	"	"	272	3.12	76	50	10.20	35,36	35	36	"	"
	"	"	"	272	3.12	75	50	10.30	36,38	36	37	"	"
	"	"	"	272	3.12	75	50	10.20	36,38	36	37	"	"
	"	"	"	334	3.84	76	50	10.20	57,59	57	58	"	"
	"	"	"	334	3.84	77	50	10.20	56,58	56	57	"	"
	"	"	"	334	3.84	75	50	10.30	54,56	54	56	"	"
Unimpreg. PCI Base, Drum No. 1	16-20	50 L./min., B.	M11	150	1.72	80	29	4.05	4.8,5.5	4.8	4.8	CK	17
	"	"	"	175	2.01	80	29	4.05	6.5,7.5	6.5	6.5	"	"
	"	"	"	200	2.30	80	29	4.05	7.2,8.5	7.2	7.2	"	"
	"	"	"	225	2.59	80	229	4.05	8.5,9.5	8.5	8.5	"	"
	"	"	"	250	2.87	80	29	4.05	9.8,11	9.8	9.8	"	"
	"	"	"	275	3.16	80	29	4.05	11,12.2	11	11	"	"
	"	"	"	300	3.45	79	30	4.05	13,15	13	13	"	"
HC3-361	16-20	50 L./min., B.	M11	143	1.64	76	50	4.23	10,13	10	11	CK	17
	"	"	"	143	1.64	74	50	4.00	11,13	11	11	"	"
	"	"	"	143	1.64	71	50	4.15	10,11	10	10	"	"
	"	"	"	143	1.64	76	50	4.06	10,12	10	10	"	"
	"	"	"	143	1.64	76	50	4.06	10,12	10	10	"	"
	"	"	"	205	2.36	76	50	4.23	21,23	21	22	"	"
	"	"	"	205	2.36	72	50	4.15	23,25	23	24	"	"
	"	"	"	205	2.36	71	50	4.13	19,21	19	20	"	"
	"	"	"	205	2.36	76	50	4.06	19,24,26	24	24	"	"
	"	"	"	205	2.36	76	50	4.06	23,25	23	23	"	"
	"	"	"	272	3.12	76	50	4.00	26,32,35	32	32	"	"
	"	"	"	272	3.12	72	50	4.15	28,33,35	33	34	"	"
	"	"	"	272	3.12	71	50	4.13	26,30,33	30	31	"	"
	"	"	"	272	3.12	75	50	4.12	35,38	35	36	"	"
	"	"	"	272	3.12	75	50	4.12	37,40	37	38	"	"

DECLASSIFIED

Table XXXVIII (Continued)

Whetlerite Designation	Sieve Fraction	Flow Rate	Type Canister	Char. Volume (ml)	λ (cm)	Temp. (°F.)	Rel.Hum. (%)	C_l (mg/L)	Break Times (min)	Std. Break (min)	Corr. Break (min)	Agent	Figure
HC3-361	16-20	50 L./min., B.	M11	334	3.84	74	50	4.00	47,55,58	55	55	CK	17
	"	"	"	334	3.84	72	50	4.14	53,56	53	55	"	"
	"	"	"	334	3.84	72	50	4.13	50,53	50	52	"	"
	"	"	"	334	3.84	73	50	4.00	47,51,54	51	51	"	"
Unimpreg. PCI Base, Drum No. 1	16-20	50 L./min., B.	M11	125	1.44	73	30	4.25	1.1,1.3	1.1	1.2	AC	18
	"	"	"	150	1.73	73	30	4.20	1.4,1.5	1.4	1.5	"	"
	"	"	"	175	2.01	73	30	4.20	1.5,1.7	1.5	1.6	"	"
	"	"	"	200	2.30	73	30	4.20	1.8,2.5	1.8	1.9	"	"
	"	"	"	225	2.59	73	30	4.05	2.5,3	2.5	2.5	"	"
	"	"	"	250	2.87	74	30	4.05	3,3.2	3	3	"	"
HC3-361	16-20	50 L./min., B.	M11	143	1.64	77	50	4.20	9,10	9	9	AC	18
	"	"	"	143	1.64	77	50	4.20	9,11	9	9	"	"
	"	"	"	205	2.36	77	50	4.20	16,21,23	21	22	"	"
	"	"	"	205	2.36	77	50	4.20	14,19,21	19	20	"	"
	"	"	"	272	3.13	77	50	4.20	33,37,38	37	39	"	"
	"	"	"	272	3.13	77	50	4.20	26,37,38	37	39	"	"
	"	"	"	334	3.84	72	50	4.00	42,46,48	46	46	"	"
	"	"	"	334	3.84	76	50	3.94	43,48,50	48	47	"	"
Unimpreg. PCI Base, Drum No. 1	16-20	50 L./min., B.	M11	125	1.44	75	30	10.23	1,1.2	1	1	SA	19
	"	"	"	150	1.73	75	30	10.28	1.2,1.4	1.2	1.2	"	"
	"	"	"	175	2.01	75	30	10.28	1.5,1.7	1.5	1.5	"	"
	"	"	"	200	2.30	75	30	10.28	1.7,2.2	1.7	1.7	"	"
	"	"	"	225	2.59	75	30	10.28	2.1,2.3	2.1	2.2	"	"
	"	"	"	250	2.87	75	30	10.28	2.2,2.4	2.2	2.3	"	"
HC3-361	16-20	50 L./min., B.	M11	134	1.54	77	50	4.25	15,17	15	16	SA	19
	"	"	"	134	1.54	75	50	4.25	17,19	17	18	"	"

DECLASSIFIED

DECLASSIFIED

Table XXXVIII (Continued)

Whetlerite Designation	Sieve Fraction	Flow Rate	Type Canister	Char. Volume (ml)	λ (cm)	Temp. (°F)	Rel.Hum. (%)	C_l (mg/L)	Break Times (min)	Std. Break (min)	Corr. Break (min)	Agent	Figure
HC3-361	16-20	50 L./min., B.	M11	153	1.76	77	50	4.25	21,24	21	22	SA	19
	"	"	"	153	1.76	75	50	4.05	23,27,28	27	27	"	"
	"	"	"	182	2.09	75	50	4.05	34,38,41	38	38	"	"
	"	"	"	182	2.09	75	50	4.05	35,39,42	39	39	"	"
	"	"	"	210	2.42	76	50	4.11	51,56,59	56	57	"	"
	"	"	"	210	2.42	76	50	4.11	50,55,58	55	56	"	"
Unimpreg. PCI Base, Drum No. 2	12-16	32 L./min., C.F.	M11	100	1.15	75	0	65.1	7,8	7	7	PS	21
	"	"	"	100	1.15	75	0	65.1	6.5,7.5	6.5	6.5	"	"
	"	"	"	150	1.73	75	0	65.1	16,18	16	16	"	"
	"	"	"	150	1.73	75	0	65.1	15,16	15	15	"	"
	"	"	"	200	2.30	75	0	65.3	24,25	24	24	"	"
	"	"	"	200	2.30	75	0	65.3	24,26	24	24	"	"
	"	"	"	250	2.87	75	0	65.3	32,34	32	32	"	"
	"	"	"	250	2.87	75	0	65.3	33,35	33	33	"	"
HC3-361	16-20	32 L./min., C.F.	M11	52.5	.60	86	50	10.48	9,10	9	9	PS	22
	"	"	"	52.5	.60	86	50	10.48	9,10	9	9	"	"
	"	"	"	76.5	.88	86	50	10.48	17,19	17	18	"	"
	"	"	"	76.5	.88	86	50	10.48	17,20	17	18	"	"
	"	"	"	96.5	1.11	90	45	10.32	32.2,35	32	33	"	"
	"	"	"	96.5	1.11	90	45	10.32	32.2,35	32	33	"	"
	"	"	"	134	1.54	86	50	10.48	49,51	49	51	"	"
	"	"	"	134	1.54	86	50	10.48	54,57	54	56	"	"
HC3-361	16-20	64 L./min., C.F.	M11	99	1.14	82	50	10.00	15,16	15	15	PS	22
	"	"	"	154	1.77	82	50	10.00	26,28	26	26	"	"
	"	"	"	209	2.40	82	50	10.00	45,47	45	45	"	"
	"	"	"	264	3.04	83	50	10.10	60.5,62	60.5	61	"	"

DECLASSIFIED
DECLASSIFIED

Table XXXVIII (Continued)

Whetlerite Designation	Sieve Fraction	Flow Rate	Type Canister	Char. Volume (ml)	λ (cm)	Temp. (°F)	Rel.Hum. (%)	C_l (mg/L)	Break Times (min)	Std. Break (min)	Corr. Break (min)	Agent	Figure
HC3-361	12-16	50 L./min., B.	M11	172	1.98	79	50	10.15	42,43	42	42	PS	23
	"	"	"	172	1.98	82	50	10.00	37,41,42	41	41	"	"
	"	"	"	196	2.26	82	50	10.15	48,49	48	49	"	"
	"	"	"	196	2.26	82	50	10.15	47,49	47	48	"	"
	"	"	"	225	2.59	79	50	10.20	56,58	56	57	"	"
	"	"	"	225	2.59	83	50	10.00	58,60	58	58	"	"
	"	"	"	248	2.85	84	50	10.00	67,69	67	67	"	"
	"	"	"	248	2.85	84	50	10.10	66,68	66	66	"	"
	"	"	"	134	1.54	79	50	10.00	24,26	24	24	"	"
	"	"	"	98	1.13	80	50	10.00	11,12	11	11	"	"
HC3-361	20-30	50 L./min., B.	M11	91	1.05	82	50	10.15	18,20	18	18	PS	23
	"	"	"	91	1.05	84	50	10.10	19,20	19	19	"	"
	"	"	"	119	1.37	79	50	10.20	26,28	26	27	"	"
	"	"	"	119	1.37	80	50	10.30	26,28	26	27	"	"
	"	"	"	148	1.70	81	50	10.00	39,41	39	39	"	"
	"	"	"	148	1.70	80	50	10.30	38,40	38	39	"	"
	"	"	"	172	1.98	81	50	10.00	46,48	46	46	"	"
	"	"	"	172	1.98	80	50	10.30	45,47	45	46	"	"
	"	"	"	76	.87	82	50	10.15	13,15	13	13	"	"
AD3-255	12-30	50 L./min., B.	M11	86	.99	95	50	10.00	7,9	7	7	PS	24
	"	"	"	86	.99	88	50	10.10	7,9	7	7	"	"
	"	"	"	129	1.48	87	50	10.10	19,21	19	19	"	"
	"	"	"	129	1.48	90	50	10.30	20,21	20	21	"	"
	"	"	"	172	1.98	90	50	10.30	33,35	33	34	"	"
	"	"	"	172	1.98	90	50	10.30	31,33	31	32	"	"
	"	"	"	210	2.41	89	50	10.10	41,43	41	41	"	"
	"	"	"	210	2.41	89	50	10.30	43,45	43	44	"	"

DECLASSIFIED

Table XXXVIII (Continued)

Whetlerite Designation	Sieve Fraction	Flow Rate	Type Canister	Char. Volume (ml)	λ (cm)	Temp. (°F)	Rel.Hum. (%)	C_l (mg/L)	Break Times (min)	Std. Break (min)	Corr. Break (min)	Agent	Figure
MIT3-4713	12-30	50 L./min., B.	M11	86	.99	88	50	10.40	14,16	14	15	PS	24
	"	"	"	86	.99	88	50	10.40	14,15	14	15	"	"
	"	"	"	129	1.48	88	50	10.40	31,33	31	32	"	"
	"	"	"	129	1.48	89	50	10.40	29,31	29	30	"	"
	"	"	"	172	1.98	89	50	10.30	48,49	48	49	"	"
	"	"	"	172	1.98	90	50	10.00	46,48	46	46	"	"
	"	"	"	210	2.41	85	50	10.00	61,62	61	61	"	"
	"	"	"	210	2.41	84	50	9.21	65,67	65	60	"	"
HC3-361	12-30	50 L./min., B.	M11	86	.99	89	50	10.15	14,16	14	14	PS	24
	"	"	"	86	.99	89	50	10.15	13,15	13	13	"	"
	"	"	"	129	1.48	90	50	10.15	23,25	23	23	"	"
	"	"	"	129	1.48	91	50	10.15	25,27	25	25	"	"
	"	"	"	172	1.98	92	50	10.00	47,48	47	47	"	"
	"	"	"	172	1.98	86	50	10.20	46,47	46	47	"	"
	"	"	"	210	2.41	93	50	10.00	53,57,59	57	57	"	"
	"	"	"	210	2.41	85	50	9.89	58,60	58	57	"	"
CC3-900	12-30	50 L./min., B.	M11	90	1.03	85	50	9.90	10,12	10	10	"	"
	"	"	"	135	1.55	85	50	9.90	28,29	28	28	"	"
	"	"	"	180	2.07	84	50	9.90	45,46	45	45	"	"
	"	"	"	220	2.53	83	50	9.95	65,67	65	64	"	"
	"	"	"	270	3.10	78	50	10.18	84,86	85	86	"	"
HC3-361	16-20	50 L./min., B.	M11	105	1.21	78	50	10.20	16,18	16	16	CG	25
	"	"	"	105	1.21	78	50	10.20	17,19	17	17	"	"
	"	"	"	143	1.64	78	50	10.45	29,31	29	30	"	"
	"	"	"	143	1.64	78	50	10.45	27,29	27	28	"	"
	"	"	"	186	2.14	78	50	10.50	43,44	43	45	"	"

DECLASSIFIED

DECLASSIFIED

Table XXXVIII (Continued)

Whetlerite Designation	Sieve Fraction	Flow Rate	Type Canister	Char. Volume (ml)	λ (cm)	Temp. (°F)	Rel.Hum. (%)	C_1 (mg/L)	Break Times (min)	Std. Break (min)	Corr. Break (min)	Agent	Figure
HC3-361	16-20	50 L./min., B.	M11	186	2.14	78	50	10.50	44,46	44	46	CG	25
	"	"	"	239	2.75	78	50	10.40	61,63	61	63	"	"
	"	"	"	239	2.75	78	50	10.40	59,60	59	61	"	"
HC3-361	16-20	32 L./min., C.F.	E2R3	105	1.60	80	50	10.40	15,17	15	16	CG	25
	"	"	"	105	1.60	80	50	10.40	16,18	16	17	"	"
	"	"	"	143	2.18	78	50	10.10	32,34	32	32	"	"
	"	"	"	143	2.18	78	50	10.10	33,35	33	33	"	"
	"	"	"	186	2.84	76	50	10.40	43,45	43	45	"	"
	"	"	"	186	2.84	76	50	10.40	42,44	42	44	"	"
	"	"	"	239	3.66	79	50	10.10	60,62	60	61	"	"
	"	"	"	239	3.66	79	50	10.10	59,61	59	60	"	"
HC3-361	16-20	64 L./min., C.F.	M11	172	1.98	76	50	9.95	18,20	18	18	CG	25
	"	"	"	172	1.98	76	50	9.95	19,21	19	19	"	"
	"	"	"	224	2.57	76	50	10.30	28,30	28	29	"	"
	"	"	"	224	2.57	76	50	10.10	27,29	27	27	"	"
	"	"	"	277	3.18	76	50	10.50	34,36	34	36	"	"
	"	"	"	277	3.18	76	50	10.30	35,37	35	36	"	"
	"	"	"	334	3.84	76	50	10.20	48,50	48	49	"	"
	"	"	"	334	3.84	76	50	10.10	49,51	49	49	"	"
HC3-361	16-20	64 L./min., C.F.	E2R3	158	2.41	78	50	10.40	15,17	15	16	CG	25
	"	"	"	158	2.41	78	50	10.40	15,17	15	16	"	"
	"	"	"	210	3.20	78	50	10.30	20,25,26	25	26	"	"
	"	"	"	210	3.20	78	50	10.30	23,25	23	24	"	"
	"	"	"	268	4.09	81	50	10.10	33,35	33	33	"	"
	"	"	"	268	4.09	81	50	10.20	32,34	32	33	"	"
	"	"	"	334	5.10	81	50	10.20	45,47	45	46	"	"
	"	"	"	334	5.10	78	50	10.30	42,47,49	47	48	"	"

DECLASSIFIED
DECLASSIFIED

Table XXXVIII (Continued)

Designation	Fraction	Flow Rate	Type Canister	Char. Volume (ml)	λ (cm)	Temp. (°F)	Rel.Hum. (%)	C_1 (mg/L)	Break Times (min)	Std. Break (min)	Corr. Break (min)	Agent	Figure
HC3-361	16-20	50 L./min., B.	E2R3	158	2.42	76	50	9.83	11,14	11	11	CG	25
	"	"	"	158	2.42	76	50	9.83	18,19	18	18	"	"
	"	"	"	210	3.21	78	49	10.05	21,23	21	21	"	"
	"	"	"	210	3.21	78	49	10.05	24,25	24	24	"	"
	"	"	"	287	4.39	74	50	9.90	34,36	34	34	"	"
	"	"	"	287	4.39	74	50	9.90	38,41	38	38	"	"
	"	"	"	334	5.10	73	51	10.20	46,49	46	47	"	"
	"	"	"	334	5.10	73	51	10.20	49,52	49	50	"	"
HC3-361	16-20	32 L./min., C.F.	M11	105	1.21	75	50	4.04	10,11	10	10	CK	26
	"	"	"	105	1.21	75	50	4.04	9,11	9	9	"	"
	"	"	"	175	2.01	77	51	3.97	24,25	24	24	"	"
	"	"	"	175	2.01	76	51	3.97	22,23	22	22	"	"
	"	"	"	235	2.70	78	49	4.00	37,40	37	37	"	"
	"	"	"	235	2.70	79	50	4.00	37,39	37	37	"	"
	"	"	"	295	3.40	79	50	4.01	50,57,59	57	57	"	"
	"	"	"	295	3.40	79	50	4.01	48,52,55	52	52	"	"
HC3-361	16-20	64 L./min., C.F.	M11	150	1.72	74	50	3.98	9,10	9	9	CK	26
	"	"	"	200	2.30	74	50	3.94	20,21	20	20	"	"
	"	"	"	245	2.82	74	50	4.00	30,31	30	30	"	"
	"	"	"	305	3.51	74	50	4.01	40,41	40	40	"	"
HC3-361	16-20	32 L./min., C.F.	M11	86	.99	77	50	4.02	10,11	10	10	AC	27
	"	"	"	86	.99	77	50	4.02	10,11	10	10	"	"
	"	"	"	124	1.43	78	50	4.02	19,20	19	19	"	"
	"	"	"	124	1.43	78	50	4.02	17,20	17	17	"	"
	"	"	"	162	1.86	80	50	3.92	30,32	30	29	"	"
	"	"	"	162	1.86	80	50	3.92	27,32,34	32	31	"	"
	"	"	"	201	2.31	81	50	3.92	35,44,46	44	42	"	"
	"	"	"	201	2.31	81	50	3.92	32,44,46	44	42	"	"

DECLASSIFIED
DECLASSIFIED

Table XXXVIII (Continued)

Whetlerite Designation	Sieve Fraction	Flow Rate	Type Canister	Char. Volume (ml)	λ (cm)	Temp. (° F)	Rel.Hum. (%)	C_1 (mg/L)	Break Times (min)	Std. Break (min)	Corr. Break (min)	Agent	Figure
HC3-361	16-20	64 L./min.,C.F.	M11	141	1.62	91	50	4.05	9,10	9	9	AC	27
	"	"	"	204	2.34	91	50	4.05	19,20	19	19	"	"
	"	"	"	270	3.10	91	50	3.99	29,31	29	29	"	"
	"	"	"	335	3.86	91	50	4.19	34,36	34	36	"	"
HC3-361	12-16	50 L./min., B.	M11	215	2.47	80	50	10.20	17,18	17	17	CG	29
	"	"	"	215	2.47	77	50	10.20	17,19	17	17	"	"
	"	"	"	272	3.12	78	50	10.20	26,28	26	27	"	"
	"	"	"	272	3.12	77	50	10.20	26,28	26	27	"	"
	"	"	"	339	3.90	78	50	10.20	42,44	42	43	"	"
	"	"	"	339	3.90	78	50	10.20	43,45	43	44	"	"
	"	"	"	401	4.60	78	50	10.20	55,57	55	56	"	"
	"	"	"	401	4.60	78	50	10.20	56,58	56	57	"	"
HC3-361	20-30	50 L./min., B.	M11	110	1.26	78	50	10.00	15,16	15	15	CG	29
	"	"	"	110	1.26	80	50	9.95	11,12	11	11	"	"
	"	"	"	110	1.26	73	50	10.20	11,12	11	11	"	"
	"	"	"	167	1.92	80	50	10.00	23,25	23	23	"	"
	"	"	"	167	1.92	73	50	9.90	21,23	21	21	"	"
	"	"	"	167	1.92	73	50	9.90	21,23	21	21	"	"
	"	"	"	239	2.74	80	50	9.95	35,37	35	35	"	"
	"	"	"	239	2.74	73	50	9.90	42,44	42	42	"	"
	"	"	"	239	2.74	75	50	9.90	41,42	41	41	"	"
	"	"	"	296	3.40	80	50	9.95	60,62	60	60	"	"
	"	"	"	296	3.40	74	50	10.20	50,52	50	51	"	"
	"	"	"	296	3.40	73	50	10.20	58,60	58	59	"	"
HC3-361	30-40	50 L./min., B.	M11	110	1.26	72	50	9.70	7,9	7	7	"	"
	"	"	"	110	1.26	72	50	9.70	6,8	6	6	"	"

DECLASSIFIED

DECLASSIFIED

Table XXXVIII (Continued)

Whetlerite Designation	Sieve Fraction	Flow Rate	Type Canister	Char. Volume (ml)	λ (cm)	Temp. (°F)	Rel.Hum. (%)	C_l (mg/L)	Break Times (min)	Std. Break (min)	Corr. Break (min)	Agent	Figure
HC3-361	30-40	50 L./min., B.	M11	153	1.76	75	50	10.10	22,24	22	22	CG	29
	"	"	"	153	1.76	75	50	10.10	19,21	19	19	"	"
	"	"	"	191	2.20	75	50	10.30	26,29	26	27	"	"
	"	"	"	191	2.20	75	50	10.30	25,28	25	26	"	"
	"	"	"	234	2.69	74	50	9.95	35,37	35	35	"	"
CC3-900	12-16	50 L./min., B.	M11	190	2.18	81	49	9.90	10,11	10	10	CG	30
	"	"	"	240	2.76	81	49	9.90	16,18	16	16	"	"
	"	"	"	280	3.22	82	49	9.90	23,25	23	23	"	"
	"	"	"	320	3.68	82	49	9.90	35,36	35	35	"	"
	"	"	"	370	4.26	80	48	10.12	45,47	45	46	"	"
CC3-900	16-20	50 L./min., B.	M11	150	1.73	83	50	9.95	12,13	12	12	CG	30
	"	"	"	200	2.30	83	50	9.95	19,20	19	19	"	"
	"	"	"	240	2.76	83	50	9.95	25,26	25	25	"	"
	"	"	"	290	3.34	83	50	9.95	39,41	39	39	"	"
	"	"	"	330	3.80	85	50	9.90	49,51	49	49	"	"
CC3-900	20-30	50 L./min., B.	M11	130	1.49	85	50	9.90	13,14	13	13	CG	30
	"	"	"	170	1.95	85	51	9.90	17,19	17	17	"	"
	"	"	"	220	2.53	87	49	9.68	35,37	35	34	"	"
	"	"	"	260	2.99	87	49	9.68	43,45	43	42	"	"
	"	"	"	300	3.45	88	49	9.68	51,52	51	49	"	"
CC3-900	30-40	50 L./min., B.	M11	110	1.27	78	52	9.95	15,16	15	15	CG	30
	"	"	"	150	1.73	78	52	9.95	25,27	25	25	"	"
	"	"	"	200	2.30	78	52	9.95	34,35	34	34	"	"
	"	"	"	240	2.76	78	52	9.95	40,42	40	40	"	"
	"	"	"	280	3.22	76	56	10.10	52,53	52	53	"	"

DECLASSIFIED

DECLASSIFIED

Table XXXVIII (Continued)

Whetlerite Designation	Sieve Fraction	Flow Rate	Type Canister	Char. Volume (ml)	λ (cm)	Temp. (°F)	Rel.Hum. (%)	C_1 (mg/L)	Break Times (min)	Std. Break (min)	Corr. Break (min)	Agent	Figure
HC3-361	12-16	50 L./min., B.	M11	215	2.47	75	50	4.01	17,20	17	17	CK	31
	"	"	"	215	2.47	74	50	3.92	13,15	13	13	"	"
	"	"	"	215	2.47	75	50	4.10	11,13	11	11	"	"
	"	"	"	272	3.13	75	50	4.01	26,29	26	26	"	"
	"	"	"	272	3.13	74	50	3.92	27,30	27	26	"	"
	"	"	"	272	3.13	75	50	4.10	27,30	27	28	"	"
	"	"	"	339	3.90	74	50	4.01	37,43,46	43	43	"	"
	"	"	"	339	3.90	74	50	3.92	40,44,47	44	43	"	"
	"	"	"	339	3.90	75	50	4.10	40,44,46	44	45	"	"
	"	"	"	401	4.61	74	50	4.01	53,59,62	59	59	"	"
	"	"	"	401	4.61	74	50	3.92	52,58,60	58	57	"	"
	"	"	"	401	4.61	75	50	4.10	47,54,57	54	55	"	"
HC3-361	20-30	50 L./min., B.	M11	110	1.27	72	50	4.13	7,8	7	7	CK	31
	"	"	"	110	1.27	74	50	4.11	5,7	5	5	"	"
	"	"	"	110	1.27	74	50	4.11	8,9	8	8	"	"
	"	"	"	167	1.92	72	50	4.13	18,20	18	19	"	"
	"	"	"	167	1.92	74	50	4.11	16,18	16	16	"	"
	"	"	"	167	1.92	74	50	3.82	17,19	17	16	"	"
	"	"	"	239	2.75	74	50	3.78	25,29,31	29	27	"	"
	"	"	"	239	2.75	74	50	4.11	30,32	30	31	"	"
	"	"	"	239	2.75	74	50	3.82	33,35	33	32	"	"
	"	"	"	296	3.40	74	50	3.93	32,40,43	40	39	"	"
	"	"	"	296	3.40	74	50	3.97	45,50,53	50	50	"	"
	"	"	"	296	3.40	74	50	3.82	48,51	48	46	"	"
HC3-361	12-16	50 L./min., B.	M11	215	2.47	74	50	3.78	20,22	20	19	AC	32
	"	"	"	215	2.47	74	50	4.00	17,20	17	17	"	"
	"	"	"	215	2.47	76	50	3.92	17,19	17	17	"	"
	"	"	"	215	2.47	76	50	3.92	16,18	16	16	"	"

DECLASSIFIED

DECLASSIFIED

Table XXXVIII (Continued)

Whetlerite Designation	Sieve Fraction	Flow Rate	Type Canister	Char. Volume (ml)	λ (cm)	Temp. (°F)	Rel.Hum. (%)	C_1 (mg/L)	Break Times (min)	Std. Break (min)	Corr. Break (min)	Agent	Figure
HC3-361	12-16	50 L./min., B.	M11	272	3.13	74	50	4.00	29,31	29	29	AC	32
	"	"	"	272	3.13	77	50	3.92	28,31	28	27	"	"
	"	"	"	272	3.13	77	50	3.92	28,30	28	27	"	"
	"	"	"	272	3.13	77	50	3.92	28,30	28	27	"	"
	"	"	"	339	3.90	77	50	3.92	41,44	41	40	"	"
	"	"	"	339	3.90	76	50	4.00	37,41,43	41	41	"	"
	"	"	"	401	4.61	74	50	3.98	51,53	51	51	"	"
	"	"	"	401	4.61	75	50	3.80	41,53	51	49	"	"
	"	"	"	401	4.61	76	50	4.17	39,49,50	49	51	"	"
	"	"	"	401	4.61	76	50	4.17	38,48,49	48	50	"	"
HC3-361	20-30	50 L./min., B.	M11	110	1.27	72	50	4.00	9,11	9	9	AC	32
	"	"	"	110	1.27	74	50	3.93	8,10	8	8	"	"
	"	"	"	167	1.92	74	50	3.93	12,14	12	12	"	"
	"	"	"	167	1.92	74	50	3.93	17,20	17	17	"	"
	"	"	"	239	2.75	74	50	3.93	33,35	33	32	"	"
	"	"	"	239	2.75	75	50	3.97	24,29,32	29	29	"	"
	"	"	"	296	3.40	76	50	3.94	38,44,47	44	43	"	"
	"	"	"	296	3.40	74	50	3.78	33,38,41	38	36	"	"
HC3-361	12-16	50 L./min., B.	M11	160	1.84	77	50	4.30	15,17	15	16	SA	33
	"	"	"	191	2.20	75	50	3.94	25,28	25	25	"	"
	"	"	"	215	2.47	75	50	3.94	32,37,39	37	36	"	"
	"	"	"	239	2.75	77	50	4.30	42,48,52,55	52	56	"	"
	"	"	"	272	3.13	77	50	4.30	55,63,68,71	68	73	"	"
HC3-361	20-30	50 L./min., B.	M11	110	1.27	77	50	4.25	15,18	15	16	SA	33
	"	"	"	110	1.27	76	50	4.05	15,18	15	15	"	"
	"	"	"	129	1.48	77	50	4.25	25,28	25	27	"	"
	"	"	"	129	1.48	76	50	4.05	26,29	26	26	"	"

DECLASSIFIED
DECLASSIFIED

Table XXXVIII (Continued)

Whetlerite Designation	Sieve Fraction	Flow Rate	Type Canister	Char. Volume (ml)	λ (cm)	Temp. (°F)	Rel.Hum. (%)	C_1 (mg/L)	Break Times (min)	Std. Break (min)	Corr. Break (min)	Agent	Figure
HC3-361	20-30	50 L./min., B.	M11	158	1.82	77	50	3.89	37,43,45	43	42	SA	33
	"	"	"	158	1.82	77	50	3.89	43,47,49	47	46	"	"
	"	"	"	191	2.20	77	50	4.10	65,74,78,80	78	80	"	"
	"	"	"	191	2.20	77	50	4.10	63,69,75,78	75	77	"	"
HC3-361	Blend B, Fig.34	50 L./min., B.	M11	196	2.25	74	48	9.95	22,24	22	22	CG	34
	"	"	"	196	2.25	74	48	9.95	22,24	22	22	"	"
	"	"	"	234	2.69	74	50	9.95	31,33	31	31	"	"
	"	"	"	234	2.69	74	50	9.95	31,32	31	31	"	"
	"	"	"	275	3.16	72	49	10.10	38,40	38	38	"	"
	"	"	"	275	3.16	72	49	10.10	40,42	40	40	"	"
	"	"	"	315	3.62	71	50	10.13	49,50	49	50	"	"
HC3-361	Blend C, Fig.34	50 L./min., B.	M11	134	1.54	83	49	10.25	9,10	9	9	CG	34
	"	"	"	177	2.04	83	49	10.25	16,18	16	16	"	"
	"	"	"	234	2.69	82	48	10.28	28,30	28	29	"	"
CC3-900	12-30	50 L./min., B.	M11	140	1.61	80	51	9.85	12,13	12	12	CG	35
	"	"	"	180	2.07	80	51	9.85	20,22	20	20	"	"
	"	"	"	230	2.64	79	52	9.95	28,29	28	28	"	"
	"	"	"	270	3.10	79	52	9.95	41,42	41	41	"	"
	"	"	"	310	3.56	80	51	9.85	51,54	51	50	"	"
HC3-361	12-30	50 L./min., B.	M11	139	1.60	81	49	10.28	10,11	10	10	CG	35
	"	"	"	139	1.60	81	49	10.28	11,12	11	11	"	"
	"	"	"	182	2.09	80	48	10.30	19,20	19	20	"	"
	"	"	"	182	2.09	80	48	10.30	20,21	20	21	"	"
	"	"	"	220	2.53	80	50	10.30	26,29	26	27	"	"
	"	"	"	220	2.53	80	50	10.30	26,28	26	27	"	"

DECLASSIFIED

DECLASSIFIED

Table XXXVIII (Continued)

Whetlerite Designation	Sieve Fraction	Flow Rate	Type Canister	Char. Volume (ml)	λ (cm)	Temp. (°F)	Rel.Hum. (%)	C_1 (mg/L)	Break Times (min)	Std. Break (min)	Corr. Break (min)	Agent	Figure
HC3-361	12-30	50 L./min., B.	M11	263	3.02	68	50	10.40	42,43	42	44	CG	35
	"	"	"	263	3.02	78	50	10.40	41,43	41	43	"	"
AD3-255	12-30	50 L./min., B.	M11	129	1.48	78	50	10.22	7,8	7	7	CG	35
	"	"	"	129	1.48	78	50	10.22	7,8	7	7	"	"
	"	"	"	162	1.86	78	50	10.22	15,16	15	15	"	"
	"	"	"	162	1.86	78	50	10.22	15,16	15	15	"	"
	"	"	"	196	2.26	77	50	10.22	23,25	23	24	"	"
	"	"	"	196	2.26	77	50	10.22	24,26	24	25	"	"
	"	"	"	230	2.64	77	50	10.15	33,35	33	33	"	"
	"	"	"	230	2.64	77	50	10.15	33,35	33	33	"	"
MIT3-4713	12-30	50 L./min., B.	M11	143	1.64	77	50	10.15	10,11	10	10	CG	35
	"	"	"	143	1.64	77	50	10.15	10,11	10	10	"	"
	"	"	"	186	2.14	77	50	10.50	17,18	17	18	"	"
	"	"	"	186	2.14	77	50	10.50	17,18	17	18	"	"
	"	"	"	229	2.64	77	48	10.34	25,26	25	26	"	"
	"	"	"	229	2.64	77	48	10.34	25,26	25	26	"	"
	"	"	"	268	3.08	76	50	10.02	30,32	30	30	"	"
	"	"	"	268	3.08	76	50	10.02	32,33	32	32	"	"
HC3-361	12-30	50 L./min., B.	M11	134	1.54	81	49	4.10	10,12	10	10	CK	36
	"	"	"	134	1.54	81	49	4.10	8,9	8	8	"	"
	"	"	"	177	2.03	82	49	4.10	16,18	16	16	"	"
	"	"	"	177	2.03	82	49	4.10	15,16	15	15	"	"
	"	"	"	220	2.53	82	50	3.93	27,30	27	26	"	"
	"	"	"	220	2.53	82	50	3.93	24,28,30	28	27	"	"
	"	"	"	263	3.02	85	48	3.93	32,37,39	37	36	"	"
	"	"	"	263	3.02	85	48	3.93	32,36,38	36	35	"	"

DECLASSIFIED
DECLASSIFIED

Table XXXVIII (Continued)

Whetlerite Designation	Sieve Fraction	Flow Rate	Type Canister	Char. Volume (ml)	λ (cm)	Temp. (°F)	Rel.Hum. (%)	C_1 (mg/L)	Break Times (min)	Std. Break (min)	Corr. Break (min)	Agent	Figure
AD3-255	12-30	50 L./min., B.	M11	134	1.54	85	48	4.08	8,9	8	8	CK	36
	"	"	"	134	1.54	85	48	4.08	7,9	7	7	"	"
	"	"	"	177	2.03	79	50	3.95	21,24	21	21	"	"
	"	"	"	177	2.03	79	50	3.95	19,22	19	19	"	"
	"	"	"	220	2.53	79	50	3.90	33,37,39	37	36	"	"
	"	"	"	220	2.53	79	50	3.90	33,36	33	32	"	"
	"	"	"	263	3.02	86	48	4.08	42,48,52,54	52	53	"	"
	"	"	"	263	3.02	86	48	4.08	41,46,49	46	47	"	"
CC3-900	12-30	50 L./min., B.	M11	140	1.61	82	50	3.84	11,12	11	11	CK	36
	"	"	"	180	2.07	82	50	3.84	20,22	20	19	"	"
	"	"	"	230	2.65	82	50	3.84	40,44,47	44	43	"	"
	"	"	"	270	3.10	81	50	3.97	58,65,68	65	64	"	"
	"	"	"	310	3.56	81	50	3.97	72,77,80	77	76	"	"
HC3-361	12-30	50 L./min., B.	M11	124	1.43	76	50	4.03	9,11	9	9	AC	37
	"	"	"	124	1.43	76	50	4.03	9,11	9	9	"	"
	"	"	"	167	1.92	78	50	4.07	18,20	18	18	"	"
	"	"	"	167	1.92	78	50	4.07	17,20	17	17	"	"
	"	"	"	210	2.42	78	50	4.07	20,24,27	24	24	"	"
	"	"	"	210	2.42	78	50	4.07	20,24,26	24	24	"	"
	"	"	"	258	2.97	81	50	3.96	19,36,38	36	36	"	"
	"	"	"	258	2.97	81	50	3.96	19,36,37	36	36	"	"
AD3-255	12-30	50 L./min., B.	M11	129	1.48	80	50	3.93	11,12	11	11	AC	37
	"	"	"	129	1.48	80	50	3.93	11,13	11	11	"	"
	"	"	"	172	1.98	80	50	3.97	20,22	20	20	"	"
	"	"	"	172	1.98	80	50	3.97	20,22	20	20	"	"

DECLASSIFIED
DECLASSIFIED

Table XXXVIII (Continued)

Whetlerite Designation	Sieve Fraction	Flow Rate	Type Canister	Char. Volume (ml)	λ (cm)	Temp. (°F)	Rel.Hum. (%)	C_1 (mg/L)	Break Times (min)	Std. Break (min)	Corr. Break (min)	Agent	Figure
AD3-255	12-30	50 L./min., B.	M11	215	2.47	78	50	4.00	30,32	30	30	AC	37
	"	"	"	215	2.47	78	50	4.00	32,35	32	32	"	"
	"	"	"	258	2.97	86	50	4.00	42,45	42	42	"	"
	"	"	"	258	2.97	86	50	4.00	42,45	42	42	"	"
	"	"	"	258	2.97	80	50	3.90	34,40,42	40	39	"	"
	"	"	"	258	2.97	80	50	3.90	34,40,42	40	39	"	"
CC3-900	12-30	50 L./min., B.	M11	140	1.61	78	50	3.93	13,14	13	13	AC	37
	"	"	"	140	1.61	85	50	4.08	13,14	13	13	"	"
	"	"	"	180	2.07	78	50	3.93	21,22	21	21	"	"
	"	"	"	180	2.07	85	50	4.08	21,22	21	21	"	"
	"	"	"	230	2.64	78	50	4.04	18,29,32	29	29	"	"
	"	"	"	230	2.64	85	50	4.08	29,32	29	30	"	"
	"	"	"	310	3.57	79	50	4.04	44,48,49	48	48	"	"
	"	"	"	310	3.57	85	50	4.05	42,51,53	51	52	"	"
HC3-361	12-30	50 L./min., B.	M11	124	1.43	81	50	3.63	16,19	16	15	SA	38
	"	"	"	124	1.43	81	50	3.63	18,21	18	16	"	"
	"	"	"	148	1.70	88	50	3.89	21,25,27	25	24	"	"
	"	"	"	148	1.70	88	50	3.89	24,28,30	28	27	"	"
	"	"	"	177	2.04	87	50	3.97	42,47,51,53	51	51	"	"
	"	"	"	177	2.04	87	50	3.97	42,47,50	47	47	"	"
	"	"	"	201	2.31	87	50	4.00	57,62,65	62	62	"	"
	"	"	"	201	2.31	87	50	4.00	55,59,61	59	59	"	"
AD3-255	12-30	50 L./min., B.	M11	124	1.43	81	50	3.91	11,13	11	11	SA	38
	"	"	"	124	1.43	81	50	3.91	10,12	10	10	"	"
	"	"	"	148	1.71	81	50	3.91	16,19	16	16	"	"
	"	"	"	148	1.71	81	50	3.91	15,18	15	15	"	"
	"	"	"	177	2.04	82	50	4.00	30,32	30	30	"	"
	"	"	"	177	2.04	82	50	4.00	30,32	30	30	"	"

DECLASSIFIED

Table XXXVIII (Continued)

Whetlerite Designation	Sieve Fraction	Flow Rate	Type Canister	Char. Volume (ml)	λ (cm)	Temp. (°F)	Rel.Hum. (%)	C_1 (mg/L)	Break Times (min)	Std. Break (min)	Corr. Break (min)	Agent	Figure
AD3-255	12-30	50 L./min., B.	M11	201	2.31	82	50	4.01	39,44,48,50	48	48	SA	38
	"	"	"	201	2.31	82	50	4.01	34,41,44	41	41	"	"
MIT3-4713	12-30	50 L./min., B.	M11	124	1.43	78	50	4.11	4,7	4	4	SA	38
	"	"	"	124	1.43	78	50	4.11	4,7	4	4	"	"
	"	"	"	148	1.71	78	50	4.11	9,14,16	14	14	"	"
	"	"	"	148	1.71	78	50	4.11	9,14,17	14	14	"	"
	"	"	"	177	2.04	80	50	3.91	21,28,32,35	32	31	"	"
	"	"	"	177	2.04	80	50	3.91	21,27,31,34	31	30	"	"
	"	"	"	201	2.31	81	50	3.65	34,42,47,50	47	43	"	"
	"	"	"	201	2.31	81	50	3.65	34,41,46,50, 53	50	45	"	"
HC3-361	12-16	50 L./min., B.	M11	172	1.98	79	50	10.15	*43	-	44	PS	39
	"	"	"	172	1.98	82	50	10.00	41	-	41	"	"
	"	"	"	196	2.26	82	50	10.15	49	-	50	"	"
	"	"	"	196	2.26	82	50	10.15	49	-	50	"	"
	"	"	"	225	2.59	79	50	10.20	58	-	59	"	"
	"	"	"	225	2.59	83	50	10.00	60	-	60	"	"
	"	"	"	248	2.85	84	50	10.00	69	-	69	"	"
	"	"	"	248	2.85	84	50	10.10	68	-	69	"	"
	"	"	"	134	1.54	79	50	10.00	26	-	26	"	"
	"	"	"	98	1.13	80	50	10.00	12	-	12	"	"
HC3-361	16-20	50 L./min., B.	M11	134	1.54	77	50	4.25	*20	-	21	SA	40
	"	"	"	134	1.54	75	50	4.05	22	-	22	"	"
	"	"	"	153	1.76	77	50	4.25	28	-	30	"	"
	"	"	"	153	1.76	75	50	4.05	29	-	29	"	"
	"	"	"	182	2.09	75	50	4.05	43	-	43	"	"

DECLASSIFIED

DECLASSIFIED

Table XXXVIII (Continued)

Whetlerite Designation	Sieve Fraction	Flow Rate	Type Canister	Char. Volume (ml)	λ (cm)	Temp. (°F)	Rel.Hum. (%)	C_l (mg/L)	Break Times (min)	Std. Break (min)	Corr. Break (min)	Agent	Figure
HC3-361	16-20	50 L./min., B.	M11	182	2.09	75	50	4.05	*44	-	44	SA	40
	"	"	"	210	2.42	76	50	4.11	61	-	63	"	"
	"	"	"	210	2.42	76	50	4.11	60	-	62	"	"
CC3-900	12-16	50 L./min., B.	M11	115	1.32	87	77	9.85	.8,1.2	.8	.8	PS	41
	"	"	"	160	1.84	87	81	9.85	2.5,3	2.5	2.5	"	"
	"	"	"	200	2.30	87	77	9.85	4.5,5.2	4.5	4.4	"	"
	"	"	"	250	2.87	87	77	9.85	8,9	8	8	"	"
	"	"	"	290	3.34	86	80	9.85	12,13	12	12	"	"
CC3-900	16-20	50 L./min., B.	M11	100	1.15	89	79	10.22	1.5,2	1.5	1.5	PS	41
	"	"	"	140	1.61	89	79	10.22	4.5,5	4.5	4.6	"	"
	"	"	"	185	2.13	90	80	10.22	8.5,9	8.5	8.7	"	"
	"	"	"	230	2.65	94	80	10.27	13,14	13	13	"	"
	"	"	"	270	3.11	94	80	10.27	19,20	19	20	"	"
CC3-900	20-30	50 L./min., B.	M11	85	.98	87	77	9.85	2.2,2.5	2.2	2.2	PS	41
	"	"	"	130	1.50	89	79	9.85	6.o,6.5	6.0	5.9	"	"
	"	"	"	170	1.96	89	79	10.22	8.8,9.5	8.8	9.0	"	"
	"	"	""	220	2.53	89	79	10.60	16,17	16	17	"	"
	"	"	"	260	2.99	89	79	10.60	22,23	22	23	"	"
CC3-900	30-40	50 L./min., B.	M11	75	.86	86	79	10.20	3.2,3.5	3.2	3.3	PS	41
	"	"	"	120	1.38	86	79	10.20	7,7.5	7	7.1	"	"
	"	"	"	165	1.90	86	81	9.75	11,12	11	11	"	"
	"	"	"	210	2.42	86	81	9.75	14,22,24	22	21	"	"
	"	"	"	250	2.87	86	81	10.20	27,28	27	28	"	"

DECLASSIFIED
DECLASSIFIED

Table XXXVIII (Continued)

Whetlerite Designation	Sieve Fraction	Flow Rate	Type Canister	Char. Volume (ml)	λ (cm)	Temp. (°F)	Rel.Hum. (%)	C_1 (mg/L)	Break Times (min)	Std. Break (min)	Corr. Break (min)	Agent	Figure
CC3-900	20-30	50 L./min., B.	M11	142	1.63	85	81	10.08	16,17	16	16	CG	42
	"	"	"	170	1.95	85	81	10.08	25,27	25	25	"	"
	"	"	"	217	2.49	83	83	9.80	37,38	37	36	"	"
	"	"	"	262	3.01	83	83	9.80	49.51	49	48	"	"
	"	"	"	300	3.45	82	81	10.20	56,58	56	57	"	"
CC3-900	12-16	50 L./min., B.	M11	175	2.01	82	80	4.17	1,1.5	1	1	CK	43
	"	"	"	220	2.53	82	80	4.17	1.2,2.2	1.2	1.2	"	"
	"	"	"	260	2.99	82	80	4.00	2.5,4.2	2.5	2.5	"	"
	"	"	"	306	3.52	82	80	4.00	5.2,7.8	5.2	5.2	"	"
	"	"	"	350	4.02	82	80	4.00	7,12,16,18	16	16	"	"
CC3-900	16-20	50 L./min., B.	M11	150	1.72	82	80	4.00	1.2,2.0	1.2	1.2	CK	43
	"	"	"	200	2.30	84	80	4.00	4.0,6.2	4.0	4.0	"	"
	"	"	"	240	2.76	84	80	4.00	9.5,11.5	9.5	9.5	"	"
	"	"	"	280	3.22	85	80	4.04	12,17,21,23	21	21	"	"
	"	"	"	330	3.79	85	80	4.04	25,35,43,48, 52,55	52	53	"	"
HH3-	16-20	50 L./min., B.	M11	125	1.44	77	50	3.92	8,9	8	8	AC	44
	"	"	"	150	1.72	78	50	4.05	12,14	12	12	"	"
	"	"	"	175	2.01	76	50	3.90	17,19	17	17	"	"
	"	"	"	200	2.30	76	50	4.20	22,26,27	26	27	"	"
	"	"	"	225	2.59	76	50	4.20	31,34	31	33	"	"
	"	"	"	250	2.87	75	50	4.04	39,41	39	39	"	"
	"	"	"	350	4.02	78	50	4.04	57,59	57	58	"	"
HH3-	16-20	50 L./min., B.	M11	125	1.44	74	80	4.04	9,11	9	9	AC	44
	"	"	"	150	1.72	73	80	4.08	14,16	14	14	"	"
	"	"	"	175	2.01	73	80	4.08	23,24	23	23	"	"
	"												

DECLASSIFIED

DECLASSIFIED

Table XXXVIII (Continued)

Whetlerite Designation	Sieve Fraction	Flow Rate	Type Canister	Char. Volume (ml)	λ (cm)	Temp. (°F)	Rel.Hum. (%)	C_1 (mg/L)	Break Times (min)	Std. Break (min)	Corr. Break (min)	Agent	Figure
HH3-	16-20	50 L./min., B.	M11	200	2.30	73	80	4.08	25,30,32	30	31	AC	44
	"	"	"	250	2.87	75	80	4.02	33,39,41	39	39	"	"
	"	"	"	350	4.02	76	80	4.16	50,65,69,70	69	72	"	"

* Indicated cumulative penetrations.

Standard Break Concentrations

Agent	Break Concentration (mmg./L.)
PS	20
CG	8
CK	8
AC	4
SA	14

Cumulative Penetrations Employed

Agent	Cumulative Penetration (mg.)
PS	6
SA	8.5

DECLASSIFIED

DECLASSIFIED

APPENDIX H

ACCURACY OF DATA

A. Reproducibility of Charcoal Volume Measurements

A measured volume of adsorbent of several sieve fractions was remeasured to determine the reproducibility of the volume determination. The results of these tests are shown in Table XXXIX.

Table XXXIX

Reproducibility of Volume Measurements

Measurement Number	Volume (ml.) for Sieve Fraction 12-16	16-20	20-30
1	200	200	200
2	200	200	199
3	200	200	199
4	199	199	200
5	199	199	199
6	199	199	199

These measurements demonstrate that adsorbent volume measurements are reprodicible to within plus or minus one ml.

B. Accuracy of Volume Measurements as Determined from Apparent Density and Constancy of Volume Fraction with Sieve Fraction

The accuracy of the adsorbent volume measurements was also checked by measurement of the apparent density for different volumes of adsorbent. This was done by weighing measured volumes of adsorbent.

These measurements were made for sieve fractions

ranging from 12-16 to 30-40, U.S.Standard. The results of these observations are shown in Table XL.

Table XL

Constancy of Apparent Density
Whetlerite: Dry HC3-361

Sieve Fraction	Volume (ml.)	Wt. (g.)	Apparent Density (g./ml.)	Avg.	Standard Deviation (g./ml.)	(%)
12-16	215	108.9	.506			
"	272	138.7	.510			
"	339	171.2	.505			
"	401	203.7	.507	.507	.002	0.4
16-20	143	75.5	.527			
"	205	106.2	.517			
"	272	139.3	.513			
"	334	171.3	.513	.517	.006	1.1
20-30	110	55.6	.506			
"	167	86.3	.516			
"	239	120.5	.504			
"	296	151.3	.511	.509	.004	0.8
30-40	110	53.5	.487			
"	153	75.0	.491			
"	191	91.3	.479			
"	234	117.4	.501	.490	.008	1.6

The linear relationship between volume and weight is apparent and the accuracy is shown to be approximately plus or minus one per cent. The apparent density for the 12-16, 16-20, and 20-30 sieve fractions is seen to be practically identical; whereas, the apparent density of the 30-40 sieve fraction is approximately four per cent lower. This may be caused by either a lower packing density or by the under-impregnation of the fine sieve fraction.

C. Volume Reduction by Blending Several Sieve Fractions

The possibility of a discrepency between the additive volume and the measured volume was investigated for blends of the standard sieve fractions. This was done to determine whether or not the finer sieve fractions fall into the instertices formed by the larger granules. This would result in a non-proportionate increase in the adsorbent bed density. The results of these investigations are shown in Table XLI.

Table XLI

Volume Reduction by Blending Sieve Fractions

Test Number	Volume of Separate Sieve Fractions (ml.) 12-16	16-20	20-30	30-40	Volume Additive (ml.)	Obs. (ml.)	Dev. (%)
1	80	160	-	-	240	238	-0.8
2	80	160	120	-	360	355	-1.4
3	80	160	120	10	370	365	-1.4
4	80	160	140	10	390	385	-1.3
5	80	160	140	20	400	392	-2.0
6	80	160	140	29	409	399	-2.4
7	100	160	140	29	429	420	-2.1
8	40	100	54	6	200	198	-1.0
9	32	98	60	10	200	197	-1.5

These results show that, although there is a slight shrinkage in volume during blending of different sieve fractions, the shrinkage is not great and averages about one to two per cent.

D. Canister Diameter, Effect on Adsorbent Bed Depth

The M11 canister is a production item which was procured by the Chemical Warfare Service under C.W.S. Specification No. 197-52-130. The inside diameter of all

canisters must pass "go-no go" type gages which are set to accept canisters with diameters varying from 4.138 to 4.145 inches. This results in an area variation of plus or minus 0.2 per cent. Since the cross-sectional area was employed to calculate the adsorbent bed depth, the same error is inherent in this dimension.

The E2R3 canister was an experimental canister and was not procured under any C.W.S. Specification. All of these canisters which were used in this work were gaged and only those with diameters between 3.620 and 3.630 were used. The resultant bed depth variation is plus or minus 0.3 per cent.

E. Air Flow Rate During Canister Tests

The air flow rate, both breather and continuous, was measured in accordance with the requirements of the applicable sections of C.W.S. Pamphlet No. 2, Part I. The orifices in the steady flow machines were calibrated frequently with a dry meter of known accuracy and were always found to be accurate within plus or minus two per cent. The same precision was found for the minute volume and the peak flow of the breather testing apparatus.

F. Gas Concentrations

Gas concentrations were determined in accordance with the applicable sections of C.W.S. Pamphlet No. 2, Part I. Basically, the method consisted of absorbing the gas contained in a known volume of air and, by a suitable titration, determining the concentration. The concentrations were so adjusted that one drop (.03 ml.)

at the end point resulted in a distinct color change. Since titres of 10 ml. or more were necessary, the accuracy of titration was approximately plus or minus 0.3 per cent. Sampling errors also were inherent in the method and were found to average plus or minus two per cent.

The precision of the methods has been established previously--prior to acceptance as a standard test procedure by the Chemical Warfare Service.

H. Gas Life

Several series of identical tests were made to determine the accuracy of the gas life measurements. Inaccuracies might be caused by variations in flow rate, concentration, break point indicators, charcoal volume, and canister diameter. The results of these tests are shown in Table XLII.

Table XLII

Precision of Gas Life Measurements
Cyanogen Chloride, 0-50, 50 L./min., Breather

Test No.	Cl (mg./L.)	Nominal Cl (mg./L.)	Obs. Break Time (min.)	Corr. Break Time (min.)	Avg. Break Time (min.)	Standard Deviation (min.)	(%)
1	4.23	4.00	10.0	10.5			
	4.00	4.00	11.0	11.0			
	4.15	4.00	10.0	10.5			
	4.06	4.00	10.0	10.0			
	4.06	4.00	10.0	10.0	10.4	0.4	3.5
2	4.23	4.00	21.0	22.2			
	4.15	4.00	23.0	23.8			
	4.13	4.00	19.0	19.5			
	4.06	4.00	24.0	24.0			
	4.06	4.00	23.0	23.0	22.5	1.6	7.1

Table XLII, Continued

Test No.	C_1 (mg./L.)	Nominal C_1 (mg./L.)	Obs. Break Time (min.)	Corr. Break Time (min.)	Avg. Break Time (min.)	Standard Deviation (min.)	(%)
3	4.00	4.00	32.0	32.0			
	4.15	4.00	33.0	34.2			
	4.13	4.00	30.0	31.0			
	4.12	4.00	35.0	36.0			
	4.12	4.00	37.0	38.0	34.2	2.5	7.3
4	4.00	4.00	55.0	55.0			
	4.14	4.00	53.0	55.0			
	4.13	4.00	50.0	51.8			
	4.00	4.00	51.0	51.0	53.2	1.8	3.4

These data show that the standard deviation of the gas life measurements is approximately 1-3 minutes. It is to be noted that the errors in this measurement are the accumulated result of all other errors involved in measuring the adsorbent volume, filling the canister, and testing.

APPENDIX I

SAMPLE CALCULATIONS

A. Step-Wise Integration for Type I Kinetics

The method of performing the step-wise integration for Type I kinetics was discussed in a qualitative manner in Appendix A. Table XLIII shows the exact method of integration for the particular values of the variables listed as Calculation No. 1, Table XXXI. Only the first two steps of the integration are shown.

B. Step-Wise Integration for Type III-A Kinetics

The method of performing the step-wise integration for Type III-A kinetics was discussed in a qualitative manner in Appendix E. Table XLIV shows the exact method of integration for the particular values of the variables listed in Table XXXIV. The integration for the first increment and the integration for an increment of bed depth 0.15 cm. from the influent face are shown. The influent concentration to the latter increment is shown in Fig. 106. It was determined by a series of step-wise calculations to this point.

C. Method of Calculation of the Break Time of Axial Flow Canister from the Break Time of Radial Flow Canister

1. Statement of Problem

The cyanogen chloride break time of a particular Type ASC impregnated whetlerite in the M10A1 canister was measured to be 65 minutes. The test conditions

DECLASSIFIED [redacted]

FIG. 106

EFFLUENT CONCENTRATION VS. TIME (CALC.)

$\lambda = 0.15$ CM.

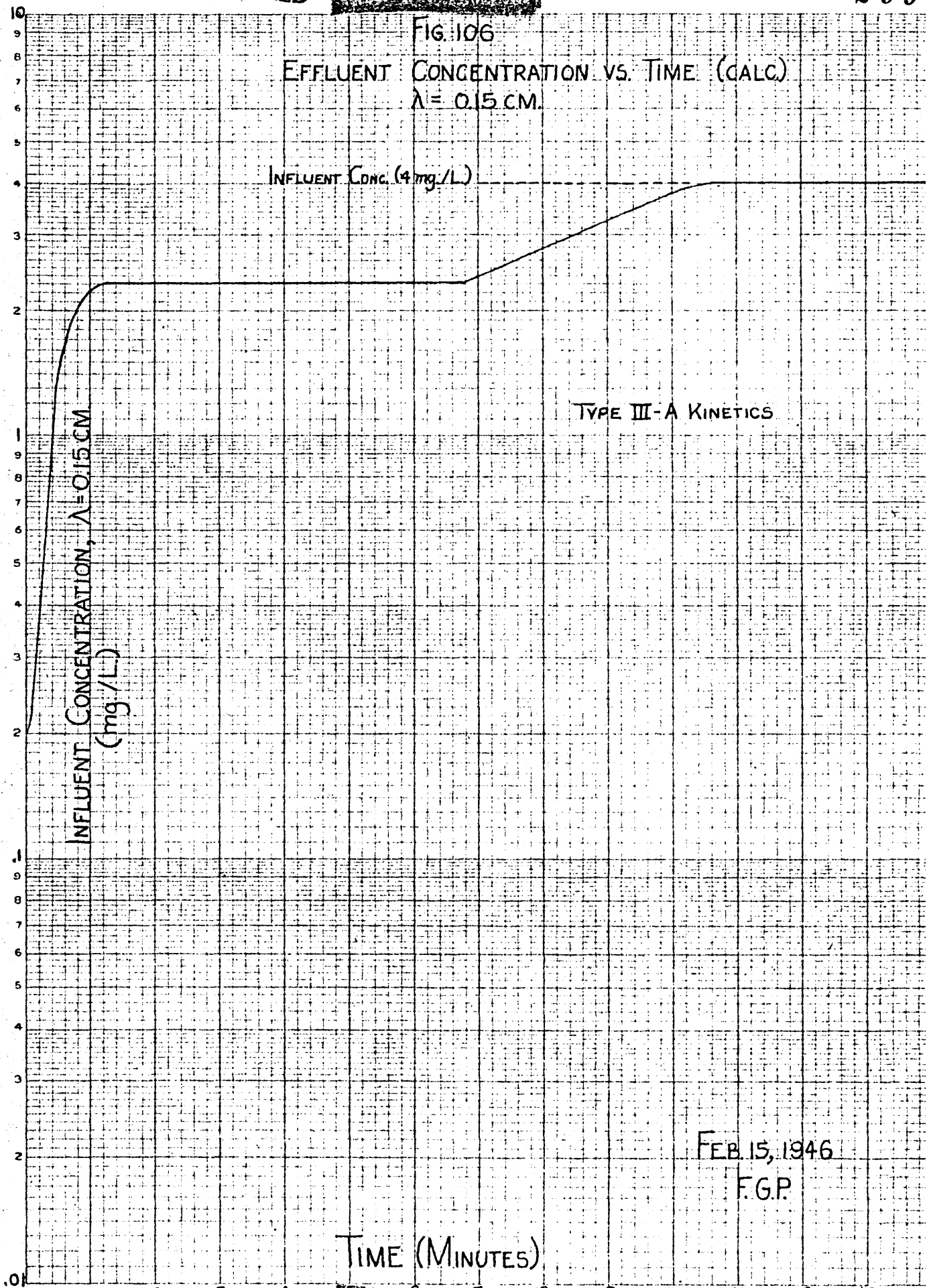

FEB. 15, 1946

F.G.P.

THE FREDERICK POST CO., CHICAGO, ILL.
336-3 SEMI-LOGARITHMIC—3 CYCLES X 70 DIVISIONS

DECLASSIFIED [redacted]

Table XLIII

Step-Wise Integration for Type I Kinetics
(Calculation No. 1, Table XXXI)

$\Delta\lambda$	C_{1a}	$(\Delta m)_a$	C_1^*	$(C_2)_1$	t	t	m_1	m_2	m_3	C_2^*	C_3^*	C_4^*	$(C_2)_2$	$(C_2)_3$	$(C_2)_4$
0-.04	10	0-100	.03	6.07	1.78	1.78	-	-	-	-	-	-	-	-	-
"	10	100-120	.73	6.35	.38	2.16	-	-	-	-	-	-	-	-	-
"	10	120-140	1.43	6.63	.41	2.57	-	-	-	-	-	-	-	-	-
"	10	140-160	2.54	7.07	.48	3.05	-	-	-	-	-	-	-	-	-
"	10	160-180	4.18	7.71	.61	3.66	-	-	-	-	-	-	-	-	-
"	10	180-200	6.51	8.63	1.02	4.68	-	-	-	-	-	-	-	-	-
"	10	200-210	8.84	9.54	1.52	6.27	-	-	-	-	-	-	-	-	-
"	10	210-211	9.81	9.92	.87	7.14	-	-	-	-	-	-	-	-	-
"	10	211-212	10.0	10.0	inf.	inf.	-	-	-	-	-	-	-	-	-
.04-.08	6.07	0- 61	.02	3.69	1.78	1.78	0- 61	-	-	-	-	-	-	-	-
"	6.35	61- 74	.10	3.88	.38	2.16	61- 74	-	-	-	-	-	-	-	-
"	6.63	74- 88	.21	4.11	.41	2.57	74- 89	74- 89	-	.22	-	-	4.11	-	-
"	7.07	89-107	.40	4.44	.48	3.05	89-107	-	-	.45	-	-	4.46	-	-
"	7.71	107-130	.90	5.03	.61	3.66	107-130	-	-	1.00	-	-	5.07	-	-
"	8.63	130-163	2.90	6.37	1.02	4.68	130-167	130-166	-	2.25	2.45	-	6.11	6.19	-
"	9.54	166-192	6.50	8.33	1.52	6.27	166-204	166-198	166-201	5.10	5.80	5.50	7.79	8.06	9.05
"	9.92	201-217	9.40	8.61	.87	7.14	201-210	201-210	201-207	8.7	8.8	8.6	9.16	9.16	9.28
"	10-	207-210	9.00	9.60	.52	7.66	-	-	-	-	-	-	-	-	-
"	10-	210-211	9.80	9.92	.87	8.53	-	-	-	-	-	-	-	-	-
"	10-	211-212	10.0	10.0	inf.	inf.	-	-	-	-	-	-	-	-	-

$(\Delta m)_a$ indicates assumed change in m; C_1^* indicates first assumed value of C^*; $(C_2)_1$ indicates first calculated value of C_2; m_1 indicates first calculated change in m; the following equations are applicable:

$$C_2 = C^* + \frac{C_1 - C^*}{e^{\frac{\Delta\lambda}{M_t}}} = C^* + \frac{C_1 - C^*}{1.65} \quad (68); \qquad \Delta m = -\frac{V}{1000}\frac{\Delta C}{\Delta\lambda}\Delta t = -\frac{575}{1000}\frac{\Delta C}{\Delta\lambda}\Delta t \quad (70)$$

DECLASSIFIED
DECLASSIFIED

Table XLIV
Step-Wise Integration for Type III-A Kinetics

A. First Increment of Bed Depth (0 to .025 cm.)

C_1	4.00	4.00	4.00	4.00	4.00	4.00	4.00	4.00	4.00	4.00		4.00	4.00	4.00	4.00
m_1	0.00	2.00	3.98	5.92	7.78	9.52	11.07	12.26	12.94	13.29		13.2	13.7	14.1	14.5
$\Delta m+\Delta n$	2.00	2.00	2.00	2.00	2.00	2.00	2.00	2.00	2.00			.5	.4	.4	.2
(Δm)	1.90	2.00	1.90	1.82	1.70	1.40	1.30	.80	.40						
(m_2)	1.90	4.00	5.88	7.74	9.48	10.92	12.37	13.06	13.34			13.7	14.1	14.5	14.7
(m_a)	.95	3.00	4.93	6.83	8.63	10.22	11.72	12.66	13.14			13.45	13.9	14.3	14.6
C^*	.015	.16	.42	.82	1.31	1.81	2.41	2.84	3.01	3.18		3.19	3.40	3.60	3.78
$C_1 - C^*$	3.98	3.84	3.58	3.18	2.69	2.19	1.59	1.16	.99			.81	.60	.40	.22
$\frac{C_1 - C^*}{1.65}$	2.41	2.32	2.17	1.93	1.63	1.33	.96	.70	.60			.49	.36	.24	.13
C_2	2.43	2.48	2.59	2.75	2.94	3.13	3.37	3.54	3.61	3.66		3.68	3.76	3.84	3.91
ΔC	1.57	1.52	1.41	1.25	1.06	.87	.63	.46	.39	.34		.32	.24	.16	.09
Δt	.032	.033	.035	.040	.047	.058	.079	.109	.128	6.20		.04	.04	.06	.05
t	.032	.065	.100	.140	.187	.245	.324	.43	.56	6.76		6.80	6.84	6.90	6.95
$\frac{\Delta M}{\Delta t}$	.064	.68	1.82	3.50	5.59	7.72	10.30	12.13	12.90	13.60					
ΔM	0.00	0.02	0.06	0.14	0.26	0.45	0.81	1.32	1.65	84.29					
M_1	0.00	0.00	0.02	0.08	0.22	0.48	0.93	1.74	3.06	4.71					
M_2	0.00	0.02	0.08	0.22	0.48	0.93	1.74	3.06	4.71	89.0					
Δm	2.00	1.98	1.94	1.86	1.74	1.55	1.19	0.68	0.35						
Δm_1	0.00	2.00	3.98	5.92	7.78	9.52	11.07	12.26	12.94	13.21					
m_2	2.00	3.98	5.92	7.78	9.52	11.07	12.26	12.94	13.29	13.2					
m_a	1.00	2.99	4.95	6.85	8.65	10.30	11.67	12.60	13.12						
$m+M$	2.00	4.00	6.00	8.00	10.0	12.0	14.0	16.0	18.0	102.2		102.7	102.7	103.1	103.5

After this point $\Delta m/\Delta t$ becomes negligible.

Chemical capacity fully utilized.

DECLASSIFIED

DECLASSIFIED

Table XLIV (Continued)

B. Increment of Bed Depth Removed from Influent Face (.150 to .200 cm.)

(C_1)	.199	.29	.75	1.03	1.31	1.60	1.91	2.12	2.29	2.33	After this point $\frac{\Delta m}{\Delta t}$ becomes negligible	2.33	2.67	2.90	3.30	3.36	4.00	4.00	4.00
m_1	0	0	1.00	1.98	2.94	3.88	5.66	7.25	8.52	9.46		10.1	10.1	10.7	11.2	11.9	12.0	13.1	14.0
$\Delta m+\Delta n$	0	1.00	1.00	1.00	1.00	2.00	2.00	2.00	2.00	2.00		53.3	60.8	68.8	78.0	86.7	102.1	.9	.2
(Δm)	0	1.00	1.00	.95	.90	1.80	1.60	1.20	.80	.60									
(m_2)	0	1.00	2.00	2.93	3.84	5.68	7.26	8.45	9.32	10.06		10.1	10.7	11.2	11.9	12.0	13.1	14.0	14.5
(m_a)	0	.50	1.50	2.45	3.39	4.78	6.46	7.85	8.92	9.76								13.5	14.2
C*	0	.004	.039	.105	.20	.40	.73	1.08	1.40	1.65								3.2	3.6
C_1- C*	.199	.286	.71	.93	1.11	1.20	1.18	1.04	.89	.68								.8	.4
$\frac{C_1- C^*}{2.72}$	.073	.105	.26	.34	.41	.44	.43	.38	.33	.25								.29	.15
C_2	.073	.109	.30	.44	.61	.84	1.16	1.42	1.73	1.90		1.95	2.24	2.44	2.77	2.82	3.36	3.49	3.75
ΔC	.126	.181	.45	.59	.70	.76	.75	.70	.56	.43		.38	.43	.46	.53	.54	.64	.51	.25
Δt	0	.276	.111	.085	.071	.131	.133	.143	.178	.232		5.40	.80	.80	.80	.80	1.11	.10	.10
t	0	.276	.387	.472	.543	.674	.807	.95	1.13	1.36		6.76	7.56	8.36	9.16	9.91	11.04	11.14	11.24
C_1	-	.29	.72	1.03	1.31	1.63	1.94	2.13	2.29	2.33									
$\frac{\Delta M}{\Delta t}$	-	.018	.167	.448	.854	1.71	3.12	5.10	5.98	7.05		7.60	8.60	9.34	10.61	10.81	12.89		
ΔM	-	0	.02	.04	.06	.22	.41	.73	1.06	1.63		41.0	6.9	7.5	8.5	8.6	14.3		
M_1	-	0	.00	.02	.06	.12	.34	.75	1.48	2.54		4.2	43.2	50.1	57.6	66.1	74.7		
M_2	-	0	.02	.06	.12	.34	.75	1.48	2.54	4.17		43.2	50.1	57.1	66.1	74.7	89.0		
Δm	-	1.00	.98	.96	.97	1.78	1.59	1.27	.94	.37									
m_1	-	0.00	1.00	1.98	2.94	3.88	5.66	7.25	8.52	9.46									
m_2	-	1.00	1.99	2.94	3.88	5.66	7.25	8.52	9.46	9.83									
m_a	-	.50	1.49	2.46	3.41	4.77	6.46	7.88	8.99	9.64									
m+M	-	1.00	2.00	3.00	4.00	6.00	8.00	10.00	12.00	14.00									

That nomenclature in parentheses-indicative of first approximation.

The funcamental relationships used for the above solution were Equations 12, 68, and 70.

DECLASSIFIED

were as follows:

Flow rate.....50 L./min., Breather
Influent Concentration..... 4 mg./L.
Effluent Concentration..... .008 mg./L.
Sieve Analysis.....12-16 30 per cent
16-20 40 per cent
20-30 30 per cent

It is desired to determine the break time of 250 ml. of this same adsorbent in the M11 canister at the same test conditions.

2. Determination of k_1

The value of k_1 is determined from the sieve analysis and Fig. 65 to be .0118.

3. Determination of Q_e

Q_e, the steady flow rate equivalent to breather flow, is a function of x and the logarithm of the concentration ratio. This function is shown in Fig. 92. The value of x is obtained from Table XXV to be 0.32, and the logarithm of the concentration ratio is equal to 6.21. Therefore, from Fig. 92, Q_e is equal to 128 L./min.

4. Determination of Critical Diameter, D_c

The critical diameter of a radial flow canister is given by the following equation:

$$D_c = \left[D_i^{x+1} + 2(x+1)k_1 \left(\frac{1000\ Q_e}{\pi\ L_b} \right)^x \ln \frac{C_1}{C_2} \right]^{\frac{1}{x+1}} \qquad (59)$$

The values of L_b, the length of the canister less the length of the baffles, and D_i, the diameter of the inner tube, are obtained from Table XXVIII to be 10.15 and 3.17 cm., respectively. Substituting the known

values of the variables into Equation 59, the following relationship is obtained:

$$D_c = \left[(3.17)^{1.32} + 2(1.32)(.0118)\left(\frac{128,000}{10.15\ \pi}\right)^{.32} \ln\frac{4}{.008}\right]^{\frac{1}{1.32}}$$

$$= 4.34 \text{ cm.}$$

5. Calculation of Capacity Constant, N

The capacity constant, N, is obtained by the solution of Equation 61. This equation is as follows:

$$t = \frac{\pi L N}{4 Q C_1}\left[D_2^2 - D_c^2 - 12 D_c k_1 \left(\frac{1000 Q_e}{\pi D_c L_b}\right)^x\right] \qquad (61)$$

D_2, the outer tube diameter, and L, the length of the canister, are obtained from Table XXVIII to be 6.79 and 11.42 cm., respectively. Substituting the known values of the variables into this equation, the following relationship is obtained:

$$65 = \frac{\pi(11.42)(N)}{(4)(50)(4)}\left[6.79^2 - 4.34^2 - 12(4.34)(.0118)\left(\frac{128,000}{\pi(4.34)(10.15)}\right)^{.32}\right]$$

Solving this equation, N is found to be equal to 65.4 mg./ml.

6. Calculation of Break Time for M11 Canister (250 ml.)

The equation for the break time of an axial flow canister (Type III-B kinetics) is as follows:

$$t = \frac{N A}{C_1 Q}\left[\lambda - k_1\left(\frac{1000 Q_e}{A_b}\right)^x \left(\ln\frac{C_1}{C_2} + 3\right)\right] \qquad (54)$$

The area of the M11 canister (4.14 inches diameter) is 87.0 sq.cm. The area at the baffles (3.64 inches diameter) is 67.2 sq.cm. The bed depth, λ, for 250 ml. of adsorbent is 2.87 cm. Substituting the known values of the variables into Equation 54, the following expression is obtained:

$$t = \frac{(65.4)(87.0)}{(4.0)(50)} \left[2.87 - (.0118)\left(\frac{128,000}{67.2}\right)^{.32} \left(\ln \frac{4}{.008} + 3\right) \right]$$

Solving this equation, the break time is calculated to be 47 minutes.

D. Calculation of the Effect of Sieve Fraction on Break Time and Air Resistance

1. Statement of Problem

The phosgene break time of a M11 canister containing 250 ml. of 12-16 sieve fraction Type ASC impregnated whetlerite (H designation) was measured to be 25 minutes at the test conditions listed below.

Influent Concentration.....10 mg./L.
Break Concentration..... .008 mg./L.
Flow Rate.....50 L./min., Breather

It is desired to determine the change in break time and air resistance of the canister if the adsorbent is changed to 250 ml. of 20-30 sieve fraction of the same whetlerite.

2. Determination of the Value of k_1

The values of k_1 for the 12-16 and the 20-30 sieve fractions are obtained from Fig. 64 to be .00524

and .00221, respectively.

3. Determination of Values of k_2

The values of k_2 for 12-16 and 20-30 sieve fractions are obtained from Fig. 68 to be 5.46 and 13.0, respectively. The correction factor to account for particle shape is obtained from Table XXIII to be unity.

4. Determination of Q_e

Q_e, the steady flow rate equivalent to breather flow is obtained from Fig. 92 to be 133 L./min. (The value of x is 0.48 from Table XXV and $\ln \frac{C_1}{C_2}$ is equal to 7.13).

5. Determination of Capacity Constant, N

The capacity constant, N, can be determined by substituting all of the known values of the variables into Equation 54 and solving for N. This is indicated in the following equation:

$$25 = \frac{(N)(87.0)}{(10)(50)}\left[2.87 - (.00524)\left(\frac{133{,}000}{67.2}\right)^{.48}\left(\ln \frac{10}{.008} + 3\right)\right]$$

The value of N is calculated to be 224 mg./ml.

6. Determination of Break Time for 20-30 Sieve Fraction (250 ml.)

Since it was shown that the value of N is independent of the sieve fraction, the break time of 250 ml. of 20-30 sieve fraction can be calculated by substitution of the calculated value of N for the 12-16 sieve fraction and the other known values of the variables into Equation 54. This substitution results in the following equation:

$$t = \frac{(224)(87.0)}{(10)(50)}\left[2.87 - (.00221)\left(\frac{133,000}{67.2}\right)^{.48}\left(\ln\frac{10}{.008} + 3\right)\right]$$

$t = 75.4$ minutes

Therefore, the increase in break time associated with a change from 250 ml. of 12-16 to 250 ml. of 20-30 sieve fraction whetlerite is 50.4 minutes.

7. Determination of Air Resistance

The air resistance of an axial flow canister is given by the following equation:

$$\Delta P = k_2 Q \left[\frac{2.00}{A_b} + \frac{\lambda - 2.00}{A}\right] \qquad (48)$$

Substituting the known values of the variables into this equation, the following expressions are obtained for the air resistance at 85 L./min.

a. 12-16 Sieve Fraction

$$\Delta P = (5.46)(85)\left[\frac{2.00}{67.2} + \frac{2.87-2.00}{87.0}\right]$$

$$= 18.5 \text{ mm. of water}$$

b. 20-30 Sieve Fraction

$$\Delta P = (13.0)(85)\left[\frac{2.00}{67.2} + \frac{2.87-2.00}{87.0}\right]$$

$$= 44.0 \text{ mm. of water}$$

Therefore, the increase in air resistance associated with a change from 250 ml. of 12-16 to 250 ml. of 20-30 sieve fraction whetlerite is 25.5 mm. of water.

APPENDIX J

LOCATION OF ORIGINAL DATA

The original data are located in the Chemical Warfare Service files at the Technical Command, Edgewood Arsenal, Maryland. The notebook pages are as follows:

C.W.S. Dev. Lab., M.I.T. Notebook Pages: 18441-18500
22521-22580
23721-23748
23763-23772
27097-27102
27109-27110
29181
50310-50323
50335
57683-58693

APPENDIX K

NOMENCLATURE

A	Area perpendicular to direction of air flow (cm^2).
a	Surface area of adsorbent per unit volume(1/cm.)
A_b	Open area at baffles (cm^2).
AC	Chemical Warfare Service symbol for hydrocyanic acid.
B	A function of $\ln \frac{C_1}{C_2}$ and x, for breather testing, dimensionless.
C	Concentration in air stream at any point (mg./L.).
C_1	Influent concentration in air stream (mg./L.).
C_2	Effluent concentration in air stream (mg./L.).
C	Concentration in equilibrium with adsorbent (mg./L.).
CG	Chemical Warfare Service symbol for phosgene.
CK	Chemical Warfare Service symbol for cyanogen chloride.
D	Diameter of radial flow adsorbent bed at any point (cm.).
d	Diameter of wetted wall absorption column (cm.).
D_c	Critical diameter of radial flow canister (cm.).
D_i	Inner tube diameter of radial flow canister (cm.).
D_p	Average particle diameter (cm.).
D_v	Diffusivity of agent being transferred ($cm.^2/sec.$).
D_2	Outer tube diameter of radial flow canister (cm.).
e	Base for natural logarithms (2.702).
F	Cumulative penetration of agent through adsorbent bed (mg.).
f	Fraction of any particular sieve fraction in adsorbent blend.
f_r	Frequency of breather flow cycle (cycles/min.).

H Experimental rate constant analogous to H_t and H_r (cm.).

H_t Height of a transfer unit, gas film (cm.).

H_r Height of a reaction unit, surface resistance (cm.).

$(H_t)_x$ Height of a transfer unit for agent x (cm.).

h Height of the "dead layer" in Mecklenberg's equation (cm.).

I Quantity of impregnant which has chemically reacted (equivalents/ml.).

$I_o(z)$ Modified Besel function, $J_o(iz)$, see p.

k's Constants

k_1 Constant in Equation , H_t (or H) = $k_1 V^x$.

k_2 Constant in pressure drop equation.

k_g Mass transfer coefficient, gas film (mg./(min.)(cm.^{2})(unit conc. gradient).

k_r Reaction rate constant, (mg./(min.)(cm.^{2})(unit grad.)

L Length of cylinder in radial flow canisters (cm.).

L_b Open length of inner tube considering restriction of baffles in radial flow canisters (cm.).

L./min. Abbreviation for liters per minute.

L./min., C.F. Abbreviation for liters per minute, constant flow.

L./min., B. Abbreviation for liters per minute, breather.

l Thickness of stagnant air film (cm.).

M Quantity of agent removed by chemical reaction with impregnants (mg./ml.).

M_s Quantity of agent in the saturated layer (mg.).

M_t Total amount of agent adsorbed by the bed (mg.).

$M.W._x$ Molecular weight of agent x.

M_1 Quantity of agent adsorbed by bed at instant influent face becomes saturated (mg.).

m Adsorbate (physically adsorbed) content of bed (mg./ml.)

N	An experimental capacity constant analogous to N_o and N_r (mg./ml.).
N_a	Quantity of agent adsorbed per unit of superficial area of the adsorbent (mg./cm.^{2}).
N_o	Saturation capacity of adsorbent for physically adsorbed material (mg./ml.).
N_r	Reactive capacity of adsorbent (mg./ml.).
n	Exponent in Freundlich's adsorption isotherm.
P	Total pressure (g./cm.^{2}).
P_{bm}	Average partial pressure of non-diffusing gas in stagnant film (g./cm.^{2}).
P_g	Partial pressure of diffusing agent in main gas stream (g./cm.^{2}).
P	Partial pressure of diffusing agent in equilibrium with adsorbent or absorbing solution (g./cm.^{2}).
ΔP	Air resistance of adsorbent bed (mm. of water).
PS	Chemical Warfare Service symbol for chloropicrin.
Q	Steady air flow rate (L./min.).
Q_e	Steady flow rate equivalent to "Breather Flow Rate" (L./min.).
R	Gas constant.
S	Slope of bed depth-break time curve (min./cm.).
S'	Slope of plot of the logarithm of the effluent concentration vs. time
SA	Chemical Warfare Service symbol for arsine.
s	Function of time in breather testing defined by the following equation: $s = 2 f_r t$.
T	Absolute temperature (^oK.).
t	Time (min.).
Δt_1	Time required to saturate influent face of adsorbent bed (min.).
V	Superficial linear air flow rate (cm./min.).
x	Exponent defined by equation H_t(or H) = $k_1 V^x$.

α	Fraction of total volume of adsorbent which is void.
ΔP	Air resistance of adsorbent bed (mm. of water).
Δt_1	Time required to saturate influent face of adsorbent bed (min.).
β	A function of n in Freundlich's adsorption isotherm.
μ	Viscosity of fluid in the stagnant film surrounding adsorbent granules or near wetted wall (g./(cm.)(sec.).
λ	Bed depth (cm.).
λ_c	Apparent critical bed depth (cm.).
λ_s	Depth of adsorbent which is completed saturated (cm.).
ρ	Density of fluid stream ($g./cm.^3$).

APPENDIX L

LITERATURE CITATIONS

1. Sherwood, T.K., "Absorption and Extraction", 1st Edition, Chapter I, McGraw-Hill Book Co., (1937).

2. Freundlich, H., "Colloid and Capillary Chemistry", London, p. 113, (1926).

3. Langmuir, I., J. Am. Chem. Soc., 40, 1361 (1918).

4. Fellenger, L., ScD Thesis, Dept. of Chem. Eng., M.I.T. (1941).

5. Chilton, T.H., Colburn, A.P. Ind. Eng. Chem., 27, 255 (1935).

6. de Saussere, T., Gilbert's Ann. der Physik, 47, 113 (1814). Ann. Phil., 6, 241 and 331 (1815).

7. Homfray, I.F., Z. Phys. Chem., 74, 129 (1910).

8. Freundlich, H., "Colloid and Capillary Chemistry", London, p. 120, (1926).

9. Bunbury, H.M., Journal Chemical Society, 121, 1525-8 (1922).

10. Arii, K. and Huzita, S., Bull. Inst. Chem. Research (Tokyo), 20, 209-17 (1941).

11. Kubelka, P., Kolloid Z., 55, 129-43 (1931).

12. Freundlich, H., "Colloid and Capillary Chemistry", London, p. 108, (1926).

13. Freundlich, H., Trans. Faraday Soc., 28, 195-201 (1932).

14. Rideal, E.K., Trans. Faraday Soc., 28, 139-47 (1932).

15. Taylor, H.S., J. Am. Chem. Soc., 53, 578-97 (1931).

16. Harned, H.S., J. Am. Chem. Soc., 42, 372-91 (1920).

17. Bergter, F., Ann. Physik, 37, 472-509 (1912).

18. McBain, J.W., Z. Physik Chemie, 68, 471-97 (1909).

19. Freundlich, H., Z. Physik Chemie, 61, 249 (1909).

[redacted] DECLASSIFIED

20.	Beel, E. and Weingaertner, E.,	Z. Physik Chemie, A173, 35-37 (1935).
21.	Damkohler, G.,	Z. Physik Chemie, A174, 222-38 (1935).
*22.	Hougen, O.A. and Dodge, F.W.,	NDRC Div. B, Formal Report No. 61 (OSRD No. 123), June 31, 1941.
23.	Marc, R.,	Z. Electrochem., 20, 515-24 (1914).
24.	Emmet, P.H. and Brunauer, S.,	J. Am. Chem. Soc., 59, 310 (1937).
25.	Taylor, H.S. and Williamson, A.J.,	J. Am. Chem. Soc., 53, 813 (1931).
26.	Sherwood, T.K. Holloway, F.A.L.,	Trans. A.I.Ch.E., 36, 21 (1940).
27.	Kowalke, O.A., Hougen, O.A., and Watson, K.M.,	Univ. Wisc. Eng. Exp. Station Bulletin 68 (1928).
28.	Chilton, T.H., Duffy, H.C., Vernon, H.C.	Ind. Eng. Chem., 29, 298 (1937).
29.	Borden, H.M., and Squires, W., Jr.,	S.M. Thesis, Dept. of Chem. Eng., M.I.T. (1937).
30.	Johnstone, H.G. Singh, A.D.,	Ind. Eng. Chem., 29, 286 (1937).
31.	Doherty, T.B. Johnson, F.C.,	S.M. Thesis, Dept. of Chem. Eng., M.I.T. (1938).
32.	Holloway, F.A.L.,	Sc.D. Thesis, Dept. of Chem. Eng., M.I.T. (1939).
33.	Gamson, B.W., Thodos, G., and Hougen, O.A.,	Trans. Am. Inst. of Chem. Eng., 39, 1 (1943).
34.	Hurt, D.H.,	Ind. Eng. Chem., 35, 522 (1943).
35.	Bohart, G.S., Adams, E.W.,	J. Am. Chem. Soc., 42, 523-44 (1920).
*36.	Danby, C.J., Davoud, J.G., Everett, J.H., Hinshelwood, C.N.,	N.D.R.C. Division 8-11, File No. B-394

[redacted] DECLASSIFIED

37.	Mecklenberg, W.,	Z. Electrochem., 31, 488-95 (1925).
38.	Mecklenberg, W.,	Kolloid Z., 52, 88-103 (1930).
39.	Beaton, R.H. and Furnas, C.C.,	Ind. Eng. Chem., 33, 1500 (1941).
40.	Engel, H.C. and Coull, H.C.,	Trans. Am. Inst. Chem. Eng., 38, 947-65 (1942).
*41.	Dole, M. and Klotz, I.M.,	"Adsorption Studies on Chloropicrin and Phosgene", OSRD Report No. 972, July 15, 1942.
*42.	Short, O.A., Pearce, F.G., Nicholls, K.R.,	M.I.T. Memorandum Report No. 97, August 25, 1944.
*43.	Dole, M.,	NDRC Misc. Pub. No. 50, Aug. 29, 1941.
*44.	Yost, D.M.,	OSRD Report No. 361, Jan. 7, 1942.
45.	Anzelius, A.,	Zeits. f. ang. Math. u. Mech., Bd. VI, S, 291 (1926).
46.	Furnas, C.C.,	Trans. Am. Inst. Chem. Eng., 24, 142 (1930).
*47.	Drew, T.B., Spooner, F.M., Douglas, J.,	NDRC Informal Report No. 10.5-14, November 17, 1944.
*48.	Wiig, E.A.,	NDRC Misc. Publication No. 254/16, p.9.
*49.	Wiig, E.A.,	NDRC Misc. Publication No. 254/17, p.2.
*50.	Wiig, E.A.,	NDRC Misc. Publication No. 254/18, p.13.
*51.	Wiig, E.A.,	NDRC Misc. Publication No. 254/19, p.11.
*52.	Wiig, E.A.,	NDRC Misc. Publication No. 254/26, p.9.
*53.	Klotz, I.M.,	NDRC Monthly Summary Report, Section 10.1, March 15, 1945.

* These reports are classified, U.S.Army documents and are filed at the Technical Command, Edgewood Arsenal, Md.

APPENDIX M

BIOGRAPHICAL SKETCH

The author was born at Terre Haute, Indiana, on Sept. 18, 1918. He attended grammar and high schools in that city and was graduated from Wiley High School in June, 1936.

He matriculated at Rose Polytechnic Institute, Terre Haute, Indiana in September, 1936, and was graduated with highest honors in May, 1940, receiving the B.S. degree in Chemical Engineering and a reserve commission in the Chemical Warfare Service of the U.S.Army.

In October, 1940, Mr. Pearce enrolled in the graduate school, Course X, at the Mass. Inst. of Technology. He passed the general doctorate examinations in May, 1941, and started a thesis on the vulcanization of Guayule rubber under Dr. E.A.Hauser in October, 1941.

On January 20, 1942, he was called into the Armed Forces and was stationed at the C.W.S. Development Lab. at M.I.T. where he worked on the development of defensive items for the Chemical Warfare Service. On Oct. 14, 1945, he was transferred to the Technical Command, Edgewood Arsenal, Md., where he was assigned the task of Actg. Chief of the Canister Branch, Protective Division.

He was placed on terminal leave from the U.S.Army from Ft. Meade, Md., on Jan. 24, 1946, and his discharge to an inactive (reserve) status will be effective on May 10, 1946.